RESOURCE SERIES 35

Alkalic Igneous Rocks of Colorado and Their Associated Ore Deposits

By James A. Cappa

Colorado Geological Survey
Department of Natural Resources
Denver, Colorado
1998

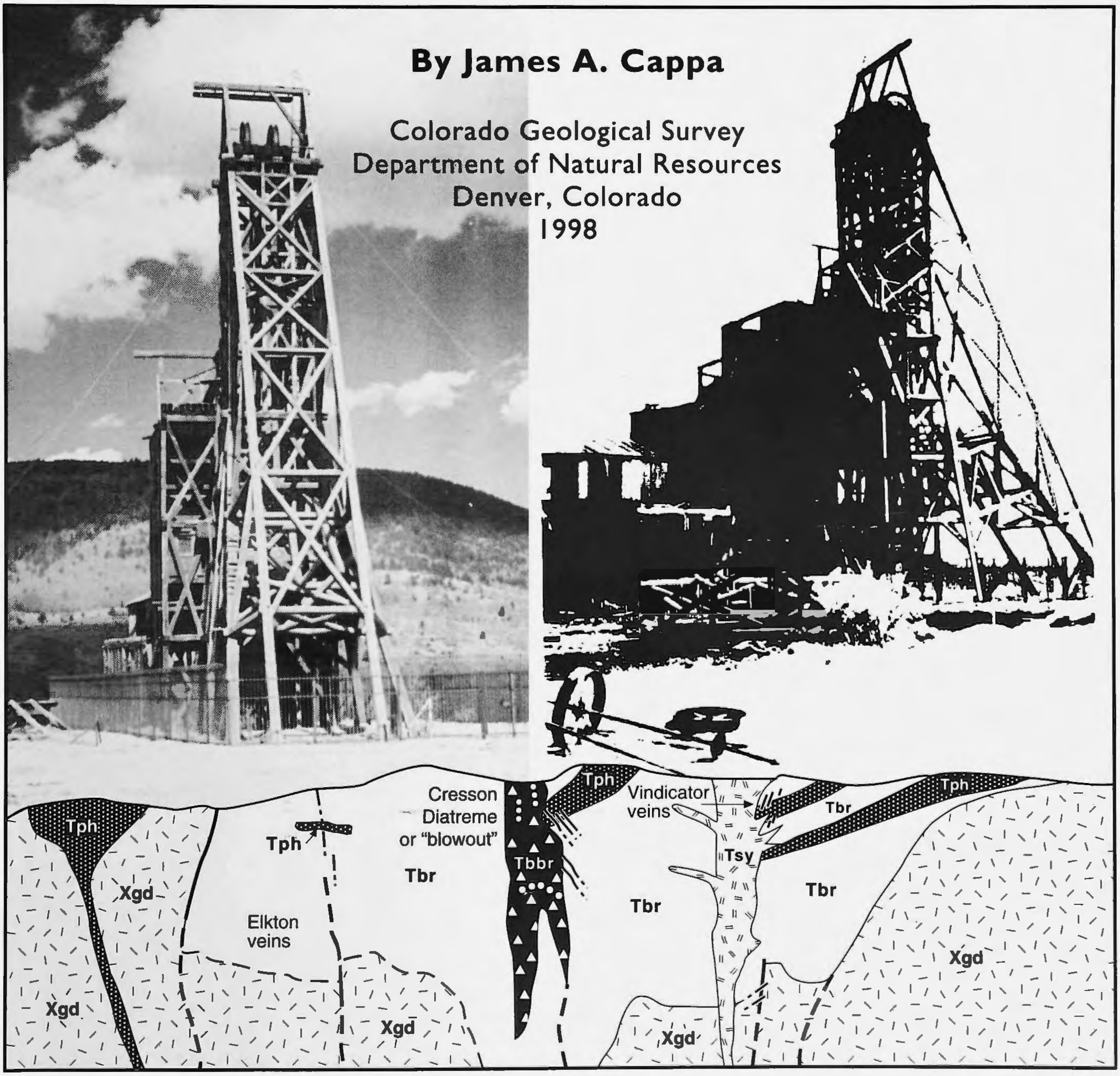

Resource Series 35

Alkalic Igneous Rocks of Colorado and Their Associated Ore Deposits

By James A. Cappa

DOI: https://doi.org/10.58783/cgs.rs35.vibz1272

Colorado Geological Survey
Department of Natural Resources
Denver, Colorado
1998

Contents

FIGURES

Preface

Alkalic igneous rocks in Colorado formed in a wide variety of tectonic settings-from the Cambrian intrusive complexes of the Wet Mountains to the late Tertiary alkalic basalts of central Colorado. They host mineral deposits as economically important as the Cripple Creek gold district, which has produced over 21 million ounces of gold since its discovery in 1891. The following chapters discuss the principal alkalic igneous complexes that are associated with economically significant mineral deposits. The final chapter describes several other alkalic igneous provinces of the state not associated with significant economic mineral deposits.

Whole rock geochemical data and the CIPW normative compositions (Best, 1982) have been included as tables in the appendix and are summarized in figures at the end of each chapter. References for each region are included at the end of the chapter.

Acknowledgements

I am especially grateful to the Colorado Geological Survey Mineral Consortium for partial funding of this project. The Consortium members are Newmont Mining Corp., Echo Bay Mines, and AMAX Gold (now a division of Cyprus Amax Minerals Company). Partial funding also came from Colorado Severance taxes, which are drived from the production of oil, gas, coal, and minerals. I would also like to thank Mary-Margaret Coates for editing and suggesting improvements to the text and Randy Streufert and Allison Lawson for their contributions on the Powderhorn district chapter, the tables, and geochemical plots.

Chapter 1

Survey of Alkalic Igneous Rocks

INTRODUCTION

Alkalic igneous rocks host many economically important and rare ore deposits in Colorado (Fig. 1), in other parts of North America, and on every continent except Antarctica. This chapter provides a review of the composition and the tectonic setting of alkalic igneous rocks, and describes the variety of ore deposits that occur in these rocks throughout the world.

COMPOSITION

Alkalic igneous rocks form a unique suite of rocks that are undersaturated with respect to silica and relatively enriched in Na_2O and K_2O. Mutschler and others (1985) defined alkalic rocks as having $Na_2O + K_2O > (0.3718) \times SiO_2 - 14.5$, where SiO_2, Na_2O, and K_2O are expressed in weight percent. Minerals that occur in alkalic rocks include alkali feldspar, plagioclase, feldspathoids such as nepheline and leucite, biotite-phlogopite, Na-Ca pyroxene, alkalic amphiboles, olivine, and Fe-Ti oxides. Alkalic rocks are range in composition from felsic to ultramafic; their silica content ranges from virtually none to rocks of intermediate silica range. Alkalic rocks also contain anomalously large amounts of rare-earth elements (REE), niobium, uranium, and other elements which occur in many of the rare minerals found in alkalic rocks.

A few of the more common aphanitic alkalic rocks include alkali olivine basalt, basanite, hawaiite, trachyte, phonolite, shoshonite, kimberlite, and lamprophyre. Phaneritic alkalic rocks include syenite, ijolite, theralite, and carbonatite. Alkalic igneous rocks are dated throughout geological time. The Poohbah Lake syenite in northwestern Ontario is the oldest documented alkalic igneous rock at 2.7 Ga (Mitchell, 1976). The youngest alkalic igneous rocks are carbonatite lavas, erupted in historical times, at Oldoinyo Lengai in East Africa. More information on the geochemistry, petrology, and geological setting of alkalic rocks can be found in several reference works including Sørensen (1974), Fitton and Upton (1987), and Mitchell (1996).

TECTONIC SETTING

Fitton and Upton (1987) classified alkalic igneous rocks on the basis of the tectonic setting in which they originated: continental rift valley magmatism, oceanic and continental intraplate magmatism, and, rarely, subduction-related magmatism.

CONTINENTAL RIFT VALLEY MAGMATISM

Continental rift valley magmatism is dominated by widespread alkalic flood basalts and more local carbonatitic flows and intrusive complexes such as are found along the East African rift. Carbonatites are one of the most unusual of alkalic rocks and much attention has been focussed on them because of their economic importance. Carbonatites are igneous rocks composed chiefly of carbonates of Na, Ca, and Mg and contain lesser amounts of feldspar, pyroxene, biotite, apatite, barite, and other unusual minerals. Carbonatites can form volcanoes, flows, and subvolcanic intrusive complexes, commonly in the form of ring dikes. More information on carbonatites can be found in several reference works including Heinrich, 1966; Tuttle and Gittins, 1966; and Le Bas, 1977.

In Colorado, alkalic basalts of middle to late Tertiary age are exposed in limited areas throughout

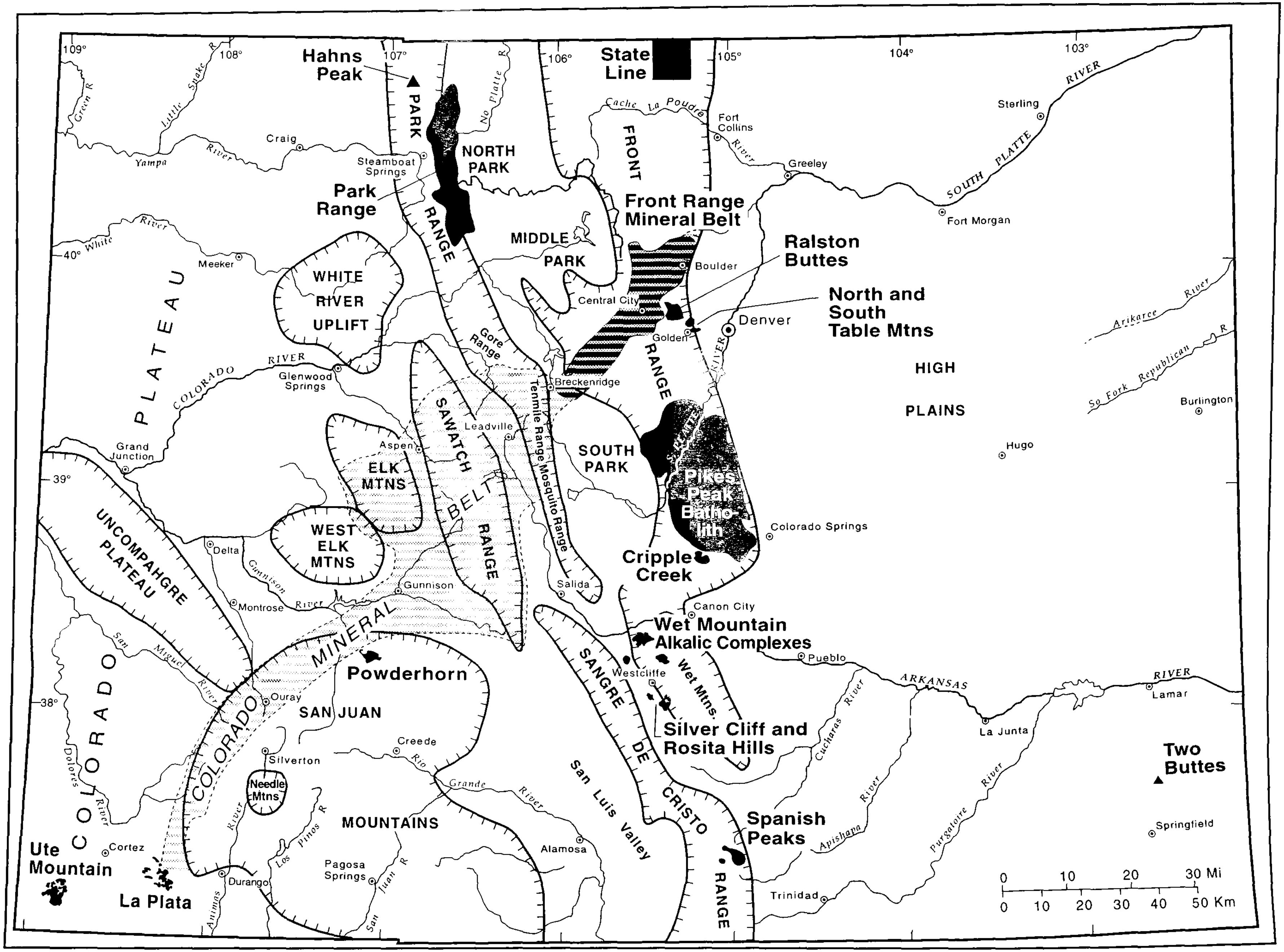

Figure 1. ndex map of alkalic rock occurrences and provinces in Colorado.

the north-central part of the state from the area around Glenwood Springs north to the Rabbit Ears and Park Ranges. The alkalic diatreme complex at Cripple Creek, Teller County, is one of the premier gold districts of North America. Both of these alkalic suites are probably related to magmatism along the Rio Grande rift zone.

OCEANIC AND CONTINENTAL INTRAPLATE MAGMATIC SETTING

The oceanic and continental intraplate magmatic setting is dominated by alkalic flood basalts often of great areal extent, such as the Paraná Basalts of Brazil and shield volcanoes such as the Galapagos Islands and the Hawaiian Islands in oceanic environments.

Ultrapotassic igneous rocks in which the K_2O/Na_2O >3 are common in continental intraplate settings. The feldspathoid mineral leucite is usually abundant in these rocks. Ultrapotassic igneous rocks are found in the Leucite Hills of southern Wyoming and in Rodalquilar gold district in the Cabo de Gato region of southeastern Spain. Müller and Groves (1995) described the relationship between potassic and ultrapotassic igneous rocks and gold-copper mineralization.

Lamprophyres are dark potassic rocks; their porphyritic texture consists of phenocrysts of ferromagnesian minerals in a groundmass of fine-grained feldspar occurs in the groundmass. Lamprophyres commonly occur as dikes and dike swarms and have been thought to be related to gold deposits in Archean terrains. Rock (1991) described the geology, chemistry, and mineralogy of lamprophyres.

Kimberlites are hybrid igneous rocks containing megacrysts of ultramafic and mafic minerals in a fine-grained matrix. Xenocrysts and xenoliths of mantle and upper and lower crustal rocks are common. Most kimberlites, the world's most prolific source of primary diamonds, are found in diatremes in intraplate continental settings. Mitchell (1986, 1995) described the mineralogy, geochemistry, and petrology of kimberlites and related rocks.

Peralkaline rocks are defined as having molecular $(K_2O + Na_2O) > H_2O$ which results in a mineralogical suite containing alkalic pyroxenes and amphiboles such as aegerine and riebeckite, rather than the more typical augite and hornblende of calc-alkalic rocks. Silicic peralkaline rocks occur in oceanic basaltic provinces and are transitional between tholeiitic and alkalic basalts. Rhyolitic ash flows and tuffs of peralkaline composition are found in the Basin and Range Province of western North America (Best, 1982).

SUBDUCTION RELATED MAGMATISM

Alkalic rocks constitute a minor part of dominantly calc-alkalic igneous complexes along subduction zones.

CLASSIFICATION

Most alkalic rocks of volcanic origin can be described by using the total alkali-silica diagram (Le Bas and others, 1986). This type of diagram compares total alkalies, Na_2O and K_2O, to silica, SiO_2. The line separating the basalt-basaltic andesite-andesite-dacite and trachybasalt-basaltic trachyandesite-trachyandesite-trachydacite fields (see Fig. 14) separates alkalic rocks on the top and subalkalic and calc-alkalic rocks below. Certain other alkalic rocks of volcanic origin, such as kimberlites, lamproites, melilites, and nephelinites do not fall readily within this scheme. These rocks can be best described by a modal-textural classification (Le Bas and Streckeisen, 1991) that is based upon the modal percentage of major minerals and the rock texture. Mineralogical-genetic classifications are based upon assemblages of characteristic minerals. For a more complete discussion of the classification of undersaturated alkalic rocks see Mitchell, 1996. In spite of various classification schemes there still remains considerable vagueness and imprecision in the naming of alkalic igneous rocks. For this report no attempt was made to reclassify the alkalic rocks; original names as published are used throughout.

ORE DEPOSITS

Mineral deposits associated with alkalic rocks are varied. Niobium, tantalum and other REE are found in carbonatites, diamonds in lamproites and kimberlites, and gold in many types of alkalic igneous rocks. The following section briefly illustrates the variety of ore deposits associated with alkalic rocks throughout the world.

NIOBIUM AND TANTALUM

Niobium and tantalum are associated with carbonatites and related alkalic igneous rocks as pyrochlore, a Nb-Ti-Ca oxide. The most significant source of niobium and tantalum are the carbonatites of the Araxá and Catalão I deposits in southern Brazil. Both of these ore deposits occur in the lateritic residuum overlying carbonatite bodies.

At Araxá, the niobium ore deposit is associated with a dolomitic carbonatite in the center of a circular carbonatite complex. The lateritic residuum can be up to 100 meters thick, and total reserves are 460 million tonnes at an approximate grade of 3 percent Nb_2O_5. Significant phosphate reserves lie approximately 1 kilometer away from the niobium ore deposit (Deans, 1978; Pell, 1996). At Catalão I a secondary Ba-Ce pyrochlore occurs in approximately 80 meters of lateritic residuum over carbonatite lenses in pyroxenite. Reserves are 3.5 million tonnes at a grade of 1.74 percent Nb_2O_5 (Deans, 1978; Pell, 1996).

In North America, significant niobium- and tantalum-bearing carbonatites occur in Quebec, Canada, and in the Powderhorn complex of Gunnison County, Colorado. Only the St. Honore deposit in near Chicoutimi, Quebec, has produced significant amounts of ore. The central core of the St. Honore deposit is a dolomitic and ankeritic carbonatite that is enriched in REE. This core is surrounded by calcitic and dolomitic carbonatites that are depleted in REE but enriched in niobium and tantalum. Reserves are approximately 12.2 million tonnes at a grade of 0.66 percent Nb_2O_5 (Pell, 1996).

RARE EARTH ELEMENTS INCLUDING YTTRIUM

The rare earth elements (REE)—lanthanum, cerium, praseodymium, neodymium, promethium, samarium, europium, gadolinium, yttrium, terbium, dysprosium, holmium, erbium, thulium, ytterbium, and lutetium—are concentrated in carbonatites and other alkalic igneous rocks, associated hydrothermal systems, and alkalic syenites. These elements also occur in skarns, pegmatites, and volatile-enriched granites. Many common minerals such as fluorite, apatite, titanite, and zircon may contain considerable amounts of REE in their atomic structure. Carbonate and fluorocarbonate minerals such as bastnäsite and parisite, which contain REE, may also be present in significant amounts. Certain phosphate minerals, monazite and xenotime, may also host REE.

The Mountain Pass deposit in southern California by itself accounts for half the world's production. The orebodies consist primarily of Late Proterozoic carbonatite dikes and other intrusive rocks containing calcite, dolomite, ankerite, siderite, barite, bastnäsite, parisite, quartz, and other minerals. The carbonatites are associated with potassic alkalic rocks, shonkinites, and saturated potassic granitic rocks. The orebodies contain approximately 40 million tons at a grade of 7.7 percent REE (Olson and others, 1954; Heinrich, 1966; Pell, 1996).

ZIRCONIUM AND HAFNIUM

Zirconium occurs within the common igneous accessory mineral zircon, a silicate, and less commonly in baddeleyite, an oxide. Alkalic igneous rocks often contain considerable amounts of baddeleyite. Most baddeleyite is recovered as a byproduct of alkalic mineral deposits mined for phosphate, niobium, and iron.

The Ilímaussaq intrusion of southern Greenland is an elliptical, intrusive complex containing several augite syenite and nepheline syenite bodies. Magmatic differentiation produced economic concentrations of REE, baddeleyite, and uranium minerals within the syenite bodies. Eudialyite (a complex Zr-Fe-Mn-Ca-Ce-Na metasilicate) cumulate layers within the syenite may contain up to 6 percent ZrO_2, 3 percent REE and 0.2 percent Nb_2O_5 (Steenfelt, 1991; Pell, 1996).

VERMICULITE

Vermiculite minerals include a variety of micaceous minerals, all hydrated silicates. They are formed chiefly as alteration products of the common mica minerals biotite and phlogopite. Most vermiculite is associated with alkalic ultramafic complexes and skarns.

The Rainey Creek alkalic-ultramafic complex near Libby, Montana, is the world's largest vermiculite deposit with approximately 90 million tonnes of ore at 30 percent vermiculite. The complex consists of successive magmatic differentiates of biotite pyroxenite, biotitite, and magnetite pyroxenite; vermiculite is associated with the altered biotite pyroxenite (Boettcher, 1967; Pell, 1996).

DIAMONDS—KIMBERLITES AND LAMPROITES

Kimberlites are small-volume, ultramafic, potassic, hybrid intrusive rocks that originate in the diamondstability region of the upper mantle. Kimberlites generally contain xenoliths and xenocrysts of mantle, crustal, and supracrustal rocks and minerals. Most of the world's primary diamonds have been produced from kimberlites (Scott-Smith, 1996a). Kimberlites occur in all regions of the earth; however, most diamondiferous kimberlites are associated with Archean age crustal complexes.

Lamproites are similar to kimberlites in many ways and the difficulty of distinguishing them has lead to confusion. The Prairie Creek, Arkansas, diamond occurrence was thought to be a peridotite kimberlite but is now recognized to be an lamproite (Bergman, 1987). One of the world's largest diamond deposits occurs in the sandy tuff lamproites of Argyle, Western Australia; this deposit is over 100 million tonnes and its phenomenal grade is about 500 carats/100 tonnes (Bergman, 1987; Scott-Smith, 1996b).

GOLD

Gold ore is associated with alkalic igneous rocks in a few localities in North America. The Cripple Creek district in Colorado (Fig. 1), which is composed of alkalic phonolites and phonolite breccias, is probably the most famous and the most productive of alkalic gold deposits in North America. The Cripple Creek district is discussed in detail in Chapter Three.

Other North American alkalic igneous rock terrains that have produced gold include the Central Montana Alkalic Province. Gold ore in the Little Rocky Mountains of the Central Montana Alkalic Province is related to the intrusion of early Tertiary, slightly alkalic, felsic porphyries. Free gold and various telluride minerals occur primarily in hydrothermal breccias that have been emplaced along northwest-trending structures. Nineteen gold deposits in the Little Rocky Mountains have produced a total of 1,250,000 ounces of gold from 1884 to 1990 (Russel, 1991).

The Little Belt Mountains of the Central Montana Alkalic Province also contain several gold districts including the Yogo and Running Wolf mining districts. Gold in these districts is related to early Tertiary alkalic syenite porphyries. A small amount of gold was produced (Woodward, 1991).

In the Kendall mining district of the North Moccasin Mountains, Montana, stratabound gold ore in Mississippian carbonate rocks is related to the intrusion of Tertiary syenite porphyries. Gold is extracted chiefly from auriferous pyrite and various telluride minerals. The Kendall district produced 450,000 ounces of gold from 1900 to 1942 (Kurisoo, 1991).

Gold ores at the Golden Sunlight Mine in southwestern Montana occur within a breccia pipe cutting Belt Supergroup sedimentary rocks. At depth the breccia grades into a Late Cretaceous rhyolite porphyry matrix and clasts of Belt Supergroup rocks. The rhyolite porphyry is inferred to grade downward into an alkalic molybdenum porphyry system. Alkalic to subalkalic lamprophyre dikes and sills that locally contain high grade gold ore were emplaced within the rhyolite porphyry along shear zones (DeWitt and others, 1996).

Lamprophyres of near-alkalic to calc-alkalic affinity have a spatial and temporal association with mesothermal gold deposits throughout the world. This association has been noted in the in many of world's great gold camps, such as the Abitibi Greenstone Belt, Canada; Yilgarn Province, Western Australia; the Porgera deposit, Papua New Guinea; Mother Lode in the Sierra Nevada foothills, California; and several other gold camps in Africa, Asia and Australia (Rock and others, 1989). Primary gold contents of all igneous rocks average 0.5 to 2.0 parts per billion. Rock and others (1989, table 2) suggest that lamprophyres from both mineralized and unmineralized regions throughout the world have a median gold content of 5 parts per billion, and that the lamprophyres are probable source rocks of gold. Many issues regarding lamprophyres as a primary gold source remain to be resolved; however, the association is intriguing and may lead to a greater understanding of the role of alkalic intrusive complexes and mesothermal gold mineralization. A contrasting view of the role of alkalic rocks in producing gold mineralization in the Superior Province of Canada is presented by Wyman and Kerrich (1989).

MOLYBDENUM

Most major molybdenum deposits in North America are associated with Tertiary calc-alkalic porphyritic intrusions. There are, however, smaller molybdenum deposits that are associated with alkalic rocks. The Mount Copeland deposit in southeastern British Columbia is composed of a basal unit of nepheline syenite gneiss, an alkalic amphibolite, and an upper calcareous syenite. The upper margin of the syenite contains anomalously large amounts of molybdenum; the highest grade ores are in pods and veins controlled by small structures (Pell, 1996).

The Cave Peak breccia pipe deposits are located in the Tertiary Trans-Pecos alkalic province of west Texas (Barker, 1987). Molybdenum, fluorite, tin, and tungsten are associated with rhyolite and rhyodacite breccia pipes that are the upper zones of a quartz monzonite porphyry (Sharp, 1979). Mercury deposits in this region are associated with quartz syenite and rhyolite intrusions (Yates and Thompson, 1959).

The Three Rivers alkalic stock in Lincoln and Otero counties, New Mexico consists of an early syenite porphyry, a later nordmarkite porphyry intruded along the northeastern boundary of the stock, and a late equigranular quartz syenite. Considerable molybdenum mineralization and hydrothermal alteration occurs along the northeast boundary of the stock and is related to the intrusion of the late quartz syenite (Giles and Thompson, 1972).

IRON

Many economically important iron deposits are associated with alkalic igneous rocks, particularly carbonatites, such as the Palabora deposit in Africa, and the Fen deposit in Norway. The Powderhorn district in Gunnison County, Colorado, which is currently (1997) being investigated for its titanium potential, was first examined for its iron ore potential.

TITANIUM

Most alkalic igneous rocks are enriched in titanium, a common constituent of rock-forming minerals such as garnet, titanite, and clinopyroxene. Titanium is present in ilmenite, magnetite, rutile, anatase, and perosvkite. The Magnet Cove complex, Arkansas, is an alkalic ring complex composed of phonolites and trachytes intruded first by jacupirangites, later by syenites and ijolites, and lastly by quartz and carbonatite veins. Titanium and vanadium resources are located in feldspar-carbonate veins and in the fenitized surrounding sediments ("novaculites") (Pell, 1996).

Perhaps the most abundant titanium resource in the world is located in Powderhorn district, Gunnison County, Colorado. This complex of carbonatites, ultramafic rocks, and syenites contains not only titanium but also REE and iron. The Powderhorn district is discussed in detail in Chapter Seven. Other titanium resource areas outside of North America include the Tapira complex in Brazil and the Afrikanda alkalic complex on the Kola Peninsula, Russia.

URANIUM AND THORIUM

Uranium is found in alkalic igneous rocks principally as disseminated mineralization in intrusive and extrusive rocks, in pegmatites, and in hydrothermal deposits.

Disseminated uranium mineralization in alkali granites, syenites, and trachytes occurs at localities around the world including Bokan Mountain, Alaska; the Front Range, Colorado; and the Ilímaussaq intrusive complex, Greenland. Alkalic pegmatites contain uranium mineralization in the Kola Peninsula and in the Ilímaussaq complex. Other sites include pegmatites in the potassic syenites of the Bear Paw Mountains, Montana. Hydrothermal vein deposits are also widespread and include the Front Range, Colorado; the Powderhorn district, Colorado; Ilímaussaq; and Bokan Mountain, Alaska (Sørenson, 1970).

Uranium is recovered from the Poços de Caldas alkalic carbonatite complex in Brazil. Pitchblende occurs in breccia pipes and other breccia bodies in phonolites of the complex. In the United States thorium-enriched veins in alkalic rocks occur at Lemhi Pass, Montana and Idaho; Hall Mountain, Idaho; the Powderhorn district and the Wet Mountains, Colorado; Capitan Mountains, New Mexico; and Mountain Pass, California (Pell, 1996).

OTHER

Copper, nickel, zirconium, hafnium, fluorspar, phosphates, and nepheline syenite are other elements, minerals, and rocks that are found in economic concentrations in alkalic igneous rocks throughout the world. There are few of these kinds of deposits in Colorado.

REFERENCES

Barker, D.S., 1987, Tertiary alkaline volcanism in Trans-Pecos, Texas, *in* Fitton, J.G., and Upton, B.G.J., eds., Alkaline igneous rocks: Geological Society of London Special Publication No. 30, p. 415–431.

Bergman, S.C., 1987, Lamproites and other potassium-rich igneous rocks: A review of their occurrence, mineralogy, and geochemistry, *in* Fitton, J.G., and Upton, B.G.J., eds., Alkaline igneous rocks: Geological Society of London Special Publication No. 30, p. 103–190.

Best, M.G., 1982, Igneous and metamorphic petrology: San Francisco, W.H. Freeman and Co., 630 p.

Boettcher, A.L., 1967, The Rainy Creek alkaline-ultramafic igneous complex near Libby, Montana, I—Ultramafic rocks and fenite: Journal of Geology, v. 75, p. 526–553.

Deans, T., 1978, Mineral production from carbonatite complexes—A world review, *in* Proceedings of the First International Symposium on Carbonatites, Poços de Caldas, Brazil, June 20–27, 1976, Brasil Ministério das Minas e Energia, Departmento Nacional da Produção Mineral, p. 123–133.

DeWitt, E., Foord, E.E., Zartman, R.E., Pearson, R.C., and Foster, F., 1996, Chronology of Late Cretaceous igneous and hydrothermal events at the Golden Sunlight gold-silver breccia pipe, southwestern Montana: U.S. Geological Survey Bulletin 2155, 48 p.

Fitton, J.G., and Upton, B.G.J., 1987, Introduction, *in* Fitton, J.G., and Upton, B.G.J., eds., Alkaline igneous rocks: Geological Society of London Special Publication No. 30, p. ix–xiv.

Giles, D.L., and Thompson, T.B., 1972, Petrology and mineralization of a molybdenum-bearing alkalic stock, Sierra Blanca, New Mexico: Geological Society of America Bulletin, v. 83, p. 2129–2148.

Heinrich, E.W., 1966, The geology of carbonatites: Chicago, Rand McNally and Company, 555 p.

Kurisoo, Peter, 1991, Gold deposits of the Kendall mining district, Fergus County, Montana, *in* Baker, D.W. and Berg, R.B., eds., Guidebook 1991, Central Montana Alkalic Province: Montana Bureau of Mines and Geology Special Publication 100, p. 39–44.

Le Bas, M.J., 1977, Carbonatite-nephelinite volcanism —An African case history: New York, Wiley Interscience, 347 p.

Le Bas, M.J., LeMaitre, R.W., Streckeisen, A.L., and Zanettin, B., 1986, A chemical classification of volcanic rocks based upon the total alkali-silica diagram: Journal of Petrology, v. 27, p. 747–750.

Le Bas, M.J., and Streckeisen, A.L., 1991, The IUGS systematics of igneous rocks: Journal of the Geological Society of London, v. 148, p. 825–833.

Mitchell, R.H., 1976, Potassium-argon geochronology of the Poohbah Lake alkaline complex, northwest Ontario: Canadian Journal of Earth Science, v. 13, p. 1456–1459.

_____1986, Kimberlites—mineralogy, geochemistry, and petrology: New York, Plenum Press, 422 p.

_____1995, Kimberlites, orangeites, and related rocks: New York, Plenum Press, 410 p.

_____1996, Classification of undersaturated and related alkaline rocks, *in* Mitchell, R.H., ed., Undersaturated alkaline rocks—mineralogy, petrogenesis, and economic potential: Mineralogical Association of Canada Short Course, v. 24, p. 1-22.

Müller, D., and Groves, D.I., 1995, Potassic igneous rocks and associated gold-copper mineralization: Berlin, Springer-Verlag, 210 p.

Mutschler, F.E., Griffin, M.E., Stevens, D.S., and Shannon, S.S., Jr., 1985, Precious metal deposits related to alkaline rocks of the North American Cordillera—An interpretive review: Geological Society of South Africa Transactions, v. 88, p. 355–377.

Olson, J.C., Shawe, D.R., Pray, L.C., and Sharp, W.N., 1954, Rare-earth mineral deposits of the Mountain Pass district, San Bernadino County, California: U.S. Geological Survey Professional Paper 261, 71 p.

Pell, J.A., 1996, Mineral deposits associated with carbonatites and related alkaline igneous rocks, *in* Mitchell, R.H., ed., Undersaturated alkaline rocks—mineralogy, petrogenesis, and economic potential: Mineralogical Association of Canada Short Course, v. 24, p. 271–310.

Rock, N.M.S., Groves, D.I., Perring, C.S., and Golding, S.D., 1989, Gold, lamprophyres, and porphyries—What does their association mean, *in* Keays, R.R., Ramsay, W.R.H., and Groves, D.I., eds., The geology of gold deposits—The perspective in 1988: Economic Geology Monograph 6, p. 609–625.

Rock, N.M.S., 1991, Lamprophyres: New York, Van Nostrand Reinhold, 285 p.

Russel, C.W., 1991, Gold mineralization in the Little Rocky Mountains, Phillips County, Montana, *in* Baker, D.W. and Berg, R.B., eds., Guidebook 1991, Central Montana Alkalic Province: Montana Bureau of Mines and Geology Special Publication 100, p. 1–18.

Scott-Smith, B.H., 1996a, Kimberlites, *in* Mitchell, R.H., ed., Undersaturated alkaline rocks—mineralogy, petrogenesis, and economic potential: Mineralogical Association of Canada Short Course, v. 24, p. 217–243.

_____1996b, Lamproites, *in* Mitchell, R.H., ed., Undersaturated alkaline rocks—mineralogy, petrogenesis, and economic potential: Mineralogical Association of Canada Short Course, v. 24, p. 259–270.

Sharp, J.E., 1979, Cave Peak, a molybdenum-mineralized breccia pipe complex in Culbertson County, Texas: Economic Geology, v. 74, p. 517–534.

Sørenson, H., 1970, Occurrence of uranium in alkaline igneous rocks—Uranium exploration geology: Vienna, International Atomic Energy Agency, p. 161–168.

_____(ed.), 1974, The alkaline rocks: New York, John Wiley and Sons, 622 p.

Steenfelt, A., 1991, High-technology metals in alkaline and carbonatitic rocks in Greenland: Journal of Geochemical Exploration, v. 40, p. 263–279.

Tuttle, O.F., and Gittens, J., 1966, Carbonatites: New York, John Wiley and Sons, 622 p.

Woodward, L.A., 1991, Metallic mineralization in the Yogo and Running Wolf mining districts, Little Belt Mountains, Montana, *in* Baker, D.W. and Berg, R.B., eds., Guidebook 1991, Central Montana Alkalic Province: Montana Bureau of Mines and Geology Special Publication 100, p. 19–27.

Wyman, D., and Kerrich, R., 1989, Archean shoshinitic lamprophyres associated with Superior Province gold deposits—Distribution, tectonic setting, noble metal abundances, and significance for gold mineralization, *in* Keays, R.R., Ramsay, W.R.H., and Groves, D.I., eds., The geology of gold deposits—The perspective in 1988: Economic Geology Monograph 6, p. 651–667.

Yates, R.G., and Thompson, G.A., 1959, Geology and quicksilver deposits of the Terlingua district, Texas: U.S. Geological Survey Professional Paper 312, 114 p.

Chapter 2

Central Front Range Mineral Belt

INTRODUCTION

The Central Front Range mineral belt consists of several mining districts—Central City, Idaho Springs, Empire, Freeland-Lamartine, Chicago Creek, Lawson-Dumont, Georgetown, Ward, Gold Hill, Apex, Jamestown, Argentine, and the Boulder County tungsten district (Fig. 2). The U.S. Geological Survey investigated most of the mining districts of the region beginning with the Georgetown quadrangle by Spurr and Garrey (1908) and the Central City district by Bastin and Hill (1917). Because of its economically important occurrences of uranium and precious metals, the Central City district was studied intensely by the U.S. Geological Survey in the 1960s (Sims, 1963, 1964; Sims and others, 1963, Sims and Sheridan, 1964, Sheridan and others, 1967). The Central City district was the most prolific producer of gold and silver in the Central Front Range mineral belt and will serve as the model for most of the deposits in the belt.

GEOLOGICAL SETTING

The Central City district and the Central Front Range mineral belt lie within a broad domal complex of Proterozoic metamorphic and igneous rocks that make up the Front Range of Colorado. Cretaceous and Tertiary alkalic and calc-alkalic porphyries intruded Proterozoic rocks during the Laramide Orogeny. Numerous vertical and near-vertical faults, many of them mineralized, cut the area. Precious- and base-metal mineralization in the Front Range mineral belt are directly related to the Laramide magmatic event (Fig. 3).

The Central Front Range mineral belt is the northeastern terminus of the Colorado mineral belt, a narrow northeast-trending zone of Laramide

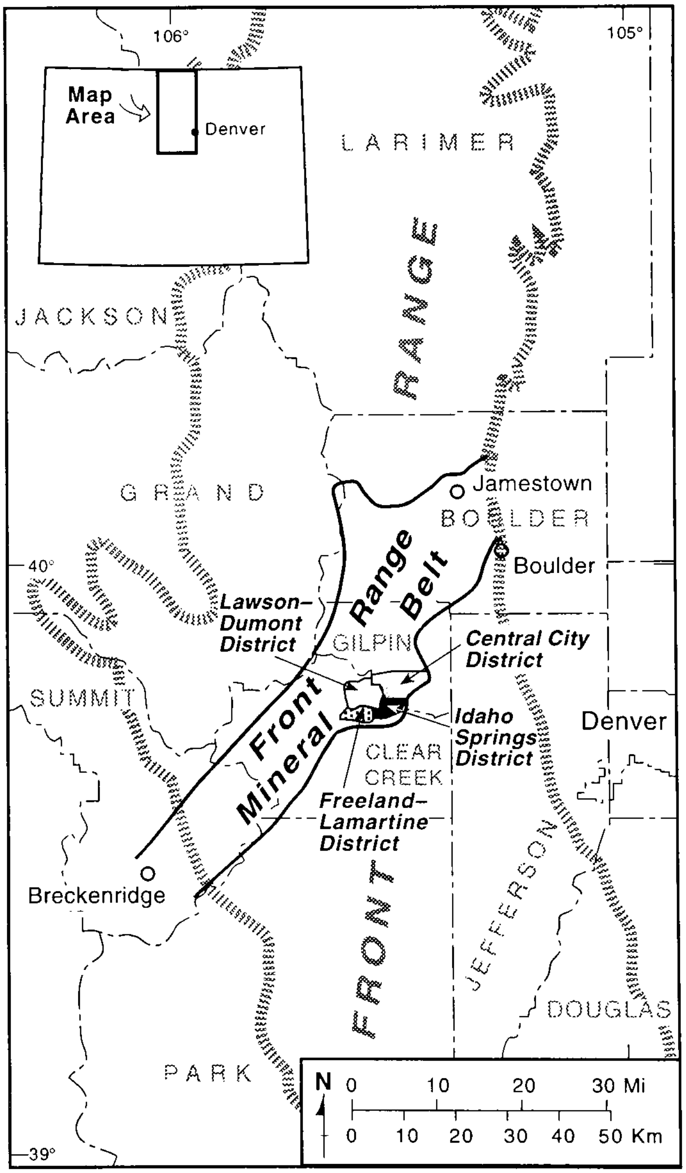

Figure 2. Index map showing the location of the Front Range mineral belt and included mining districts, Colorado. (Modified from Tweto and Sims, 1963)

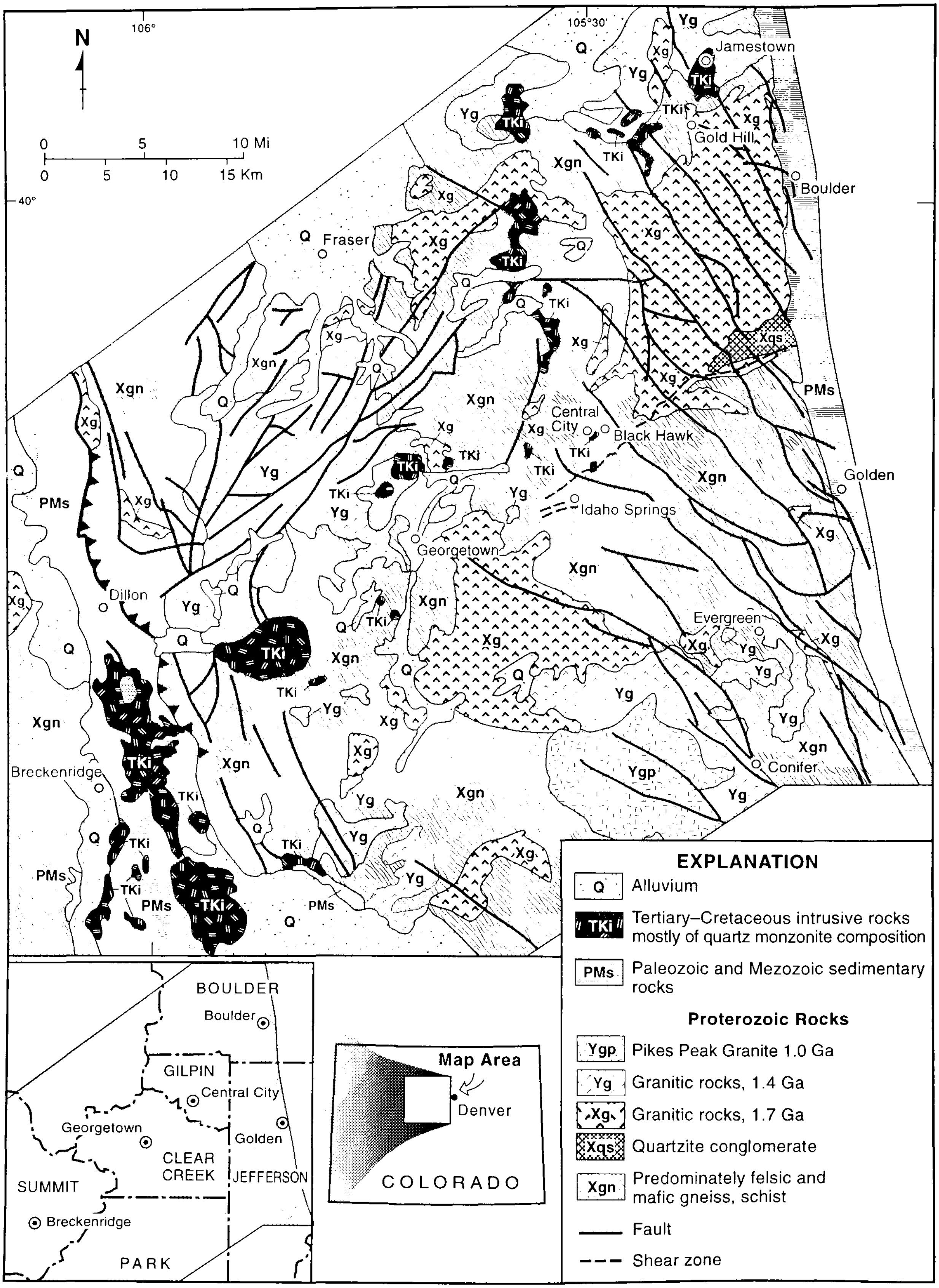

Figure 3. Geologic map of the central Front Range mineral belt, Colorado. (Modified from Lovering and Goddard, 1953)

intrusive rocks that host most of Colorado's important mining districts (Fig. 2). The Colorado mineral belt is located along a zone of weakness defined by northeast-trending shear zones within Proterozoic rocks (Tweto and Sims, 1963).

PROTEROZOIC METAMORPHIC ROCKS (Xgn)

The Proterozoic metamorphic rocks consist primarily of well foliated, gray, medium- to fine-grained, biotite-quartz-plagioclase gneiss which locally contains sillimanite, microcline gneiss, and lesser amounts of amphibolite. Rare cordierite-amphibole gneiss and lime-silicate gneiss contain variable amounts of garnet, quartz, pyroxene, hornblende, plagioclase, and epidote (Fig. 3).

Dark gray to black amphibolite occurs in equigranular, massive, or foliated masses that contain approximately equal amounts of hornblende and plagioclase. Amphibolite forms large discreet layers in the gneissic rocks.

The chemical and mineralogical compositions of the gneissic rocks suggest that these rocks derived from the metamorphism of interbedded graywacke, shale, feldspathic sandstone, and minor carbonate rock. The amphibolite masses probably derived from the metamorphism of local mafic volcanic rocks (Sims and Gable, 1967). Rubidium-strontium dating of whole rock and feldspar samples indicate that the regional metamorphism of the Central Front Range occurred about 1,750 Ma (Hedge and others, 1967).

PROTEROZOIC QUARTZITE (Xqs)

A small local area in Coal Creek Canyon north of Golden along the eastern border of the Central Front Range (Fig. 3) contains a thick section of Proterozoic quartzite, mica schist, and conglomerate. The quartzite unit contains interlayered, micaceous, well foliated, fine- to coarse-grained quartzite and conglomeratic quartzite. The conglomeratic quartzite consists of rounded quartzite pebbles. The conglomerate and quartzite are generally even-bedded although locally cross-bedding does occur.

Three major mica schist units are interlayered within the quartzite unit. The schist is well foliated, and most of it shows a conspicuous mineral lineation. The main minerals are muscovite, biotite, and quartz; locally andalusite, cordierite, garnet, plagioclase, and staurolite are prominent (Wells, 1967; Wells and others, 1964).

PROTEROZOIC GRANODIORITE (Xg)

The composition of the rocks labeled granodiorite is variable; however, they generally resemble a granodiorite. The rocks are gray to mottled black and white, medium-grained, and equigranular. They have a gneissic texture, and contain plagioclase, microcline, quartz, and variable amounts of biotite and hornblende. Small bodies of the granodiorite have a wholly gneissic structure; the larger bodies tend to have weakly foliated interiors and strongly foliated borders. The foliation is generally parallel to that in the surrounding metamorphic gneisses and is interpreted to have resulted from syntectonic emplacement (Sims and Gable, 1967).

In the central Front Range this syntectonic granodiorite is known locally as the Boulder Creek Granite (Fig. 3). Peterman and others (1968) reported a whole rock rubidium-strontium age date of 1,700 ± 40 Ma for the Boulder Creek Granite. Stern and others (1971) using a uranium-lead discordia method on zircons from the Boulder Creek Granite determined a date of 1,714 ± 22 Ma.

PROTEROZOIC GRANITES — YOUNGER (Xg AND Yg)

Within the central Front Range two younger Proterozoic granitic bodies, the Silver Plume Granite and the Pikes Peak Granite, intrude both the older metamorphic gneisses and the Boulder Creek granites (Fig 3.). The Silver Plume Granite (Xg) is well exposed in the Georgetown and Empire districts. It also occurs less extensively in the Freeland-Lamartine, Lawson-Dumont, and Idaho Springs districts (Harrison and Wells, 1959; Hawley and Moore, 1967; Moench and Drake, 1966). It is a gray to buff, fine- to medium-grained granitic rock composed of quartz, microcline, and plagioclase; biotite and muscovite are minor constituents. Most of the granitic bodies are massive; locally, however, a foliation reflects parallel alignment of microcline crystals. This foliation is interpreted as a primary flow layering (Braddock, 1969; Spurr and Garrey, 1908). The Silver Plume Granite has been dated by rubidium-strontium methods in the northern Front Range at 1,420 ± 30 Ma (Peterman and others, 1968).

The Pikes Peak Granite (Yg), which forms the largest batholith in Colorado, is exposed only in the southern part of the Front Range. It is a coarse-grained, granular to porphyritic, pink granite (Lovering and Goddard, 1950). It has been dated by potassium-argon and rubidium-strontium methods at 1,020 Ma (Peterman and Hedge, 1968).

CRETACEOUS-TERTIARY INTRUSIVE ROCKS (TKi)

Cretaceous-Tertiary intrusive rocks, which are generally porphyritic, can be divided into the seven main types listed below from oldest to youngest. Descriptions of the intrusives are based upon Sims and others (1963) and Wells (1960). The age of intrusive events in the Central City district ranges from 63 to 59 Ma; the mineralization event was determined as 59.1 ± 1 Ma (Rice and others, 1982). Cunningham and others (1994) reviewed older published age dates and presented new data on the age of the intrusive, alteration, and mineralization events in parts of the Central Front Range mineral belt.

Leucocratic Granodiorite Porphyry

Leucocratic granodiorite porphyry occurs as irregular plutons up to 3,000 feet across and, less commonly, as associated dikes. The rock has a light gray, fine-grained groundmass consisting of plagioclase, microcline, and quartz. The phenocrysts are mostly light gray oligoclase, although all types of feldspars occur as phenocrysts.

Alkalic Syenite Porphyry

Alkalic syenite porphyry occurs as a small pluton and associated dike swarm near Banta Hill in the Central City district. The rock is a light brownish gray with conspicuous dark gray, diamond-shaped, plagioclase feldspar phenocrysts that compose 25 to 50 percent of the rock. The groundmass of the porphyry is mostly small laths of plagioclase with antiperthite intergrowths of potassic feldspar, sparse quartz, and ferromagnesian minerals.

Quartz Monzonite Porphyry

Quartz monzonite porphyry is the most abundant and variable Tertiary intrusive rock in the Central Front Range mineral belt. The porphyry is light to medium gray and contains subangular feldspar phenocrysts. Two phases dominate: one has small phenocrysts and sparse ferromagnesian minerals; the other has relatively large phenocrysts and several percent of ferromagnesian minerals. Phenocrysts in the phase dominated by small crystals consist of oligoclase, orthoclase, albite, and sanidine. Phenocrysts in the phase characterized by coarse crystals are mostly oligoclase. Much of the groundmass and ferromagnesian minerals have been altered to epidote, chlorite, clay, and carbonate.

Bostonite Porphyry

Bostonite porphyry occurs throughout the Central Front Range mineral belt. In the Central City district the porphyry is found in two dike systems that form one or both walls of economically important vein systems. In the Empire district the bostonite porphyry occurs as a small plug and several dike complexes.

The bostonite porphyry has a seriate porphyritic texture; 15 to 30 percent of the phenocrysts are white plagioclase, orthoclase feldspar, and a dark-colored, altered ferromagnesian mineral, probably aegerine-augite. Andradite garnet locally makes up about 5 percent of the phenocrysts of the porphyry. A lilac-colored groundmass consists of albite, potassium feldspar, and minor quartz.

Trachytic Granite Porphyry

A small dike of trachytic granite porphyry is exposed near Russell Gulch in the Central City district, near the town of Lawson, and along Chicago Creek. The porphyry has a seriate porphyritic texture and an aphanatic, pale red groundmass. Unlike bostonite porphyry, it contains large, almond-shaped, white to pink feldspar phenocrysts. The groundmass mineralogy is similar to that of bostonite porphyry.

Quartz Bostonite Porphyry

Quartz bostonite porphyry forms thin, steeply dipping anastomosing dikes throughout the Central Front Range mineral belt. The porphyry contains as much as 25 percent phenocrysts of anorthoclase which commonly possess argillic alteration. The aphanatic, lilac-colored groundmass contains quartz and feldspar.

Limburgite Porphyry

Limburgite porphyry occurs as northeast-trending dikes only within the Boulder County tungsten district. These dikes are contemporaneous with the early stages of vein formation. Phenocrysts of coarse-grained, altered olivine crystals and medium-grained augite crystals lie in a groundmass of very fine grained augite with a trachytic texture, analcite, and isotropic minerals (Lovering and Tweto, 1953).

Biotite Latite Porphyry

Dikes of biotite latite porphyry are found in the Boulder County tungsten district (Lovering and Tweto, 1953), the Lawson-Dumont district (Hawley and Moore, 1967), the Chicago Creek area (Harrison and Wells, 1959), and the Idaho Springs district (Moench and Drake, 1966). Phenocrysts of plagioclase, biotite, hornblende, and minor apatite comprise about two-thirds of the latite. The hornblende crystals are usually strongly altered; in contrast, the plagioclase and the biotite look fresh. The groundmass is made up of very fine grained feldspar laths (Lovering and Tweto, 1953).

Hornblende Granodiorite Porphyry

Hornblende granodiorite porphyries differ from the leucocratic granodiorites in their greater content of hornblende, biotite, and calcic plagioclase. Exposures of this rock type are common in the Idaho Springs district along Fall River. Phenocrysts are usually plagioclase, but in some varieties quartz and biotite are common. The groundmass contains variable amounts of feldspar, quartz, hornblende, biotite, and pyroxene. Two samples of zircon from the hornblende granodiorite porphyry from the Apex stock were dated by the fission track method at 61.7 ± 6.3 and 58.5 ± 5.2 Ma (Cunningham and others, 1994).

STRUCTURE

The Proterozoic gneisses and some of the Proterozoic granitic intrusive rocks have a well-defined foliation and lineation. The foliation in the gneisses, especially those of meta-sedimentary origin, thought to be parallel to original bedding (Sims and Gable, 1967).

Numerous folds in the Proterozoic rocks are mostly open with steeply dipping axial planes; however, local zones contain tight isoclinal folds. The Central City anticline is a broad, northeast-trending, open fold that exposes microcline gneiss in its core and biotite gneiss on its limbs. It is at least 10 miles long and cuts across the entire Central City district. The axes of numerous minor folds parallel the Central City anticline, but small folds whose axes bear normal to the dominant northeast direction also occur throughout the district (Sims, 1964; Sims and others, 1963; Taylor, 1976).

There are two main groups of faults in the Central City district: an older set of Proterozoic(?) faults that strike northwest or north-northeast, and Laramide faults that strike east, east-northeast, or northeast. Most of the faults have steep dips and a dominant horizontal relative displacement of only a few feet. Older faults are usually long, continuous fractures or fracture zones that commonly are intruded by Laramide dikes and associated vein deposits. Tweto and Sims (1963, p. 1001) list convincing evidence for the Precambrian origin of these sets of faults. The younger set of faults cuts both the older faults and the Laramide intrusive rocks and forms a mesh pattern. Displacements are usually less than 20 feet. Some of the most valuable mineral deposits in the Central City district occur in the eastward-trending faults (Sims and others, 1963).

The structural setting of the Lawson-Dumont district, Chicago Creek area, Freeland-Lamartine district, the Idaho Springs district, the Empire district, the Wood and East Calhoun mines, the Ward district, and the Georgetown district is broadly similar to that found in the Central City district (Hawley and Moore, 1967; Harrison and Wells, 1959; Harrison and Wells, 1956; Moench and Drake, 1966; Braddock, 1969; Drake, 1957; Worcester, 1920; Spurr and Garrey, 1908).

The older Laramide intrusive rocks generally form as steep-sided plutons with radiating dike swarms. The younger intrusives form dikes almost exclusively. Tweto and Sims (1963) proposed that the Laramide intrusive rocks of the Central Front Range mineral belt were emplaced along a northeast-trending Precambrian shear zone named the Idaho Springs-Ralston shear zone.

GEOCHEMISTRY

The total alkalies versus silica plot shows the strongly alkalic nature of the Tertiary monzonite, syenite, sanidinite, gabbro, and bostonites (Fig. 4). Granodiorites, diorites, granites, and the metamorphic rocks are subalkalic in chemistry. Alkalic and subalkalic rocks are about evenly distributed in the Front Range mineral belt. The Harker variation diagrams (Fig. 5) also demonstrate the enrichment of Na_2O and K_2O in these rocks. Table 1 in the appendix lists the geochemical analyses and CIPW norms used in the diagrams.

ECONOMIC GEOLOGY

The principal ore deposits of the Central Front Range mineral belt are veins that formed as fracture and fissure fillings. Stockwork systems and

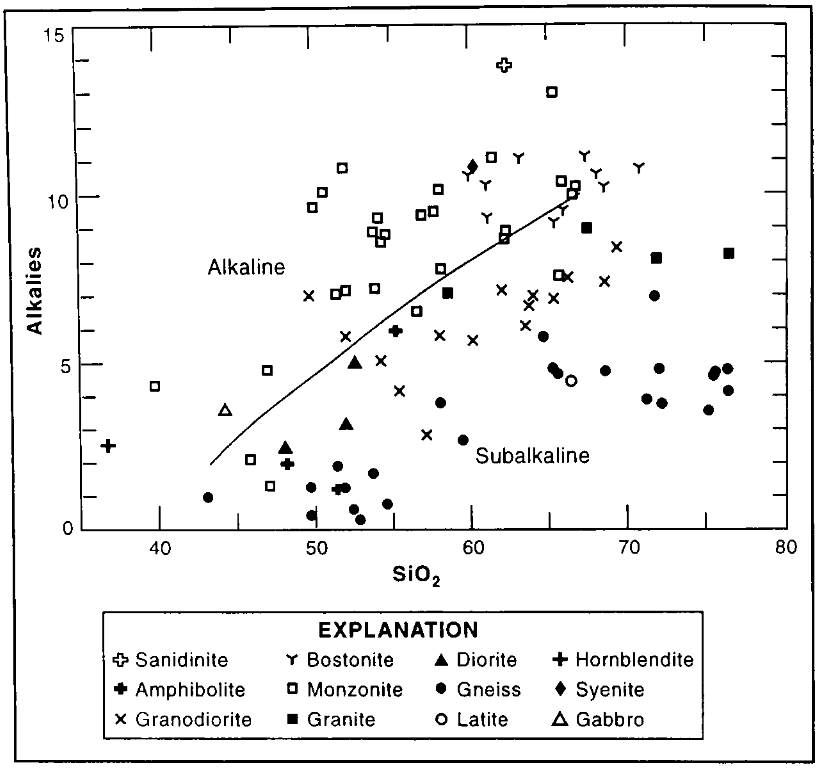

Figure 4. Plot of alkalies versus silica of representative rock samples from the Front Range mineral belt. (Plot design after Irvine and Baragar, 1971)

magmatic segregation ore deposits also occur in the belt; however, they are not as economically valuable as the vein deposits.

VEINS AND FRACTURE FILLINGS

Veins in the Central City district range from a few hundred to a few thousand feet in length and have depths approximately comparable to their length. The veins almost always have a steep dip, greater than 60 degrees. A prominent vein system, the Gardner-California-Mammoth lode, was mined locally for a distance of more than 12,000 feet and persisted to a depth of 2,200 feet, the deepest in the district. Veins are generally 1 to 3 feet wide, but locally they are up to 30 feet wide.

The veins fill the faults and fractures and often show evidence of repeated movement. They may form simple, well-defined, fissure fillings or complex, anastomosing vein systems. The simple veins have smooth sharp walls bounded by a narrow zone of altered wallrock. The complex veins comprise several subparallel veins and zones of altered wallrock with many small veinlets of quartz and sulfide minerals.

The veins within the Central City district are not uniformly mineralized and economic deposits form distinct ore "shoots". Their size ranges from pods and lenses containing only a few tons to shoots containing several thousand tons. The largest ore shoot is in the California Mine; it has a plunge length greater than 2,100 feet, a breadth of 800 feet, and a stope length of about 1,000 feet. Ore shoots have a consistent direction of plunge that can be related to dips of the Central City anticline. The ore shoots on the northwest side of the anticline plunge westward, whereas those on the southeast side plunge generally to the east.

Vein Mineralogy

The veins of the Central City district are divided in two distinct but gradational mineralogical types: pyrite veins and galena-sphalerite veins. Pyrite and quartz dominate the pyrite veins; lesser amounts of chalcopyrite, tennantite, sphalerite, galena, and enargite are also present. Gold that occurs in both vein types is almost always very fine grained and not visible to the naked eye. The average grade of direct shipping ore from pyrite veins in several Central City mines ranged from 1 to 5 ounces of gold per ton, 2 to 12 ounces of silver per ton, and copper contents of greater than 1.5 percent.

Sims and others (1963) subdivided the pyrite veins on the basis of the quantity and proportion of the contained metallic minerals into those pyrite veins nearly devoid of base-metal sulfides and sulfosalts (type A), those that contain abundant copper minerals (type B), and those that contain sphalerite, galena, and copper minerals (type C).

The galena-sphalerite veins contain sparse pyrite, chalcopyrite, and tennantite. Quartz, carbonate minerals, and fluorite are common gangue minerals. The veins contain zones of breccia, variable amounts of gangue, and local stringers and pods of base-metal sulfides. Interlacing veinlets of sulfide minerals may form a crudely layered ore. The galena-sphalerite veins generally contain lesser amounts of gold and copper and more silver and lead than

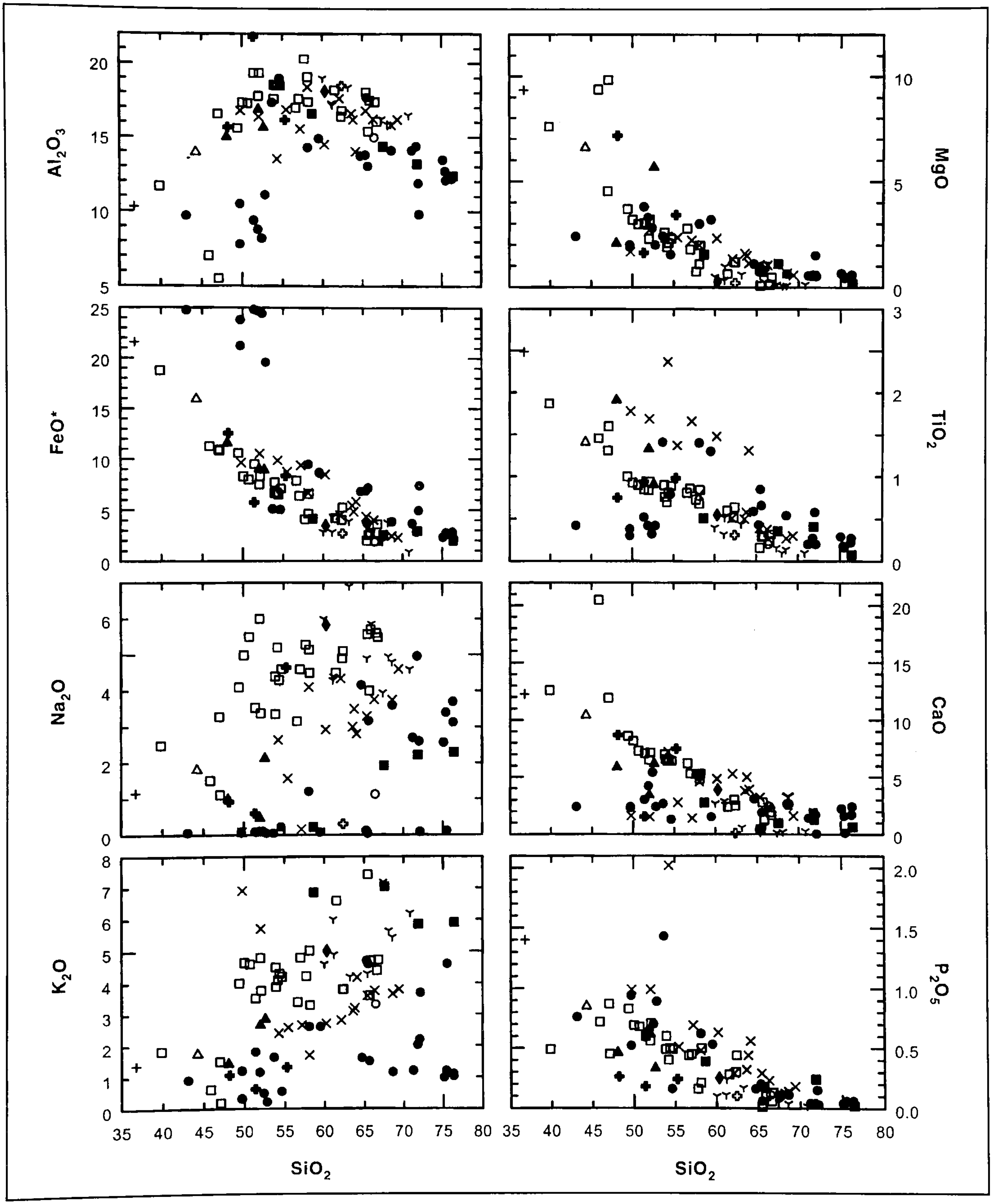

*Figure 5. Harker variation diagram of representative rock samples from the Front Range mineral belt. Refer to the explanation on Fig. 4. (*includes Fe_2O_3)*

the ore of the pyrite veins. Other minerals of economic importance that occur in the veins of the Central Front Range mineral belt include molybdenite, chalcocite, silver, bismuth, uraninite (pitchblende), ferberite, wolframite, and sylvanite (Sims and others, 1963; Bastin and Hill, 1917).

Other less common types of vein deposits occur throughout the Central City district. Gold and silver tellurides occur in thin, 1 to 3 inch thick, veins with dark gray quartz (the dark gray color may be due to minute inclusions of molybdenite), pyrite, purple fluorite, and tennantite. Uraninite and secondary uranium minerals occur sporadically along pyrite and galena- sphalerite veins.

Quartz-ferberite (iron tungstate) veins of ore grade occur in the Boulder County tungsten district. Locally, pyrite and marcasite are found in the quartz-ferberite veins. Veins have an average width of less than a foot; however, in sheeted zones (a localized area of several closely-spaced subparallel veins) the width of mineralized rock can be up to 20 feet (Lovering and Tweto, 1953; George, 1909).

Zoning

A concentric zoning of ores is shown by the distribution of the pyrite and galena-sphalerite veins (Fig. 6a, 6b) (Sims and others, 1963). The central zone contains mostly pyrite veins of type B and is characterized by a low silver-gold ratio. The intermediate zone contains pyrite veins of type C. Gold is an important constituent of these ores and the silver:gold ratio is slightly greater than in the central zone. The peripheral zone is characterized by galena-sphalerite veins. The internal distribution of base- and precious-metal content in this zone is variable, but gold in this zone was rarely of ore grade. The barren zone contains low grade veins that were rarely economic to mine.

Alteration

The wall rocks of the Central Front Range mineral belt have been hydrothermally altered to varying degrees. The width of the altered zones ranges from a few inches up to tens of feet. E.W. Tooker (1963) divided the wallrock alteration into four main zones: 1) fresh rock, 2) weak argillic alteration, 3) strong argillic alteration, and 4) sericite-quartz-pyrite. Fresh rock of zone 1 grades into the weak argillic alteration of zone 2 by the partial alteration of plagioclase and hornblende into clay minerals. The transition from zone 2 to the strong argillic alteration of zone 3 is marked by the almost total alteration of plagioclase and hornblende and the partial alteration of biotite to clay minerals. The final stage of alteration, zone 4, is characterized by the almost complete sericitization of most of the remaining rock-forming minerals and clay minerals of the zones 2 and 3, and the recrystallization of quartz into aggregates of small strain-free crystals. Potassium feldspar is not visibly altered in zone 4. In some locations, alteration zones overlap and others are missing. The argillic alteration zones comprises mixed clay assemblages of montmorillonite, illite, mixed layer montmorillonite-illite, chlorite, kaolinite, and halloysite (Tooker, 1963).

Supergene alteration occurred in the upper part of the vein systems above the water table and resulted in a locally significant enrichment of gold. There is also a zone of secondary sulfide enrichment that lies below the water table.

Paragenesis

Alteration of the wallrock preceded the deposition of the ore minerals in the veins of the Central Front Range mineral belt. The earliest stage of mineralization (Fig. 7), the uranium stage is characterized by quartz, uraninite, and minor pyrite. The pyrite stage came after a period of fracturing and brecciation and consisted primarily of quartz and pyrite. The final stage, the base metals stage, followed a second period of fracturing and brecciation and consisted of minor quartz and carbonate minerals and most of the base metal sulfides. Gold and silver were deposited in all three stages; however, the majority of the precious metals was deposited in the base-metals stage. Telluride veins are associated with the quartz bostonite dikes and possibly represent the last phase of hydrothermal mineralization in the mineral belt (Rice and others, 1985).

Vein Control

Two main types of structural control influenced the grade and tonnage of the ore shoots: physical character and structure of the wallrock, and vein intersections and junctions. The gneiss, especially the microcline gneiss, is relatively competent and usually deforms in a brittle fashion making it most likely to host vein deposits. Veins that are nearly normal to foliation of the surrounding gneiss wallrock tend to be wide, persistent, and strongly mineralized, whereas those nearly parallel to foliation tend to be thin and barren. Irregularities along faults such as a change in dip or strike and splits, branches, and other subsidiary fractures also are

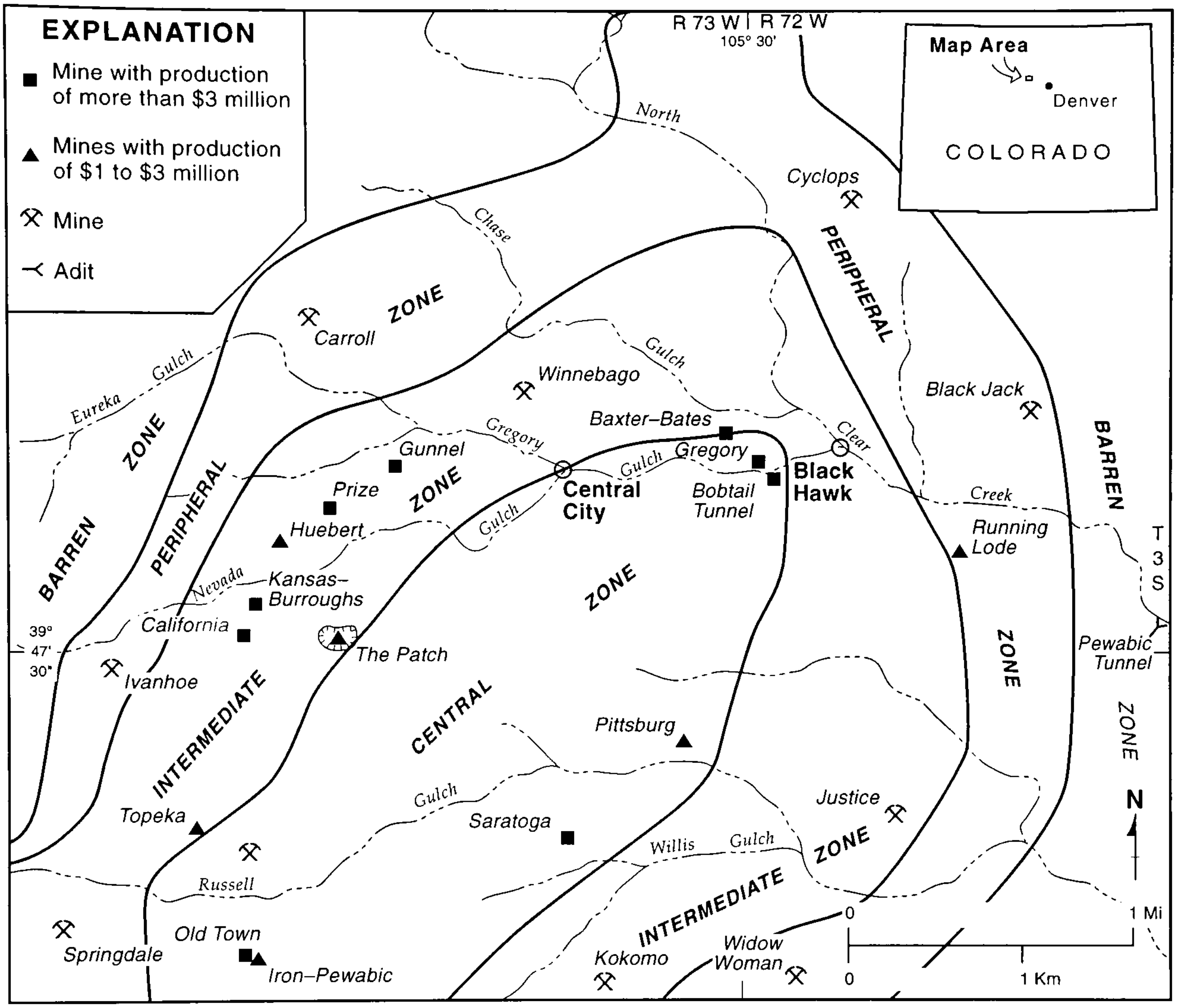

Figure 6a. Map of Central City district showing zoning of mineral deposits. (From Sims and others, 1963)

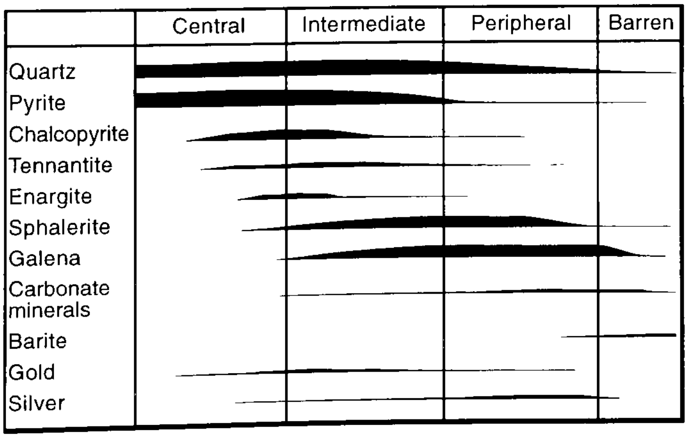

Figure 6b. Zonal distribution of vein-forming minerals. (From Sims and others, 1963)

important loci of ore deposition. Many high grade ore shoots occur at the intersection of two or more veins. Generally ore shoots occur where veins intersect at an acute angle.

STOCKWORKS

The Patch in the Central City district is the most significant of the few stockwork deposits in the Central Front Range mineral belt. The Patch is oval in plan view; its east-west axis is 750 feet long and its north-south axis is 450 feet long, and it extends at least 1,600 feet deep. The deposit consists of fractured and brecciated rock, principally microcline gneiss. A bostonite porphyry dike cuts the stock-

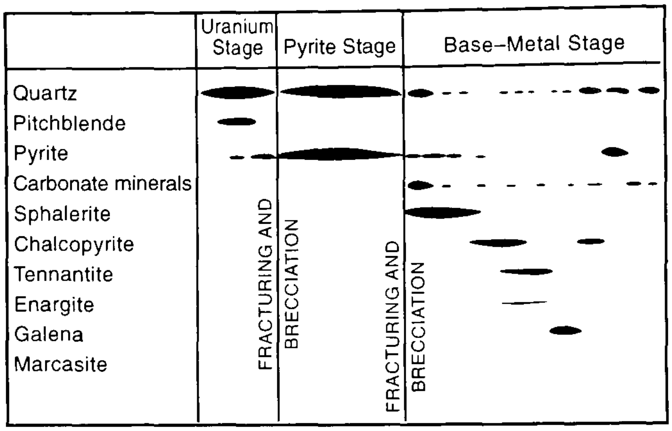

Figure 7. Generalized sequence of deposition of principal vein-forming minerals, Central City district. (From Sims and others, 1963)

work breccia. The entire stockwork is altered without regard to intensity of brecciation. Economic mineralization contains sulfide minerals and precious metals—mainly pyrite, chalcopyrite, tennantite, and sphalerite, gold, and silver; and gangue minerals—mostly quartz with lesser amounts of ankerite(?), formed in the matrix of the breccia fragments.

The average grade of ore taken from the San Juan Mine in the Patch from 1888 to 1909 was 2.09 ounces of gold per ton, 6.81 ounces of silver per ton silver, and 1.5 to 9 percent copper. The lower part of the Patch stockwork was intersected at a depth of 1,600 feet by the Argo Tunnel. The weighted average grade of the Patch in the Argo Tunnel is 0.071 ounce of gold per ton and 0.489 ounce of silver per ton (Sims and others, 1963, p. 95).

MAGMATIC SEGREGATIONS

There are two small, economically insignificant ore deposits in the Central Front Range mineral belt that do not fall into the vein and stockwork categories. The Evergreen Mine in the Apex district of Gilpin County is located at the contact of the Proterozoic gneiss and several small dikes of quartz monzonite porphyry, probable offshoots from a nearby quartz monzonite stock (Lovering and Goddard, 1950). The dikes are generally similar to the quartz monzonite but differ in their greater amounts of quartz, wollastonite, and garnet. Disseminated chalcopyrite and bornite occur within the dikes and along micro-veinlets and fractures. Mineralization also occurred within the igneous matrix of a contact breccia composed of gneiss and schist clasts. Bastin and Hill (1917) hypothesized that the ore minerals and elements necessary to form wollastonite, garnet, and the copper sulfides were assimilated by deep portions of the quartz monzonite magma and moved into fissures along the contact zone.

The Caribou-Grand Island district is located in the west-central part of Boulder County and is noted primarily for its rich silver vein deposits in a Laramide monzonite porphyry (Lovering and Goddard, 1950; Smith, 1938). Within the porphyry there is a small percentage of gabbro, pyroxenite, hornblendite, peridotite, and titaniferous magnetite. A significant deposit of titaniferous iron ore occurs in a magnetite pyroxenite. Bastin and Hill (1917) reported that the ore contained 23.9 to 64.7 percent Fe_3O_4 and 2.5 to 4.5 percent TiO_2.

ORIGIN AND MODEL OF ORE DEPOSITS

Geological relations and the close association between the ages of the hornblende granodiorite, the bostonite, the quartz bostonite, and the main sulfide ores support the strong connection between the Laramide alkalic and calc-alkalic intrusions and precious and base metal mineralization in the Central Colorado mineral belt. Sims and others (1963) and most previous investigators interpret the ores of the Central City district to have been deposited from hydrothermal fluids related to the Laramide magmatic event.

Following the development of the district fracture pattern, hydrothermal solutions rose along the fractures, mixed with meteoric waters, and deposited the early alteration minerals, sericite and potassium feldspar. Changes in the chemistry of the hydrothermal fluids led to the deposition of pyrite and uranium minerals. Later movements opened spaces along the fracture systems, and the base- and precious-metals were deposited in the fractures. Analysis of sphalerite indicates that temperature of formation varied between 620° to 150° C. A gross regularity in the temperature is indicated by the sphalerite; however, several anomalous patterns occur throughout the district (Sims and others, 1963; Sims and Barton, 1961, 1962).

A close geographical relationship and similar minor element content suggest that the uranium minerals were derived directly from the late alkalic magmas (Sims, 1963). Significant uranium mineralization did not correspond to the pattern of the base- and precious-metal mineralization. Studies by Phair (1952) and Wells (1960) indicated that the younger Laramide intrusions were progressively enriched in uranium minerals culminating with the alkalic magmas of the quartz bostonite porphyry.

The telluride ores are nearly always found in different veins and fractures than the dominant base- and precious-metal sulfide mineralization. Paragenesis of the tellurides indicates that they were deposited late in mineralization events. Sims and others (1963) suggest that the telluride minerals are related to the late biotite-quartz latite porphyry.

There is no strong evidence that can correlate the dominant base- and precious-metal ores to any particular intrusive body. Rice and others (1982) suggested that a deep-seated source magma of mixed composition supplied the hydrothermal fluids that travelled along fractures to produce the zoning pattern of the district, and that mineralization occurred during a relatively short period of 1 My at 59 ± 1 Ma. They further suggest that only the uranium mineralization is correlated with a particular intrusive, the quartz bostonite porphyry.

EXPLORATION AND PRODUCTION HISTORY

The Central City district and its discovery are an important part of Colorado's history as it marks the beginning of the development of Colorado's mineral resources and the modern settlement of Colorado. Vague and poorly documented reports of gold in Colorado date back to 1758; however, none of these attracted much attention. In 1849 a party of prospectors from Georgia on their way to gold fields of California camped near the present site of Denver. They found small amounts of placer gold in Cherry Creek and in a branch of Clear Creek but not enough to stay them from their original destination. In the spring of 1858 the same prospectors returned; they traversed from the Cherry Creek and Clear Creek sites into the area of the Central City district and found rich gold placers in Russell Gulch. In January 1859 they discovered another placer gold deposit near the mouth of Chicago Creek close to the present site of Idaho Springs.

By the fall of 1858 rumors flew throughout the country about the new gold discovery in the Rocky Mountains.Beginning in the spring of 1859 hundreds of gold-seekers arrived every week in the new town at the confluence of Cherry Creek and the Platte River that would eventually become Denver. In May 1859 John Gregory, another prospector from Georgia, discovered the first lode gold deposit in the Rocky Mountains between the present cities of Central City and Blackhawk at a site that now bears his name, Gregory Gulch. During 1859 and 1860 several more placer and lode deposits were discovered in the district and in the Central Front Range mineral belt.

During the early days of the district most of the ore was produced from placer deposits and oxidized surface gossans, which could be processed easily and cheaply. Primary sulfide ores were found at depths of less than 100 feet and so began an early period of processing experimentation that led to the construction several stamp mills using the amalgamation process. In 1866 Nathaniel Hill established the first smelter in the district at Blackhawk. Other smelters soon followed in Empire and Idaho Springs and later in Golden and Denver. Since the 1930s, most of the amalgamation plants have been replaced by flotation plants and mills (Bastin and Hill, 1917; Sims and others, 1963).

Gilpin County contains approximately 95 percent of the Central City district, and from 1859 to 1990 it produced more than 4.25 million ounces of gold, 11.3 million ounces of silver, 26.2 million pounds of copper, and 38.1 million pounds of lead along with zinc and some minor uranium. Clear Creek County contains a small portion of the Central City district as well as the Idaho Springs, Empire, Freeland-Lamartine, Lawson-Dumont, Georgetown, and Argentine mining districts. Production from Clear Creek County from 1859 to 1990 was 1.4 million ounces of gold, 62.0 million ounces of silver, 15.0 million pounds of copper, and 205.0 million pounds of lead as well as zinc and minor amounts of uranium. (Sims and others, 1963; U.S. Bureau of Mines Yearbooks, 1954–1990)

The Central City district reached its zenith in 1871 when $3,359,240 worth of ore was produced. Production from the district declined rapidly between 1914 and 1920; approximate annual production during the 1920s was only $100,000. During the Depression exploration and production in the Central City district increased; however, the beginning of World War II and the cessation of gold mining in the United States when the War Production

Board issued limitation order L-208 signaled the end of the Central City district as a significant producer of metals in Colorado (Sims and others, 1963; U.S. Bureau of Mines Yearbooks, 1954–1990).

The black "barren" mineral found in the Nederland and Ward areas of Boulder County was recognized as wolframite by John Knight in 1899. One year later, W. H. Wannamaker discovered ferberite float in the main part of the Boulder County tungsten district. Wannamaker and his partner, S. T. Conger, mined 40 tons of high grade ore from the surface on the Sherril prospect. They quickly discovered and developed the Conger, Oregon, Denver, Illinois, Charley, and other tungsten-bearing veins. A tungsten rush ensued and several new tungsten prospects were discovered and developed into producing mines.

The zenith of the Boulder County tungsten district came in the years around World War I, 1915–1918, when tungsten was in very high demand to harden steel. The peak year of production was 1917 when 2,707 tons of concentrate (60 percent WO_3) was produced. Production and prices declined in the period between the wars. World War II briefly increased prices and production; however, in the years after 1945 the district declined rapidly (Lovering and Tweto, 1950).

REFERENCES

Bastin, E.S., and Hill, J.M., 1917, Economic geology of Gilpin County and adjacent parts of Clear Creek and Boulder Counties, Colorado: U.S. Geological Survey Professional Paper 94, 379 p.

Braddock, W.A., 1969, Geology of the Empire quadrangle, Grand, Gilpin, and Clear Creek Counties, Colorado: U.S. Geological Survey Professional Paper 616, 56 p.

Cunningham, C.G., Naeser, C.W., Marvin, R.F., Luedke, R.G., and Wallace, A., 1994, Ages of selected intrusive rocks and associated ore deposits in the Colorado mineral belt: U.S. Geological Survey Bulletin 2109, 31 p.

Drake, A.A., Jr., 1957, Geology of the Wood and East Calhoun Mines, Central City district, Gilpin County, Colorado: U.S. Geological Survey Bulletin 1032-C, p. 129–170.

George, R.D., 1909, The main tungsten area of Boulder County, Colorado, with notes on the intrusive rocks by R.D. Crawford: Colorado Geological Survey First Report, 1908, p. 7–103.

Harrison, J.E., and Wells, J.D., 1956, Geology and ore deposits of the Freeland-Lamartine district, Clear Creek County, Colorado: U.S. Geological Survey Bulletin 1032-B, p. 33–127.

_____1959, Geology and ore deposits of the Chicago Creek area, Clear Creek County, Colorado: U.S. Geological Survey Professional Paper 319, 92 p.

Hawley, C.C., and Moore, F.B., 1967, Geology and ore deposits of the Lawson-Dumont-Fall River district, Clear Creek County, Colorado: U.S. Geological Survey Bulletin 1231, 92 p.

Hedge, C.F., Peterman, Z.E., and Braddock, W.A., 1967, Age of the major Precambrian regional metamorphism in the northern Front Range, Colorado: Geological Society of America Bulletin, v. 78, p. 551–558.

Irvine, T.N., and Baragar, W.R.A., 1971, A guide to the chemical classification of the common volcanic rocks: Canadian Journal of Earth Sciences, v. 8, p. 523–548.

Lovering, T.S., and Goddard, E.N., 1950, Geology and ore deposits of the Front Range, Colorado: U.S. Geological Survey Professional Paper 223, 319 p.

Lovering, T.S., and Tweto, O., 1953, Geology and ore deposits of the Boulder County tungsten district, Colorado: U.S. Geological Survey Professional Paper 245, 199 p.

Moench, R.H., and Drake, A.A., Jr., 1966, Economic geology of the Idaho Springs district, Clear Creek and Gilpin Counties, Colorado: U.S. Geological Survey Bulletin 1208, 91 p.

Peterman, Z.E., and Hedge, C.E., 1968, Chronology of Precambrian events in the Front Range, Colorado: Canadian Journal of Earth Sciences, v. 5, p. 749–756.

Peterman, Z.E., Hedge, C.E., and Braddock, W.A., 1968, Age of Precambrian events in the northeastern Front Range, Colorado: Journal of Geophysical Research, v. 73, no. 6, p. 2,277–2,296.

Phair, George, 1952, Radioactive Tertiary porphyries in the Central City district, Colorado, and their bearing upon pitchblende deposition: U.S. Geological Survey TEI-247, issued by U.S. Atomic Energy Commission Technical Information Service, Oak Ridge, Tennessee.

Rice, C.M., Harmon, R.S., and Sheperd, T.J., 1985, Central City, Colorado—The upper part of an alkaline porphyry molybdenum system: Economic Geology, v. 80, p. 1,769–1,796.

Rice, C.M., Lux, D.R., and Macintyre, R.M., 1982, Timing of mineralization and related intrusive activity near Central City, Colorado: Economic Geology, v. 77, p. 1,655–1,666.

Sheridan, D.M., Maxwell, C.H., Albee, A.L., 1967, Geology and uranium deposits of the Ralston Buttes district, Jefferson County, Colorado: U.S. Geological Survey Professional Paper 520, 120 p.

Sims, P.K., 1963, Geology of uranium and associated ore deposits, central part of the Front Range mineral belt: U.S. Geological Survey Professional Paper 371, 118 p.

_____1964, Geology of the Central City quadrangle, Colorado: U.S. Geological Survey Geological Quadrangle Map GQ-267, 1:24,000.

Sims, P.K., and Barton P.B., 1961, Some aspects of the geochemistry of sphalerite, Central City district, Colorado: Economic Geology, v. 56, p. 1211–1237.

_____1962, Hypogene zoning and ore genesis, Central City district, Colorado: Geological Society of America Buddington Volume, p. 373–396.

Sims, P.K, Drake, A.A., Jr., and Tooker, E.W., 1963, Economic geology of the Central City district, Gilpin County, Colorado: U.S. Geological Survey Professional Paper 359, 231 p.

Sims, P.K., and Gable, D.J., 1967, Petrology and structure of Precambrian rocks, Central City quadrangle, Colorado: U.S. Geological Survey Professional Paper 554-E, 56 p.

Sims, P.K., and Sheridan, D.M., 1964, Geology of uranium deposits of the Front Range, Colorado: U.S. Geological Survey Bulletin 1159, 116 p.

Smith, W., 1938, Geology of the Caribou stock in the Front Range, Colorado: American Journal of Science, 5th Series, v. 36, p. 8–26

Spurr, J.E., and Garrey, G.H., 1908, Economic geology of the Georgetown quadrangle, Colorado, with a section on General geology, by S.H. Ball: U.S. Geological Survey Professional Paper 63, 422 p.

Stern, T.W., Phair, G., Newell, M.N., 1971, Boulder Creek batholith, Colorado, Part II: Isotopic age of emplacement and morphology of zircon: Geological Society of America Bulletin, v. 82, p. 1615–1634.

Taylor, R.B., 1976, Geologic map of the Black Hawk quadrangle, Gilpin, Jefferson, and Clear Creek Counties, Colorado: U.S. Geological Survey Geological Quadrangle Map GQ-1248, scale 1:24,000.

Tooker, E.W., 1963, Altered wallrocks in the central part of the Front Range mineral belt, Gilpin and Clear Creek Counties, Colorado: U.S. Geological Survey Professional Paper 439, 102 p.

Tweto, O., and Sims, P.K., 1963, Precambrian ancestry of the Colorado mineral belt: Geological Society of America Bulletin, v. 74, p. 991–1014.

Wells, J.D., 1960, Petrography of radioactive Tertiary igneous rocks, Front Range mineral belt, Colorado: U.S. Geological Survey Bulletin 1032-E, p. 223–272.

_____1967, Geology of the Eldorado Springs quadrangle, Boulder and Jefferson counties, Colorado: U.S. Geological Survey Bulletin 1221-D, 85 p.

Wells, J.D., Sheridan, D.M., and Albee, A.L., 1964, Relationship of Precambrian quartzite-schist sequence along Coal Creek to Idaho Springs Formation, Front Range, Colorado: U.S. Geological Survey Professional Paper 454-O, p. O1–O25.

Worcester, P.G., 1920, The geology of the Ward region, Boulder County, Colorado: Colorado Geological Survey Bulletin 21, 74 p.

Chapter 3

Cripple Creek District

INTRODUCTION

The Cripple Creek district is located in the southern part of Teller County (Fig. 8) well south of the Colorado Mineral Belt. The district is the most important gold-producing camp in the state; it has produced more than 21 million ounces of gold since its discovery in 1891. In comparison, the entire state of Colorado has produced about 44 million ounces since the first discovery in Gregory Gulch in 1860 (Davis and Streufert, 1990).

The earliest geological work on the district was completed by Cross and Penrose (1895) and by Penrose (1895). Later Lindgren and Ransome (1906) published a significant description of the geology and mineralogy of the district. These early authors theorized that the Cripple Creek volcanic complex was explosive. Loughlin and Koschmann (1935) recognized the role of subsidence in forming some of the breccia complexes. Koschmann (1949) reiterated the importance of subsidence in the volcanic complex and noted the importance of buried Proterozoic horsts or "ridges" in the localization of gold-bearing vein complexes. Gold-bearing veins that extended to depths of greater than 3,000 feet with only insignificant changes in mineralogy were noted by Loughlin (1927).

GEOLOGICAL SETTING

The Cripple Creek district is located within a small (approximately 6 square miles), Oligocene alkalic, intrusive-diatreme complex emplaced at the junction of four Proterozoic igneous and metamorphic units (Fig. 9 and 10). There are older Oligocene andesites, conglomerates, and rhyolitic ash flow tuffs just to the south of the district. The district is further localized along generally northwest-trending faults that parallel regional mid-Tertiary extensional systems.

PROTEROZOIC ROCKS (Xgn, Xgd, Ycc, AND Ypp)

The oldest Proterozoic unit is a biotite-quartz-plagioclase gneiss (Xgn) which was intruded by a 1,700 Ma hornblende or biotite granodiorite (Xgd). The Cripple Creek Quartz Monzonite (Ycc) (age 1,400 Ma) and the Pikes Peak Granite (Ypp) (age 1,000 Ma) intruded the older Proterozoic rocks (Wobus and others, 1976).

OLIGOCENE VOLCANIC AND VOLCANICLASTIC ROCKS (Ttml, Ttc, Twm)

Several volcanic rock units in the area of the Cripple Creek district pre-date the intrusive-diatreme complex that hosts the gold mineralization. The Lower Thirty Nine Mile Andesite is composed of a dark gray to purple pyroxene andesite. The Tallahassee Creek Conglomerate (Ttc) is composed of fluvial arkoses and conglomerates. The Wall Mountain Tuff (Twm) is a rhyolitic ash flow tuff that has a reported potassium-argon date of 35.7 Ma (Wobus and others, 1970).

OLIGOCENE DIATREME COMPLEX

The Cripple Creek intrusive-diatreme complex consists primarily of a large mass of heterolithic breccia. Phonolite, latite-phonolite, syenite, and alkali basalt intrude the breccia throughout the complex. The entire district is centered over a gravity and magnetic low interpreted by Kleinkopf and others (1970) to represent a large batholith at depth.

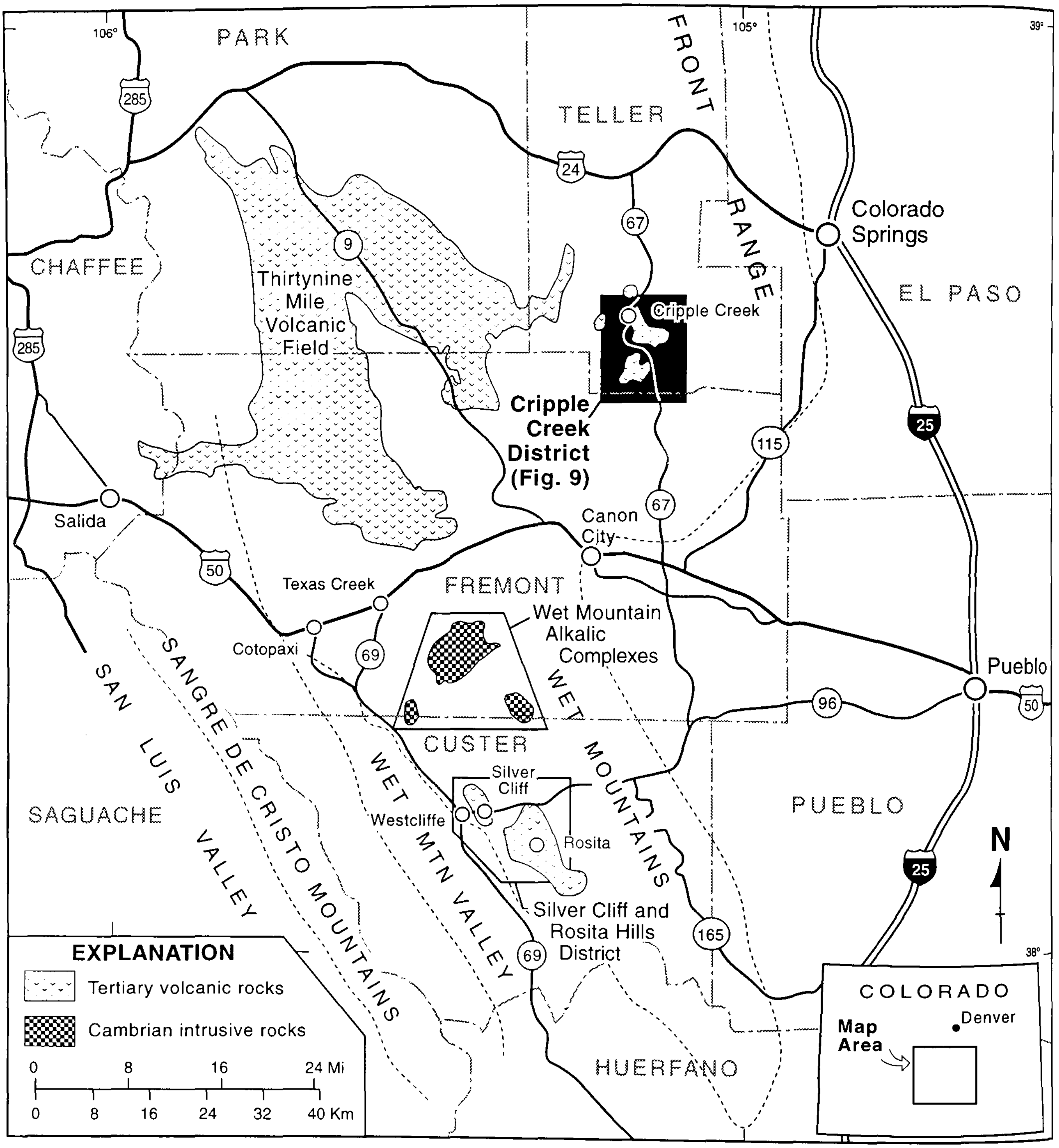

Figure 8. Index map showing location of the Cripple Creek district, Silver Cliff and Rosita Hills district, and the Wet Mountains alkalic complexes.

Breccia (Tbr)

The Cripple Creek breccia is a heterolithic breccia and tuff composed of angular to subangular fragments of Proterozoic igneous and metamorphic rocks and Tertiary rocks. It has a well-sorted matrix of quartz, microcline and rock fragments. The breccia appears massive in outcrop; however, it is locally stratified. The breccia is at least 3,300 feet thick

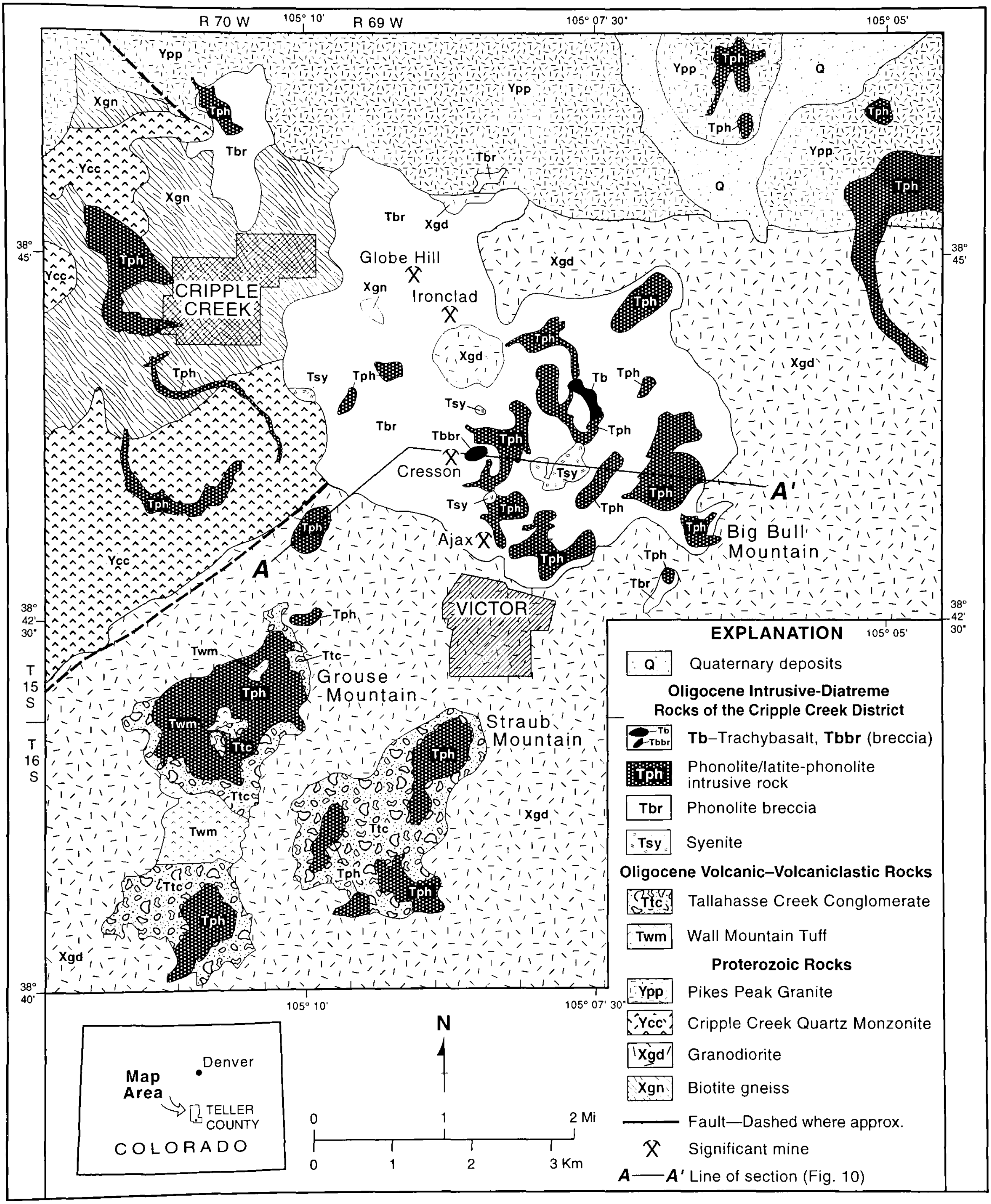

Figure 9. Simplified geologic map of the Cripple Creek district, Teller County, Colorado. (From Wobus and others, 1976)

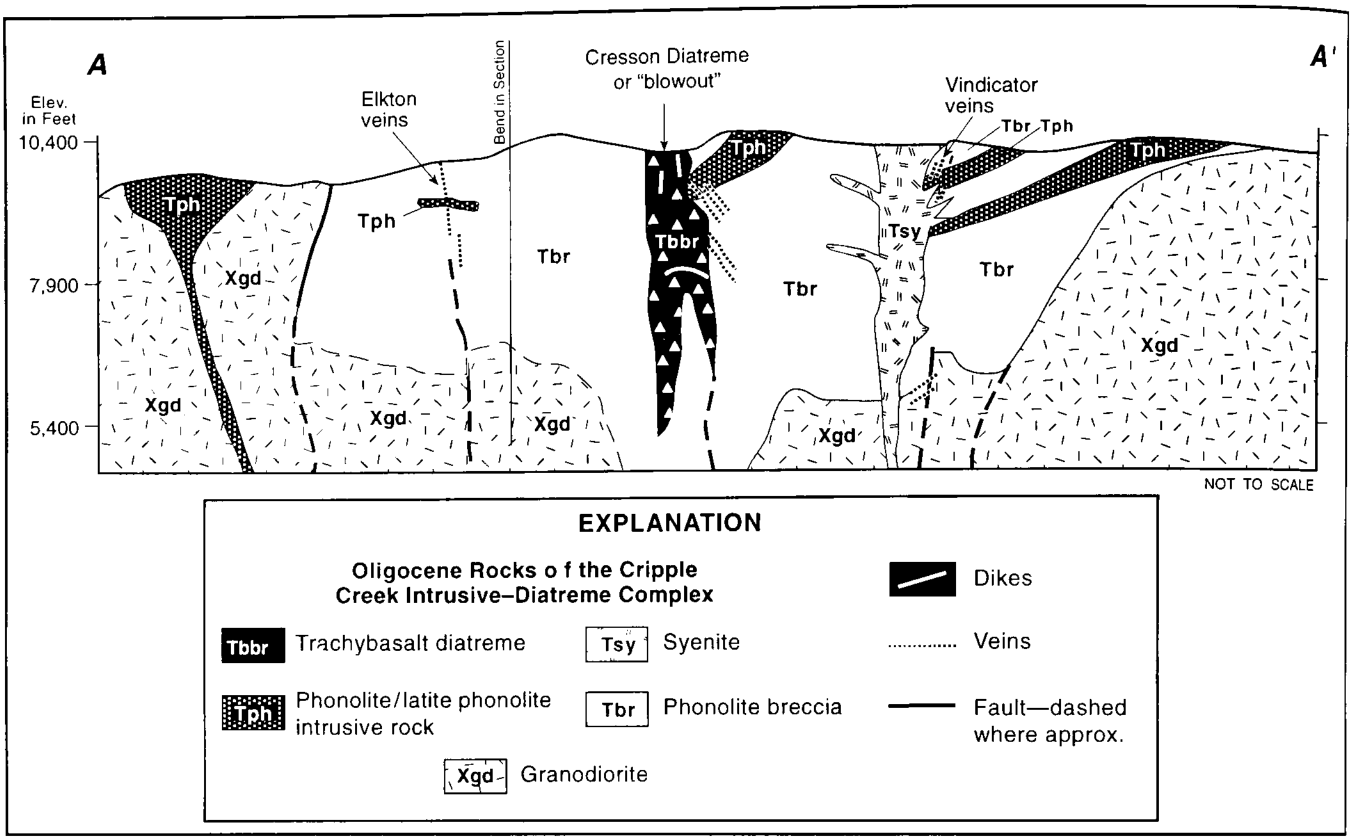

Figure 10. Geological cross section A—A' across Cripple Creek district. (From Thompson and others, 1985)

(Thompson and others, 1985) and occupies three separate subbasins (Loughlin and Koschmann, 1935). There are fluvial and lacustrine sediments interbedded with the Cripple Creek breccia in the eastern half of the complex. Carbonized tree trunks and coal layers are also present within the breccia at depths up to 800 feet (Lindgren and Ransome, 1906).

Phonolite (Tph)

Phonolite and latite-phonolite are the most widespread igneous rocks in the Cripple Creek district. They form bold hilly outcrops outside the district at Straub, Big Bull, and Grouse Mountains (Fig. 9). The latite-phonolite is a distinctly porphyritic phase with phenocrysts of orthoclase, oligoclase, and pyroxene up to 1 centimeter in size (Thompson and others, 1985). Nepheline, sodalite, and analcite occur with those minerals within the finer-grained portion of the phonolite (Lindgren and Ransome, 1906). The phonolite occurs as dikes, upward-flaring domes, flows, and tabular bodies. Although it is generally aphanitic, locally it is slightly porphyritic with mostly sanidine phenocrysts. Detailed descriptions of the petrography and mineralogy of the phonolites and latite phonolites can be found in Lindgren and Ransome (1906). Wobus and others (1976) reported potassium-argon dates of 27.9 and 29.3 Ma for the phonolite. Argon-argon isotope dates on sanidine from the phonolite by Kelley and others (1993) indicate an emplacement age of 31.4 to 32.5 Ma.

Syenite (Tsy)

Syenite occurs as dikes and stocks of limited areal extent that intrude the Cripple Creek breccia. The syenite is a medium to dark gray, medium- to fine-grained granular rock composed of orthoclase, plagioclase, pyroxene, hornblende, biotite, and sodalite. Apatite, sphene, and magnetite are common accessory minerals (Wobus and others, 1976).

Trachybasalt (Ttb)

Alkalic basalts occur as dikes and sills cutting all the other rocks of the Cripple Creek diatreme and some of the older Proterozoic rocks as well. Several varieties of alkalic basalt have been described by Loughlin and Koschmann (1935) and Lindgren and Ransome (1906): trachydolerite, vogesite, monchiquite (lamprophyre), and melilite basalt. Their textures range from aphanatic to porphyritic.

The composition of the trachybasalt varies within the district. The Isabella dike in the Isabella Mine contains plagioclase ranging from andesine to bytownite, pyroxene, olivine, and lesser amounts of orthoclase and analcite. The Anna Lee vogesite dike in the Portland Mine contains orthoclase, hornblende, pyroxene, biotite, analcite, and local plagioclase feldspar. The monchiquites vary in granularity from aphanitic to porphyritic. Monchiquite phenocrysts are pyroxene and olivine in a fine-grained matrix of analcite (Lindgren and Ransome, 1906).

The Cresson "blowout" in the Cresson Mine is composed of an alkalic basalt breccia (Tbbr) with fragments of alkalic basalts, all the other volcanic and igneous rocks of the diatreme, and Proterozoic rocks. The matrix contains significant secondary pyrite and dolomite. Several dikes and sills composed of the alkalic basalt cut the Cresson blowout.

STRUCTURE

In a general sense the Cripple Creek basin is elongated in a northwest-southeast direction (Fig. 9), which probably reflects a major tectonic direction in the underlying Proterozoic rocks. The basin walls are generally steely-dipping, 65° to 80°, and irregular in form (Fig. 10). There are local overhangs especially in the southwestern part of the basin. The overall Cripple Creek basin has been divided into three subbasins that are separated in the northern part by "islands" of Proterozoic gneiss and granodiorite (Fig. 9). Another ridge of Proterozoic rock that separates the southern and eastern basins is only known in the subsurface; it trends southeast from the granodiorite "island" near Globe Hill.

The ore-bearing veins and vein systems of the Cripple Creek district are radially dispersed about the central granite island and are related to structural features in the underlying Proterozoic rocks, such as buried granite horsts, and zones of sharp bending in the contact of the volcanic basin rocks and Proterozoic rocks (Koschmann, 1949).

Aeromagnetic and gravity data (Kleinkopf and others, 1970) show a prominent gravity low over the intrusive-diatreme complex and a negative magnetic anomaly which corresponds with known surface gold-silver-tellurium geochemical anomalies (Gott and others, 1967, 1969). Local gravity minima are probably related to deep fissure zones. The gravity and magnetic lows probably indicate alteration processes within a large alkalic igneous body at depth below the intrusive-diatreme complex.

GEOCHEMISTRY

The total alkalies versus silica plot shows the strongly alkalic nature of most of the Tertiary volcanic rocks of the Cripple Creek district (Fig. 11). Phonolites, plagioclase phonolites, and trachytes are most alkalic. The monchiquites have low silica contents, 36 to 42 percent, and relatively low contents of alkalies. Of note, also, is the slightly alkalic nature of the Proterozoic gneiss and granite samples (Fig. 11). The normative diagram (Fig. 12) differentiates between the Tertiary alkalic rocks and the subalkalic Proterozoic gneiss and granite. The volcanic rocks are strongly nepheline normative; only the monchiquite is olivine normative. Another normative diagram (Fig. 13) demonstrates the weakly potassic nature of the Tertiary volcanic rocks. A Le Bas plot (Fig. 14) demonstrates a modern classification scheme for the volcanic rocks of the Cripple Creek district. The Harker variation diagrams (Fig. 15) also demonstrate the enrichment of Na_2O and K_2O in these rocks. Table 2 in the appendix lists the geochemical analyses and CIPW norms used in the diagrams.

ECONOMIC GEOLOGY

Four main types of ore deposits are found within the Cripple Creek district: vein deposits, diatreme-hosted deposits, hydrothermal breccia-hosted deposits, and bedded rock-hosted deposits (Thompson, 1992).

VEIN DEPOSITS

The vein and fissure vein deposits of the Cripple Creek district were the first discovered and are, historically, the most productive type of ore deposit. The veins generally dip steeply and show a general radial pattern within the district; however, they are best developed over "horsts" or ridges in the underlying Proterozoic rocks (Fig. 10). The veins of the district range from simple fissure fillings less than an inch thick to sheeted zones that are several feet, and as much as 100 feet, in width.

The Ajax vein system is typical of the district and has been the subject of recent geological research (Dwelley, 1984; Thompson and others, 1985). The Ajax vein is exposed throughout a vertical range of greater than 3,000 feet with virtually no change in ore grade or mineralogy. The Ajax Mine began production in 1895 and produced more than 700,000 ounces of gold at grades of 0.6 to 1.04 ounces per ton. Individual veins cut the Proterozoic granodiorite, where they are narrow, well-defined sheeted zones, and the Cripple Creek phonolite breccia, where they anastomose (Fig. 6, Thompson and others, 1985).

Early-stage minerals within the Bobtail and Newmarket veins of the Ajax vein system include quartz, fluorite, adularia, pyrite, sphalerite, galena, and local dolomite and marcasite. Later-stage minerals include most of those and the gold telluride, calaverite, and the silver sulfide, acanthite.

The principal ore minerals in the Cripple Creek district are calaverite, and rarely sylvanite and petzite.

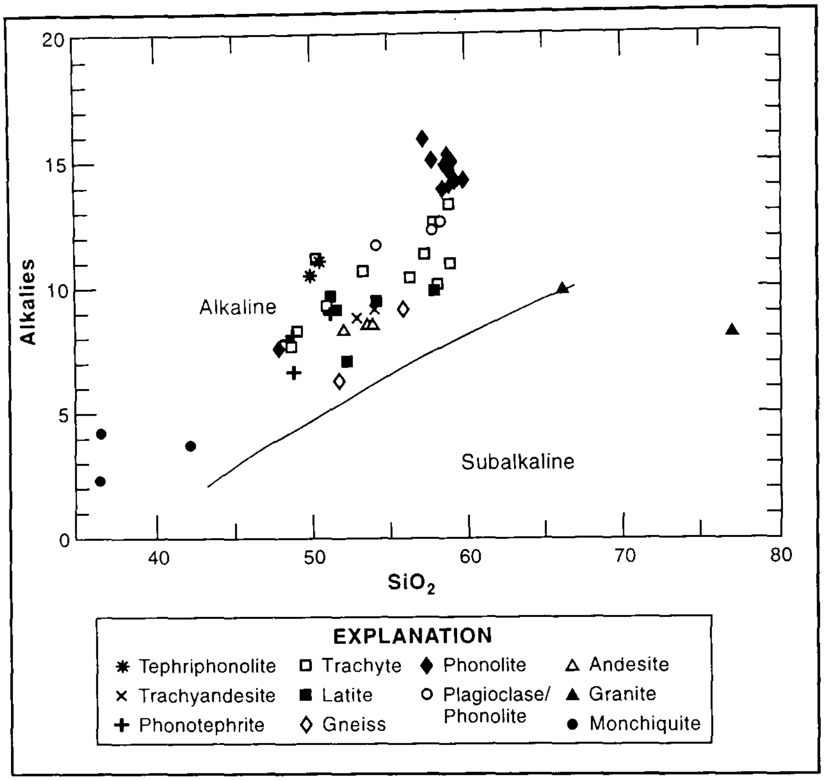

Figure 11. Plot of alkalies versus silica of representative rock samples from the Cripple Creek district.

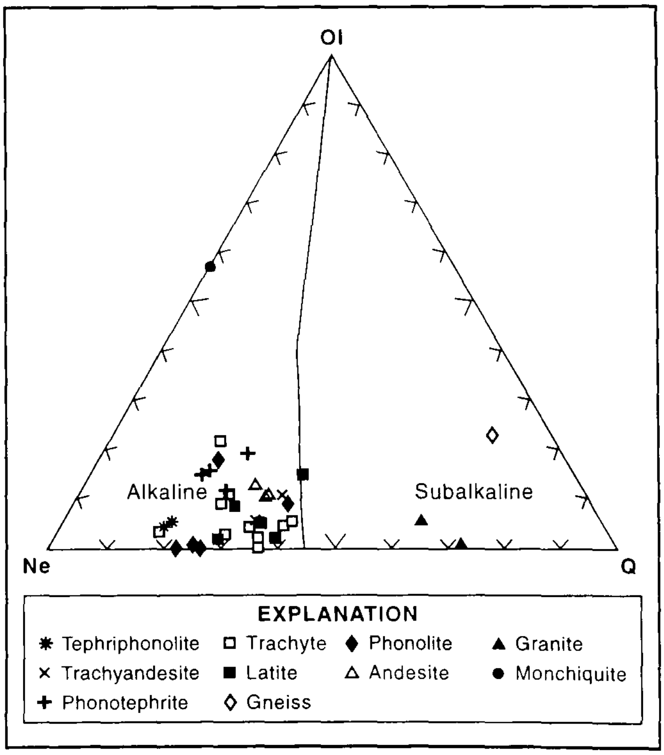

Figure 12. Normative diagram; Ne-Ol-Q of representative rock samples from the Cripple Creek district.

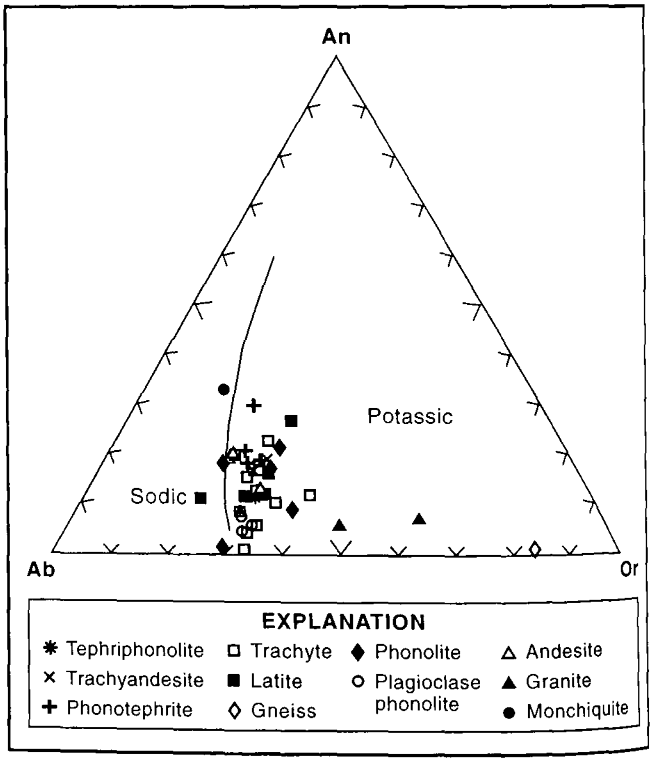

Figure 13. Normative diagram; Ab-An-Or of representative rock samples from the Cripple Creek district.

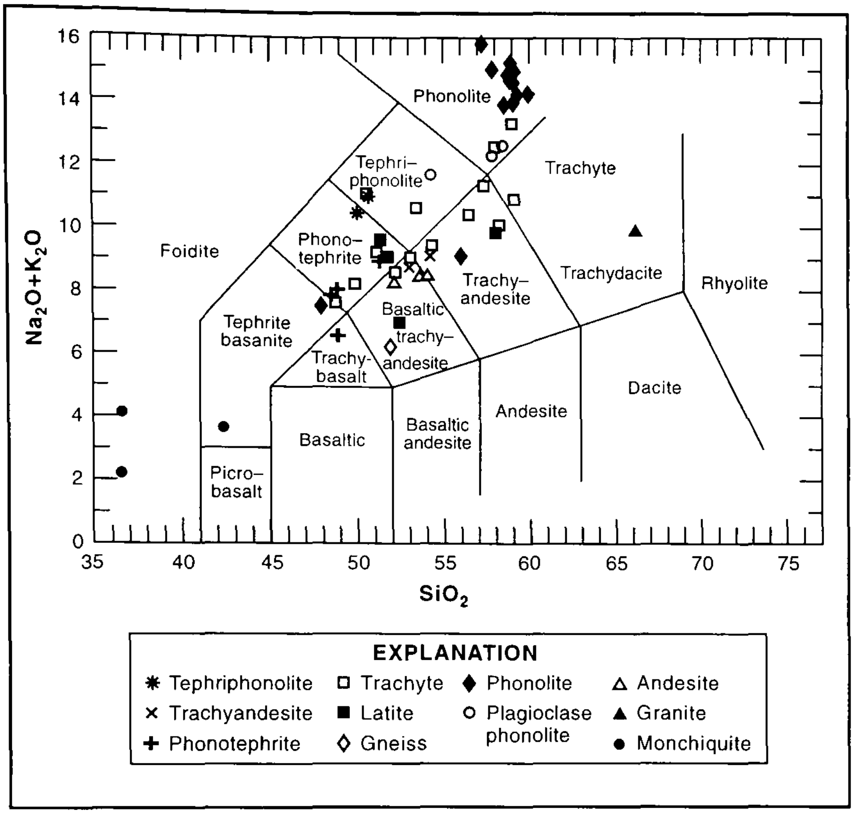

Figure 14. Le Bas diagram of representative rock samples from the Cripple Creek district.

Calaverite from district mines contains 39 percent to 43 percent gold and minor amounts of silver (Lindgren and Ransome, 1906). Wall rock alteration adjacent to the fissure veins is of limited extent and is best developed in the Cripple Creek breccia. The inner zone is dominated by secondary potassium feldspar, dolomite, roscoelite (vanadium mica), and pyrite. The outer zone of alteration consists of sericite, montmorillonite, magnetite, minor potassium feldspar, and pyrite (Thompson and others, 1985).

DIATREME-HOSTED DEPOSITS

The most economically valuable diatreme-hosted deposit in the Cripple Creek district is the Cresson Mine. It yielded 28.3 million tons of ore at a grade of 0.55 ounces of gold per ton from 1904 to 1959. The mine's production of over 15 million ounces of gold was about 70 percent of the district's total production. In 1914 a very rich part of the deposit known as the Cresson Vug was discovered at the 1200 level of the Cresson Mine; during a period of four weeks it yielded approximately 58,000 ounces of gold from an open cavity 23 feet by 13 feet by 40 feet high (Pontius and Butts, 1991).

Gold and silver telluride ores occur within a heterolithic breccia pipe (Fig. 10). The breccia is a medium to dark gray, matrix-supported, heterolithic, moderately propylitized mafic breccia. The breccia fragments consist of Proterozoic granitic rocks and the trachybasalt. There are several trachybasalt dikes and sills within the diatreme body.

Ore deposits in the Cresson Mine were located in both steeply-dipping and flat-lying fissures and sheeted zones. The steeply dipping fissures were commonly located at the contact of the Cresson Breccia Pipe. Flat-lying structures were found within the outer portions of the pipe especially along the southeast flank of the pipe. The principal ore minerals in the Cresson Pipe are calaverite, rarely petzite, and free gold which is intimately associated with melonite. Hildebrand and Gott (1974) suggested that the free gold exsolved from the melonite. Fluid inclusion data from Nelson (1989) indicate that the ore-forming fluids in the Cresson breccia were of low salinity, approximately 3 percent weight equivalent NaCl, had a pH of 5 to 6, and had temperatures ranging from 135° to 175° C.

HYDROTHERMAL BRECCIA DEPOSITS

The northern subbasin of the Cripple Creek district is dominated by hydrothermal breccia gold deposits. These deposits consist of low grade, native gold ores within strongly altered and hydrothermal brecciated pyroxene-bearing alkali trachyte porphyry (referred to as phonolite and latite-phonolite in older literature). The hydrothermal breccias of the Globe Hill and Ironclad deposits were mined during the period from 1992 to 1995.

Four separate structural events (Trippel, 1985) occurred at the Globe Hill deposit. Stage 1, the earliest event, created a northwest-trending zone of altered hydrothermal breccia along existing faults

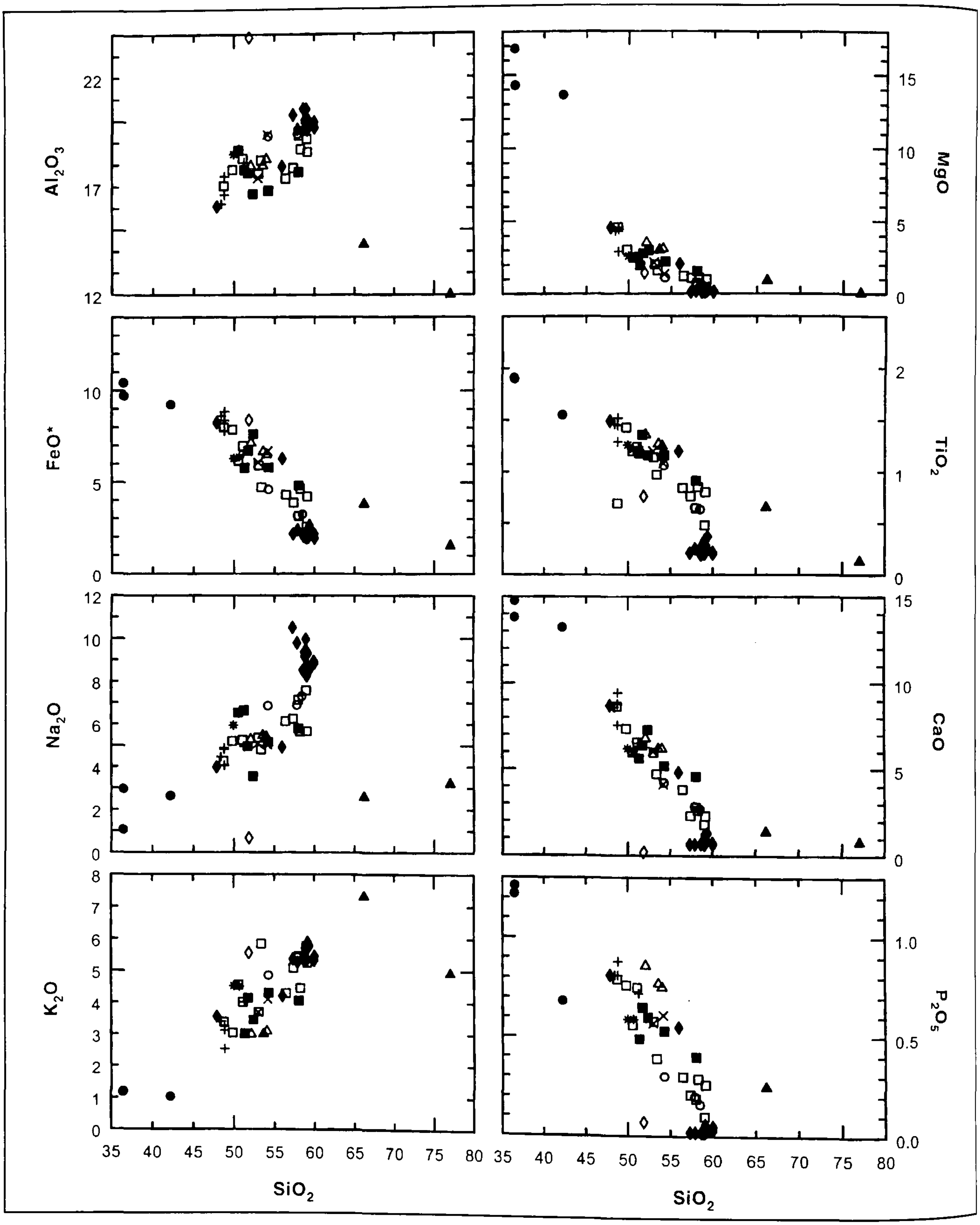

*Figure 15. Harker variation diagram of representative rock samples from the Cripple Creek district. Refer to the explanation on Fig. 14. (*includes Fe_2O_3)*

and joints. The breccias are crudely zoned from a breccia-dominated core to a crackle breccia-dominated halo, and into jointed wall rock. The breccia fragments range in size from 1 millimeter to 3 centimeters; they are generally monolithic and have subangular to subrounded shapes. The mineralization associated with stage 1 breccias produced veins, breccia matrix fillings, and weak disseminations into breccia fragments and adjacent wall rock. The open space vein fillings consist of either quartz-celestite-carbonate-fluorite or quartz-fluorite-pyrite. Ores in the breccia matrix filling is composed of quartz-celestite-pyrite-fluorite-carbonate. Base metal sulfides, specularite, rutile, and calaverite occur in minor amounts within stage 1 structures.

Stage 2 is characterized by steeply dipping tectonic structures of indeterminate displacement. The structures are usually filled with gouge material, a mixture of unsorted, very small wall rock fragments and rock flour. Mineralization associated with stage 2 structures produced veins along early structures and disseminations into the adjacent wall rock. The veins are composed of quartz-celestite-fluorite-(pyrite-carbonate-adularia). Base metal sulfides and calaverite also occur in lesser amounts. The wall rocks are characterized by zones of pyrite, other base metal sulfides, and calaverite.

Stage 3 produced an intrusive breccia body below the Globe Hill open pit. The breccia contains unsorted, subangular to well-rounded heterolithic fragments less than 8 centimeters in size. This breccia does not host any ores.

The stage 4 event is represented by a pipe-like hydrothermal breccia in the Globe Hill area. The central part of this breccia body contains heterolithic, subangular to subrounded matrix-supported fragments. The peripheral breccia halo consists of fragment-supported angular to subangular wall rock fragments that grade into a crackle-brecciated wall rock. The matrix of the central part of the stage 4 breccia consists of anhydrite-carbonate-celestite-fluorite and base metal sulfides. The peripheral breccia halo is partially cemented and cut by veins of massive montmorillonite. There are only trace amounts of gold in the stage 4 breccias.

The Ironclad breccia pipe is another hydrothermal breccia just to the south of the Globe Hill breccia deposit. It is located in a plagioclase phonolite rock at the intersection of a prominent northeast-trending structure and a northwest-trending structure. Like the Globe Hill breccia, the Ironclad breccia pipe has a complex history of brecciation and mineralization. Brecciation event 1 (Seibel, 1991) is the earliest event and is significant because native gold was precipitated during this event. The matrix of these plagioclase phonolite breccias contains drusy quartz, fluorite, carbonate and celestite. Brecciation event 1 fluids were boiling CO_2-rich fluids, with a pH of 5 to 6.5 and temperatures below 186° C. The gold was transported as a bisulfide complex and precipitated in open structures.

Brecciation event 2 at the Ironclad deposit brought more oxidized hydrothermal fluids that overprinted earlier breccias. The breccias contain anomalously large amounts of manganese and iron oxides in the matrix. The gold ore resulted from the incorporation of breccia fragments from breccia event 1. Brecciation event 3 introduced no new minerals into the deposit.

BEDDED ROCK-HOSTED DEPOSITS

Fluvial, lacustrine, and airfall bedded rocks are common in the eastern subbasin of the Cripple Creek intrusive-diatreme complex (Wood, 1990). Some of the sedimentary units within the complex, probably related to the Tallahassee Creek Conglomerate, contain cobbles of Proterozoic rocks and are thought to predate the intrusive-diatreme complex. The sedimentary and pyroclastic deposits associated with the intrusive-diatreme complex include conglomerates, sandstones, siltstones, claystones, and organic limestones. Sedimentary structures including evidence of subaerial deposition, raindrop impacts, are found in the sedimentary rocks. Silicic, argillic, and potassic alteration are common in these rocks. Sedimentary rocks are found at the surface and in the deepest mine workings, 3,200 feet below the surface (Koschmann, 1949), indicating a substantial amount of subsidence within the complex.

Disseminated gold ore resulted from circulating hydrothermal fluids that replaced crystal fragments and volcanic glass. These fluids also added dolomite, pyrite, and fluorite to the rock. The Cameron Mine contains disseminated gold in sediments and pyroclastic rocks. Gold assays of a green clay or lithic wacke completed in the 1930s range from less than 0.05 ounce per ton to 3.4 ounces per ton. Later exploration drilling in the 1980s did not confirm these earlier reports (Wood, 1990).

ORIGIN OF THE ORE DEPOSITS

The Cripple Creek district consists of a broad uplifted area of Proterozoic igneous and metamorphic rocks that was intruded by an alkalic intrusive-diatreme complex during the late Oligocene (approximately 32 Ma for the most differentiated intrusive rocks to 28 Ma for samples from the more mafic phonolites [Kelley and others, 1993]). The origins of this intrusive complex, well outside the northeast-trending Colorado mineral belt, are still debatable; however, Thompson and others (1985) indicated that the early stages of the opening of the Rio Grande Rift, which extends from New Mexico through central Colorado, were responsible for the alkalic intrusive-diatreme complex. The rocks of the intrusive-diatreme complex were probably derived from alkalic basalts formed by partial melting of the upper mantle. Differentiation of the of the melt as it moved through the crust may have created a monchiquite magma that underwent further fractionation to form the phonolite intrusives (Birmingham, 1987).

At the time of the intrusive episode the landscape was wet, as indicated by the diatreme style of volcanism. Intrusions that encountered abundant water produced phreatic and phreatomagmatic explosions that in turn produced diatremes. Other parts of the intrusive complex formed small coalescing stocks, dikes, sills, and probably local eruptive centers.

The main episode that produced all of the various types of ore deposits in the Cripple Creek district followed the main stage of intrusive and diatreme emplacement. The minerals formed by potassic alteration—adularia, potassium feldspar, and secondary biotite—related to vein emplacement have argon-argon dates ranging from 30 to 28 Ma (Kelley, and others, 1993). The first hydrothermal event was essentially a high temperature event (>350° C) resulting in widespread propylitic alteration and enhanced rock permeability. The second hydrothermal event had many stages all at approximately 180° C with low salinities. An extensive amount of the potassium feldspar alteration is associated with this hydrothermal event (Pontius, 1993). The mineralizing fluids followed structural zones and other permeable pathways to create the large vertical extent of mineralization of both gold tellurides and the free gold.

The gold was probably transported by a tellurium or bisulfide complex in magmatic fluids. The system began with the deposition of the free gold and pyrite minerals in permeable intrusive rocks. As this system evolved the permeability decreased and repeated structural activity opened the structural conduits and the provided open space for the gold telluride vein deposits to form. The last stage of the intrusive complex was the intrusion of the more mafic and ultramafic intrusives resulting in the formation of the hydrothermal breccias and breccia pipes. Supergene alteration followed the main hydrothermal events (Pontius, 1993).

EXPLORATION AND PRODUCTION HISTORY

Early reports of gold ores in the district in 1874 and 1884 did not result in the establishment of the vibrant mining district of later years (Penrose, 1895). A local rancher named Robert Womack made a gold discovery in 1891 and located the El Paso claim in Poverty Gulch which was later developed into the Gold King Mine, the first of series of gold discoveries which lead to the rapid development of the district. The rich underground mines in the early years of the district's history had an average grade of 1 to 2 ounces of gold per ton.

The Cripple Creek district produced more than 21 million ounces of gold and 2 million ounces of silver. In the peak year of production, 1900, 879,000 ounces of gold were produced. By 1920 production from the district had declined because of labor shortages, wage disputes, and water problems. In 1933 the price of gold increased from $20.67 to $35.00 an ounce which fostered mining in the district until the outbreak of World War II and the closure of all non-essential mines by the War Production Board in 1942. All restrictions on the price of gold were lifted during the mid-1970s and interest focused on low grade, bulk-tonnage gold deposits in the district.

The main areas of interest in the recent years are the low-grade, hydrothermal breccia deposits at Globe Hill and Ironclad. Texasgulf Minerals and Metals Co. and Golden Cycle Corporation formed the Cripple Creek and Victor Gold Mining Company (CCVGMC) and explored the area in the early 1980s. CCVGMC processed some old dump materials. Nerco Minerals bought Texasgulf Minerals and Metals Co. interest in 1989 and formed Pikes Peak Mining Company (PPMC). At that time there where no economic reserves known in the district. In the years from 1990 to 1993 PPMC completed more than 900,000 feet of exploration drill holes mostly in the area of the Cresson Mine and the Globe Hill and Ironclad open pit mines. They discovered a drill-indicated resource of 3,400,000 ounces of gold that has within it a proven and probable reserve of about 1,850,000 ounces (Pontius, J.A., PPMC, written communication, 1993).

During 1991 PPMC produced 15,500 ounces of gold and 10,000 ounces of silver from old waste dumps in the district. Mining operations commenced at the Globe Hill and Ironclad open pits late in that year. The announced reserve was 4 million tons of ore at 0.04 ounces per ton. In 1992 production from the two open pit mines jumped up to 42,400 ounces of gold and 11,900 ounces of silver. Gold Production in 1993 was 49,100 ounces of gold and 7,900 ounces of silver. Mining operations at the Globe Hill open pit mine ceased during 1993 and the Ironclad Mine closed in 1994.

In May 1993, Independence Mining announced that it had acquired 100 percent of PPMC. Plans for the future include the construction of the new Cresson open pit mine scheduled to be in production by 1995. The ore deposit at the new Cresson open pit mine is a disseminated, low-grade, bulk-tonnage type ore body in contrast to the historical high grade veins and "vugs" of the Cresson Mine. Rock types in the new open pit mine include phonolites, hydrothermal breccias, syenites, and various primitive ultramafic lamprophyres. The primary mineralized structural trend is north-northwest which follows pre-existing structures in the Proterozoic basement rocks. Alteration is ubiquitous and ranges from propylitic to strong argillic and potassic. The new Cresson deposit contains only native gold associated with pyrite and hydrous iron and manganese oxides. No telluride mineralization has been discovered in the disseminated deposit (Pontius and Butts, 1991).

Mining at the Cresson open pit began in December 1994. In 1995 the mine produced 7,155,400 tons of ore at a grade of 0.033 ounce of gold per ton for a total of 76,589 ounces of gold. In 1996 production increased to 174,000 ounces of gold. Production in 1997 increased to 228,000 ounces of gold. The Cresson deposit had a 1994 proven and probable reserve of 73 million tons at a grade of 0.03 ounce of gold per ton for a total of 2.2 million ounces (J.A. Pontius, PPMC, oral communication 1996).

REFERENCES

Birmingham, S.D., 1987, The Cripple Creek volcanic field, central Colorado: Austin, Univ. of Texas at Austin, M.A. thesis, 295 p.

Cross, W., and Penrose, R.A.F. Jr., 1895, Geology and mining industries of the Cripple Creek district, Colorado: U.S. Geological Survey Sixteenth Annual Report, Part 2, p. 1–109.

Davis, M.W., and Streufert, R.K., 1990, Gold occurrences of Colorado: Colorado Geological Survey Resource Series 28, 101 p.

Dwelley, P.C., 1984, Geology, mineralization, and fluid inclusion analysis of the Ajax vein system, Cripple Creek mining district, Colorado: Fort Collins, Colorado State University, M.S. thesis, 167 p.

Eriksson, C.L., 1987, Petrology of the alkalic hypabyssal and volcanic rocks at Cripple Creek, Colorado: Golden, Colorado School of Mines, M.S. thesis, 114 p.

Gott, G.B., McCarthy, J.H., Van Sickle, G.H., and McHugh, J.B., 1967, Distribution of gold, tellurium, silver and mercury in part of the Cripple Creek district, Colorado: U.S. Geological Survey Circular 543, 8 p.

_____1969, Distribution of gold and other metals in the Cripple Creek district, Colorado: U.S. Geological Survey Professional Paper 625A, 17 p.

Hildebrand, F.A., and Gott, G.B., 1974, Coloradoite, acanthite, and jarosite from the Cripple Creek district, Teller County, Colorado: U.S. Geological Survey Journal of Research, v. 2, no. 3, p. 339–340.

Kelley, K.D.,1996, Origin and timing of magmatism and mineralization in the Cripple Creek district, Colorado: Golden, Colorado School of Mines, Ph.D. dissertation, 259 p.

Kelley, K.D., Snee, L.W., and Thompson, T.B., 1993, ^{40}Ar/^{39}Ar isotopic dates from the Cripple Creek gold-telluride district, Colorado—Constraints on the timing of magmatism and mineralization [abs.]: Geological Society of America Abstracts with Programs, v. 25, no. 5, p. 61.

Kleinkopf, M.D., Peterson, D.L., and Gott, G.B., 1970, Geophysical studies of the Cripple Creek mining district, Colorado: Geophysics, v. 35, p. 490–500.

Koschmann, A.H., 1949, Structural control of the gold deposits of the Cripple Creek district, Teller County, Colorado: U.S. Geological Survey Bulletin 955-B, p. 19–60.

Lindgren, W., and Ransome, F.L., 1906, Geology and gold deposits of the Cripple Creek district, Colorado: U.S. Geological Survey Professional Paper 54, 516 p.

Loughlin, G.F., 1927, Ore at deep levels in the Cripple Creek district, Colorado: American Institute of Mining and Metallurgical Engineers Technical Publication 13, 32 p.

Loughlin, G.F., and Koschmann, A.H., 1935, Geology and ore deposits of the Cripple Creek district, Colorado: Colorado Scientific Society Proceedings, v. 13, no. 6, p. 215–435.

Nelson, S.E., 1989, Geology, alteration, and mineral deposits of the Cresson diatreme, Cripple Creek district, Colorado: Fort Collins, Colorado State University, M.S. thesis, 147 p.

Penrose, R.A.F. Jr., 1895, Mining geology of the Cripple Creek district, Colorado: U.S. Geological Survey Sixteenth Annual Report, Part 2, p. 111–209.

Pontius, J.A., 1993, Field guide—Gold deposits of the Cripple Creek mining district, Colorado, USA: Unpublished report.

Pontius, J.A., and Butts, R.A., 1991, Geology and gold deposits of the Cresson deposit, Cripple Creek, Colorado: 97th Annual Northwest Mining Association Convention, Spokane Washington, December 4–6, 1991.

Seibel, G.E., 1991, Geology of the Victor Mine, Cripple Creek mining district, Colorado: Fort Collins, Colorado State University, M.S. thesis, 133 p.

Thompson, T.B., 1992, Mineral deposits of the Cripple Creek district: Mining Engineering, v. 44, no. 2, p. 135–138.

Thompson, T.B., Trippel, A.D., and Dwelley, P.C., 1985, Mineralized veins and breccias of the Cripple Creek district, Colorado: Economic Geology, v. 80, p. 1669–1688.

Trippel, A.D., 1985, Hydrothermal mineralization and alteration at the Globe Hill deposit, Cripple Creek district, Colorado: Fort Collins, Colorado State University, MS thesis, 93 p.

Wobus, R.A., Epis, R.C., and Scott, G.R., 1976, Reconnaissance geological map of the Cripple Creek-Pikes Peak area, Teller, Fremont, and El Paso Counties, Colorado: U.S. Geological Survey Miscellaneous Field Map, MF-805.

Wood, M.R., 1990, Geology and alteration of the eastern Cripple Creek mining district, Teller County, Colorado: Fort Collins, Colorado State University, M.S. thesis, 186 p.

Chapter 4

State Line Kimberlite District

INTRODUCTION

The State Line kimberlite district is located in the northern Front Range of Colorado and the geologically continuous Laramie Range of southern Wyoming (Fig. 16). In 1960 exotic blocks of Ordovician and Silurian fossiliferous limestones were found at the site of the Ferris kimberlite; however, they were not recognized as being part of a kimberlite diatreme complex. These exotic blocks were the first documented occurrence of lower Paleozoic rocks in the northern Front Range. The discovery of the Sloan kimberlite in 1964 established the true nature of these exotic rocks as xenolithic fragments within a kimberlite diatreme complex (McCallum and others, 1975). Additional discoveries of kimberlites were made in the ensuing years from localities as far south as Green Mountain just west of Boulder, Colorado to the Iron Mountain district, west of Wheatland, Albany County, Wyoming (McCallum and Mabarak, 1976). About 100 kimberlite diatremes have been identified in the region of northern Colorado and southern Wyoming including the State Line district.

GEOLOGICAL SETTING

The State Line kimberlite district is located along the eastern flank of the Front Range in Colorado and the Laramie Range of Wyoming. The oldest rocks in the region are metasedimentary gneisses of Proterozoic age (Fig. 17). Two younger Proterozoic batholiths, the Log Cabin Granite and the Sherman Granite, and some associated mafic intrusive rocks intrude the older gneisses and form the Virginia Dale ring complex. The deposition of Lower Paleozoic clastic and carbonate sedimentary rocks is confirmed by the presence of exotic blocks of those rocks in the kimberlite intrusive diatremes of the district. The kimberlites were emplaced during the Devonian (Eggler, 1968). After the kimberlites were intruded the entire region of the Front Range was uplifted and all in situ Lower Paleozoic rocks were eroded away.

GNEISS (Xgn)

The oldest rocks in the State Line district are Early Proterozoic metasediments composed of hornblende and biotite gneisses to the south and quartz monzonite gneiss to the northeast. Mineral assemblages indicate that these rocks attained the almandine-amphibolite facies of metamorphism. These rocks have been dated at 1,750 Ma (Eggler, 1968; Peterman and others, 1966).

VIRGINIA DALE RING COMPLEX

The Virginia Dale ring complex is a prominent circular feature composed primarily of granites and diorites that intrude the older gneissic metasedimentary terrain. The feature is approximately 9 miles in diameter.

Diorite (XYd)

The earliest rock units found within the ring complex are several types of basic rocks which include diorite, hornblende gabbro, andesite, and dacite. These various units are shown as diorite in Fig. 17. The diorite, andesite, and dacite are apparently contemporaneous; however, the age relationship between the dioritic rocks and hornblende gabbro is unknown. Isolated outcrops of the diorite around the northern edge of the complex indicate that the diorite and associated rocks extended around the perimeter of the ring complex prior to the intrusion of the later granitic rock units.

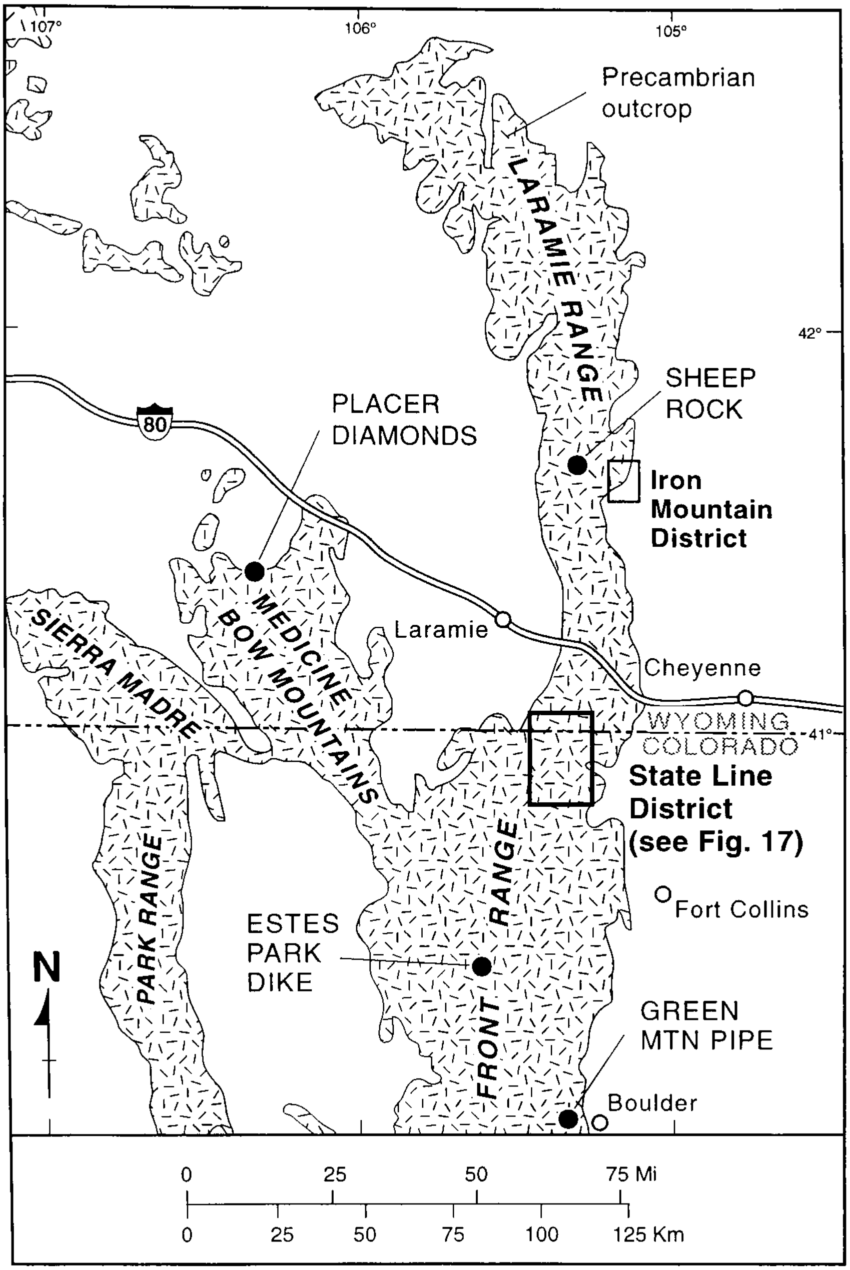

Figure 16. Location map of Front Range-Laramie Range kimberlites. (From Hausel, McCallum, and Roberts, 1985)

Sherman Granite

Darton and others (1910) described several facies of a coarse-grained granite batholith in the southern Laramie Range and gave it the name "Sherman Granite." In the Virginia Dale area two facies of the Sherman Granite were mapped, a granite and a quartz monzonite.

Trail Creek Granite (Ystc) The most widespread facies, informally named the Trail Creek granite, forms a portion of the batholith immediately north and east of the complex and the outer ring dike. The Trail Creek granite is a red, equigranular granite with conspicuous clots of hornblende and biotite (Eggler, 1968).

Cap Rock Quartz Monzonite (Yscr) The other facies of the Sherman Granite, a pinkish-gray, porphyritic, biotite, quartz monzonite, was informally named the Cap Rock quartz monzonite. It has a foliation defined by the planar alignment of microcline crystals, inclusions, and biotite streaks. Eggler (1968) divided the Cap Rock quartz monzonite into two distinct units. The "outer Cap Rock quartz monzonite" has smaller and better aligned phenocrysts and biotite streaks than the "inner Cap Rock quartz monzonite." The contact between the two zones is gradational. Recent work has indicated that locally the Cap Rock quartz monzonite appears to be part of a younger granitic system, the Log Cabin granite (H.G. Coopersmith, Diamond Co. N.L., oral communication, 1993)

Several small dikes and lenses of quartz monzonite intrude the diorite complex at the contact zone between the diorite complex and the outer Cap Rock quartz monzonite. Adjacent to these intrusive bodies, there are unusual hybrid rocks that are intermediate in composition between quartz monzonite and diorite (Eggler, 1968).

The Sherman Granite, which includes the Trail Creek granite and the Cap Rock quartz monzonite, has a rubidium-strontium isochron date of 1,410 + 30 Ma (Peterman and others, 1968).

Log Cabin Granite (Ylc)

Boos and Boos (1933) applied the name "Log Cabin Granite" to a biotite-muscovite granite batholith that is younger than the rocks of the Virginia Dale ring complex in the northern Front Range of Colorado. The Log Cabin Granite may be distinguished from the Sherman Granite by the Log Cabin's finer grain size, primary muscovite, and

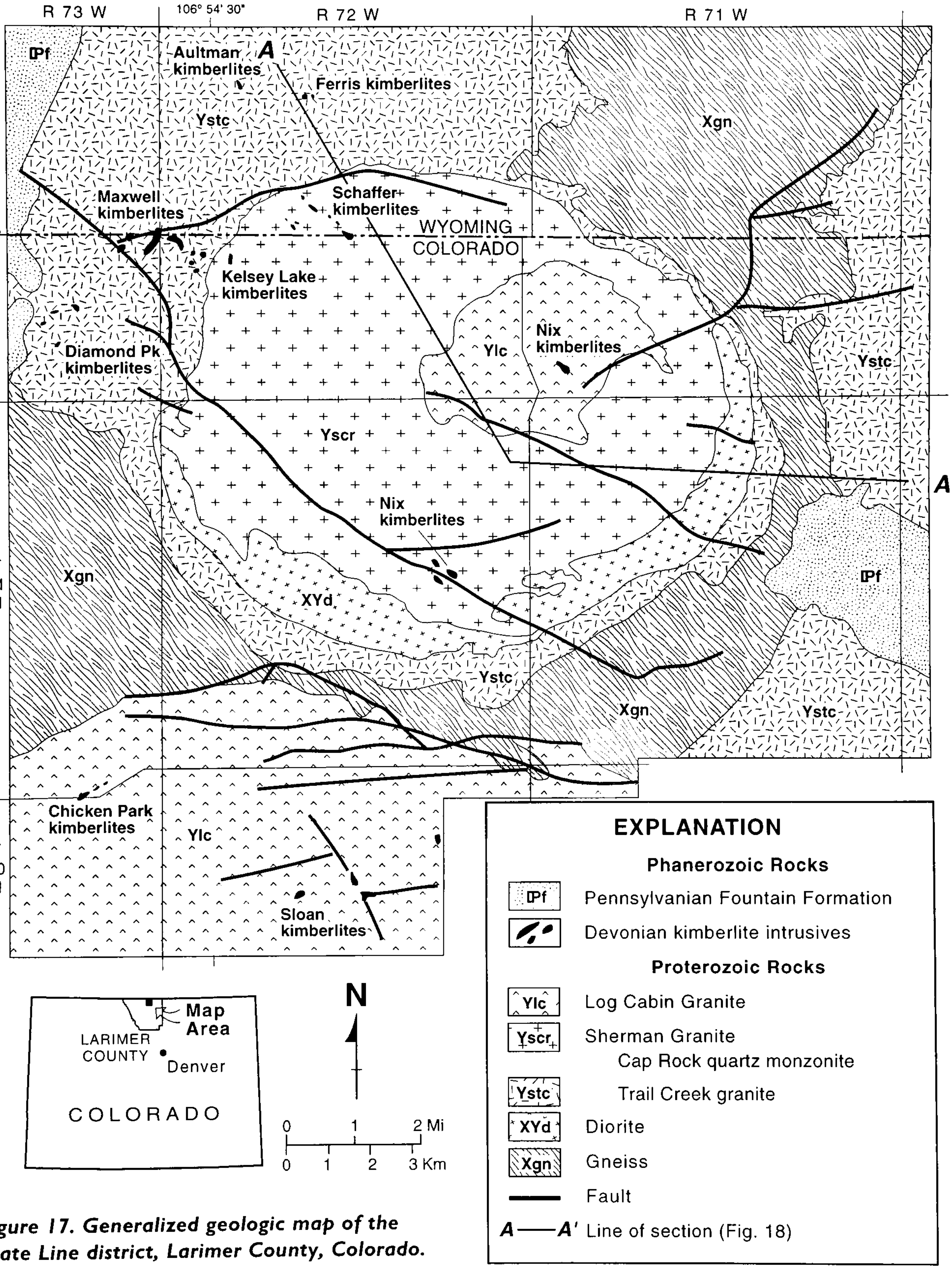

Figure 17. Generalized geologic map of the State Line district, Larimer County, Colorado. (From Hausel, McCallum, and Roberts, 1985)

abundant pegmatites and aplites (Eggler, 1968). Six samples from the Log Cabin Granite define a rubidium-strontium isochron date of 1,420 ± 30 Ma indicating that the age difference between the Sherman Granite and the Log Cabin Granite is probably less than 40 Ma (Peterman and others, 1968).

The Sherman Granite is intruded by a swarm of porphyritic andesite dikes in the State Line district. Further south the dikes are cut and hydrothermally metamorphosed by the Silver Plume Granite, which is thought to be correlative to the Log Cabin Granite (Eggler, 1968).

PHANEROZOIC SEDIMENTS

There are no in-place, Phanerozoic sedimentary rocks in the State Line district; however, a few miles to the northwest and southeast, red beds of the Pennsylvanian Fountain Formation (IPf)are exposed. Exotic blocks and fragments of limestone, dolomite, sandstone, and conglomerate of Cambrian, Ordovician, Silurian and possibly Early Devonian age have been found in a substantial number of the kimberlite diatremes. This indicates that Lower Paleozoic sediments were deposited in a shallow marine environment in this part of the Rocky Mountains. Later, during the Devonian, these marine rocks were intruded by the kimberlite diatremes. All the Lower Paleozoic rocks throughout the region of the present-day Front Range were removed by a later pre-Pennsylvanian erosion event. These exotic blocks of Lower Paleozoic rocks are the only record of Early Paleozoic events in the northern Front Range (McCallum and others, 1975).

STRUCTURE

Gravity models (Eggler, 1968) supplemented by surface data indicate that the outer granite zone, composed of the Trail Creek granite, forms a ring dike whose walls dip steeply outward. The contacts of the Trail Creek granite with the surrounding rocks are always sharp (Fig. 18). There is no evidence that foliation of the older gneisses was deformed.

Unlike the foliation in the outer ring dike, the foliation in the inner Cap Rock quartz monzonite core zones defines a circular pattern in which the dips become shallower inward. The contact between the Cap Rock quartz monzonite and the Trail Creek granite is sharp, steep, and parallels alignment of phenocrysts in the quartz monzonite.

The core zone of the Log Cabin granite is considered to be a central stock. Consideration of the modelled gravity values indicates

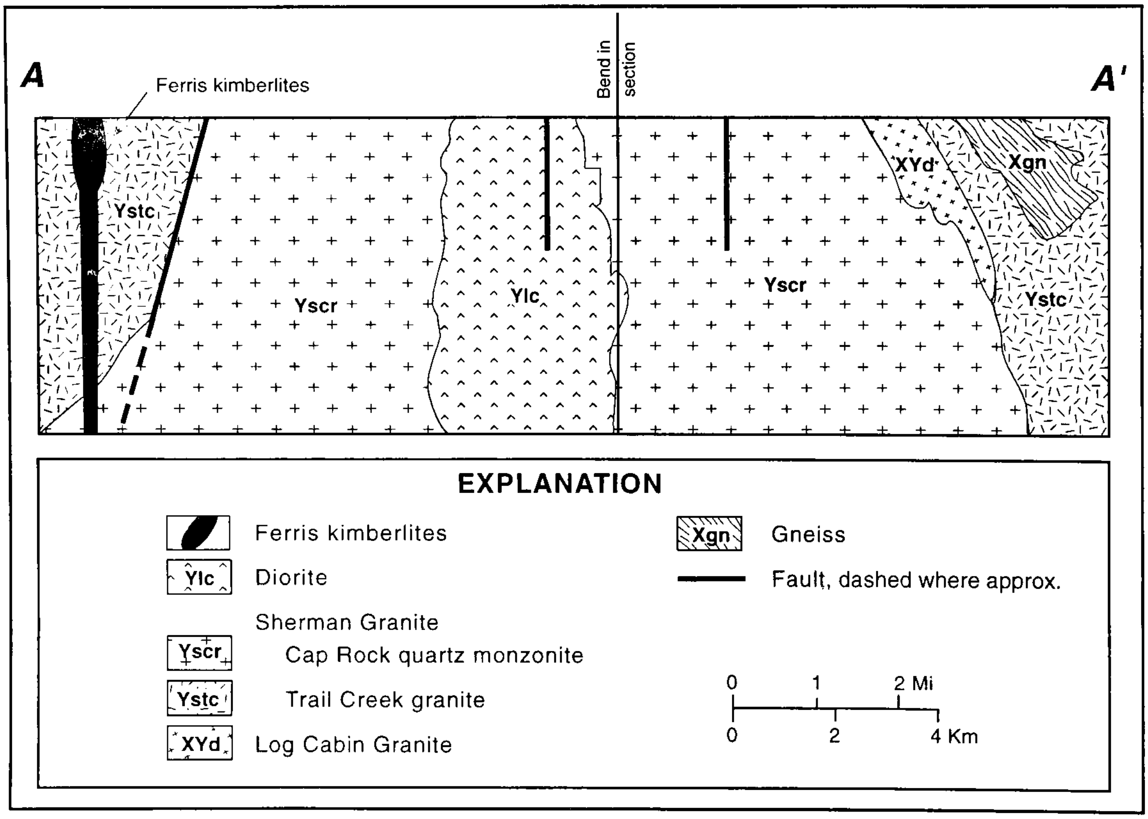

Figure 18. Generalized cross-section of the Virginia Dale ring complex. (From Hausel, McCallum, and Roberts, 1985)

that a stock emplacement model is more realistic than a cauldron subsidence model. The observed foliation pattern indicates that some sagging took place in the magma chamber, possibly after a period of magma withdrawal (Eggler, 1968).

GEOCHEMISTRY

The plot of total alkalies versus silica (Fig. 19) shows the subalkaline (calc-alkalic) nature of the Proterozoic granites, diorites, and monzonites. The kimberlites, eclogite, and peridotite contain low amounts of silica and alkalies; however, they plot in the alkaline area of the diagram. The Harker diagram (Fig. 20) illustrates the large amount of calcium and magnesium oxides, presumably from garnet and pyroxene minerals, and decreased aluminum oxide in the kimberlites. Table 3 in the appendix lists the geochemical analyses and CIPW norms used in the diagrams.

ECONOMIC GEOLOGY

The host rocks for the diamond deposits of the State Line district are Devonian kimberlites. Kimberlites are a rare and unique hybrid rock found in only a few places in the world. The term "kimberlite" was first applied to the diamond-bearing "blue ground" breccias of the Kimberly district in South Africa. According to Mitchell (1991) there are two main groups of kimberlites: group 1—olivine- rich, monticellite serpentine calcite kimberlites (prefixes are used to indicate the dominant matrix minerals); and group 2—micaceous kimberlites.

Group 1 kimberlites are complex hybrid rocks consisting of minerals including diamond that were derived from the fragmentation of upper mantle xenoliths such as ilherzolite, from megacrysts or discrete nodules, and from the primary phenocryst and matrix minerals. There is a large variation in the appearance and mineralogy of kimberlites because of the significant differences in the percentage contribution of each source rock or mineral.

Group 1 kimberlites are defined as carbon dioxide-rich, potassic ultrabasic rocks that occur in small diatremes, or in dikes and sills of limited extent. Commonly, they possess a distinctive inequigranular texture with megacrysts and macrocrysts set in a fine-grained matrix. The megacryst assemblage comprises anhedral crystals of olivine, magnesian ilmenite, chromium-poor pyrope garnet, chromium-poor clinopyroxene, phlogopite, enstatite, and titanium-poor chromite. The fine-grained matrix consists of olivine, phlogopite, perovskite, spinel, monticellite, apatite, calcite, and serpentine. Group 1 kimberlites do not contain primary diopside; the sparse diopside is an alteration product related to contamination from silica-rich country rocks. Mantle-derived xenocrysts of magnesian aluminous chromite, chromium diopside, and chromium pyrope garnet are common.

Group 2 kimberlites consist of rounded olivine macrocrysts set in a matrix of phlogopite, diopside, spinel, perovskite, and calcite. They have been found only in southern Africa.

There are approximately 40 kimberlite diatremes and dikes in the State Line district, most of which are known to be diamondiferous. They range in size from a few feet to nearly 1,800 feet in diameter and generally have an ellipsoidal to elongate shape. Only a few of the diatremes show a definite structural control, mostly along east-west and northwest-trending structures. Others, such as the Schaffer

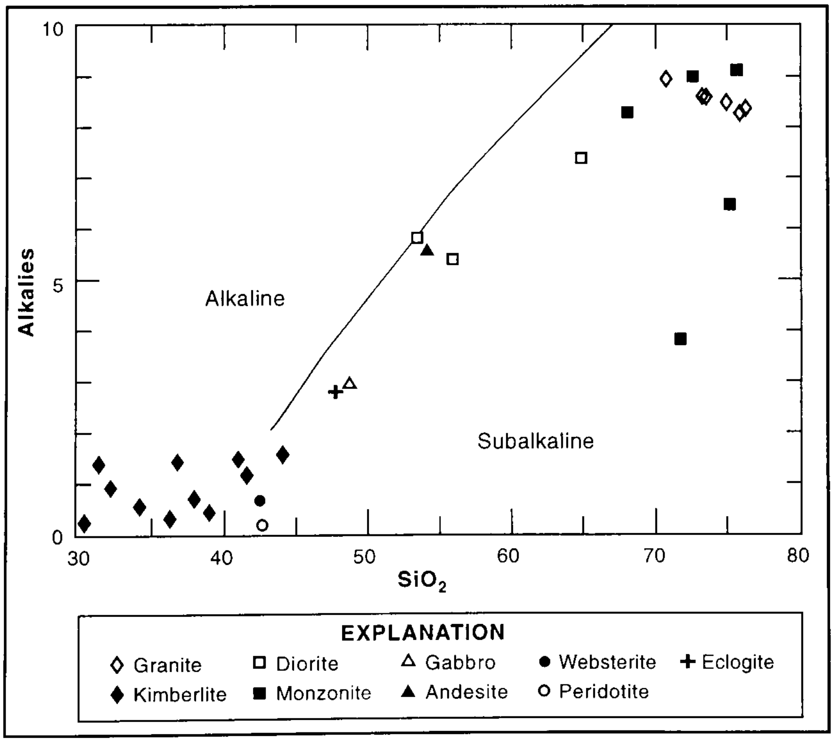

Figure 19. Plot of alkalies versus silica of representative rock samples from the State Line district.

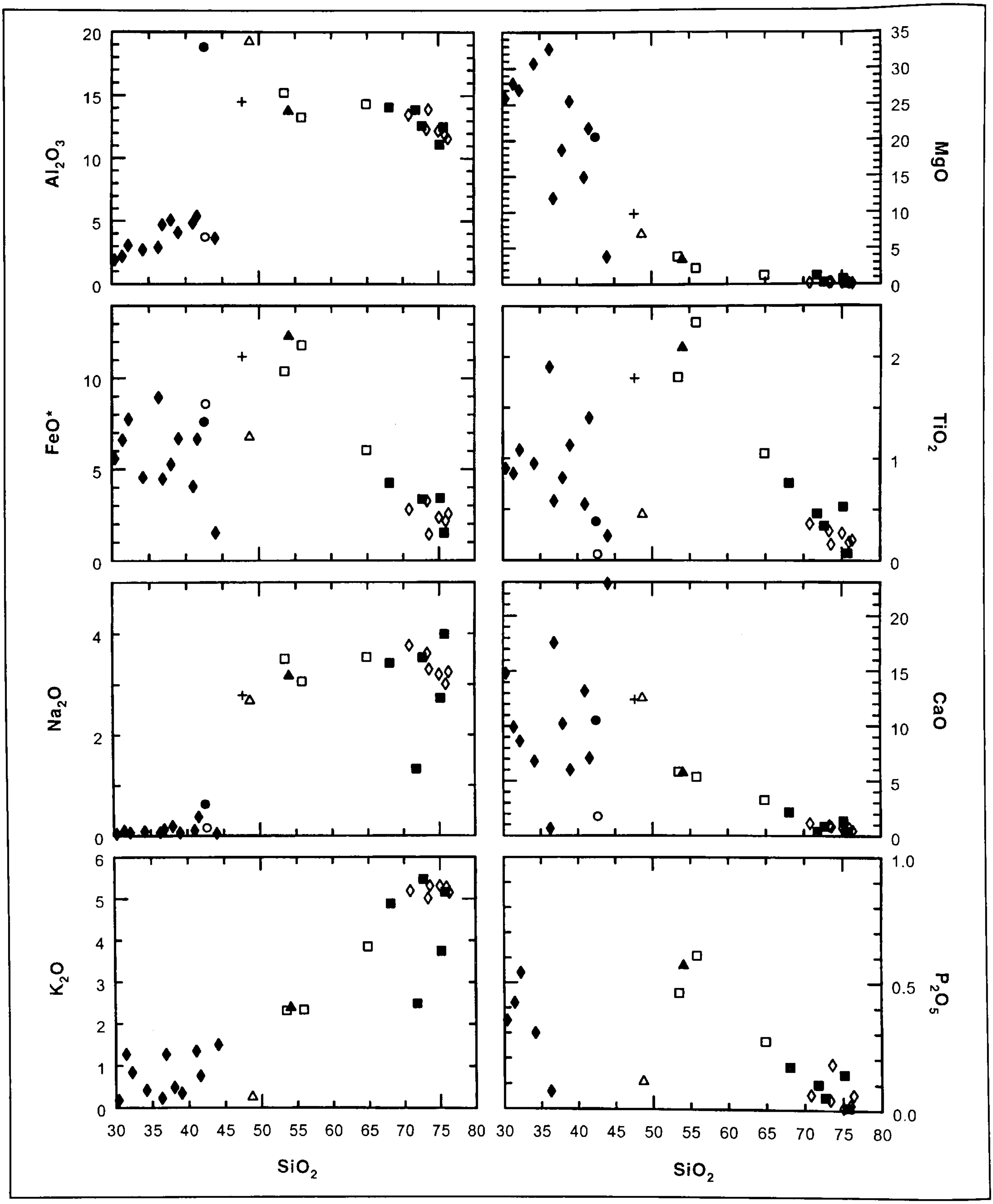

*Figure 20. Harker variation diagram of representative rock samples from the State Line district. Refer to the explanation on Fig. 19. (*includes Fe$_2$O$_3$)*

diatremes, are aligned in a northwest direction, oblique to the local fracture direction (Hausel and others, 1985).

Diatreme facies kimberlites (Fig. 21) differ from hypabyssal kimberlites because they are volcanic breccias. They contain clasts of the country rock, fragments of hypabyssal kimberlites, and rounded pelletal lapilli. Crater facies kimberlites are volumetrically insignificant; however, they do contain important diamond deposits such as Orapa in Botswana.

Four main varieties of kimberlite have been recognized in the State Line district: massive to porphyritic, carbonate-rich massive to porphyritic, breccia, and carbonate-rich breccia (Smith and others, 1979). The massive to porphyritic kimberlite is best exposed in the Iron Mountain district of Wyoming and in the kimberlite dikes near Estes Park, Colorado. This type of kimberlite contains up to 50 percent rounded to subrounded olivine and enstatite phenocrysts set in a fine-grained matrix of serpentine, calcite, dolomite, phlogopite, magnetite, perovskite, and other minerals. Serpentine, dolomite, hematite, magnetite, and iddingsite replace olivine phenocrysts. Massive to porphyritic kimberlite contains only a small percentage of lithic xenoliths.

The carbonate-rich massive to porphyritic kimberlite is texturally similar to the massive to porphyritic kimberlite variety; however, it contains a much greater amount of carbonate minerals, most of which replace phenocrysts, xenocrysts, and serpentine in the matrix.

Kimberlite breccia and carbonate-rich kimberlite breccia contain significant numbers of xenoliths: Lower Paleozoic sedimentary rocks; Proterozoic crystalline rocks including granites and schists; and upper mantle nodules of spinel and garnet peridotite, garnet clinopyroxenite and websterite, dunite, eclogite, monomineralic megacrysts, and carbonatite. The xenoliths and olivine phenocrysts are set in a fine-grained matrix of serpentine, carbonate, perovskite, magnetite, hematite, and other secondary minerals.

The Schaffer number 3 diatreme (Fig. 17) has been dated at 377 Ma by the fission track method on zircons (Naeser and McCallum, 1977). The presence of xenoliths of fossiliferous Ordovician and Silurian clastic and carbonate rocks in the kimberlites confirm this date.

Kimberlite from the Green Mountain area west of Boulder (Fig. 16) differs from the State Line district kimberlites in that the Green Mountain kimberlite has larger phenocrysts of ilmenite and olivine, up to a centimeter in diameter. The Green Mountain kimberlite does not contain any xenoliths of Phanerozoic rocks. Kridelbaugh and others (1972) suggested that this diatreme was emplaced during the Precambrian based on reconnaissance paleomagnetic considerations. Later investigations by Larson and Amini (1981) established a Devonian age of 367 Ma for sphene from the Green Mountain kimberlite. The lack of xenoliths of Paleozoic rocks and the large size of the phenocrysts suggest that the Green Mountain kimberlite may be either a blind hypabyssal pipe or it may represent a normal kimberlite eroded to a deeper level, the root zone facies, than the nearby State Line district diatreme facies kimberlites (Fig. 21).

The Estes Park kimberlite is a short distance south of the town of Estes Park and was discovered in 1975. The dike is one to two yards wide and trends in a northerly direction for approximately a quarter mile. It is characterized by rounded megacrysts of partially chloritized phlogopite. Like all the other kimberlite bodies in the Wyoming-Colorado region it has an age of 377 to 395 Ma based upon the rubidium-strontium radiometric technique (Smith, 1979).

The Kelsey Lake kimberlites form a small group of eight irregular pipes and fissures mostly of diatreme and hypabyssal facies kimberlite. The pipes intrude the Sherman granite and are structurally controlled by joint patterns in the granite. The Kelsey Lake 1 kimberlite consist of multiple phases of diatreme and possible crater facies kimberlite. The Kelsey Lake 2 pipe is a multiphase diatreme facies complex with four phases of serpentine kimberlite breccia (Coopersmith and Schulze, 1996).

Late stage alteration and weathering have affected the primary mineralogy of the Kelsey Lake kimberlites. Phenocrysts of olivine have been replaced by serpentine. Carbonate alteration usually accompanies the serpentinization. Groundmass minerals and megacrysts and xenocrysts of ilmenite, garnet, spinel, phlogopite, and diopside are generally not strongly altered. Mantle-derived xenoliths and xenocrysts include diamond (no diamond-bearing xenoliths have been recovered), altered peridotite fragments, eclogites, megacrysts of ilmenite, garnet, and green clinopyroxene; xenocrysts of garnet, ilmenite, chromite, chrome diopside. Most of the garnets are derived from peridotite, have a purple and red color, and have compositions ("G9" and

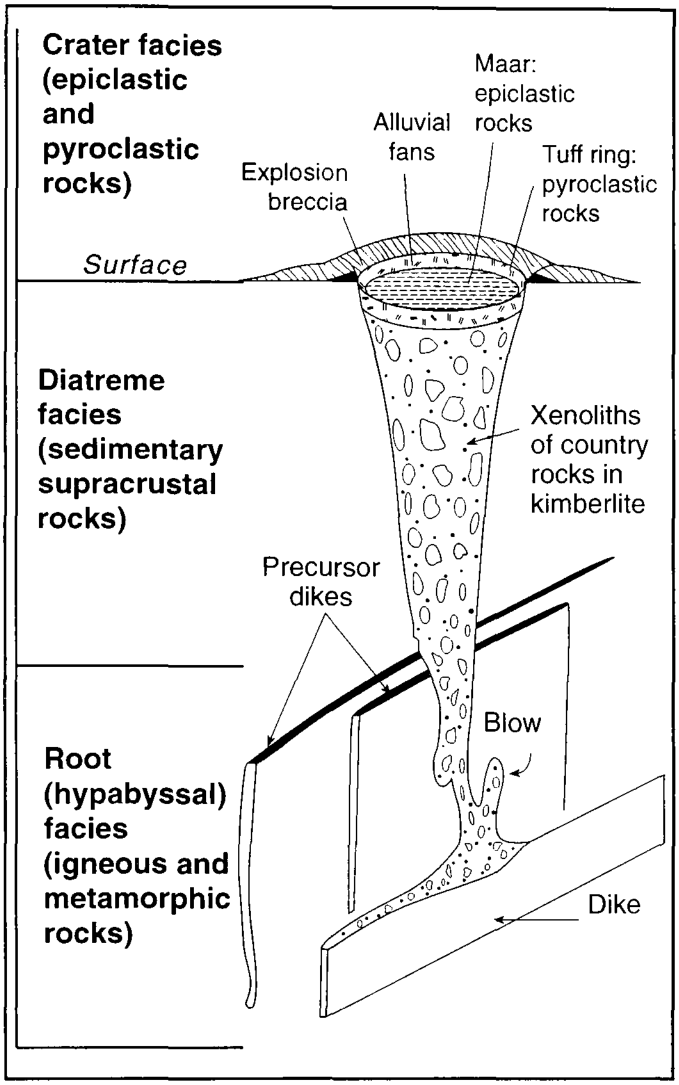

Figure 21. Model of kimberlite maar-diatreme complex showing the relationship between crater, diatreme, and root facies. (From Mitchell, 1986)

"G10", Gurney 1984) that are consistent with the presence of diamonds (Coopersmith and Schulze, 1996).

Most of the diamonds show well developed octahedral faces. Growth forms range from simple to complex. Dodecahedra, transitional octahedra-dodecahedra, and macles and aggregate forms are also found. The diamonds are predominately colorless to white, though some are grayish-black owing to inclusions of graphite (McCallum and others, 1979).

ORIGIN OF ORE DEPOSITS

Diamonds form in nature under only the extreme conditions found in the upper mantle: pressures of greater than 50 kilobars and temperatures of 900 to 1,300° C and possibly higher (Kirkley and others, 1992). Kimberlites are magmatic bodies that originate in the upper mantle and intrude upward through the lower and upper crust, eventually reaching the earth's surface as a maar-diatreme complex (Fig. 21). Kimberlites have three facies depending upon their position in the mantle and crust; the root facies, the diatreme facies, and the crater facies (Mitchell, 1986). The shape of the kimberlite is as pictured in Figure 21, similar to a carrot, a comparatively wide upper zone, up to several hundred meters in diameter, in the diatreme and crater facies, which narrows down to a thin intrusive dike, possibly only a meter thick, in the root facies. The forceful intrusion of the kimberlite fractures and brecciates the surrounding rocks of the upper mantle and crust and incorporates them as xenoliths.

Peridotite and eclogite xenoliths both host diamonds. Diamonds are probably more abundant in peridotites, although that rock disaggregates more readily than eclogite. Harzburgite, a variety of peridotite that consists primarily of olivine and orthopyroxene is the most likely to contain diamonds. Eclogites are an unusual rock composed of red pyrope garnets and a rare, green, sodium-rich pyroxene known as omphacite. Eclogites are thought to form at higher temperatures and pressures than peridotites (Kirkley and others, 1992).

Recent dating of inclusions in diamonds from kimberlite and lamproite pipes, mainly in South Africa and Australia, indicate that diamonds formed as early as 3,300 Ma and as late as 990 Ma, an extended period of the earth's history. Diamonds can be vastly older than their host kimberlites. Diamonds from the Kimberly Mine in South Africa were dated at 3,300 Ma although the host kimberlite was not intruded until 100 Ma (Richardson and others, 1984).

The carbon in diamonds from peridotite xenoliths has a narrow range of $\delta^{13}C$ values, –2 to –9‰; whereas, carbon in diamonds from eclogite xenoliths has a wide range of $\delta^{13}C$ values, +3 to –34‰. The wide range of $\delta^{13}C$ values from samples of eclogites is typical of carbon isotopes values found in near- surface sediments and surficial biogenic environments, indicating that eclogites may be formed from the melting of subducted supracrustal rocks (Kirkley and others, 1992).

Kimberlites ascend rapidly to the earth's surface at rates thought to be on the order of 10 to 30 kilometers per hour. There is usually no evidence of any substantial thermal reaction with the surrounding country rock. In the near-surface environment velocities may increase to several hundreds of kilometers per hour because of gas expansion in the ascending magma and reaction with water (Kirkley and others, 1992). Craters, tuff rings and maars are formed as the highly charged kimberlite magma erupts at the surface (Fig. 21). Kimberlites, though rare, are widespread throughout the surface of the earth. Most well known diamond-producing pipes are small, 12 to 75 acres, and they generally occur in clusters, typically, six to forty pipes in any one cluster.

Almost all diamond-bearing kimberlites are found in the stable Archean cratons of the continents, never in oceanic crust or in younger tectonic mountain belts. The presence of supracrustal sediments and volcanic rocks overlying ancient cratonic rocks is a favorable factor because it indicates that the wider, and therefore more economically exploitable, diatreme and crater zones of the kimberlite have probably been preserved (Kirkley and others, 1992).

Most of the economic value from diamondiferous kimberlites lies in the fraction of diamonds that are of gem quality. Most economic kimberlite ore bodies contain about 20 to 40 percent gem-quality diamonds. The grade of ore bodies, which includes industrial to gem-quality diamonds, varies from 10 to 20 carats per 100 tons up to hundreds of carats per 100 tons.

EXPLORATION AND PRODUCTION HISTORY

The diamonds in the kimberlites of the State Line district were discovered in 1975 when a U.S. Geological Survey technician was having difficulties making a thin section of a serpentinized garnet peridotite nodule from one of the State Line district kimberlites. After noting deep scratches on a grinding plate used in preparing thin sections, the technician found that the scratches were made by a tiny white diamond crystal, less than 1 millimeter in diameter. Several other small diamonds were found in the sample (McCallum and Eggler, 1976).

The Superior Oil Company which acquired leases in and around the Sloan kimberlites (Fig. 17) in 1980, initiated a four-year diamond testing program. Because the kimberlite was poorly exposed, techniques other than surficial geological mapping were necessary. Basic prospecting for kimberlite boulders in the eluvial soil layer and analysis of heavy mineral concentrations in soil and stream sediments outlined the target area of the Sloan kimberlite. Exploration trenching supplemented by a rotary drilling program confirmed a connection between two separated bodies of Sloan kimberlite (Shaver, 1988).

Superior conducted geophysical and soil geochemical surveys over the Sloan kimberlite. The most successful of these techniques was a very low frequency resistivity survey (Fig. 22). A robust contrast was noted because the kimberlites were much more weathered than the surrounding granitic rocks. Ground magnetics was less definitive the kimberlites and the granitic rocks lack a strong magnetic contrast. Concentrations of nickel and chromium in soil samples taken over the kimberlite were anomalously high (Shaver, 1988).

Superior built a test plant near the Sloan kimberlite for bulk testing the kimberlite ores. Two types of samples were collected: a bulk sample of 50 metric tons assayed for macroscopic diamonds, and several 25 kilogram samples from the bulk samples and drill core assayed for microscopic diamonds. More than 2,500 metric tons of material were processed at the plant. The grade of the Sloan 1 kimberlite is 8 carats per 100 metric tons, and the grade of the Sloan 2 is 20 carats per 100 metric tons. Fifteen percent of the diamonds were gem quality, 65 percent were near-gem, and 20 percent were industrial. However, the economic potential of the prospect was limited by a lack of large stones; the average weight of the diamonds was 0.01 carat and the largest was only 1.24 carats (Shaver, 1988).

Similar geophysical and geochemical surveys and bulk sampling were completed by Cominco American, Inc. at the Schaffer and Aultman kimberlites (Fig. 17). As at the Sloan kimberlite, resistivity surveys were the most effective geophysical tool and nickel and chromium in soil were the most effective geochemical indicators. Approximately 8,000 metric tons of kimberlite were bulk sampled and the grades ranged from 0.5 to 1.0 carat per 100 tons; the ratio of gem stones to industrial grade stones was about the same as found in South African kimberlites, 1 to 5 (Lincoln, 1982).

The Kelsey Lake prospect (Fig. 17) consists of eight kimberlite pipes. In 1995 Colorado Diamond Co., a subsidiary of Redaurum Red Lakes Mines Ltd. of Toronto, announced a 300,000 ton per year

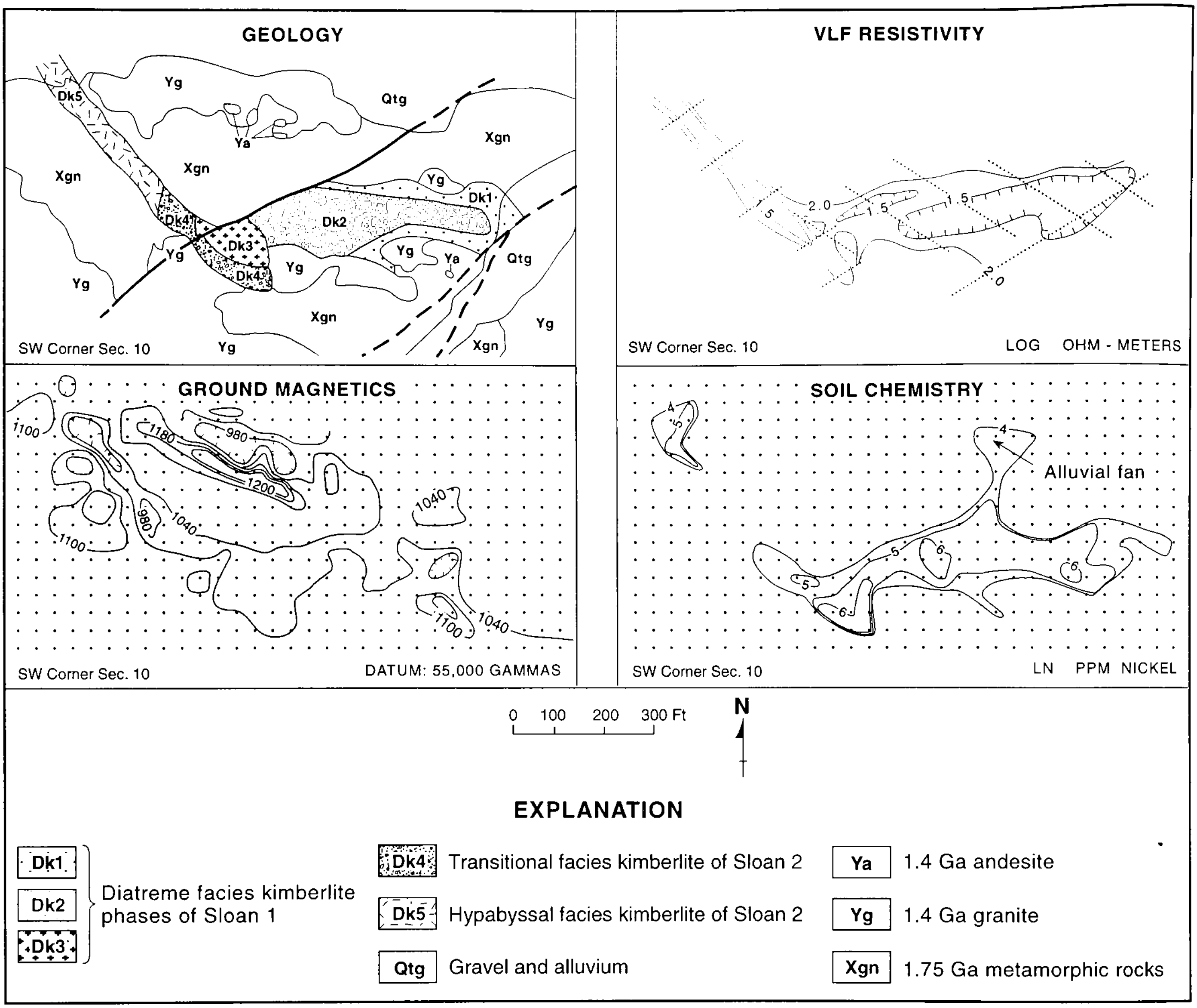

Figure 22. Comparison of geophysical and geochemical exploration techniques with the geology of the Sloan 1 and 2 kimberlite (see Fig. 17). (From Shaver, 1988)

trial mining program on their Kelsey Lake kimberlite prospect. Open pit mining began in late 1996 on the Kelsey Lake 1 and Kelsey Lake 2 kimberlites, the two largest pipes, which have a surface area of about 20 acres. The $2 million processing plant began production in the spring of 1996. The Kelsey Lake Mine is North America's first commercial diamond producer since the turn of the century. The mine and processing plant will be upgraded to 1 million tons per year production after the two year trial mining program.

The Kelsey Lake kimberlites contain predominantly diatreme-facies kimberlite, with minor local hypabyssal and crater facies. Alteration and weathering of the kimberlites is pervasive. Olivine phenocrysts and macrocrysts are replaced by serpentine and carbonate. Groundmass minerals consist of diopside, perovskite, apatite, and calcite. Macrocrysts and xenocrysts of ilmenite, garnet, spinel, phlogopite, and diopside are well preserved (Coopersmith, 1997).

A 14.2 carat, gem-quality white diamond was recovered from the Kelsey Lake kimberlite during bulk sample testing in 1994. During the summer of 1996, a 28.3 carat, gem-quality yellow diamond was unearthed. These two diamonds were the largest ever recovered from the State Line district. The 28.3 carat yellow diamond is the fifth largest found in the United States. In July 1997 the company recovered two gem-quality stones weighing 28.2 and 16.3 carats. Colorado Diamond Co. expected the mine to produce about 25,000 carats of diamonds in 1996 and 100,000 carats in 1997. To 1997 about 65 percent of the recovered diamonds from the Kelsey Lake Mine were of gem-quality.

REFERENCES

Ater, P.C., Eggler, D.H., and McCallum, M.E., 1984, Petrology and geochemistry of mantle eclogite xenoliths from Colorado-Wyoming kimberlites: Recycled ocean crust?, *in* Kornprobst, J., ed., Kimberlites II: The mantle and crust relationships—Proceedings of Third International Kimberlite Conference, Summer 1982, Clermont-Ferrand, France, Amsterdam, Elsevier, p. 309–318.

Boos, M.F., and Boos, C.M., 1933, Granites of the Front Range: The Log Cabin Granite [abs.]: Geological Society of America Proceedings, p. 69.

Coopersmith, H.G., 1991, Geology and exploration of the Kelsey Lake diamondiferous kimberlite, Colorado: Presented at the Society of Mining Engineers Annual Meeting, Denver, Colorado, February,1991.

_____1997, Kelsey Lake: first diamond mine in North America: Mining Engineering, v. 49, no. 4, p. 30–33.

Coopersmith, H.G., and Schulze, D.J., 1996, Development and geology of the Kelsey Lake Diamond Mine, Colorado, *in* Thompson, T.B., ed., Diamonds to Gold, I. State Line Kimberlite District, Colorado, II. Cresson Mine, Cripple Creek District, Colorado: Society of Economic Geologists Field Conferences Guidebook Series, v. 26, p. 5–19.

Darton, N.H., Blackwelder, E., and Siebenthal, C.E., 1910, Laramie-Sherman Folio: U.S. Geological Survey Folio 173, 17 p.

Eggler, D.H., 1968, Virginia Dale Precambrian ring dike complex, Colorado-Wyoming: Geological Society of America Bulletin, v. 79, p. 1545–1564.

Eggler, D.H., McCallum, M.E., and Kirkley, M.B., 1987, Kimberlite transported nodules from Colorado-Wyoming—A record of enrichment of shallow portions of an infertile lithosphere, *in* Morris, E., and Pasteris, J.D., eds., Mantle metasomatism and alkaline magmatism: Geological Society of America Special Paper 215, p. 77–90.

Eggler, D.H., McCallum, M.E., and Smith, C.B., 1979, Megacryst assemblages in kimberlite from northern Colorado and southern Wyoming—Petrology, geochemistry-barometry, and areal distribution, *in* Boyd, F.R. and Meyer, H.O.A., eds., The mantle sample—Inclusions in kimberlites and other volcanics, Volume 2: Proceedings of the Second International Kimberlite Conference, American Geophysical Union, Washington, D. C., p. 213–225.

Gurney, J.J., 1984, A correlation between garnets and diamonds, *in* Glover, G.J., and Harris, P.G., eds., Kimberlite occurrence and origin—A basis for conceptual models in exploration: Perth, University of Western Australia Publication 8, p. 143–166.

Hausel, W.D., McCallum, M.E., and Roberts, J.T., 1985, The geology, diamond testing procedures, and economic potential of the Colorado-Wyoming kimberlite province—A review: Geological Survey of Wyoming Report of Investigation 31, 22 p.

Kirkley, M.B., Gurney, J.J., and Levinson, A.A., 1992, Age, origin and emplacement of diamonds—a review of scientific advances in the last decade: Canadian Institute of Mining and Metallurgy Bulletin, v. 84, no. 956, p. 48–57.

Kridelbaugh, S.J., Hobblitt, R., Kellogg, K., and Larson, E., 1972, Petrologic and paleomagnetic implications of the Green Mountain diatreme [abs.]: Geological Society of America Abstracts with Programs, v. 4, no. 6, p. 386.

Larson, E.E., and Amini, M.H., 1981, Fission-track dating of the Green Mountain kimberlite diatreme, near Boulder, Colorado: The Mountain Geologist, v. 18, no. 1, p. 19–22.

Lincoln, J.B., 1982, Schaffer-Aultman kimberlite complexes, Albany County, Wyoming, *in* The genesis of Rocky Mountain ore deposits—Changes with time and tectonics: Denver, Proceedings of the Denver Region Exploration Geologists Society Symposium, p. 71–77.

McCallum, M.E., and Eggler, D.H., 1976, Diamonds in an upper mantle peridotite nodule from kimberlite in southern Wyoming: Science, v. 192, p. 253–256.

McCallum, M.E., Eggler, D.H., and Burns, L.K., 1975, Kimberlitic diatremes in northern Colorado and southern Wyoming: First International Conference on Kimberlites, September 24–28, 1973, Cape Town, South Africa: Physics and Chemistry of the Earth, v. 9, p. 149–161.

McCallum, M.E., and Mabarak, C.D., 1976, Diamond in State-Line kimberlite diatremes, Albany County, Wyoming and Larimer County, Colorado: Geological Survey of Wyoming Report of Investigation 12, 36 p.

McCallum, M.E., Mabarak, C.D., and Coopersmith, H.G., 1979, Diamonds from kimberlites in the Colorado-Wyoming State Line district, *in* Boyd, F.R. and Meyer, H.O.A., eds., Kimberlites, diatremes, and diamonds—Their geology, petrology, and geochemistry, Proceedings of the Second International Kimberlite Conference, v. 1, Washington, D.C., American Geophysical Union, p. 42–58.

McCallum, M.E., and Smith, C.B., 1978, Minor and trace element contents of kimberlites of the Front Range, Colorado and Wyoming: U.S. Geological Survey Open File Report 78-1011.

Mitchell, R.H., 1986, Kimberlites: mineralogy, petrology and chemistry: New York, Plenum Press, p. 442.

_____1991, Kimberlites and lamproites—Primary sources of diamond: Geoscience Canada, v. 18, p. 1–16.

Naeser, C.W., and McCallum, M.E., 1977, Fission-track dating of kimberlitic zircons [extended abs.] Second International Kimberlite Conference, Santa Fe, New Mexico, no pagination.

Peterman, Z.E., Hedge, C.E., and Braddock, W.A., 1966, Precambrian geochronology of the northeastern Front Range, Colorado [abs.], Geological Society America Special Paper 87, p. 127.

_____1968, Age of Precambrian events in the northeastern Front Range, Colorado: Journal of Geophysical Research, v. 73, p. 2,277–2,296.

Richardson, S.H., Gurney, J.J., Erlank, A.J., and Harris, J.W., 1984, Origin of diamonds in old enriched mantle: Nature, v. 310, p. 198–202.

Shaver, K.C., 1988, Exploration of the Sloan Ranch complex—a diamondiferous kimberlite prospect in northern Colorado: Mining Engineering, v. 40, no. 1, p. 45–48.

Smith, C.B., 1979, Rb-Sr mica ages of various kimberlites: Kimberlite Symposium II, Cambridge, England, v. 1, p. 61–64.

Smith, C.B., McCallum, M.E., Coopersmith, H.G., and Eggler, D.H., 1979, Petrochemistry and structure of kimberlites in the Front Range and the Laramie Range, Colorado-Wyoming, *in* Boyd, F.R., and Meyer, H.O.A., eds., Kimberlites, diatremes, and diamonds: Their geology, petrology, and geochemistry, Proceedings of the Second International Kimberlite Conference, v. 1, Washington, D.C., American Geophysical Union, p. 178–189.

Chapter 5

La Plata District

INTRODUCTION

The La Plata district (also called the California district) is located in the La Plata Mountains in Montezuma and La Plata counties just to the northwest of the City of Durango (Fig. 23). Some mention of the La Plata district was made by the geologists of the Hayden Survey shortly after the discovery of the district (Holmes, 1877). The laccolithic nature of the La Plata Mountains was recognized soon after the discovery of precious metals in the district (Cross, 1894). The first detailed description of the geology and ore deposits of the district was completed in 1899 as part of the U.S. Geological Survey's Atlas series (Cross and others, 1899). The most thorough study of the geologic setting, ore deposits, and mines of the district was reported in U.S. Geology Survey Professional Paper 219 (Eckel, 1949). Other pre-1949 references describing individual mines and ore deposits were listed by Eckel (1949, p. 6–7). No geological investigations or theses of the district were published until Werle and others (1984) produced a study on the Allard stock, one of the alkalic intrusive stocks of economic importance in the La Plata Mountains.

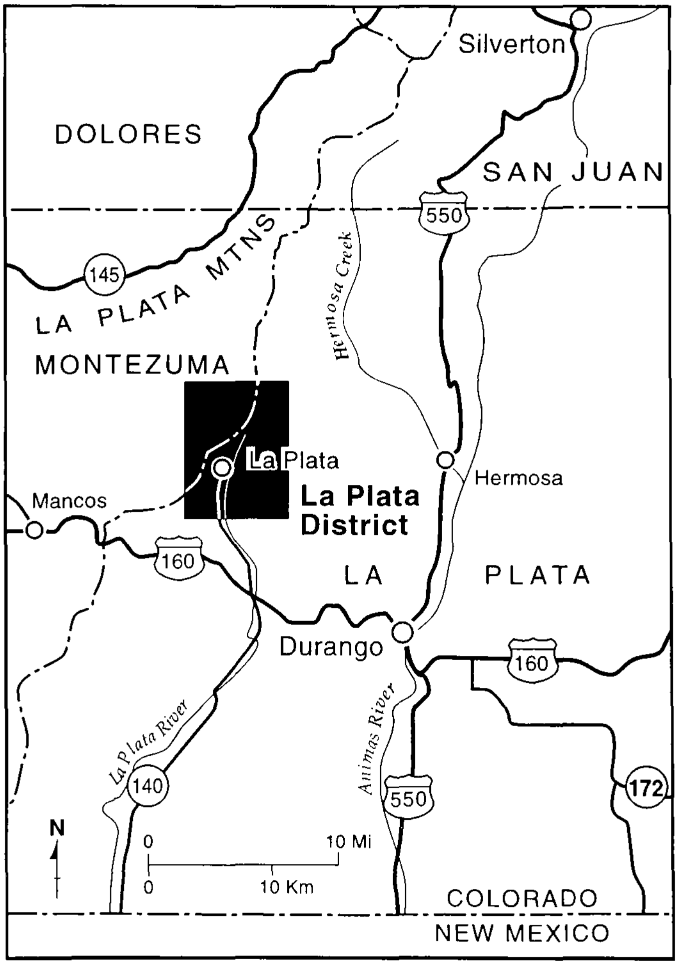

Figure 23. Index map showing the location of the La Plata district, La Plata County, Colorado.

GEOLOGICAL SETTING

The La Plata district is located just to the southeast of the San Juan volcanic field at the southernmost end of the Colorado Mineral Belt (Fig. 23 and Fig. 24). The region consists of a sequence of nonmarine to marine sedimentary rocks of late Paleozoic to late Mesozoic age. These sedimentary rocks were intruded during the Laramide Orogeny, Late Cretaceous to early Tertiary, by sills and laccoliths of alkalic porphyritic rocks. This intrusive event caused the broad structural doming of the region. A somewhat younger intrusive event emplaced five generally equigranular, alkalic stocks of syenite, diorite, and monzonite. The younger stocks are related to contact metamorphism, hydrothermal alteration, and stockwork veining. Formation descriptions are adapted from Eckel (1949) unless otherwise noted.

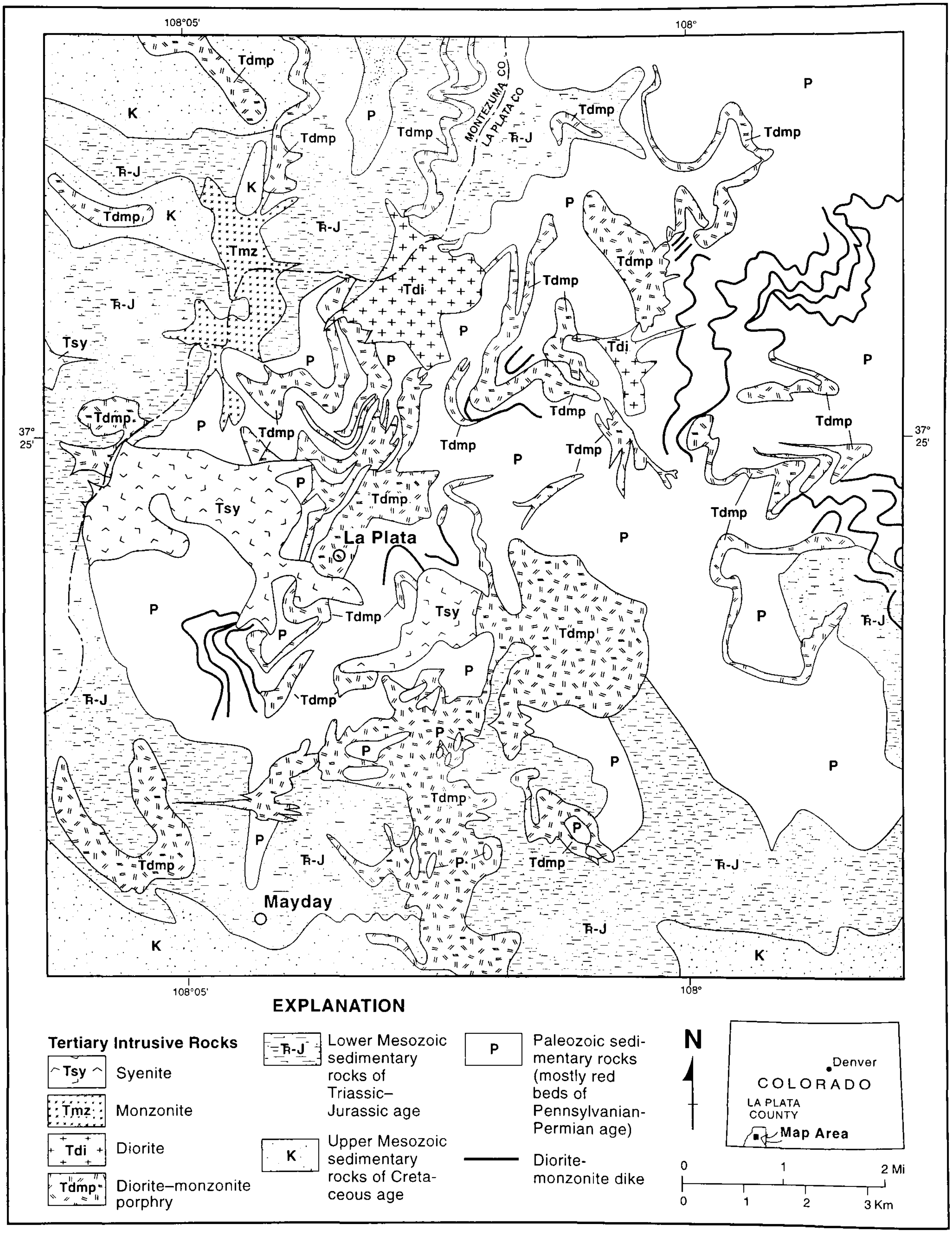

Figure 24. Simplified geological map of the La Plata district, La Plata County, Colorado. (Modified from Eckel, 1949)

PALEOZOIC SEDIMENTARY ROCKS (P)

Hermosa Formation

The Hermosa Formation of Pennsylvanian age is exposed in only a limited area of the La Plata district. It consists primarily of gray and red arkosic sandstone, shale, fossiliferous limestone, and gypsum. The thickness of the Hermosa Formation in the La Plata district is unknown; however, to the east in the Animas River Valley it is 2,751 feet thick.

Rico Formation

The Rico Formation of Permian age consists of about 300 feet of dull-red to maroon sandstone, arkose, and conglomerate. There is also a minor proportion of interbedded shales and sandy to shaley fossiliferous limestone.

Cutler Formation

The Cutler Formation of Permian age consists of 1,400 to 2,200 feet of reddish-brown mudstone, shale, sandstone, and conglomerate. There are minor limestone nodules which locally are metamorphosed to calc-silicate minerals.

MESOZOIC SEDIMENTARY ROCKS (TR-J AND K)

Dolores Formation

The Dolores Formation of Triassic to Jurassic age consists primarily of 400 to 700 feet of reddish-brown mudstone with lesser amounts of maroon to gray, fine-grained sandstone. The base of the Dolores Formation is marked by a 7-feet-thick bed of limestone conglomerate.

Entrada Sandstone

The upper Jurassic Entrada Sandstone consists of 40 to 50 feet of buff to pinkish white fine-grained sandstone. The Entrada Sandstone makes bold outcrops and has striking large-scale cross-bedding.

Wanakah Formation

The Wanakah Formation of upper Jurassic age is 25 to 150 feet thick in the La Plata district. It has been divided into three members from the base of the formation: the Pony Express limestone, the Bilk Creek sandstone, and the Marl member.

The Pony Express limestone consists of up to 30 feet of dark gray to dark blue, bituminous limestone. It has an average thickness of 3 feet and in most places the limestone consists of a single massive bed; however, locally it is composed of three or more beds, each about one foot thick. In some layers there is a suggestion of oolitic or pisolitic structures. The Pony Express limestone hosts several rich ore deposits.

The Bilk Creek sandstone member consists of about 20 feet of white to light-colored, friable, fine-grained sandstone. The uppermost one to two feet of the sandstone are hard and calcareous, and they contain grains of red chert.

The Marl member ranges from 25 to 100 feet in thickness and is composed of pinkish-red to greenish-gray marl, mudstone, and sandstone. In some places a 6-feet-thick bed of sandstone marks the base of the member.

Junction Creek Sandstone

The Junction Creek Sandstone is of Late Jurassic age and consists of 200 to 500 feet of white to light buff, friable, cross-bedded sandstone that contains numerous partings of arkose and greenish-gray to light-red shale. The Junction Creek Sandstone, which strongly resembles the Entrada Sandstone, hosts several ore deposits.

Morrison Formation

The Morrison Formation of Late Jurassic age consists of 400 to 625 feet of lenticular beds of brilliant green shales and light-colored sandstone.

Dakota Sandstone

The Dakota Sandstone of Upper Cretaceous age consists of about 100 feet of conglomeratic sandstone and shale. It is exposed only in the southernmost part of the La Plata district.

Mancos Shale

Like the underlying Dakota Sandstone, the Mancos Shale is found only in the southernmost part of the district. It consists of about 1,000 feet of dark gray to black clay shale.

Laramide Intrusive Rocks

There are two suites of intrusive rocks in the La Plata district. The older suite consists of diorite and monzonite porphyries, generally laccoliths that are related to the doming of the La Plata Mountains. The younger suite consists of equigranular syenites, monzonites, and diorites that occur primarily as irregular stocks and associated sills. These nonporphyritic rocks are associated with intense hydrothermal alteration.

Porphyritic Rocks (Tdmp)

The diorite-monzonite porphyry contains phenocrysts of white plagioclase and dark hornblende in a gray-green groundmass of orthoclase, quartz, and accessory minerals. The porphyries, which are most numerous near the center of the La Plata dome, occur as stocks, dikes, sills, and laccoliths. A zircon from a sample of diorite-monzonite porphyry near Snowstorm Mountain yielded a fission-track date of 59.8 ± 6.3 Ma (Cunningham and others, 1994).

Syenite porphyries are closely related to the diorite and monzonite porphyries and in some areas grade into each other. The syenite porphyry contains phenocrysts of orthoclase, plagioclase, hornblende, and pyroxene. Biotite from unaltered syenite porphyry of the Allard stock yielded a potassium-argon date of 67.8 ± 1.6 Ma (Cunningham and others, 1994). Within the porphyritic rocks there are small intrusive breccia bodies and dikes and sills of fine-grained ferromagnesian rocks.

EQUIGRANULAR ROCKS (Tmz, Tdi, Tsy)

A single stock contains light-gray to pinkish-gray, medium- to fine-grained equigranular monzonite (Tmz). Orthoclase and plagioclase feldspar are the dominant minerals in the monzonite; lesser amounts of augite, hornblende, and biotite also occur. The age of the monzonite as determined by potassium-argon methods is 65.0 Ma (Armstrong, 1969). Two irregularly shaped stocks are composed of a gray, fine-grained diorite (Tdi) that is very similar to the monzonite, differing only in a greater percentage of ferromagnesian minerals and plagioclase feldspar. A potassium-argon date of 67.5 ± 1.6 Ma is reported for the diorite (Cunningham and others, 1977).

Two large stocks of augite syenite (Tsy) crop out in the central part of the district south of the monzonite and diorite stocks. In most places the syenite is strongly altered. Fresh samples contain mostly alkalic feldspars, such as orthoclase, anorthoclase, and microperthite. Augite and lesser amounts of hornblende and biotite constitute the ferromagnesian minerals. Potassium-argon dates for the syenite range from 67.8 ± 1.6 to 72.8 ± 5.5 Ma (Cunningham and others, 1977).

STRUCTURE

The La Plata Mountains are formed by broad domal uplift that is slightly elongate in a northeast direction and is about 15 miles in diameter. The dome is a result of the intrusion of the porphyritic laccolith, which displaced the older sedimentary beds without altering them. The later equigranular intrusive rocks intruded the already existing La Plata dome.

The district contains both early barren faults and later ore-bearing faults. The early barren faults are located predominately in the northwestern and southern parts of the La Plata dome. They are characterized by comparatively large displacements and can be up to several miles in strike length. The younger ore-bearing faults tend to be radially distributed with respect to the La Plata dome and generally have displacements of less than 30 feet. They strike mostly northeasterly and easterly and have lengths of up to a few hundred feet (Eckel, 1949).

GEOCHEMISTRY

Only rock samples from the syenite at Allard Stock have published whole rock analyses. Figure 25 demonstrates that some of the syenites are nepheline normative and have an alkalic character; others are quartz normative and may indicate silica enrichment. The normative feldspar diagram (Fig. 26) demonstrates that all the samples from the Allard Stock are strongly potassic. The Harker diagram (Fig. 27) shows the variation of the major oxides with silica. Table 4 in the appendix lists the geochemical analyses and CIPW norms used in the diagrams.

ECONOMIC GEOLOGY

The six main types of ore deposits in the La Plata district are: quartz-telluride veins, telluride replacement bodies, gold-bearing exoskarns, quartz gold-sulfide veins, breccias, and copper porphyry-type deposits.

QUARTZ-TELLURIDE VEINS

The quartz-telluride veins are the most economically valuable ore deposit type and account for more than 90 percent of the production from the district. The May Day, Idaho, Neglected, Incas, and Gold King were all important mines containing quartz-telluride veins. In general, these deposits are irregular discontinuous veins occupying faults and fractures. The veins average 3 to 5 feet wide but can be as much as 15 feet in width. The main gangue material of the veins is white, green, and dark gray quartz. The green color is reportedly due to roscoelite, a vanadium-rich mica. Other gangue

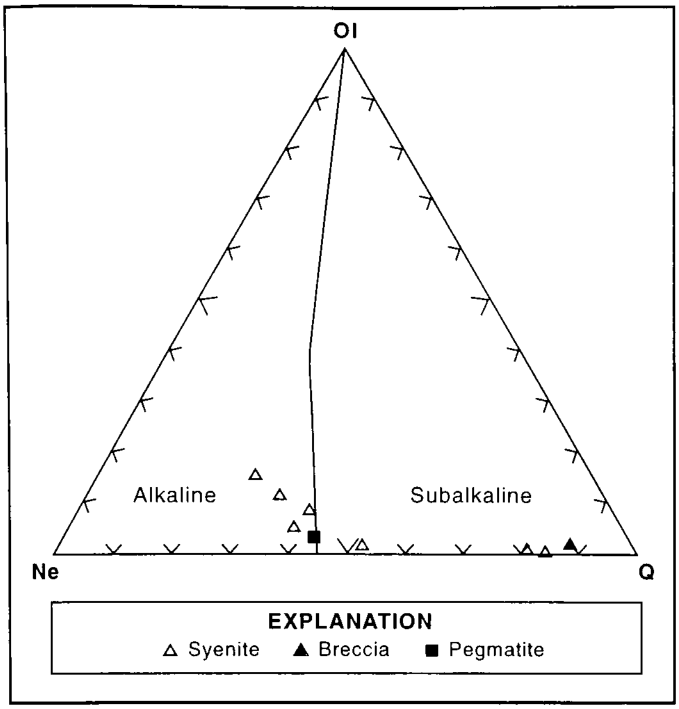

Figure 25. Normative diagram; Ne-Ol-Q of representative rock samples from the La Plata district.

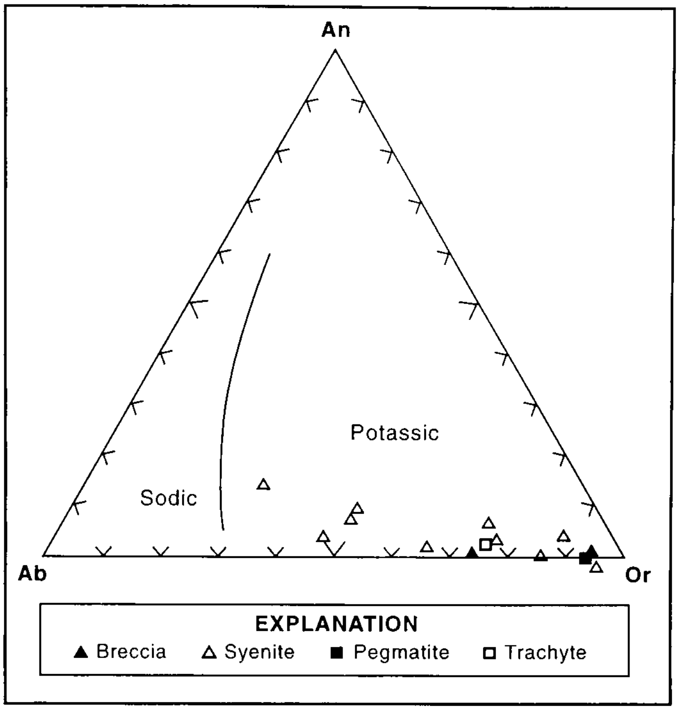

Figure 26. Normative diagram; Ab-An-Or of representative rock samples from the La Plata district.

minerals include barite, ankerite, calcite, fluorite, and dickite (Eckel, 1949).

The main ore minerals are gold tellurides including sylvanite ($AuAgTe_4$), calaverite ($AuTe_2$), hessite ($AgTe_2$), krennerite ($(Au,Ag)Te_2$), and petzite ($AuAg_3Te_2$). Coloradoite (HgTe) is also common in all the telluride ore deposits and may have been the source of the free mercury reported by the earliest prospectors in the district (Eckel, 1949). Native gold and the base metal sulfides including pyrite, arsenopyrite, tetrahedrite, galena, and sphalerite are common in the quartz-telluride veins. The ore minerals form irregular masses intergrown with the gangue minerals (Eckel, 1949).

The Bessie G Mine is composed of two en-echelon vein segments which trend approximately N. 70° E., cutting the Dolores and Cutler Formations. It is parallel to some and cuts across other nearby diorite dikes. The most abundant telluride is coloradoite. The most common precious metal-bearing tellurides are hessite and petzite; less common are sylvanite and krennerite. The Bessie G vein contains abundant native gold commonly associated with telluride minerals. The gold, which contains up to 15 percent silver, is commonly coarse-grained with individual crystals up to a millimeter in diameter. It occurs as isolated grains within late fractures in quartz (Saunders and May, 1986).

Some deposits grouped into this ore type contain only a small percentage of telluride minerals and are characterized by an abundance of base metal sulfides. The Red Arrow and adjacent Outwest Mines are the most productive of this sub-type of quartz-telluride vein deposit. Pyrite, chalcopyrite, galena, sphalerite, tetrahedrite, and arsenopyrite occur within these deposits along with small amounts of telluride minerals. Gold occurs in the native state and is generally coarse grained. The average grade at the Red Arrow mine is one to two ounces per ton of gold, but ranges up to several hundred ounces per ton. Quartz veins with ruby silver, pyrargyrite and proustite, as at the Cumberland Mine, are probably related to this type of ore deposit.

TELLURIDE REPLACEMENT BODIES

Some of the richest ore in the district, up to 400 ounces of gold per ton, came from telluride replacement ores in the Pony Express limestone member of the Wanakah Formation. In the May Day, Incas, and Idaho Mines the replacement ores are associated with ore-bearing telluride veins, barren faults, and porphyry dikes.

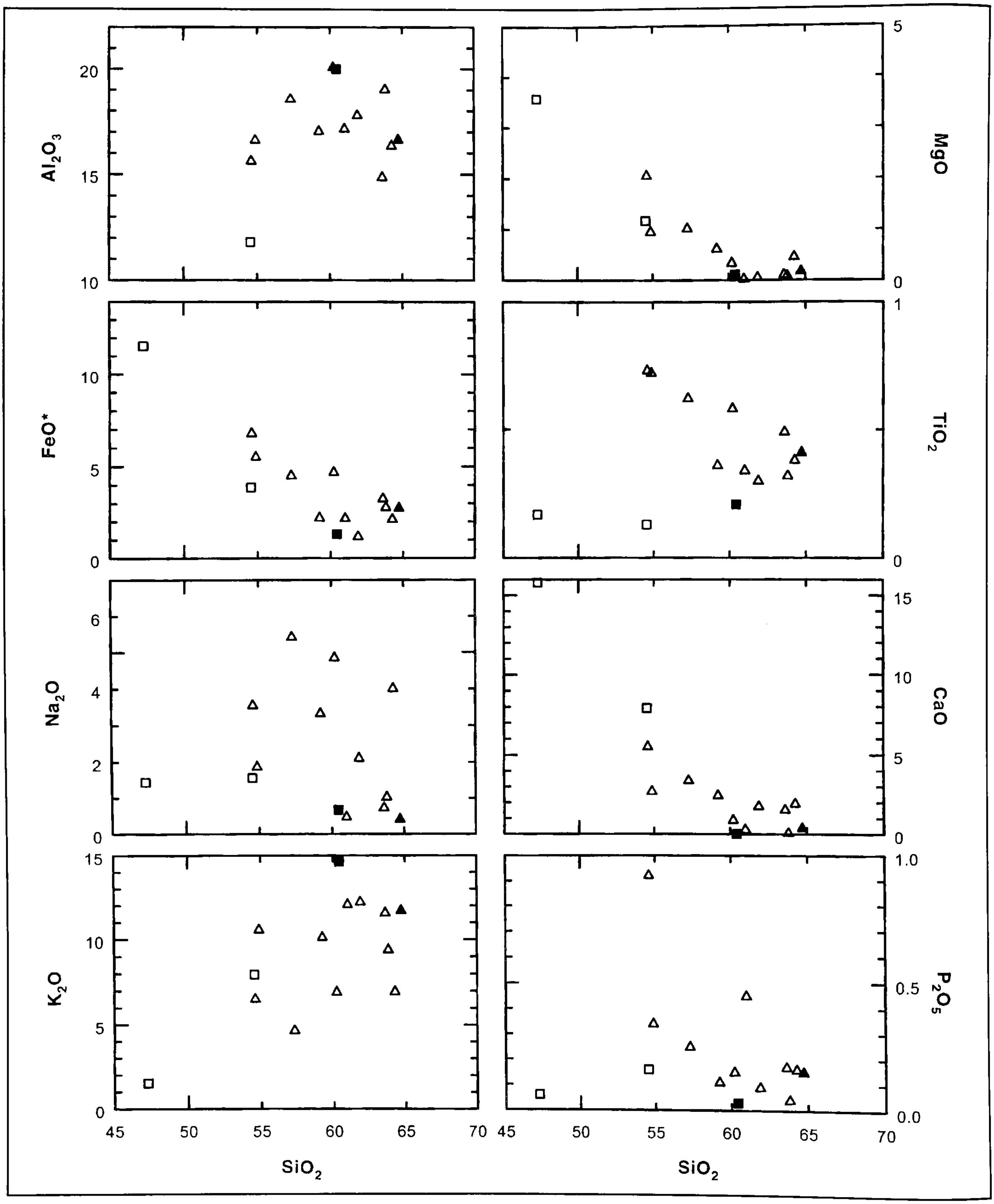

*Figure 27. Harker variation diagram of representative rock samples from the La Plata district. Refer to the explanation on Fig. 26. (*includes Fe_2O_3)*

The replacement gangue minerals consists primarily of calcite, ankerite, and other carbonate minerals. The ore minerals consist of the telluride minerals, free gold, and base metal sulfides. Solid masses of telluride ore, several feet in diameter, have been found some places (Eckel, 1949).

GOLD-BEARING EXOSKARNS

Skarn deposits of variable size occur in the carbonate-rich beds of the Pony Express limestone member and the Dolores Formation. They contain minor gold mineralization associated with base metal sulfides in a gangue of andradite, augite, magnetite, hematite, hornblende, epidote, and minor quartz and calcite. The richest ore of this type was mined from the "Bay City limestone," a 10-feet-thick limestone unit at the base of the Dolores Formation, in the Bay City Mine. Most of the other skarn deposits in the district are small and low grade. All the known economic skarn deposits are wholly or partially oxidized.

QUARTZ-GOLD-SULFIDE VEINS AND REPLACEMENT BODIES

Quartz veins with fine-grained pyrite, chalcopyrite, and barite occur within narrow steeply-dipping shear zones. Low-grade gold mineralization, approximately 0.2 ounce per ton, is probably associated with the pyrite. Only the oxidized portions of these veins were successfully exploited.

The Doyle Mine and the Peerless Mine contain replacement bodies of quartz, pyrite and associated native gold within the Pony Express limestone and calcareous units at the contact of the Dolores and Entrada Formations. There are no tellurides or silicate minerals in this ore type. Unoxidized ore samples contain 0.20 to 0.35 ounces of gold per ton. The oxidized parts of the replacement bodies contain up to 0.75 ounces per ton.

BRECCIAS

There are two broad northeast-trending breccia zones within the La Plata district. Pyrite which contains minor amounts of gold is common throughout the shear zones. Greater amounts of pyrite are concentrated into quartz-gold-sulfide veins where they have been successfully mined. The shear zones between the veins contain gold with grades of 0.03 to 0.05 ounces per ton (Eckel, 1949).

There is one breccia body not associated with the shear zones. The Little Kate breccia is an irregular mass of breccia over 2,250 feet long, 200 to 650 feet wide, and 600 feet deep. The breccia fragments, which consist of sedimentary and igneous rocks, are set in a fine-grained matrix. Quartz gold-sulfide veins with widths from 6 inches to 10 feet are found throughout the breccia. The breccia is reported to contain from 0.01 to 0.04 ounces of gold per ton (Eckel, 1949).

COPPER PORPHYRY-TYPE DEPOSITS

The Copper Hill deposit yielded over 223,000 pounds of copper at a recovered grade of 5 percent copper from the Allard Syenite and associated replacement bodies in sedimentary rocks. Several stages of syenite plutons and hydrothermal alteration were documented by Werle and others (1984):

Stage 1: forceful injection of gray syenite plutons
Stage 2: intense argillic hydrothermal alteration of Stage 1 syenite
Stage 3: intrusion of mafic (greater amounts of hornblende and augite) syenite along northeast-trending shear zones cutting the Stage 1 syenite
Stage 4: formation of breccia pipes by violent escape of volatile gases
Stage 5: intense potassium metasomatism, replacement of argillically altered feldspars in Stage 1 syenite by sanidine
Stage 6: emplacement of trachyte and pegmatite dikes marking the transition from dominantly magmatic to pneumatolitic activity
Stage 7: hydrothermal solutions deposit metallic minerals, sanidine, calcite, and fluorite as veinlets and disseminated masses throughout the stock

The richest ore deposit in the La Plata district, which was worked by the May Day and Idaho Mines, produced 123,000 ounces of gold and 1,142,000 ounces of silver during the period 1903 to 1943. Three main types of ore occur at the May Day and Idaho deposit: quartz telluride veins, limestone replacements, and porphyry-type. The most productive ore type was quartz telluride veins that were emplaced in the Entrada Sandstone, the Pony Express limestone, and the Morrison Formation. Limestone replacements were formed mostly in the Pony Express limestone adjacent to the primary quartz telluride veins. Mineralized porphyry was noted in the mine at the time of active mining, but it was not economic (Eckel, 1949).

EXPLORATION AND PRODUCTION HISTORY

The La Plata Mountains were named by eighteenth century Spanish explorers who reportedly found silver mines there in 1776 (Eckel, 1949, p. 51). Placer gold was discovered along the La Plata River in 1873. The first lode claim was located in June 1874 on the South Comstock vein and by 1880 several lode mines including the Comstock, the Ashland, the Century, and the Cumberland were in production. The most prolific producers were the May Day and Idaho Mines, discovered in 1902 and 1903 respectively. These two mines produced about $3 million worth of ore, about half the total district's production, through 1937. None of the other individual mines of the district were large producers.

From 1878 to 1980 the La Plata district produced 203,227 ounces of gold, 2,037,060 ounces of silver, 280,476 pounds of copper, and 726,083 pounds of lead. Production from the mines of the La Plata district declined rapidly after World War II ended in 1945. Less than 4,000 ounces of gold were produced in the years from 1945 through 1980 (Henderson, 1926; U.S. Bureau of Mines Mineral Resources of the United States, 1924–1931; U.S. Bureau of Mines Mineral Yearbooks 1932–1980).

In the 1980s Exxon Minerals conducted an aggressive exploration program in the La Plata Mountains focussing their attention on the Bessie G Mine. In succeeding years several other exploration companies have conducted exploration in the district; however, no new large or high grade ore deposit has been discovered in the region.

REFERENCES

Armstrong, R.L., 1969, K-Ar dating of laccolithic centers of the Colorado Plateau and vicinity: Geological Society of America Bulletin, v. 80, p. 2,081–2,086.

Cross, W., 1894, The laccolithic mountain groups of Colorado, Utah, and Arizona: U.S. Geological Survey 14th Annual Report, pt. 2, p. 157–241.

Cross,W., Spencer, A.C., and Purington, C.W., 1899, The La Plata quadrangle: U.S. Geological Survey Atlas, La Plata Folio no. 60.

Cunningham, C.G., Naeser, C.W., and Marvin, R.F., 1977, New ages for intrusive rocks in the Colorado mineral belt: U.S. Geological Survey Open File Report 77-573, 7 p.

Cunningham, C.G., Naeser, C.W., Marvin, R.F., Luedke, R.G., and Wallace, A.R., 1994, Ages of selected intrusive rocks in the Colorado mineral belt: U.S. Geological Survey Bulletin 2109, 31 p.

Eckel, E.B., 1949, Geology and ore deposits of the La Plata District, Colorado: U.S. Geological Survey Professional Paper 219, 179 p.

Henderson, C.W., 1926, Mining in Colorado—A history of discovery, development, and production: U.S. Geological Survey Professional Paper 138, 263 p.

Holmes, W.H., 1877, Report as a geologist of the San Juan division: U.S. Geological and Geographical Survey of the Territories (Hayden), 9th Annual Report for 1875, p. 237–276.

Saunders, J.A., and May, E.R., 1986, Bessie G: A high-grade epithermal gold telluride deposit, La Plata County, Colorado, *in* McDonald, J.A., ed., Proceedings of Gold '86, an International Symposium on the Geology of Gold: Toronto, p. 436–444.

U.S. Bureau of Mines, 1924–1931, Mineral Resources of the United States.

_____1932–1980, Mineral Yearbooks.

Werle, J.L., Ikramuddin, M., Mutschler, F.W., 1984, Allard Stock, La Plata Mountains, Colorado—an alkaline rock-hosted porphyry copper—precious metal deposit: Canadian Journal of Earth Science, v. 21, p. 630–641.

Chapter 6

Hahns Peak District

INTRODUCTION

Hahns Peak forms a unique cone-shaped mountain about 15 miles west of the Park Range. The small villages of Columbine and Hahns Peak survive mainly as tourist camps. The area is accessible by county road from Steamboat Springs (Fig. 28).

GEOLOGICAL SETTING

The oldest rocks in the region surrounding Hahns Peak are Proterozoic gneisses, schists, quartzite, metaconglomerate, and amphibolite. Younger rocks include Triassic through Tertiary sedimentary rocks and a late Tertiary porphyritic intrusive complex which is the primary host for the lode mineralization in the district (Segerstrom and Young, 1972). Only Jurassic and younger rocks are shown on Figure 28 and described below.

MESOZOIC AND CENOZOIC SEDIMENTARY ROCKS

Morrison Formation, Jurassic (Jm)

The Morrison Formation is generally poorly exposed in the Hahns Peak area. The best exposure is on the north side of Hahns Peak where it consists of 267 feet of greenish gray and reddish brown sandstone, claystone, and fresh water limestone (Barnwell, 1955). On the west side of Hahns Peak the Morrison Formation is bleached white and contains fine-grained, disseminated pyrite due to hydrothermal alteration (Segerstrom and Young, 1972).

Dakota Formation, Cretaceous (Kd)

The Dakota Sandstone is approximately 90 to 120 feet thick and consists of consists of a basal unit of cross-bedded chert and quartz pebble conglomerate, a middle unit of medium-grained sandstone, and an upper unit of sandstone and interbedded shale (Barnwell, 1955). The basal conglomerate is usually strongly silicified (Casaceli, 1983).

Mancos Formation, Cretaceous (Km)

The Mancos Formation consists of 900 feet of black shale, bentonite, and limestone (Barnwell, 1955) and may, locally, develop slaty cleavage owing to contact metamorphism.

Browns Park Formation, Tertiary (Tb)

The Browns Park Formation of Miocene and Pliocene age consists of coarse conglomerate, red to yellow sandstone, and minor volcanic ash (Segerstrom and Young, 1972).

TERTIARY PORPHYRITIC INTRUSIVE AND EXTRUSIVE ROCKS (Tp AND Tpa)

The Hahns Peak porphyry is a composite stock that is composed primarily of quartz latite. A potassium-argon date of 10.0 ± 0.3 Ma was obtained on a sanidine crystal from a unit named the 7D Porphyry. A slightly older date of 11.5 ± 0.4 Ma was obtained on a sanidine from a dike that cuts the Hahns Peak porphyry. A reasonable age estimate for the intrusion of the stock is 12 Ma (Segerstrom and Young, 1972).

The composite porphyry stock has been divided into smaller units by various workers. Dowsett (1980) divided the porphyry into three smaller stocks, whereas Casaceli (1983) subdivided the porphyry into five separate stocks. The oldest stock is the Beryl porphyry which is a dark green to black, quartz latite porphyry with phenocrysts of plagio-

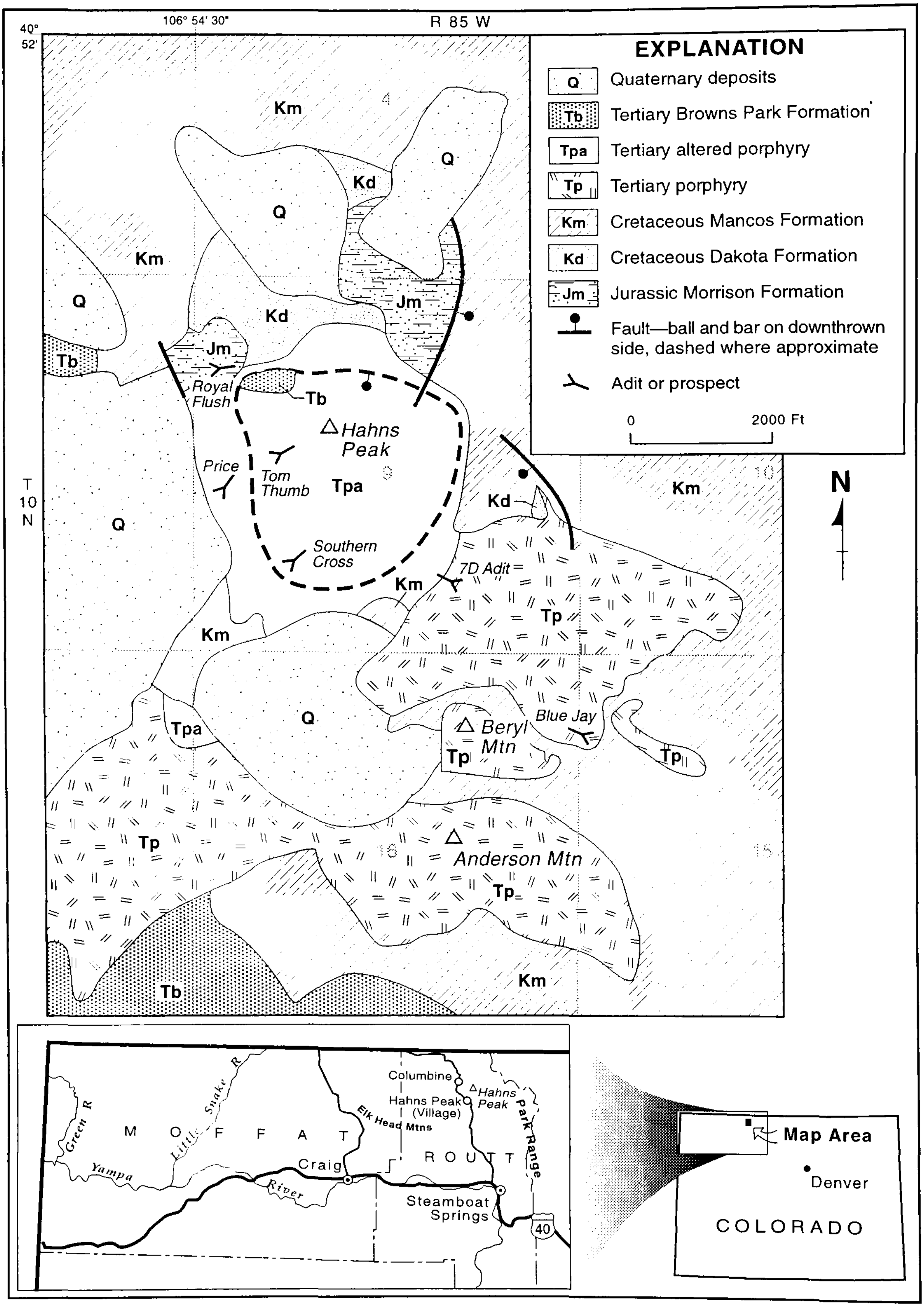

Figure 28. Geologic and index map of the Hahns Peak district, Routt County, Colorado. (From Segerstrom and Young, 1972)

clase, biotite, quartz, sanidine, and trace amounts of hornblende, apatite, and sphene. The other intrusive units named by Casaceli (1983) are all varieties of quartz latite with different colors, alteration styles, structures, and slightly differing amounts of phenocrysts. Intrusive breccias, both heterolithic and monolithic, and aplite and porphyry dikes are found within the porphyritic rocks.

Breccias and volcaniclastic rocks have been described on Hahns Peak and in the region by various authors. Dowsett (1980) and Segerstrom and Young (1972) interpreted the breccia units as tectonic breccias, whereas Casaceli (1983) proposed that the breccias were of hydrothermal origin and described the volcaniclastic units as a vent complex consisting of tuff, lapilli, and bomb sized airfall beds and a base surge deposit.

STRUCTURE

Hahns Peak is located at the eastern end of a series of Tertiary intrusive and extrusive rocks in the Elkhead Mountains. Structurally, Hahns Peak is a composite laccolith within in a horst block between two major east-trending faults, the King Solomon Fault and the Grouse Mountain Fault.

The sedimentary rocks surrounding Hahns Peak have been domed by the intrusion of the porphyry. Locally, some of the sedimentary rocks are overturned or are steeply-dipping. In one drill hole rocks of the Morrison Formation were found at a depth of 2,500 feet below the intrusive (Young and Segerstrom, 1973). Several normal and reverse faults cut the porphyry and influence the mineralization, brecciation, and hydrothermal alteration.

HYDROTHERMAL ALTERATION

The Hahns Peak porphyry shows two periods of alteration. Early stage alteration consists primarily of a silicification and sulfide mineralization that occurred before intrusion of the porphyry. Pyrite and minor amounts of molybdenite in silica stockwork systems were deposited during this stage of alteration (Casaceli, 1983).

The main stage of alteration occurred during the emplacement of the Hahns Peak porphyry and consists of an inner phyllic zone grading outward into mixed phyllic-argillic, argillic, and propylitic zones. The propylitic zone is moderately developed and consists of albite, calcite, montmorillonite, chlorite, and sericite. The argillic zone is also moderately developed and consists of montmorillonite, kaolinite, and sericite with lesser amounts of chlorite and quartz; disseminated pyrite is found throughout. The mixed phyllic-argillic zone consists of sericite, quartz, kaolinite, and montmorillonite, and disseminated pyrite (average content of 1.5 percent). The phyllic zone consists of sericite, quartz, and minor kaolinite. The plagioclase feldspar phenocrysts are completely replaced by sericite, quartz, and kaolinite. Disseminated pyrite is common throughout the phyllic zone. There are small zones of advanced argillic alteration associated with fine-grained pebble breccias. (Casaceli, 1983).

GEOCHEMISTRY

Whole rock analyses from the Tertiary porphyritic rocks and Proterozoic igneous and metamorphic rocks are shown on a Le Bas diagram (Fig. 29). The trachytes, trachyandesite, andesine trachybasalt, latite, rhyodacite, and rhyolite all plot in the alkalic region of the Le Bas diagram. The Harker variation diagram (Fig. 30) shows the major oxides against silica. Of interest is the constant sodium oxide content of all rocks from the district. Table 5 in the appendix lists the geochemical analyses and CIPW norms used in the diagrams.

ECONOMIC GEOLOGY

Early mineralization at Hahns Peak occurred during the early stage hydrothermal alteration event when minor amounts of pyrite and molybdenite were deposited in a silica stockwork system. According to Casaceli (1983) two late mineralization events occurred during the formation of the hydrothermal breccias. Pyrite, galena, sphalerite, and chalcopyrite occur within the breccia matrix and in altered porphyry. The distribution pattern of anomalous lead, silver, and manganese is coincident the breccia. Anomalous amounts of gold and silver are found in the upper portions of the breccia bodies and was probably the source of the placer gold that occurs is in streams surrounding Hahns Peak.

The highest base metal values noted by Casaceli (1983) came from a pebble dike in a breccia in the 7D adit: copper, 1,660 parts per million (ppm); lead, 7,700 ppm; zinc, 18,000 ppm; molybdenum, 2,200 ppm; and silver, >100 ppm. A sample taken from the adjacent wall rock was also anomalous: copper, 615 ppm; lead, 3,200 ppm; zinc, 3,300 ppm,

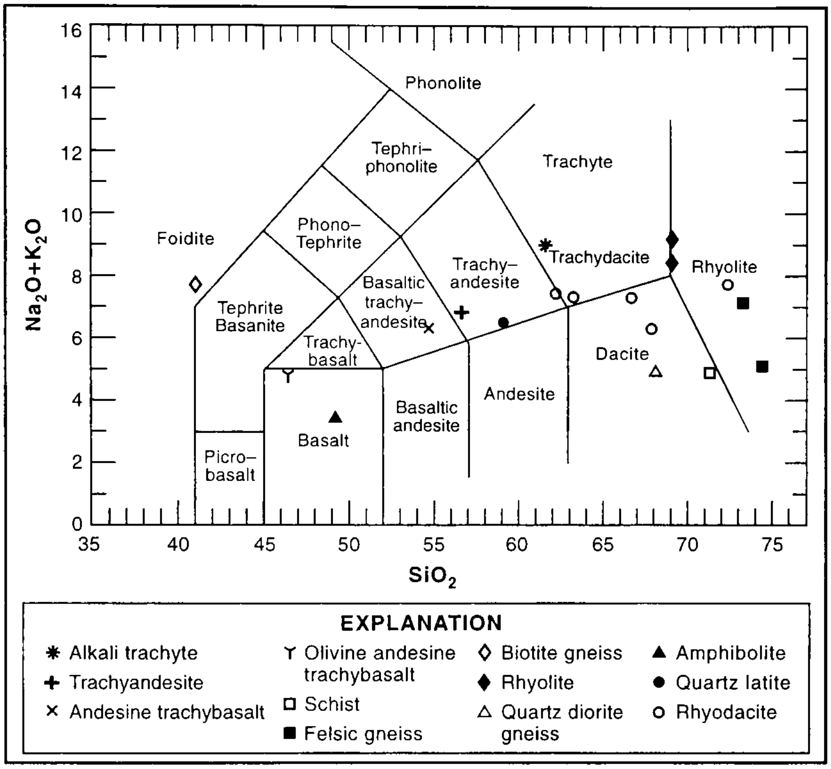

Figure 29. Le Bas diagram of representative rock samples from the Hahns Peak district.

molybdenum, 17 ppm; and silver, 18 ppm. A sample of the hydrothermal breccia near the Tom Thumb Mine contained 24 ppm gold.

EXPLORATION AND PRODUCTION HISTORY

The Hahns Peak gold placers were first noted in 1864 by a Captain Way but were developed by Joseph Hahn and W. A. Doyle in 1865 and 1866. According to George and Crawford (1909), $200,000 to $500,000 was a conservative estimate of gold production between 1866 and 1909. Placer mining continued at a much diminished scale up through the 1950s (Parker, 1974). Production from 1933 to 1945 from the Hahns Peak district (including lode mines) was worth only $16,800 (Vanderwilt, 1947). Lode mining attempts produced fairly high grade ore (about $60 to $70 per ton) from the Tom Thumb and Minnie D. Mines (Gale, 1905). However, limited tonnage and poor transportation from this remote part of the state contributed the lack of profitability of these operations (George and Crawford, 1909).

REFERENCES

Barnwell, W.W., 1955, The geology of the South Hahns Peak district, Routt County, Colorado, in Guidebook to the geology of northwest Colorado, Intermountain Association of Petroleum Geologists 6th Annual Field Conference, 1955: Salt Lake City, Utah, p. 73–74.

Casaceli, R.J., 1983, The geology and mineral potential of the Hahns Peak intrusive porphyry, Routt County, Colorado: Corvallis, Oregon State University, M.S. thesis, 223 p.

Dowsett, F.R., 1980, Hydrothermal alteration of the Hahns Peak stock, Routt County, Colorado: Economic Geology, v. 75, p. 30–44.

Gale, H.S., 1905, The Hahns Peak gold field, Colorado: U.S. Geological Survey Bulletin 285, p. 28–34.

George, R.D., and Crawford, R.D., 1909, The Hahns Peak region, Routt County, Colorado, an outline survey: Colorado Geological Survey First Report, 1908, p. 189–229.

Segerstrom, K., and Young, E.J., 1972, General geology of the Hahns Peak and Farwell Mountain quadrangles, Routt County, Colorado: U.S. Geological Survey Bulletin 1349, 62 p., scale 1:24,000.

Parker, B.H., Jr., 1974, Gold placers of Colorado, Book 2 of 2 books: Colorado School of Mines Quarterly, v. 69, no. 4, 224 p.

Vanderwilt, J.W., 1947, Mineral resources of Colorado: Denver, State of Colorado Mineral Resources Board, 547 p.

Young, E.G., and Segerstrom, K., 1973, A disseminated silver-lead-zinc sulfide occurrence at Hahns Peak, Routt County, Colorado: U.S. Geological Survey Bulletin 1367, 33 p.

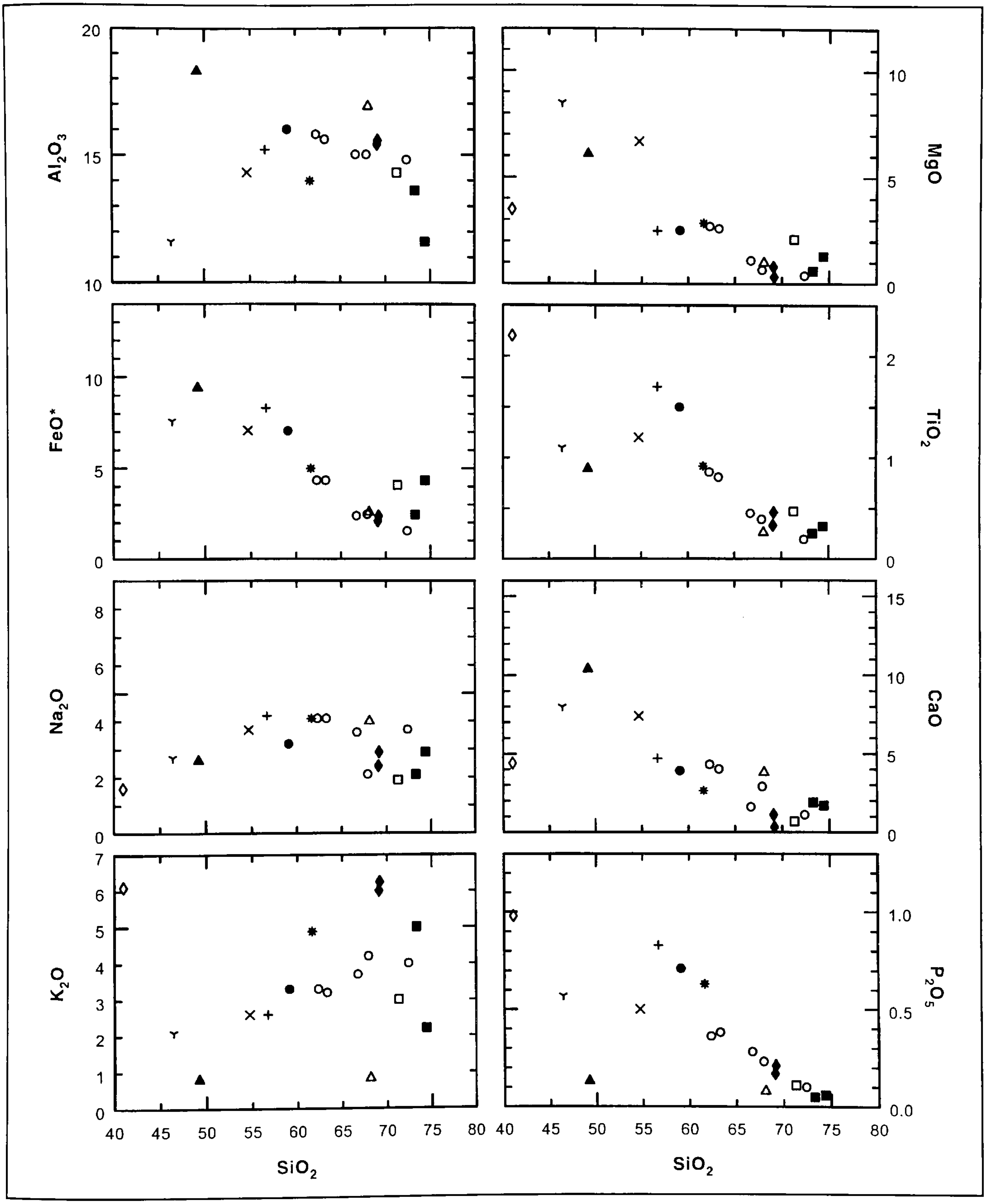

*Figure 30. Harker variation diagram of representative rock samples from the Hahns Peak district. Refer to the explanation on Fig. 29. (*includes Fe_2O_3)*

Chapter 7

Iron Hill Alkalic Complex, Powderhorn District

INTRODUCTION

The Powderhorn district is located in southern Gunnison County in an area of Proterozoic basement rocks on the northwest side of the San Juan volcanic field. The area is bisected by Cebolla Creek, a tributary of the Gunnison River which currently drains into Blue Mesa Reservoir. Access is via Colorado State Highway 149, 29 miles east of Lake City (Fig. 31).

The Powderhorn district contains the largest known reserves of both titanium and niobium in the United States. The district is also enriched in rare-earth minerals, thorium, iron, uranium and vanadium, and it contains economic deposits of vermiculite. Early economic interest in the district focused primarily on its vermiculite resources and small amounts were produced in the 1930s and 1940s (Temple and Grogan, 1965). The large resource of titanium in the Powderhorn district, contained in the mineral perovskite, was first described by Olson and Wallace (1956); however, attempts at development have not yet been successful. Neither have niobium or rare-earth resources been exploited.

Larsen (1942) published the first comprehensive report on the geology, geochemistry, petrology, and mineralogy of the Iron Hill complex. The geology and economic potential of the district was detailed by Temple and Grogan (1965) and reviewed by Armbrustmacher (1981). Rubidium-strontium age dates were provided by Olson and Marvin (1971) and Fenton and Faure (1971). Thorium resources were described by Olson and Wallace (1956), Armbrustmacher (1981), and Olson and Hedlund (1981). Olson and Wallace (1956) also discussed rare-earth minerals. Analyses of apatites from several rock types by Nash (1972), include rare-earth element data. Rose and Shannon (1960) and Thompson (1987) described the titanium and iron ores. The early report provided several tables of drill core assays.

GEOLOGICAL SETTING

The Iron Hill carbonatite complex was intruded into the surrounding middle Proterozoic Powderhorn Granite, other unnamed granites and felsite porphyries, and metamorphic rocks in very earliest part of the Cambrian Period (see Fig. 31). Some of the Proterozoic granites and felsite porphyries have been fenitized near the contacts of the Iron Hill carbonatite intrusive complex (Olson and others, 1977; Hedlund and Olson, 1975).

In surface expression, the Iron Hill complex is a pear-shaped mass of carbonatite and other alkalic rocks. Surface exposure of the complex covers 31 square kilometers immediately south and east of the town of Powderhorn. Core drilling indicated that the complex tapers at depth giving it a funnel shape in vertical section (Temple and Grogan, 1965). These rocks may be well or poorly exposed. The older alkalic rocks of the complex are softer than either the surrounding granitic host rock or the carbonatites, and they occupy topographic lows owing to the effect of differential erosion. Contacts are frequently defined by a break in slope.

The northwest part of the complex is covered by a series of Oligocene volcanic and volcaniclastic rocks that include ash-flow tuffs, air-fall tuffs, and rhyodacite and quartz latite flows. The southwest portion of the complex is overlain by Quaternary talus deposits and alluvium of the Cebolla Creek and its tributaries.

The alkalic rocks composing the complex, from oldest to youngest, are pyroxenite, uncompahgrite,

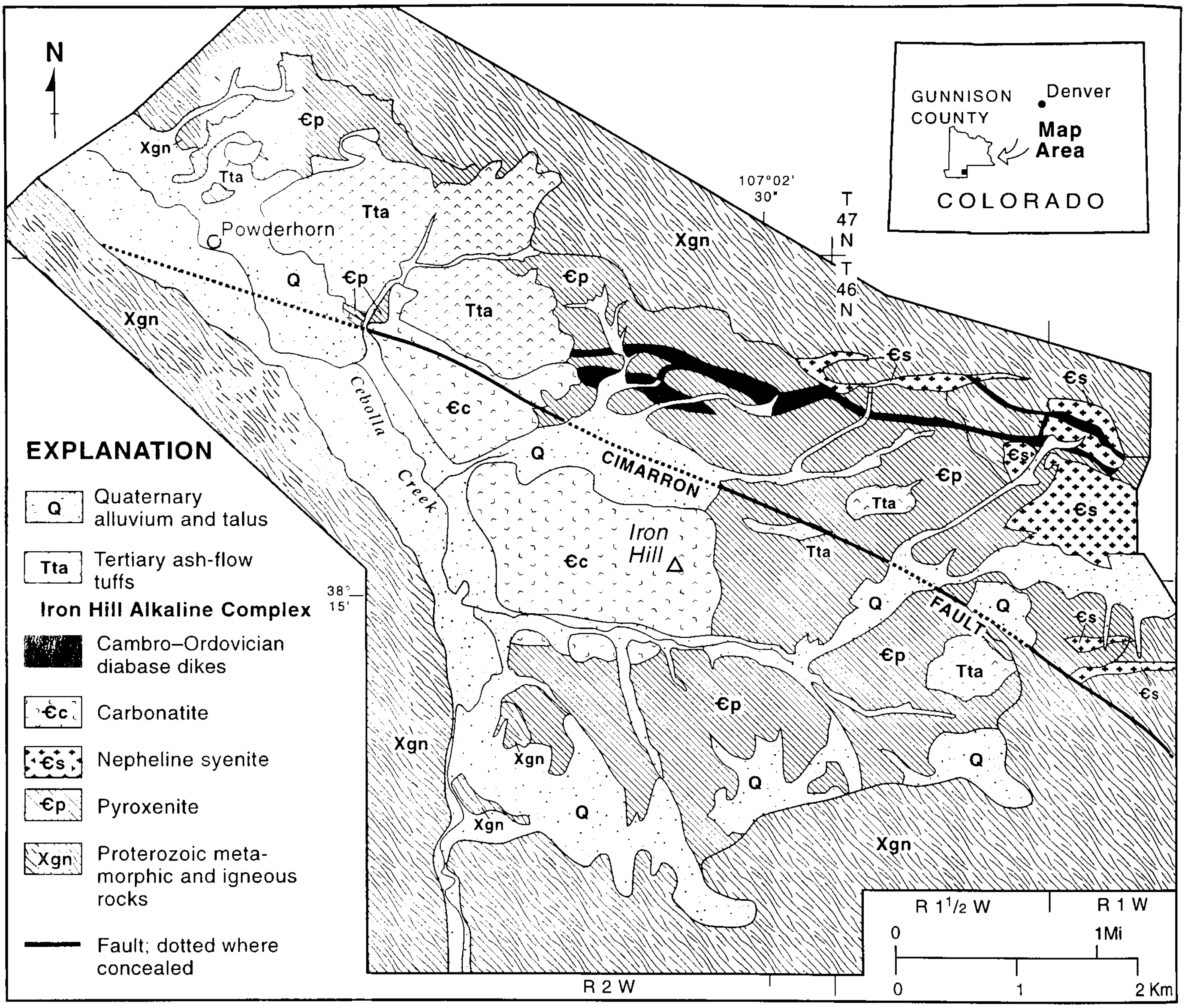

Figure 31. Geological and index map of the Iron Hill alkalic complex, Powderhorn district, Gunnison County, Colorado. (Modified from Armbrustmacher, 1981)

ijolite, nepheline syenite, and carbonatite. Potassium-argon age determinations from a number of minerals gave an age of emplacement for the complex at 570 Ma, while a rubidium-strontium isochron based on four micas and one whole-rock analysis indicated an apparent age of 579 Ma for the pyroxenite and syenite (Olson and others, 1977). A fission-track age of 550 Ma was obtained on sphene from the ijolite (Wooley, 1987).

PYROXENITE (Ꞓp)

Pyroxenite, which underlies 70 percent of the area, is the most commonly exposed rock type in the Iron Hill complex; it has sharp contacts with the surrounding host rocks and occupies a topographic low which surrounds carbonatite on all but the west side. Pyroxenite was the earliest rock to be emplaced and is cut by all the other carbonatite complex rocks (Temple and Grogan, 1965).

Primary internal structures within the pyroxenite consist of a persistent layering of pyroxene-rich units alternating with biotite or vermiculite-rich units. The pyroxenite lacks a fine-grained chill zone near its contacts indicating a lack of temperature contrast with the surrounding rock at the time of intrusion (Olson and Hedlund, 1981).

The pyroxenite is medium- to coarse-grained, locally pegmatitic, and generally contains 55 to 70 percent diopsidic augite, 10 to 15 percent ilmenite and magnetite, 5 to 25 percent melanite, 5 percent fluorapatite, and 10 percent biotite and phlogopite. Common accessory minerals are sphene, brown amphibole, calcite, perovskite, leucoxene, sodic amphibole, melilite, sericite, pyrite, chalcopyrite, and pyrrhotite. Vermiculite and titaniferous iron ores occur locally in pod-like bodies (Hedlund and Olson, 1975).

The calcium titanate mineral, perovskite ($CaTiO_3$), is present in sufficient quantities locally in the pyroxenite at Iron Hill to be an ore of titanium. Ore zones occur as segregations of ilmenite and perovskite encapsulated by titaniferous magnetite, and as relatively pure perovskite masses in dike-like bodies. Most of the dikes are less than 60 centimeters and are traceable for less than 30 meters (Olson and Hedlund, 1981).

UNCOMPAHGRITE

Uncompahgrite crops out in the southern part of the complex and consists mainly of medium- to coarse-grained melilite with lesser amounts of pyroxene, magnetite, and perovskite. Small dikes of uncompahgrite intrude pyroxenite in Beaver Creek valley. Uncompahgrite is included with the map unit of pyroxenite (€p) in Figure 31.

IJOLITE

Small bodies of fine- to coarse-grained ijolite intrude pyroxenite and uncompahgrite, mainly in the southeastern portion of the complex (Wooley, 1987). The ijolite is hypidiomorphic and commonly consists of 30 to 50 percent nepheline, 30 to 40 percent aegirine-augite, and 10 to 30 percent melanite garnet, with minor amounts of orthoclase, magnetite, and apatite (Hedlund and Olson, 1975). In places the nepheline content of the rock is as high as 80 percent. In most cases the nepheline has been altered to a very fine grained mixture of sericite, cancrite, natrolite and other minerals. In fine-grained ijolite, the pyroxene is a light green, diopsidic variety common to most of the pyroxenite phases of the complex (Temple and Grogan, 1965). Ijolite is included with the map unit of pyroxenite (€p) in Figure 31.

NEPHELINE SYENITE (€s)

Light gray, medium- to coarse-grained nepheline syenite is exposed in the eastern portion of the Iron Hill alkalic complex, emplaced as small stocks and dikes in Proterozoic granite, fenite, and pyroxenite of the Iron Hill carbonatite complex. Olson and Hedlund (1981) noticed that fenitization of the granite country rock is most extensive in the vicinity of the nepheline syenites. These rocks contain about 75 percent microperthite, albite, and aegirine-augite, with accessory melanite, magnetite, sphene, biotite, apatite, calcite, sericite, and zircon (Hedlund and Olson, 1975).

A nepheline syenite-pyroxenite breccia occurs in the eastern part of the complex consisting of fractured pyroxenite invaded by numerous nepheline syenite dikelets and narrow seams of nepheline. At contacts between nepheline syenite and pyroxenite, alteration and replacement of pyroxene by nepheline attests to the late stage nature of this rock type (Temple and Grogan, 1965).

CARBONATITE (€c)

This rock type forms the prominent topographic features of Big and Little Iron Hills, which rise nearly 1,000 feet above the Cebolla Valley and the area underlain by pyroxenite. Outcrops of carbonatite are characterized by foliated or banded, brown, gneissoid, granular, ankeritic dolomite; outcrops also commonly contain white, coarsely crystalline dolomite (Temple and Grogan, 1965).

Carbonatite, the youngest rock type of the complex, forms a stock of approximately 800 acres intruded into pyroxenite, fenite, and other alkalic rocks. Numerous carbonatite dikes cut pyroxenite, granite, and fenitized rock. A mixed zone 350 to 1,000 feet wide, characterized by biotite and sodic amphibole minerals, lies along the southern and eastern margins of the stock near contacts with pyroxenite and uncompahgrite (Wooley, 1987). Contacts of the carbonatite stock are generally not well exposed; however, on the western and northwestern margin of the stock carbonatite is in sharp contact with fenite (Temple and Grogan, 1965).

The carbonatites are light brown to very light gray, foliated to massive rocks composed of dolomite, ankerite, calcite, siderite, fluorapatite, fluorite, barite, pyrochlore, synchisite, parisite, pyrite, pyrrhotite, chalcopyrite, galena, sphalerite, and sodic amphibole. The stocks of Iron Hill are predominantly dolomite and ankeritic dolomite (Hedlund and Olson, 1975). Grain size in the carbonatites can range from fine-grained to pegmatitic (Wooley, 1987).

The internal structure and texture of the carbonatite is very complex. These structures and textures include the grain size variations documented by Wooley (1987), varying degrees of foliation, drag folds, shear zones, and partially replaced xenoliths of the surrounding country rocks. Most of the internal structures are considered primary, formed during or shortly after intrusion (Olson and Hedlund, 1981).

GEOCHEMISTRY

A plot of the total alkalies versus silica (Fig. 32) demonstrates the strongly alkalic nature of all of the intrusive rocks of the Powderhorn district except the granite and gabbro. The Harker diagram (Fig. 33) shows the variation of the major oxides against silica. Table 6 in the Appendix lists the chemical analyses and CIPW norms used in the diagrams.

ECONOMIC GEOLOGY

THORIUM

Thorium occurs in six distinct deposit types in and around the alkalic rock complex of the Powderhorn district: thorite veins, in the Iron Hill carbonatite, carbonatite dikes, trachyte dikes, magnetite-ilmenite-perovskite dikes, and segregations and disseminations in small plutons which are older than the Iron Hill alkalic complex itself (Olson and Hedlund, 1981).

The highest thorium concentrations in the district are in veins consisting of potassic feldspar, quartz, calcite, barite, goethite, and hematite, with accessory thorite, jasper, magnetite, pyrite, galena, chalcopyrite, sphalerite, synchisite, and other minerals. Thorite veins occur primarily within steeply dipping shear zones in the Proterozoic rocks. The veins range in thickness from about an inch to 17 feet and can be up to 3,000 feet in length, though most are less than 300 feet. The ThO_2 content ranges from 0.01 percent to 4.9 percent; however, the average is less than 1 percent (Olson and Hedlund, 1981).

The Iron Hill carbonatite stock contains thorium concentrations ranging from 6 parts per million (ppm) thorium to 150 ppm thorium. The average is 36.2 ppm. Thorium concentrations of this magnitude are not economic unless augmented with concomitant production of niobium, titanium, and rare-earth minerals (Armbrustmacher, 1980). The Iron Hill carbonatites do contain titanium and rare-earth metals.

Carbonatite dikes associated with the Iron Hill alkalic complex are the most naturally radioactive rocks of the Powderhorn district. These rocks can contain from 30 ppm to 3,200 ppm Th and from a trace to 1.5 percent rare-earth oxides (Olson and Hedlund, 1981). Trachyte dikes and magnetite-ilmenite-perovskite dikes generally contain a couple of tenths of a percent ThO_2 and are not considered to be of economic value. Deposits of thorium in the Powderhorn district are generally of too low a concentration to be produced as a "stand-alone" commodity.

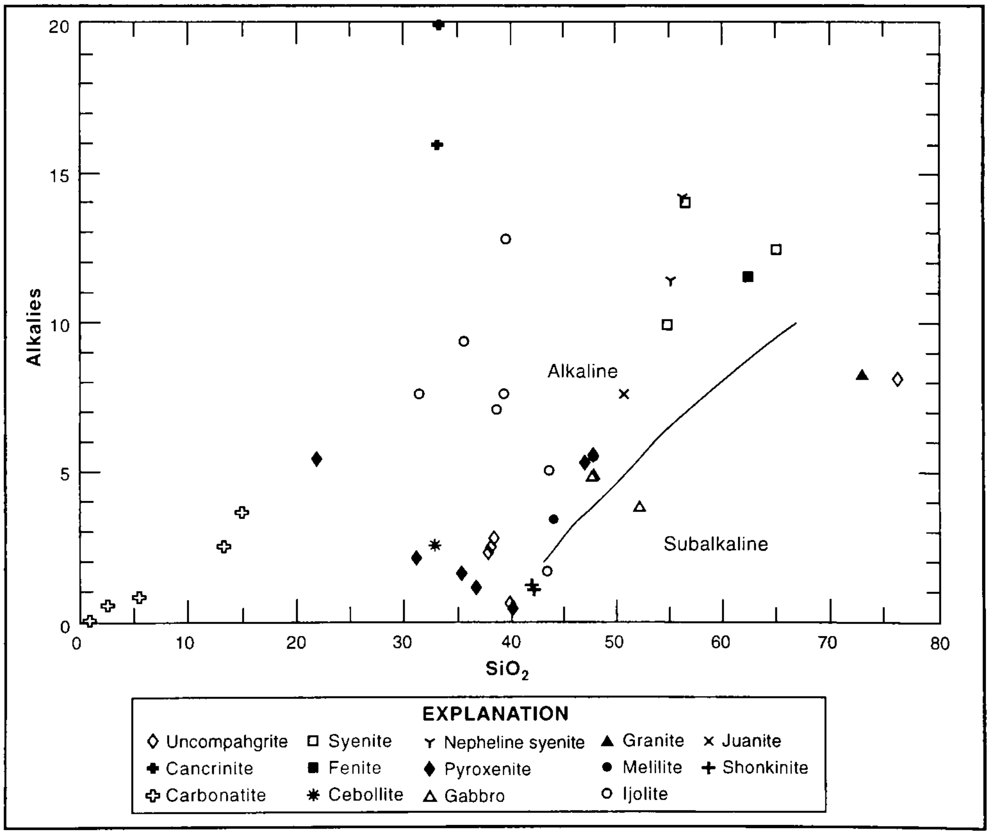

Figure 32. Plot of alkalies versus silica of representative rock samples from the Powderhorn district.

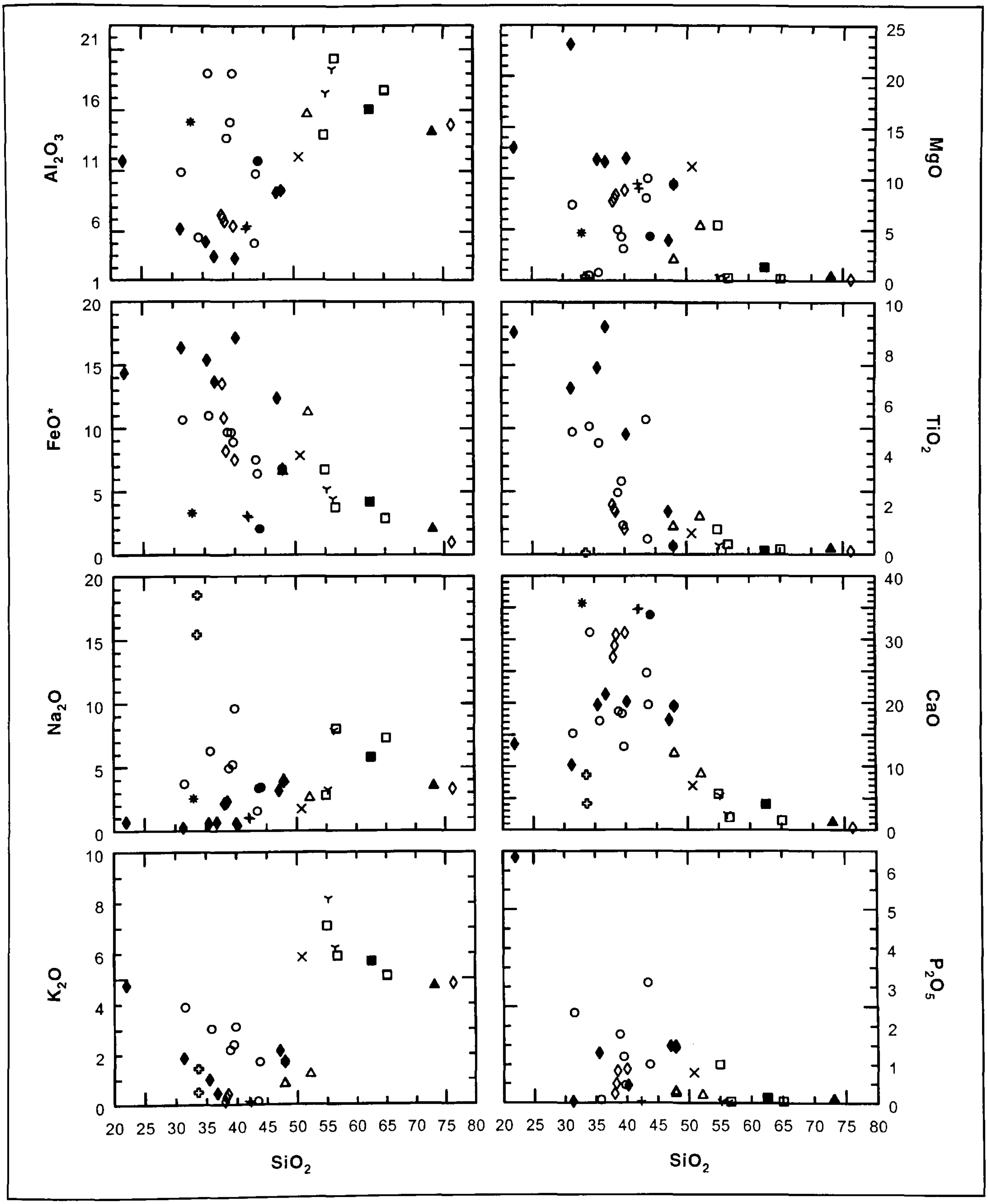

*Figure 33. Harker variation diagram of representative rock samples from the Powderhorn district. Refer to the explanation on Fig. 32. (*includes Fe_2O_3)*

NIOBIUM

The Iron Hill carbonatite stock contains an estimated 100,000 tons of Nb_2O_5, as indicated by test drilling conducted by E.I DuPont Co. in 1957 and 1958. Niobium occurs predominantly in the mineral pyrochlore, which is disseminated throughout the dolomitic carbonatite. Average niobium concentrations in these rocks are 0.25 percent Nb_2O_5 (Temple and Grogan, 1965). Pyrochlore is most abundant in fine-grained carbonatite, but it also occurs in shear zones associated with fluorapatite (Olson and Hedlund, 1981).

Niobium occurs in lesser concentrations in other minerals of the Iron Hill stock. Perovskite from magnetite-ilmenite-perovskite rock has niobium concentrations of 0.17, 0.2, and 0.7 percent. Niobium is a trace element in ilmenite, sphene, magnetite, and melanite analyzed from the Powderhorn district (Olson and Hedlund, 1981).

The thorite veins of the Powderhorn district commonly contain niobium, some in the mineral columbite. The concentrations of niobium in thorite veins ranges from 30 ppm to 1,500 ppm Nb_2O_5; the thorium to niobium ratios in the veins is usually around 7. The thorium to niobium ratio decreases with decreasing distance to the alkalic complex at Iron Hill. In the carbonatite of the complex itself, Nb_2O_5 concentrations exceed greatly those for ThO_2 (Olson and Hedlund, 1981).

TITANIUM

The resource of titanium at Powderhorn is believed to be the largest in the United States, composing over half of the known usable resource of titaniferous raw material (Thompson, 1987). The main ore mineral is perovskite, a calcium-titanium oxide. Titanium resources have been estimated at 390,000,000 tons of ore assaying 11.5 percent TiO_2. A newspaper article (Denver Post, February 25, 1976, p. 31) quotes a Kaiser Engineers Company report listing an indicated titanium reserve of 419,000,000 tons of ore assaying 12 percent TiO_2 (Olson and Hedlund, 1981).

Published figures quantifying the Powderhorn titanium resource are based on volume estimates of pyroxenite that contains numerous magnetite-perovskite veinlets. Many of these estimates are misleading because perovskite is considered as "disseminated" when actually only about 8 percent of perovskite is separable, rather than the reported 12 percent. Separable perovskite averages 45 to 50 percent TiO_2, 1.5 percent rare-earth metals, and 0.5 percent Nb_2O_5 (Thompson, 1987).

Several titanium-bearing minerals are present in the pyroxenite of the Iron Hill complex including perovskite, ilmenite, leucoxene, sphene, melanite, garnet, and titaniferous magnetite. Minor amounts of titanium occur in diopside and biotite. Magnetite, ilmenite, and perovskite occur as intergrowths, in segregations and dikes, and as disseminations in pyroxenite.

Random crystals of perovskite up to 3 inches in length are found and usually contain up to 1.5 percent rare-earths and 0.3 to 0.5 percent Nb_2O_5 (Thompson, 1987). Southeast of Powderhorn, a dike of magnetite-ilmenite-perovskite rock is 150 feet wide and extends for an undetermined distance under a cap of Oligocene welded tuff. Magnetite-ilmenite-perovskite rock can locally contain up to 40 percent TiO_2 (Hedlund and Olson, 1975). An analysis of 441 samples taken from drill core indicates a TiO_2 content range from 0.3 to 11.9 percent, with an average of 5.8 percent, for the Iron Hill pyroxenites (Rose and Shannon, 1960). Perovskite concentrates contain about 51 percent TiO_2, magnetite-ilmenite rock contains 6 to 19 percent, and melanite concentrates contain 5 percent TiO_2 (Olson and Hedlund, 1981).

Titanium-rich pyroxenite is defined by abundant apatite, olivine, nepheline, feldspar, and melanite garnet containing up to 5 percent TiO_2. Garnet and sphene are secondary minerals formed apparently after perovskite (Force, 1991).

The major problem confronting development of the titanium resources at Powderhorn has been the difficulty of processing perovskite and other complex ore minerals. Ores invariably contain trace amounts of rare-earths, thorium, or uranium-vanadium, increasing the beneficiation costs associated with these source materials. Only the perovskite can be liberated by standard metallurgical techniques. The recovered TiO_2 is generally less than 40 percent of the total chemical TiO_2. Alteration of perovskite to leucoxene also reduces recovery percentages (Thompson, 1983). A description of the processing techniques and economics of recovering titanium-oxide for commercial use is given in Thompson (1987).

RARE EARTH ELEMENTS

Rare earth elements (REE) are ubiquitous in the thorium deposits of the Powderhorn district. The

REE occur in the minerals monazite, thorite, rhabdophane, synchisite, and bastnäsite. A rough correlation exists between content of carbonate minerals in a deposit and the relative concentration of cerium-group (light) rare earths to yttrium-group (heavy) rare earth metals. At decreasing distances from the carbonatite stock at Iron Hill, deposits contain increasing carbonate mineral content and higher proportions of cerium in relation to other rare earth metals (Olson and Hedlund, 1981).

IRON

The Powderhorn district was recognized as a source of iron as early as 1880. The iron ore is magnetite-ilmenite-perovskite rock. The iron content of this material, 11.7 percent average for more than 100,000,000 tons of magnetite-bearing pyroxenite (Rose and Shannon, 1961), is insufficient to attract mining for iron alone (Olson and Hedlund, 1981). Small iron deposits have also been prospected in the Iron Hill carbonatite stock. The deposits consist of martite-apatite veins and small bodies of limonite and hematite (Olson and Hedlund, 1981).

URANIUM

Uranium concentrations in the Powderhorn district are generally low, rarely exceeding 10 ppm. Thorium to uranium ratios are high in most rocks of the district.

VANADIUM

Vanadium is a potentially recoverable metal from Powderhorn ores. The concentration of V_2O_5 in magnetite from uncompahgrite rock is 0.21 percent. Magnetite from a magnetite-ilmenite-perovskite dike contained 0.14 percent V_2O_5. Vanadium also occurs in melanite garnet (0.2 percent V_2O_5), perovskite (0.06 percent V_2O_5), and diopside (0.05–0.07 percent V_2O_5) (Olson and Hedlund, 1981). Fisher (1975) estimated a resource of 50,000 tons of vanadium contained in 100 million tons of magnetite-ilmenite-perovskite rock of the alkalic complex at Iron Hill.

EXPLORATION AND PRODUCTION HISTORY

In the 1880s the first patented mining claims were located on Big Iron Hill for iron because of the prominent reddish-brown color of the hill. A group of Minnesota investors acquired the property in the 1930s to exploit the vermiculite resources. In 1951 the Humphrys Engineering Company of Denver acquired the property and evaluated its titanium potential. The property passed to DuPont in 1956 and it explored for niobium and columbium resources.

In 1968 Buttes Gas and Oil Company of Moab, Utah acquired the property and conducted several drilling programs and geophysical surveys looking primarily for titanium. Buttes also conducted reserve assessments, marketing studies, and metallurgical processing research. In 1990 Teck Resources leased the Buttes Oil and Gas Company property and began evaluating the titanium resources of the Powderhorn district. In 1996 Teck started the second phase of pilot metallurgical tests which consist of converting the perovskite concentrate to titanium dioxide for the pigment industry.

REFERENCES

Armbrustmacher, T.J., 1980, Distribution and abundance of thorium in the carbonatite stock at Iron Hill, Powderhorn district, Gunnison County, Colorado: U.S. Geological Survey Professional Paper No. 1049-B, 12 p.

_____1981, The complex of alkaline rocks at Iron Hill, Powderhorn district, Gunnison County, Colorado, *in* Epis, R.C., and Callendar, J.F., eds., Western Slope Colorado: New Mexico Geological Society, Proceedings of the 32nd Field Conference, Oct. 8–10, 1981, Socorro, New Mexico, 1981, p. 293–296.

Fenton, M.D., and Faure, G., 1971, Rb-Sr whole-rock age determinations for the Iron Hill and McClure Mountain carbonatite-alkalic complexes, Colorado: Mountain Geologist, v. 7, no. 4, p. 269–275.

Fisher, R.P., 1975, Vanadium resources in titaniferous magnetite deposits: U.S. Geological Survey Professional Paper No. 926-B, 10 p.

Force, E.R., 1991, Geology of titanium-mineral deposits: Geological Society of America Special Paper No. 259, Boulder, Colorado, 1991, 112 p.

Hedlund, D.C., and Olson, J.C., 1975, Geologic map of the Powderhorn quadrangle, Gunnison and Saguache counties, Colorado: U.S. Geological Survey Map GQ-1178, scale 1:24,000.

Larsen, E.S., Jr., 1942, Alkalic rocks of Iron Hill, Gunnison County, Colorado: U.S. Geological Survey Professional Paper No. 197-A, p. 1–64.

Nash, W.P., 1972, Mineralogy and petrology of the Iron Hill carbonatite complex, Colorado: Geological Society of America Bulletin, v. 83, p. 1,361–1,382.

Olson, J.C., 1974, Geologic map of the Rudolph Hill quadrangle, Gunnison, Hinsdale, and Saguache counties, Colorado: U.S. Geological Survey Map GQ-1177, scale 1:24,000.

Olson, J.C., and Hedlund, D.C., 1981, Alkalic rocks and resources of thorium and associated elements in the Powderhorn district, Gunnison County, Colorado: U.S. Geological Survey Professional Paper No. 1049-C, 34 p.

Olson, J.C., and Marvin, R.F., 1971, Rb-Sr whole rock age determinations of the Iron Hill and McClure Mountain carbonatite-alkalic complexes, Colorado—Discussion: Mountain Geologist, v. 8, no. 4, p. 221.

Olson, J.C., Marvin, R.F., Parker, R.L., and Mehnert, H.H., 1977, Age and tectonic setting of lower Paleozoic alkalic and mafic rocks, carbonatites, and thorium veins in south-central Colorado: U.S. Geological Survey Journal of Research, v. 5, p. 673–687.

Olson, J.C., and Wallace, S.R., 1956, Thorium and rare earth minerals in the Powderhorn district, Gunnison County, Colorado: U.S. Geological Survey Bulletin 1027-O, p. 693–723.

Rose, C.K., and Shannon, S.S., 1960, Cebolla Creek titaniferous iron deposits, Gunnison County, Colorado: U.S. Bureau of Mines Report of Investigations 5679, 30 p.

Temple, A.K., and Grogan, R.M., 1965, Carbonatite and related alkalic rocks at Powderhorn, Colorado: Economic Geology, v. 60, p. 672–692.

Thompson, J.V., 1987, Titanium resource in Colorado equals all other U.S. deposits: Engineering and Mining Journal, v. 188, p. 27–30.

_____1983, Economic potential of the carbonatite and alkalic stock at Powderhorn, Gunnison County, Colorado, *in* Gunnison Gold Belt and Powderhorn Carbonatite Field Trip Guidebook, 1983, Denver, Denver Region Exploration Geologists Society.

Wooley, A.R., 1987, Iron Hill (Powderhorn), Colorado, *in* Alkaline rocks and carbonatites of the world—Part I: North and South America: Austin, University of Texas Press, 1987, 79 p.

Chapter 8

Silver Cliff and Rosita Hills District

INTRODUCTION AND HISTORY

The Silver Cliff and Rosita Hills district is located at the northern end of the Wet Mountains, Custer County (see Fig. 34). From 1872 to 1958 the Silver Cliff and Rosita Hills district produced an estimated 110,000 ounces of gold, 4,744,000 ounces of silver, 626,000 pounds of copper, and 12,000,000 pounds of lead (Henderson, 1926; Vanderwilt, 1947: Del Rio, 1960). There is no record of metal production from the district after 1958.

The Maverick Vein near the ghost town of Rosita was the initial discovery of the Rosita Hills district in 1872. Two years later the Humboldt-Pocahontas vein was discovered and developed into a significant and steady silver producer. Emmons (1896) reported that the mine produced over $900,000 (nineteenth century prices) of silver. The Bassick Mine, which was discovered in 1877, was the single most prolific producer of silver and gold ore in the district. The mine was developed to a depth of 1,400 feet and produced about $2 million worth of gold and silver ore and was reportedly still in ore when it was abandoned (Emmons, 1896).

In 1878 silver was discovered in what was to become the Silver Cliff district with the location of the Silver Cliff and Racine Boy claims (Emmons, 1896). The most important mine in the Silver Cliff district is the Bull Domingo pipe, a breccia pipe hosted in Proterozoic gneiss.

GEOLOGICAL SETTING

The Silver Cliff and Rosita Hills district lies near the intersection of the Wet Mountains and the Sangre de Cristo Mountains. The Wet Mountain Valley is the physiographic expression of the Wet Mountain rift zone, an axial rift zone of the Rio Grande Rift. The alkalic volcanic rocks of the Silver Cliff and Rosita Hills district and the Cripple Creek district (Fig. 35) are a result of magmatic and tectonic forces associated with the formation of the rift.

The oldest rocks of the district are Proterozoic gneisses and granites. The volcanic rocks of the Silver Cliff and Rosita Hills form two distinct intrusive caldera complexes which were emplaced in the Proterozoic rocks during Oligocene and Miocene time (Sharp, 1978). A narrow zone of flows, plugs and dikes connects the two centers. Precious- and base-metal ores are found within veins and breccia pipes in the volcanic complex (with the exception of the Bull-Domingo Mine discussed later). The host for the more significant ore deposits is the Rosita Andesite.

A simplified geological map of the Silver Cliff and Rosita Hills district is shown in Figure 35. The two volcanic complexes, the Rosita Hills and Silver Cliff, are described separately even though it is thought that the volcanism was coeval. The following lithological descriptions of the map units are, except where noted, from Sharp (1978). The map units are listed in the order of oldest to youngest.

PROTEROZOIC UNDIFFERENTIATED (XYgg)

The Proterozoic rocks consist of X age felsic and mafic gneisses of probable equivalence to the Idaho Springs Formation of the Front Range and the Y age San Isabel Granite, a coarse-grained, porphyritic, biotite granite. The granites have a lead-alpha date of 1,430 ± 200 Ma (Boyer, 1962). These rocks are locally cut by syenite dikes of Cambrian age (not shown on Fig. 35).

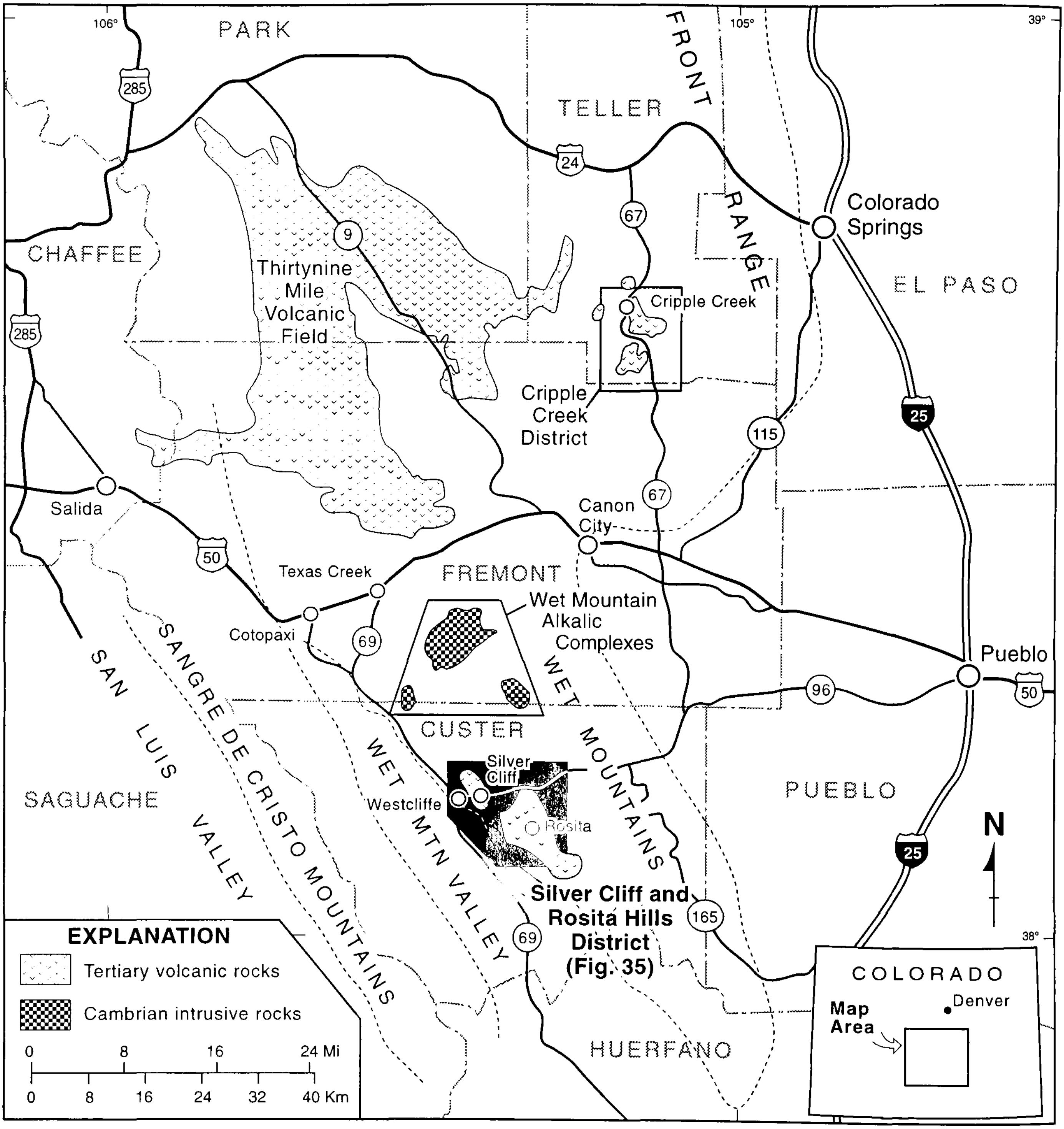

Figure 34. Index map showing location of the Cripple Creek district, Silver Cliff and Rosita Hills district, and the Wet Mountains alkalic complexes.

ROSITA HILLS COMPLEX

Rhyolite Flows and Volcaniclastic Rocks, Oligocene (Tdr)

These early volcanic and volcaniclastic rocks are composed of pink to white rhyolitic tuffs, welded ash flow tuffs, laharic breccias and conglomerates, pumice-bearing ashy sandstones and gravel deposits. A biotite-rich pumice bed was dated at 32.1 ± 0.9 Ma and a welded ashflow unit at 27.5 ± 2.8 Ma by fission track methods (Scott and Taylor, 1975).

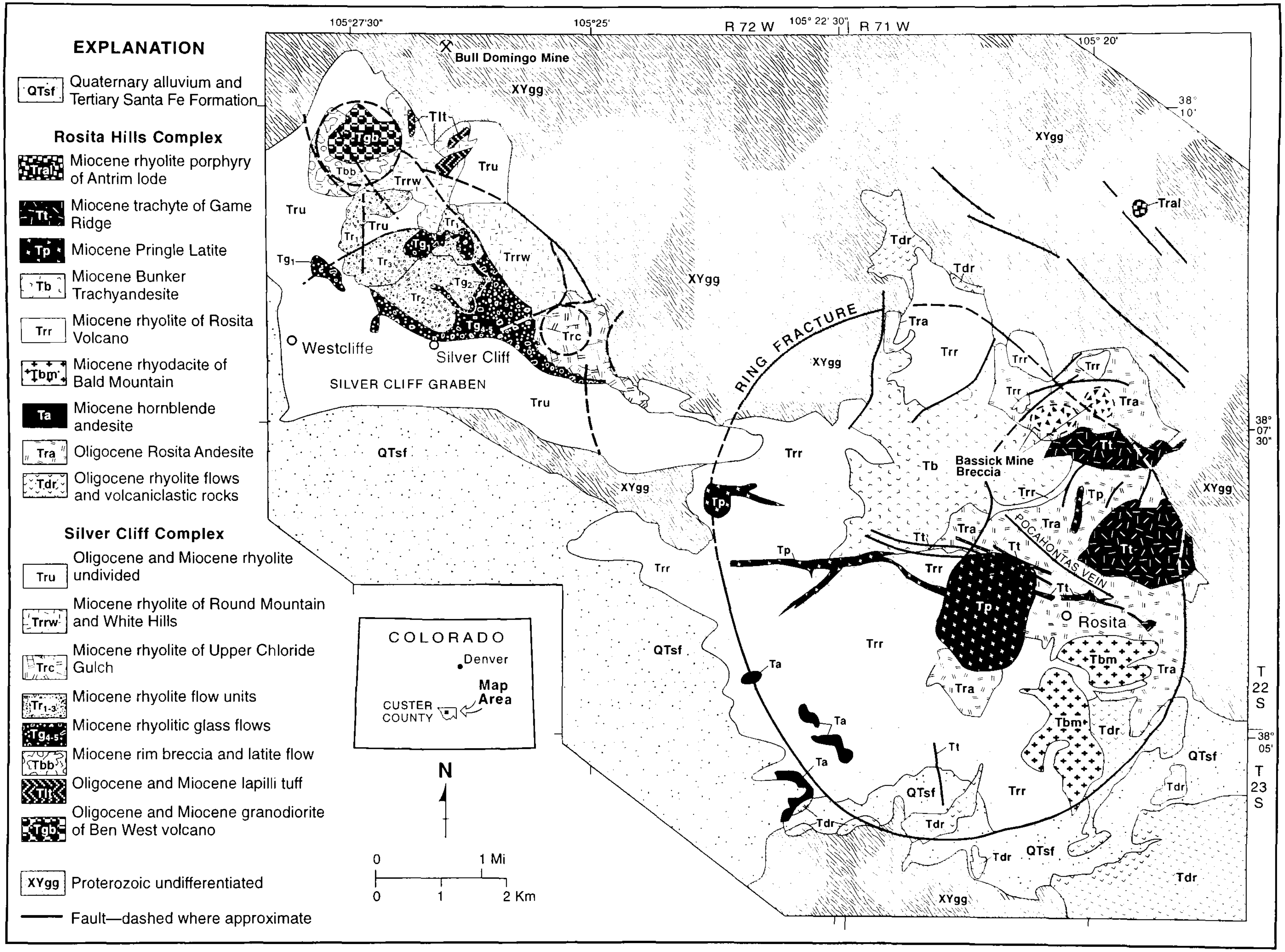

Figure 35. Simplified geological map of the Silver Cliff and Rosita Hills district, Custer County, Colorado. (Modified from Sharp, 1978)

Rosita Andesite, Oligocene (Tra)

The Rosita Andesite is composed of dark brownish gray, holocrystalline, fine- to medium-grained alkali andesite flows and associated flow breccias and has a variable thickness up to 1,300 feet. The rock has a porphyritic texture and contains phenocrysts of potassium feldspar and sodic plagioclase. Amphibole, augite, and biotite are also present. The formation also contains lesser amounts of laharic breccias, tuffs of andesitic to rhyolitic composition, and andesitic agglomerates (Siems, 1967, 1968). The Rosita Andesite is the result of dominantly andesitic volcanism at the Rosita Hills complex. The pipes and vents of this volcanic cycle are hydrothermally altered and generally mineralized. The "Bassick Agglomerate" named by Cross (1896) is now recognized as a breccia pipe within the Rosita Andesite. The prolific Bassick Mine is located in the "Bassick Agglomerate" (Siems, 1967).

Hornblende andesite, Miocene (Ta)

The dark gray, fine-grained, holocrystalline andesite of this unit was emplaced primarily along ring fracture zones of the Rosita volcanic center. The rock consists principally of elongate blue-black hornblende crystals, biotite flakes, and plagioclase crystals; augite, sphene, magnetite, zircon, and topaz occur in lesser amounts.

Rhyodacite of Bald Mountain, Miocene (Tbm)

The rhyodacite is fine grained and holocrystalline and consists of potassium feldspar, albite, calcic plagioclase, and quartz. Biotite and amphibole are common. These rocks were emplaced as domes and flows in a small area south of the town of Rosita around Bald Mountain (Siems, 1968).

Rhyolite of Rosita Volcano, Miocene (Trr)

This heterogeneous unit consists of a pink to white, vitrophyric to finely granular, banded, massive and fragmental quartz and sanidine rhyolite with a slightly porphyritic texture. The rhyolite forms vent and dome breccias, dikes, flows, glassy flows, and welded ash-flow tuffs. The rocks were formed dominantly along ring fractures. Rocks at the vent sites are commonly altered to an assemblage of alunite, quartz, illite, and pyrophyllite. Glassy rocks and welded ash flow tuffs are commonly altered to zeolite-bearing rocks. The Rhyolite of Rosita volcano represents a mainly rhyolitic stage of volcanism following the more mafic Rosita Andesite episode.

Bunker Trachyandesite, Miocene (Tb)

The main body of the Bunker Trachyandesite is a dark greenish gray, fine-grained, equigranular to slightly porphyritic, intrusive trachyandesite. Phenocrysts consist of plagioclase and potassium feldspar; augite, amphibole, rare hypersthene, biotite, and apatite are also present. There is also a later intrusive phase of this formation that consists of fine-grained syenodiorite. Carbonate alteration and minor mineralization is associated with the trachyandesite.

Pringle Latite, Miocene (Tp)

Stocks and dikes of gray to greenish gray latite and quartz monzonite make up the Pringle Latite. The latite consists of sodic plagioclase, sanidine, biotite, augite, and hornblende. The mafic minerals are commonly altered to iron oxide minerals. This unit forms a large stock at Pringle Hill.

Trachyte of Game Ridge, Miocene (Tt)

Pinkish-gray syenite porphyry and trachyte intrude all other rocks of the Rosita volcanic complex. All phases of the trachyte, whether intrusive, dike, or flow, have a porphyritic texture. Glassy sanidine crystals and sodic plagioclase are the common phenocrysts. Breccia-filled explosive vents and quartz "blowouts" occur in the dikes and are generally mineralized. Ores within the Rosita complex are associated with this final volcanic event.

Rhyolite porphyry of Antrim Lode, Miocene (Tral)

This intrusive dome and others (not shown on the map) are thought to be the final volcanic event of the Rosita volcanic complex. They are associated with the east ring fracture of the complex (Siems, 1968). The rock is a white to light gray rhyolite porphyry and consists of quartz and sanidine phenocrysts with associated smaller biotite flakes. This rock was dated at 26.3 ± 0.7 Ma (Scott and Taylor, 1975).

SILVER CLIFF COMPLEX

Granodiorite of Ben West Volcano, Oligocene and Miocene (Tgb)

The granodiorite of Ben West volcano, the subvolcanic intrusive phase of the Silver Cliff volcanic complex, consists of a gray to pink granodiorite porphyry. The phenocrysts are sanidine and partially resorbed quartz.

Lapilli Tuff, Oligocene and Miocene (Tlt)

The lapilli tuff is a dark, finely layered, air-fall tuff. It is locally altered to a white clay material with illite and quartz; generally contains pyrite and is altered to dark iron and manganese oxides.

Rim Breccia and Latite Flow, Miocene (Tbb)

The rim breccia consists of completely altered blocks of rhyolite? and latite. The breccia fragments now consist of quartz, illite, pyrite, and jarosite. The unit is mineralized along the concentric faults and fractures of the Ben West volcano.

Rhyolitic Glass Flows, Miocene (Tg_{1-5})

Gray, brown, and varicolored, altered to fresh, volcanic glass flows are numbered one through five. The flows are dominantly of rhyolitic composition and usually possess a cherty spheroidal upper phase. Flow unit Tg_2 contains spectacular spherulites up to six feet in diameter. Altered glass flows consist of mordenite, kaolinite, and illite.

Rhyolite Flow Units, Miocene (Tr_{1-3})

Gray to white, banded, locally porcellaneous rhyolite flows and minor dikes form three units. In Tr_3 several fracture zones are filled with iron and manganese oxides that produced significant amounts of silver. Locally, the rhyolite contains lithophysae of topaz and garnet.

Rhyolite of Upper Chloride Gulch, Miocene (Trc)

The rhyolite of Upper Chloride Gulch is a red to pink, banded rhyolite with flow and vent breccia. The rhyolite is usually dense and glassy but locally contains crystals of sanidine and quartz and lithophysae of garnet and alkali feldspar.

Rhyolite of Round Mountain and White Hills, Miocene (Trrw)

The rhyolite of Round Mountain and White Hills is a white and pink, densely welded flow and vent breccia, ash-flow tuff, and air-fall tuff. Vent material is often altered to alunite; concentric fractures contain sulfosalts of copper and silver.

Rhyolite Undivided, Oligocene and Miocene (Tru)

Some rhyolite flows and associated pyroclastic rocks are not assigned to other formations. In the Silver Cliff graben just south of the town of Silver Cliff the undivided rhyolite unit is several thousand feet thick and contains lacustrine and fluvial deposits.

QUATERNARY ALLUVIUM AND TERTIARY SANTA FE FORMATION, (QTsf)

Poorly sorted sand and boulder deposits and sandy silt make up this map unit.

STRUCTURE

The uplift of the Wet Mountains during the Laramide orogenic event reactivated many of the Proterozoic northwest-trending faults in the Rosita Hills and Silver Cliff districts (Boyer, 1962). There are also minor north and northeast-trending faults within the districts. Volcanism began about 27 to 31 Ma, approximately the same time as the initiation of rifting in the Rio Grande Rift (Lipman and Mehnert, 1975). Many structures in the Oligocene and Miocene volcanic rocks of the district, such as the Antrim Lode and the Humboldt-Pocahontas Vein (Fig. 35), were emplaced along the reactivated Proterozoic structures. The eruption of the early rhyolites and the andesites of the Rosita Andesite caused doming and subsidence and eventual caldera formation. Ring fractures and breccia pipes in the district, such as the Bassick Breccia, are related to this subsidence event. There are other ring fracture systems in the Silver Cliff district. A ring fracture separates volcanic rocks from Proterozoic rocks on the east side of Round Mountain and a ring fracture passes through the Defender Mine and is exposed for 7,000 feet within the volcanic rocks (Siems, 1968).

GEOCHEMISTRY

Figure 36 is a Le Bas diagram that plots total alkalies against silica. The latite, trachyte, rhyodacite, gabbro and andesite plot well above into the alkalic range. The rhyolites plot in the rhyolite field of the diagram; however, they lie along the extension of the dividing line between alkalic and subalkalic rocks. The Rosita Hills suite of volcanic rocks is more alkalic than the Silver Cliff complex which is composed mostly of rhyolite. The normative diagram (Fig. 37) demonstrates the potassic nature of all the rocks of the district. The Harker variation diagram (Fig. 38) also shows the potassic nature of the rocks in the district. Table 7 in the Appendix

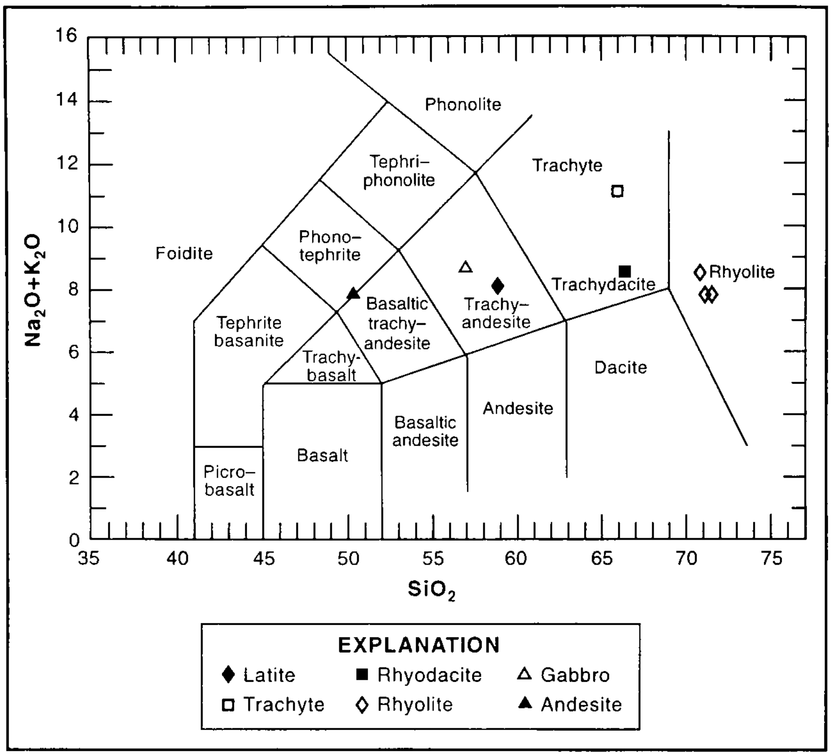

Figure 36. Le Bas diagram of representative rock samples from the Silver Cliff and Rosita Hills district.

lists the chemical analyses and CIPW norms used in the diagrams.

ECONOMIC GEOLOGY

Within the Rosita Hills and Silver Cliff districts there are two main types of ore bodies, breccia pipes and veins or fracture fillings. Both types are controlled by faults and joints related to the caldera subsidence. The best (and only) descriptions of the underground relationships of the mines come from Cross (1896).

BRECCIA PIPES

Breccia pipes in the volcanic rocks and Proterozoic rocks have been the most significant producers of precious metal ore in the district. The breccia pipe at the Bassick Mine in the Rosita Hills was the single largest producer; more than $2 million (1896 prices) of metal came from the mine. The breccia is composed of argillically altered fragments of Rosita Andesite ranging in size from a few inches to blocks 3 feet in diameter. The breccia pipe has an elliptical plan with short axis dimensions of 20 to 30 feet and long axis dimensions of 100 feet. The walls of the breccia are generally vertical and extend to a depth of at least 1,400 feet where mining ceased.

The ore and associated gangue minerals at the Bassick breccia pipe were deposited in concentric rings around the breccia fragments. The inner most zone is a thin layer, up to 5 millimeters thick, consisting of sphalerite, galena, and antimony sulfide. It contains gold at a grade of 1 to 3 ounces per ton and silver at a grade of about 60 ounces per ton. The second layer is similar in composition but lighter in color and contains more precious metal, up to 100 ounces of gold and 150 to 200 ounces of silver per ton. The third layer is a 5-millimeter to 5-centimeter thick zone of crystalline sphalerite which contains 60 to 120 ounces of silver and 15 to 50 ounces of gold per ton. The third layer often is the outermost layer. The fourth layer when present is composed of a 1- to 2-centimeter layer of chalcopyrite with higher grades of precious metals. The fifth and outermost layer consists of pyrite and kaolin. Silica, tetrahedrite, smithsonite, and charcoal fragments occur in the matrix of the breccia. Pyrite commonly occurs with the argillically altered fragments of the Rosita Andesite in the ore body.

The Bull Domingo Mine is located within the Precambrian metamorphic rocks of the Blue Hills just on the north side of the Silver Cliff district. The mine probably produced between 0.5 and $1.0 million (1896 prices) worth of silver and lead prior to 1896. The ore body is a steeply-dipping breccia complex with a elliptical shape, 90 by 40 feet on the 150 level, that extended to a depth of 550 feet where mining ceased.

The breccia fragments consist of rounded clasts of gneiss, granite, pegmatite, and syeniteof Cambrian age. No clasts of volcanic rocksrelated to the Silver Cliff or Rosita Hills complexes are reported from the Bull Domingo Mine. The ore minerals are deposited as layers around the clasts. The inner most layer consists of galena and locally sphalerite and pyrite. The remaining layers are all gangue minerals: dolomite, ankerite or siderite, calcite, and white or yellow chalcedony. The ore contains 10 to

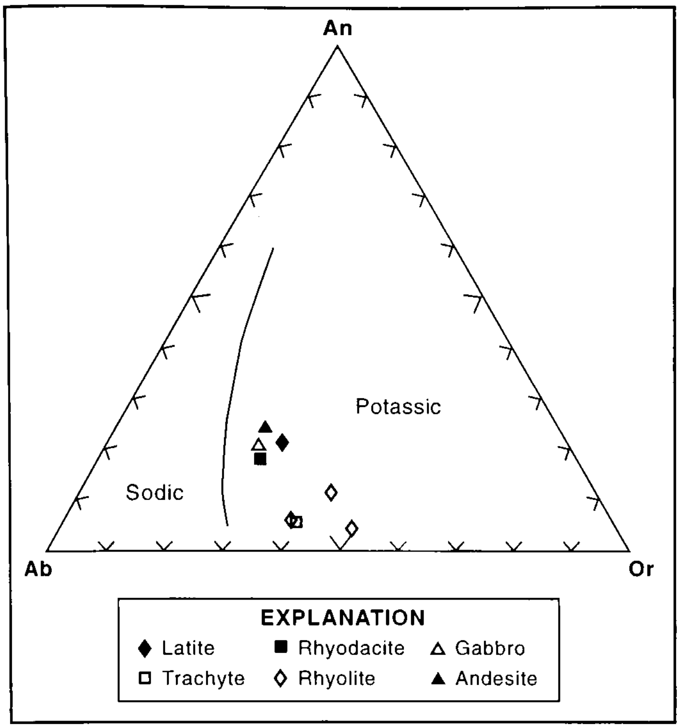

Figure 37. Normative diagram; Ab-An-Or of representative rock samples from the Silver Cliff and Rosita Hills district.

12 ounces of silver per ton and about 10 percent lead; silver is associated with the galena.

VEINS AND FRACTURE FILLINGS

Veins and mineralized fractures occur mostly in the younger trachytes and consist of tetrahedrite, pyrite, calcite, and barite. The Humboldt-Pocahontas Vein and associated shoots have a length of about 8,000 feet and several mines and prospects were located along this feature. The Humboldt Mine produced approximately $500,000 worth of silver ore prior to 1878. The vein in the Humboldt Mine was developed down to the 800 level and consisted of argillically altered trachyte, pyrite, chalcopyrite, galena, tetrahedrite, stephanite, and the gangue minerals barite and calcite.

In the Silver Cliff district mineralized veins and fractures generally occupy ring fractures of the Silver Cliff caldera. Most of the mines developed on Silver Cliff veins had limited production. The ore minerals consist of pyrite, galena, sphalerite, and chalcopyrite.

The Silver Cliff and Racine Boy deposits are vein stockwork systems within fractured rhyolite.

Emmons (1896) describes the Silver Cliff deposit as banded rhyolite with oxides of manganese and iron carrying little flakes of silver chloride. The ore minerals were later determined to be bromargyrite (AgBr), argentian cryptomelane (a silver-bearing potassium manganese oxide), and native silver (Hildebrand and Mosier, 1974). The grade of the deposit mined in the nineteenth century was 35 to 50 ounces of silver per ton. The mineralization in the rhyolites is strongly structurally controlled as the overlying obsidian flows cut off mineralization (Fieldman and Crowley, 1980). The total value of production from the Silver Cliff Mine was approximately $400,000.

REFERENCES

Anderson, F.G., Selvig, W.A., Baur, G.S., Colbassani, P.J., and Bank, W., 1956, Composition of perlite: U.S. Bureau of Mines Report of Investigation 5199, 13 p.

Boyer, R.F., 1962, Petrology and structure of the southern Wet Mountains, Colorado: Geological Society of America Bulletin, v. 73, p. 1,047–1,070.

Cross, W., 1896, Geology of Silver Cliff and Rosita, Colorado: U.S. Geological Survey 17th Annual Report, part 2, p. 263–403.

Del Rio, S.M., 1960, Mineral resources of Colorado First Sequel: Denver, State of Colorado Mineral Resources Board, 764 p.

Emmons, S.F., 1896, The mines of Custer County, Colorado: U.S. Geological Survey 17th Annual Report, part 2, p. 405–472.

Fieldman, D.W., and Crowley, F.P., 1980, Silver deposits of the southern portion of the Silver Cliff Caldera, *in* Babcock, J.W., and King, J.R., eds., Silver Cliff volcanic center and Tallahassee Creek uranium deposits: Denver Region Exploration Geologists Society First Annual Field Trip Guidebook.

Henderson, C.W., 1926, Mining in Colorado—A history of discovery, development, and production: U.S. Geological Survey Professional Paper 138, 263 p.

Hildebrand, F.A., and Mosier, E.I., 1974, Argentian cryptomelane and bromargyrite in volcanic rocks near Silver Cliff, Colorado: U.S. Geological Survey Bulletin 1382-C, 23 p.

Lipman, P.W., and Mehnert, H.H., 1975, Late Cenozoic basaltic volcanism and development of the Rio Grande depression in the Southern Rocky Mountains, *in* Curtis, B.F., ed., Cenozoic history of the Southern Rocky Mountains: Geological Society of America Memoir 144, p. 119–154.

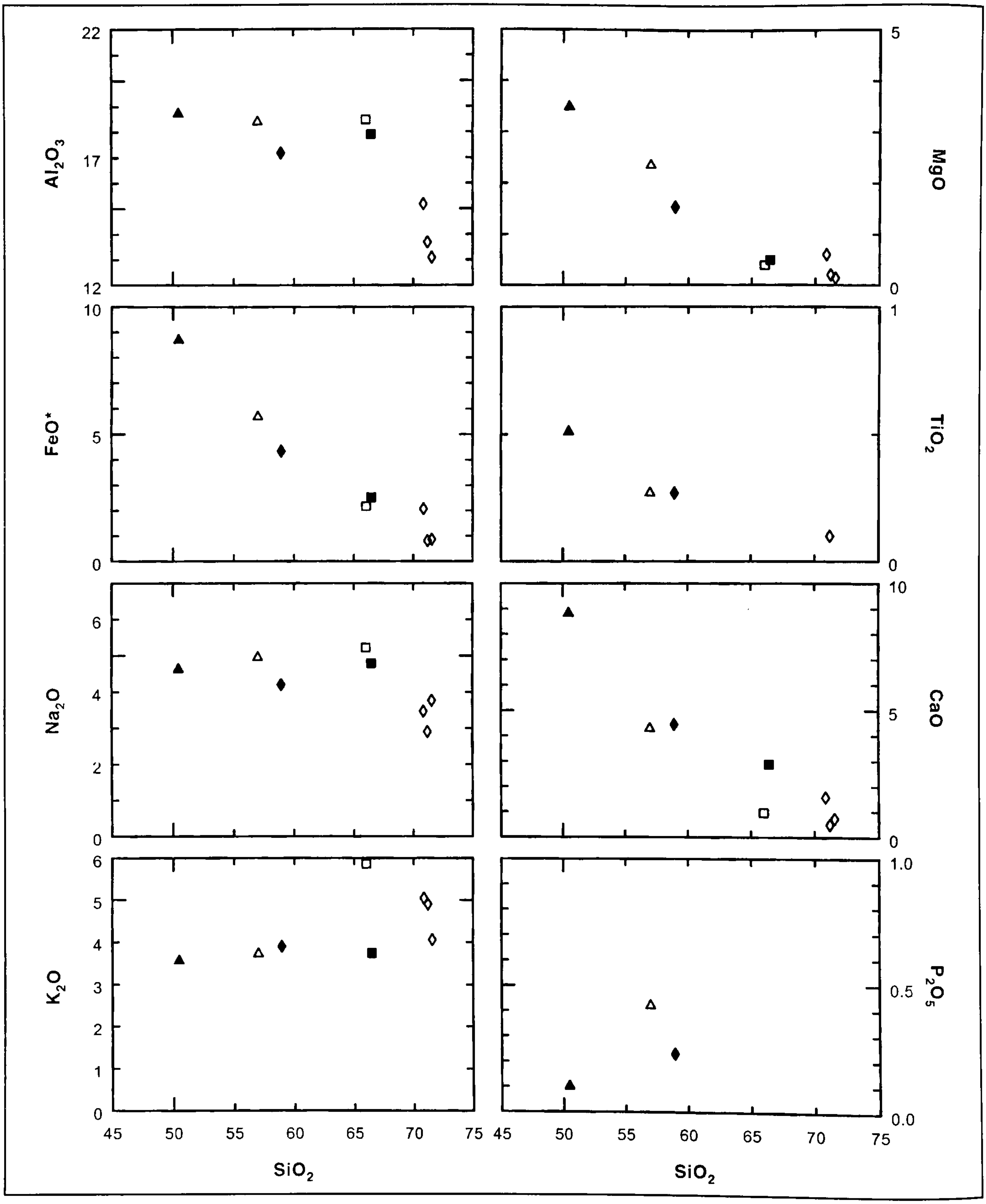

*Figure 38. Harker variation diagram of representative rock samples from the Silver Cliff and Rosita Hills district. Refer to the explanation on Fig. 37. (*includes Fe_2O_3)*

Scott, G.R., and Taylor, R.B., 1975, Post-Paleocene Tertiary rocks and Quaternary volcanic ash of the Wet Mountain Valley, Colorado: U.S. Geological Survey Professional Paper 868, 15 p.

Sharp, W.N., 1978, Geologic map of the Silver Cliff and Rosita volcanic centers, Custer County, Colorado: U.S. Geological Survey Miscellaneous Investigation Series Map I-1081, scale 1:24,000.

Siems, P.L., 1967, Volcanic and economic geology of the Rosita Hills and Silver Cliff districts, Custer County, Colorado: Golden, Colorado School of Mines, D.Sc. dissertation, 222 p.

Siems, P.L., 1968, Volcanic geology of the Rosita Hills and Silver Cliff district, Custer County, Colorado: Colorado School of Mines Quarterly, v. 63, no. 3, p. 89–124.

Vanderwilt, J.W., 1947, Mineral resources of Colorado: Denver, State of Colorado Mineral Resources Board, 547 p.

Chapter 9

Wet Mountain Alkalic Complexes

INTRODUCTION AND HISTORY

The Wet Mountain alkalic complexes, which were first recognized by Parker and Hildebrand (1963), are located at the northern end of the Wet Mountains just north of the towns of Westcliffe and Silver Cliff (Fig. 39). Three distinct complexes, the Gem Park, the Democrat Creek, and McClure Mountain (Fig. 40) each contain a series of carbonatites, syenites, lamprophyres, and mafic and ultramafic rocks.

A small amount of titaniferous magnetite was produced from mafic and ultramafic rocks at the Iron Mountain Mine in the McClure Mountain complex as early as 1873 (Becker and others, 1961). Although there has been no significant mineral production from the carbonatites, they do contain anomalously high concentrations of niobium, thorium, REE, and phosphorous. Small deposits of vermiculite, copper, iron, silver, and nickel are also found within the complexes.

GEOLOGICAL SETTING

From approximately 520 to 500 Ma the rocks of the alkalic complexes intruded into the surrounding Proterozoic gneisses and granites. Locally, Tertiary volcaniclastic and clastic rocks (Fig. 40) were deposited. The Texas Creek Fault and the Ilse Fault are northwest-trending faults that form the boundaries of the structural block containing the alkalic complexes (they are not in the area shown by the geological map in Fig. 40). Several northwest-trending faults within the block are the loci of syenites, carbonatites, lamprophyres, and other intrusives and veins related to the alkalic intrusive event.

PROTEROZOIC UNDIFFERENTIATED (XYgg)

The Proterozoic rocks consist of felsic and mafic gneisses of probable equivalence to the Idaho Springs Formation, 1,720 Ma (X) of the Front Range and medium-grained quartz monzonite of Silver Plume age, 1,450 Ma (Y); and quartz diorites (Taylor and others, 1975a, 1975b).

McCLURE MOUNTAIN COMPLEX

The McClure Mountain complex is the largest of the three Wet Mountain alkalic complexes and consists of mafic and ultramafic rocks, syenites, and dikes of carbonatite, lamprophyre, and syenite.

Mafic and Ultramafic Rocks (Ꞓmg)

Mafic and ultramafic rocks form discordant intrusions and layered cumulate bodies in the area around Iron Mountain. Gabbro, dunite, anorthosite, and pyroxenite, the main compositional layers in the cumulate rocks, are interlayered with thicknesses ranging from a fraction of an inch to tens of feet. The complex forms a spoon-shaped body with a thickness of several thousand feet. Layers of titaniferous magnetite were exploited at the Iron Mountain Mine in the nineteenth century. The magnetite occurs as equidimensional grains containing intergrowths of ilmenite (Shawe and Parker, 1967). The ore contains 47.86 percent iron, 12.95 percent titanium oxide, and 0.03 percent phosphorous (Singewald, 1913).

Mafic and ultramafic discordant intrusions lack layering, contain xenoliths of the cumulate layered rocks, and have discordant contacts. They are similar in composition to the layered rocks. Mafic nepheline-clinopyroxene rocks termed ijolite intrude

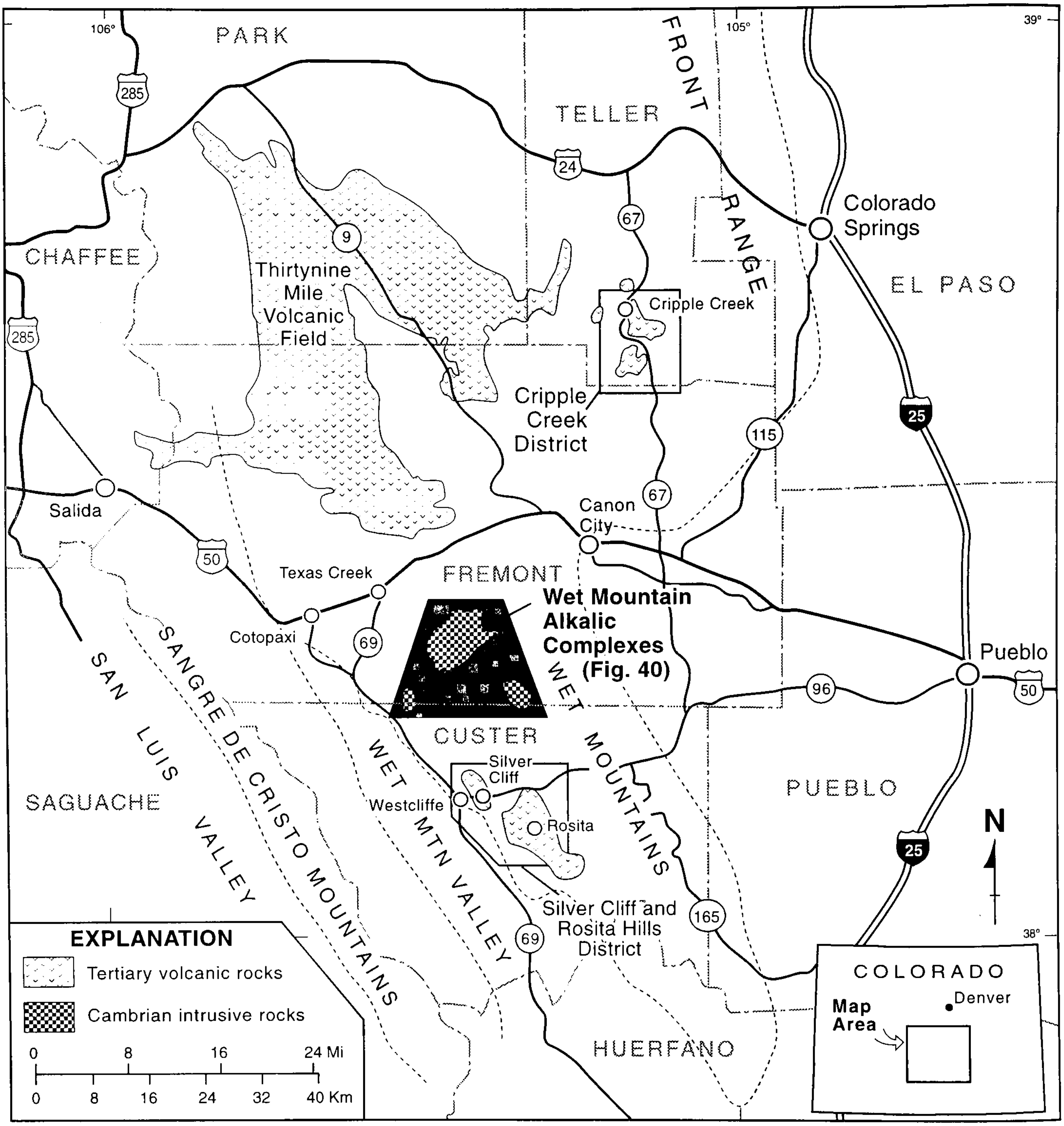

Figure 39. Index map showing location of the Cripple Creek district, Silver Cliff and Rosita Hills district, and the Wet Mountains alkalic complexes.

syenites in parts of the McClure Mountain complex (Armbrustmacher, 1984).

Syenites (€mh, €mn)

There are two distinct types of syenite in the McClure Mountain complex, a hornblende-biotite syenite and a younger nepheline syenite. These rocks intrude the mafic and ultramafic rocks of the complex. Fenitization of the rocks adjacent to the syenite intrusions is common (Armbrustmacher,

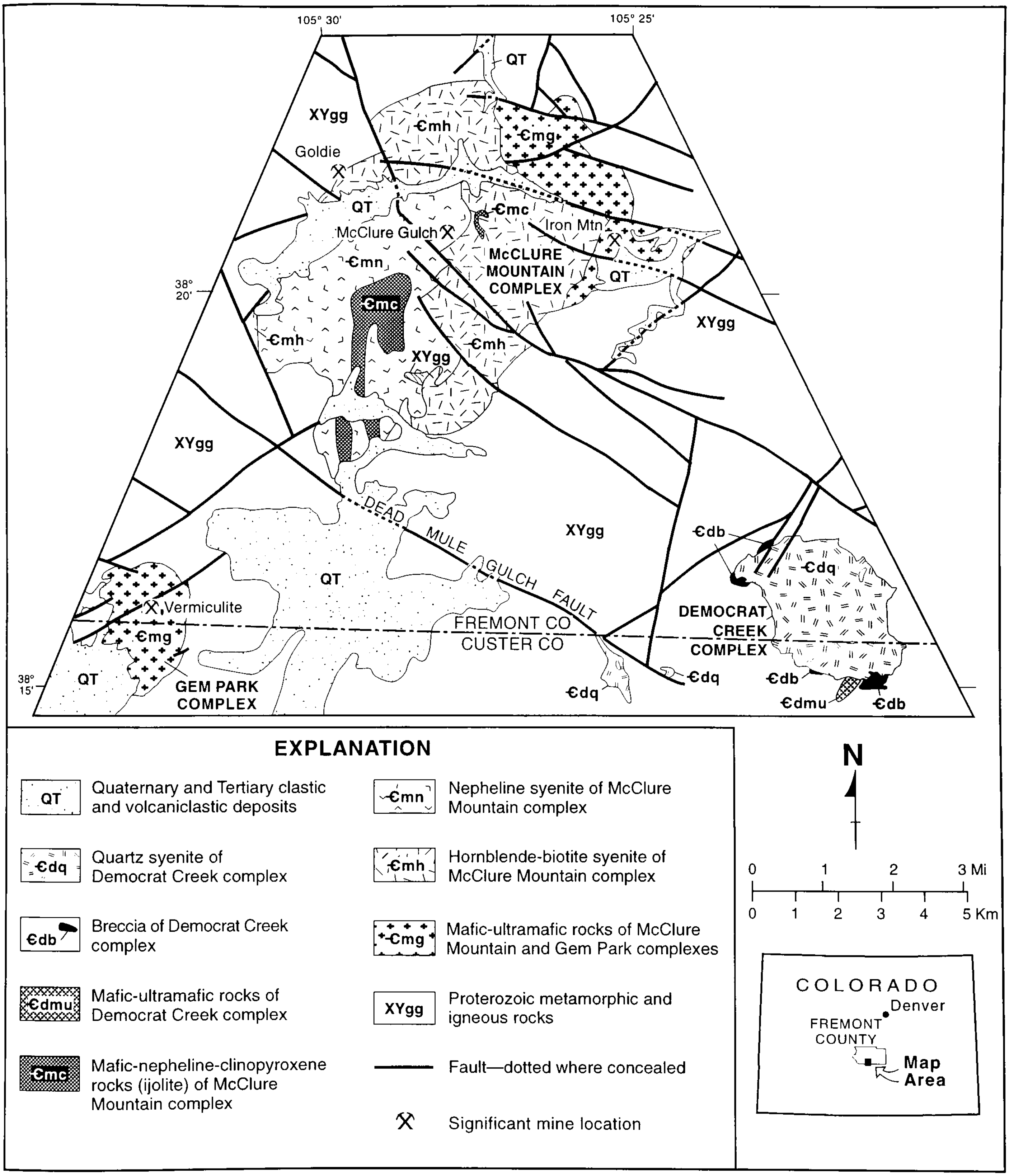

Figure 40. Geologic map of the Wet Mountains alkalic complexes, Fremont and Custer Counties, Colorado. (Modified from Taylor and others, 1975a and 1975b; Olson and others, 1977; and Armbrustmacher, 1984)

1984). Rubidium-strontium age dates of the syenites obtained by Fenton and Faure (1970) indicate a date of 517 ± 14 Ma. Olson and others (1977) reported ages of 520 Ma on hornblende using the potassium-argon method, 521 Ma using the rubidium-strontium isochron method, 508 Ma on biotite using the potassium-argon method, 506 Ma using the sphene fission track method, and a rubidium-strontium isochron date of 495 Ma for a late, red syenite dike. Armbrustmacher (1984) reported an age of 535 ± 5 Ma for the syenites of McClure Mountain.

Carbonatites

Carbonatites of the McClure Mountain complex were classified by Armbrustmacher (1979) as replacement and primary intrusive bodies (not shown on the geologic map, Fig. 40). Replacement carbonatites occur only as dikes, have replacement textures, and commonly contain calcite, hematite, monazite and lesser amounts of dolomite. Primary carbonatites have xenomorphic granular textures and are generally coarse- grained. They commonly contain barite, calcite, dolomite, hematite, and quartz. They contain higher levels of typical carbonatite elements including manganese, barium, strontium, lanthanum, cerium, yttrium, ytterbium, lead, thorium, and other rare earth elements.

The Goldie deposit is a 750 foot long carbonatite vein associated with a cogenetic lamprophyre dike. It contains a unique assemblage of rare aluminofluoride minerals including cryolite, pachnolite, prosopite, and ralstonite (Heinrich, 1977).At McClure Gulch a multiple carbonatite dike with a sulfide-bearing phase and a coarse- grained phase was described by Armbrustmacher and others (1979). The sulfide-bearing phase contains enriched amounts of Fe, La, Pb, Ce compared to the coarse-grained phase.

GEM PARK COMPLEX

The Gem Park alkalic complex is roughly a mile in diameter (Fig. 40) and consists primarily of ultramafic and mafic rocks, and lesser amounts of lamprophyre, syenite, and carbonatite. The complex was intruded into the surrounding Proterozoic rocks and was, at least partially, covered by Tertiary volcanic rocks of the Thirtynine Mile volcanic field (Parker and Sharp, 1970; Armbrustmacher, 1984).

Mafic and Ultramafic Rocks (Ꞓmg)

The mafic and ultramafic rocks of the Gem Park complex consist of pyroxenite and gabbro cumulate intrusions similar to those described in the McClure Mountain complex. The pyroxenite contains mostly clinopyroxene but also lesser amounts of brown amphibole, green amphibole, and plagioclase; accessory magnetite, apatite, and sphene; and local pyrite, chalcopyrite, and pyrrhotite. The gabbro at Gem Park is composed primarily of labradorite, clinopyroxene, olivine, brown amphibole, and magnetite.

Both the pyroxenite and gabbro and the surrounding Proterozoic rocks have locally been metasomatized to fenite, which consists of blue sodic amphibole, aegerine, tremolite-actinolite, augite, phlogopite, vermiculite and other minerals. Vermiculite was mined at the Vermiculite and Niles Mines from fenitized pyroxenite and gabbro. Rare niobium minerals along with pyrochlore, columbite, thorianite, natrolite, and monazite occur within the fenite zone (Parker and Sharp, 1970).

Syenite and Lamprophyre

A nepheline syenite pegmatite body composed of coarse-grained perthite crystals, interstitial nepheline, and dark green pyroxene is exposed at one locality in the Gem Park complex (not shown on the geologic map, Fig. 40). Lamprophyre and syenite porphyry dikes intrude the Gem Park pyroxenites and gabbros in several localities (Parker and Sharp, 1970).

Carbonatites

The carbonatite dikes (not shown on the geologic map, Fig. 40) have been grouped according to their composition by Parker and Sharp (1970): dolomite-pyrochlore, the most widespread type; dolomite-apatite; dolomite-blue amphibole-pyrochlore, noticeably radioactive because of thorium-bearing pyrochlore; and dolomite-barite-monazite, strongly radioactive.

Several carbonatite dikes are intruded into the Proterozoic granitic and metamorphic rocks outside the Gem Park alkalic complex. At the Gem Mine a carbonatite dike consisting primarily of dolomite, calcite and minor sulfide minerals, intruded both the Gem Park pyroxenite and the surrounding Proterozoic gneissic granite. Niccolite, annabergite, a nickel cobalt arsenate, and native silver were produced in the nineteenth century.

DEMOCRAT CREEK COMPLEX

The Democrat Creek complex is composed primarily of syenite with lesser amounts of mafic and ultramafic rocks and carbonatite dikes (Armbrustmacher, 1984).

Mafic and Ultramafic Rocks (Ꞓdmu)

The mafic and ultramafic rocks of the Democrat Creek complex consist of two pyroxenes, a calcium-rich clinopyroxene and a calcium-poor orthopyroxene, plagioclase, tremolite-actinolite?, and accessory apatite and magnetite. Armbrustmacher (1984, p. 13) states that the two-pyroxene assemblage is more typical of tholeitic mafic rocks than alkalic complexes.

Quartz Syenite (Ꞓdq)

The quartz syenite is variable in texture ranging from equigranular, medium-grained to pegmatitic. The feldspars, microcline, microperthite, and albite, are the most abundant constituents. Quartz occurs interstitially and varies from 2 to 32 percent by volume (Armbrustmacher, 1984). A potassium-argon date of 500 ± 25 Ma for biotite from the syenite was reported by Brock and Singewald (1968). A rubidium-strontium isochron age date of 511 ± 8 Ma is reported for the syenite of the Democrat Creek complex (Armbrustmacher and Hedge, 1982).

STRUCTURE

The northern end of the Wet Mountains is dominated by northwest-trending normal faults. Northeast-trending normal faults may be younger, as they offset Tertiary volcanic rocks near the Gem Park complex. The shape of mafic and ultramafic cumulate bodies are generally concentric, parallel to the circular outlines of the Iron Mountain-McClure Mountain and Gem Park complexes. Planar structure in the gabbros dips consistently towards the center of the complexes suggesting a funnel-shaped layered intrusive body. The syenites and carbonatite dikes were intruded later into the mafic and ultramafic rocks (Boyer, 1962).

GEOCHEMISTRY

The normative diagram (Fig. 41) demonstrates the changes in the chemistry of the various pyroxenite rocks, from the clinopyroxenite to the clinopyroxene olivinites, of the Wet Mountains district. The syenites are very low in normative olivine and show a clear trend from normative nepheline to normative quartz. Figure 42, an albite-anorthite-orthoclase normative diagram, shows the syenite and clinopyroxenite samples as being slightly potassic. The other rock samples that were analyzes plot along the albite-anorthite join line; they are more calcic than sodic. The Harker diagrams (Fig. 43) show the alka-

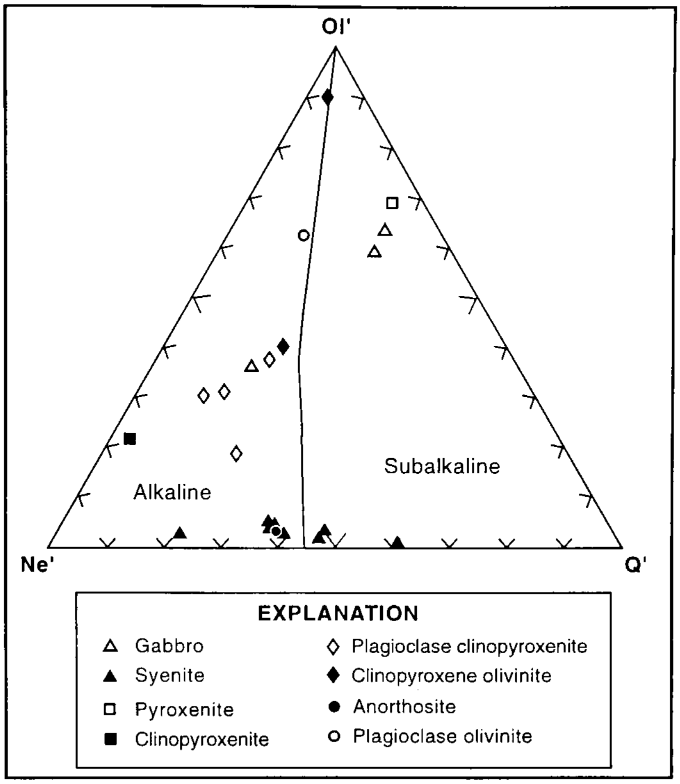

Figure 41. Normative diagram; Ne-Ol-Q of representative rock samples from the Wet Mountains alkalic complexes.

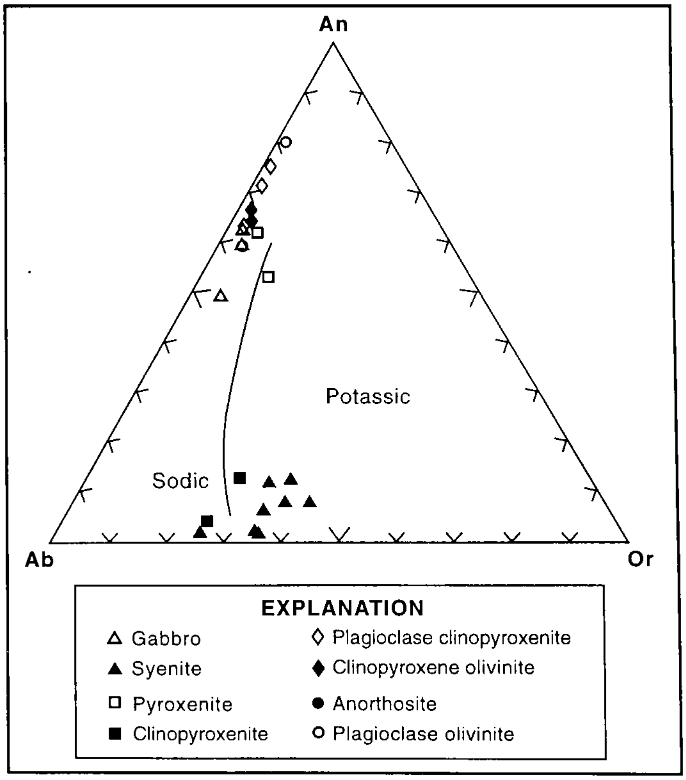

Figure 42. Normative diagram; Ab-An-Or of representative rock samples from the Wet Mountains alkalic complexes.

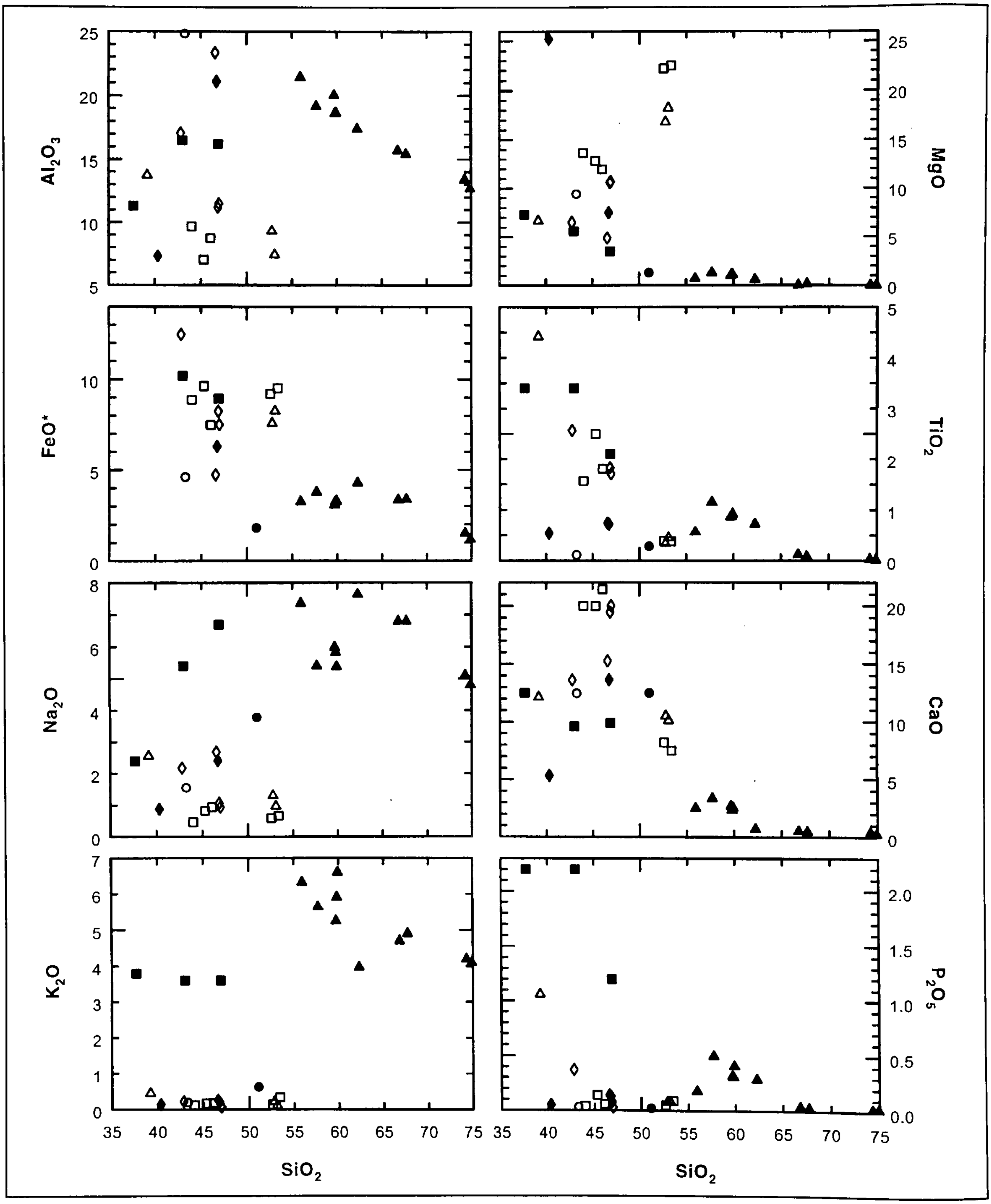

*Figure 43. Harker variation diagram of representative rock samples from the Wet Mountains alkalic complexes. Refer to the explanation on Fig. 42. (*includes Fe_2O_3)*

lic nature of the syenite rocks and the relatively high iron content of the pyroxenite and olivinite rocks. Table 8 in the Appendix lists the chemical analyses and CIPW norms used in the diagrams.

ECONOMIC GEOLOGY

The only deposits that were mined within the Wet Mountain alkalic complexes are titaniferous magnetite at the Iron Mountain Mine in the McClure Mountain complex; vermiculite from the Niles and Vermiculite Mines; and nickel and silver from the Gem Mine in the Gem Park complex. These deposits are described in the preceding pages. None of these deposits were economic successes. Several quartz-barite-carbonate veins with anomalous amounts of thorium were described by Christman and others (1959) in the Wet Mountain area especially the Democrat Creek complex. The niobium and rare earth resources of the carbonatites are a future target depending upon establishment of a market, metallurgical procedures, and increased commodity prices.

REFERENCES

Armbrustmacher, T.J., 1979, Replacement and primary carbonatites from the Wet Mountains area, Fremont and Custer Counties, Colorado: Economic Geology, v. 74, p. 888–901.

_____1984, Alkalic rock complexes in the Wet Mountains area, Custer and Fremont Counties, Colorado: U.S. Geological Survey Professional Paper 1269, 33 p.

Armbrustmacher, T.J., Brownfield, I.K., and Osmonson, L.M., 1979, Multiple carbonatite dike at McClure Gulch, Wet Mountains alkalic province, Fremont County, Colorado: The Mountain Geologist, v. 16, no. 2, p. 37–45.

Armbrustmacher, T.J., and Hedge, C.E., 1982, Genetic implications of minor-element and Sr-isotope geochemistry of alkaline rock complexes in the Wet Mountains area, Fremont and Custer Counties, Colorado: Contributions to Mineralogy and Petrology, v. 79, p. 424–435.

Becker, R.M., Shannon, S.S., Jr., and Rose C.K., 1961, Iron Mountain titaniferous magnetite deposit, Fremont County, Colorado: U.S. Bureau of Mines Report of Investigations 5864, 18 p.

Boyer, R.F., 1962, Petrology and structure of the southern Wet Mountains, Colorado: Geological Society of America Bulletin, v. 73, p. 1,047–1,070.

Brock, M.R., and Singewald, Q.D., 1968, Geologic map of the Mount Tyndall quadrangle, Custer County, Colorado: U.S. Geological Survey Geological Quadrangle Map GQ-596, scale 1:24,000.

Christman, M.R., Brock, M.R., Pearson, R.C., and Singewald, Q.D., 1959, Geology and thorium deposits of the Wet Mountains, Colorado—A progress report: U.S. Geological Survey Bulletin 1072-H, p. 491–533.

Fenton, M.D., and Faure, G., 1970, Rb-Sr whole rock age determinations of the Iron Hill and McClure Mountain carbonatite-alkalic complexes, Colorado: The Mountain Geologist, v. 7, no. 4, p. 269–275.

Heinrich, E.W., 1977, Aluminofluoride minerals of the Goldie carbonatite, Fremont County, Colorado, Mountain Geologist, v. 14, no. 2, p. 33–46.

Olson, J.C., Marvin, R.F., Parker, R.L., and Mehnert, H.H., 1977, Age and tectonic setting of lower Paleozoic alkalic and mafic rocks, carbonatites, and thorium veins in south-central Colorado: U.S. Geological Survey Journal of Research, v. 5, p. 673–687.

Parker, R.L., and Hildebrand, F.A., 1963, Preliminary report on alkalic intrusive rocks in the northern Wet Mountains, Colorado, in Geological Survey Research, 1962: U.S. Geological Survey Professional Paper 450-E, p. E8–E10.

Parker, R.L., and Sharp, W.N., 1970, Mafic-ultramafic igneous rocks and associated carbonatites of the Gem Park complex, Custer and Fremont Counties, Colorado: U.S. Geological Survey Professional Paper 649, 24 p.

Shawe, D.R., and Parker, R.L., 1967, Mafic-ultramafic layered intrusion at Iron Mountain, Fremont County, Colorado: U.S. Geological Survey Bulletin 1251-A, p. 1–27.

Singewald, J.T., 1913, The titaniferous iron ores in the United States: U.S. Bureau of Mines Bulletin 64, 145 p.

Taylor, R.B., Scott, G.R., Wobus, R.A., Epis, R.C., 1975a, Reconnaissance geological map of the Royal Gorge quadrangle, Fremont and Custer Counties, Colorado: U.S. Geological Survey Miscellaneous Investigation Series Map, I-869, scale 1:62,500.

_____1975b, Reconnaissance geological map of the Cotopaxi 15-minute quadrangle, Fremont and Custer Counties, Colorado: U.S. Geological Survey Miscellaneous Investigation Series Map, I-900, scale 1:62,500.

Chapter 10

Ralson Buttes District

INTRODUCTION AND HISTORY

The Ralston Buttes district is located within the Front Range mineral belt in Jefferson County just north of the city of Golden (Fig. 44). Uranium ores in the Proterozoic rocks of the Front Range were first documented in the late 1940s when Fred Schwartzwalder brought to the attention of the Atomic Energy Commission ore samples from an old copper prospect, the Hoffmeister prospect (later called the Mena Mine). Several other uranium occurrences were discovered during the early 1950s (Adams and others, 1953). The most important producer in the district was the Schwartzwalder Mine, which produced more than 17 million pounds of U_3O_8 from 1953 through 1986, its last year of recent production (Cotter Corporation, oral communication 1995). Several other mines including the Mena, the Aubrey Ladwig, the Ohman, and the Ascension all shipped lesser amounts of ore (Sheridan and others, 1967). In 1997 the Schwartzwalder Mine reopened as economic conditions for uranium production improved.

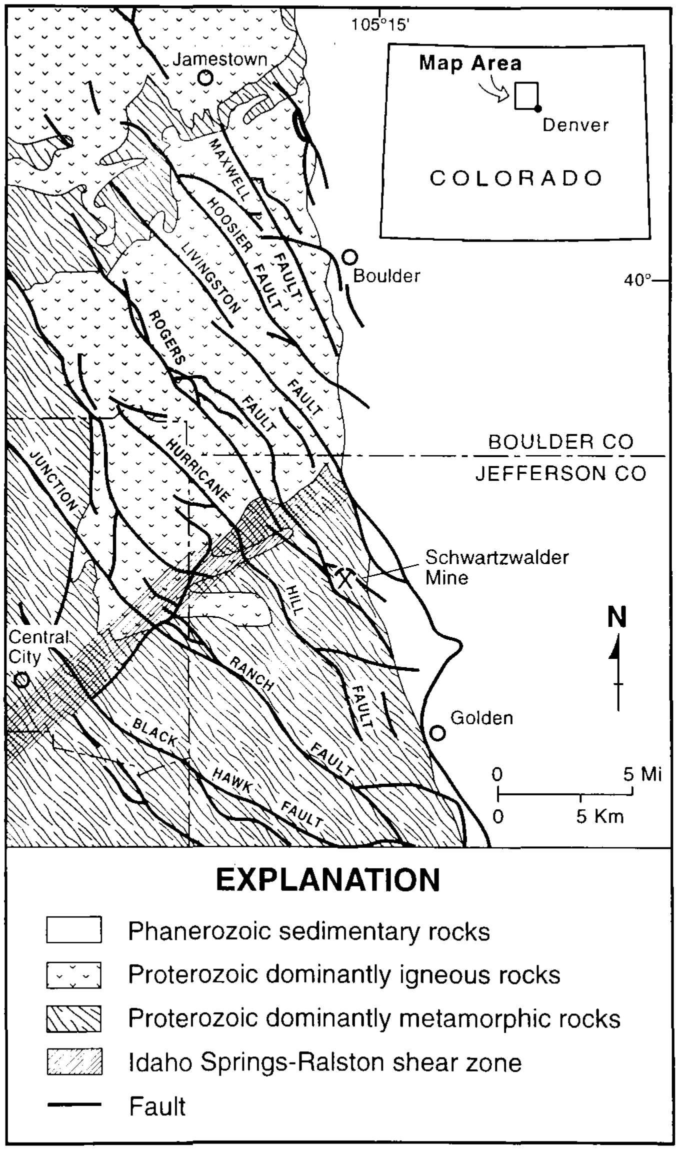

Figure 44. Breccia faults and general geology of the Ralston Buttes district, central Front Range Colorado. (From Wallace and Karlson, 1985)

GEOLOGICAL SETTING

Uranium (pitchblende) in the Ralston Buttes district is found solely within the Proterozoic metasediments and metavolcanics. Pennsylvanian to Permian redbeds of the Fountain Formation and younger sedimentary rocks crop out less than a mile to the east of the Schwartzwalder Mine. Ore occurs in steeply-dipping hydrothermal veins that occupy breccia zones and related fractures (Fig. 45).

METAMORPHIC ROCKS

A mica schist unit that crops out widely in the area south of the Schwartzwalder Mine is thought to be

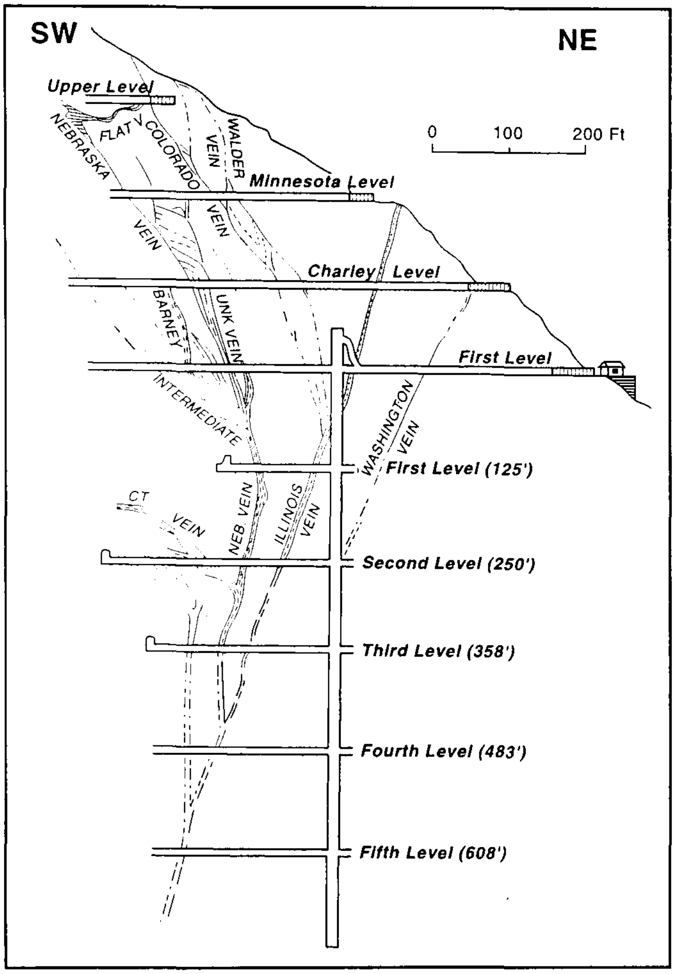

45. Cross section of the Schwartzwalder Mine, normal to the plane of the principle veins. (From Downs and Bird, 1965)

the oldest Proterozoic unit in the area. Hornblende gneiss, microcline-quartz-plagioclase-biotite gneisses and quartzites all occur either as distinct mappable units or as complexly interfingered units (Sheridan and others, 1967). Protoliths of these metamorphic rocks were deposited in a volcanic arc and back-arc basin prior to about 1,730 Ma (Hills and Houston, 1979).

IGNEOUS ROCKS

The Boulder Creek Granodiorite and an unnamed quartz monzonite intrude the older metamorphic rocks. Weakly- to moderately-developed foliation within these two large intrusive units indicate that they were syn-metamorphic or slightly post-metamorphic, approximately 1,700 Ma.

Hornblende diorite occurs as dikes within the foliated metamorphic rocks. The hornblende diorites have a metamorphic texture and are probably similar in age to the metamorphic rocks. The hornblende diorite consists principally of hornblende and plagioclase. Accessory minerals include biotite, apatite, magnetite, rutile, and sphene.

Hornblende-biotite lamprophyres occur as widely scattered small dikes and sills. The dikes are about 15 feet thick but can be traced only short distances along strike. The lamprophyres contain microcline, hornblende, and biotite. Accessory minerals are epidote, sphene, apatite, allanite, and zircon. The radioactivity of the lamprophyres is reported to be twice to three times that of the surrounding rocks. The high radioactivity is thought to be related to anomalous amounts of zircon and allanite.

Granitic pegmatites and aplites are also found throughout the foliated rocks. They consist principally of quartz and microcline and lesser amounts of plagioclase, biotite, muscovite, and tourmaline. Locally the pegmatites contain beryl, chrysoberyl, apatite, magnetite-ilmenite, garnet, allanite, monazite, triplite, and sillimanite (Sheridan and others, 1967).

STRUCTURE

Major folds in the Precambrian rocks of the Ralston Buttes area trend east to northeast.

Fault systems and fracture zones, like those that host the Schwartzwalder Mine, trend northwest and some cut both Proterozoic rocks and the younger sedimentary formations (Fig. 44). The northeast-trending Idaho Springs-Ralston shear zone, a zone of regional cataclasis, is located about 4 miles to the northwest of Schwartzwalder Mine (Sheridan and others, 1967).

GEOCHEMISTRY

The total alkali versus silica plot (Fig. 46) demonstrates the alkalic nature of the Proterozoic monzonite from the Ralston Buttes area. The biotite gneiss and amphibolite are also strongly alkalic. The presence of garnet in the biotite gneiss causes an increase in the silica content and subsequently they plot in the subalkaline field. The Harker diagram (Fig. 47) shows the variation of the major oxides against silica. Table 9 in the Appendix lists the chemical analyses and CIPW norms used in the diagrams.

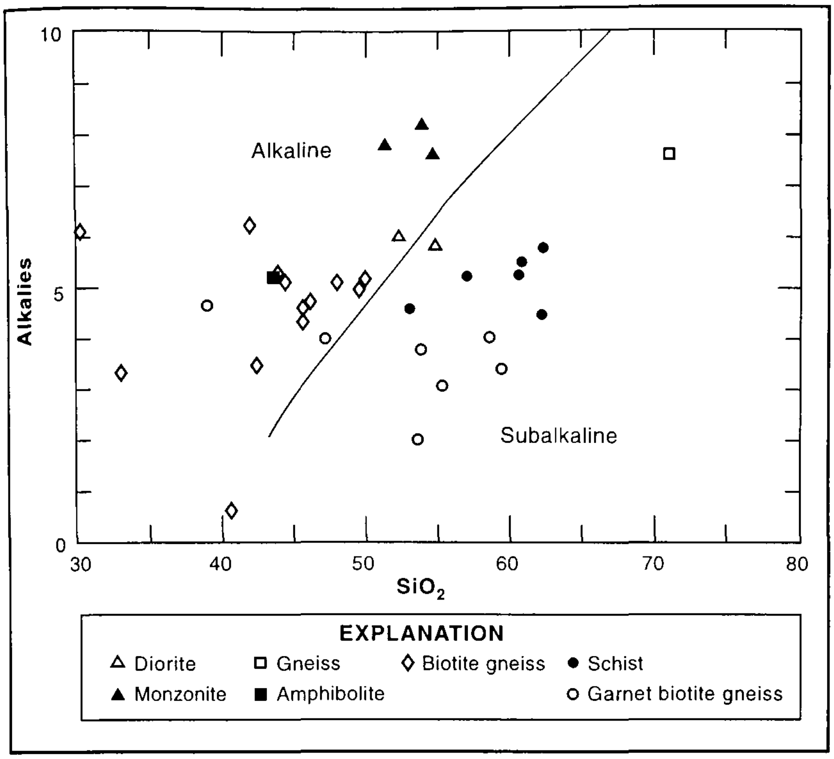

Figure 46. Plot of alkalies versus silica of representative rock samples from the Ralston Buttes district.

ECONOMIC GEOLOGY

The uranium deposits of the Ralston Buttes district can be divided into two main areas: the Ralston Creek area, which contains the Schwartzwalder Mine, and the Golden Gate Canyon area. Pitchblende and other minor uranium oxide minerals and base metal sulfides are found in steeply-dipping hydrothermal veins developed along breccia and fracture zones (Fig. 45). Deposits in the Golden Gate Canyon area possess epithermal features such as simple mineralogy and voids and crustification whereas those in the Ralston Creek area are thought to be mesothermal because of their more complex mineralogy. The host rocks of the Schwartzwalder Mine are a garnet-biotite gneiss and quartzite which form a thin transition zone between the more regionally extensive hornblende gneiss and mica schist units (Sims and Sheridan, 1964).

The main fissure veins of the Schwartzwalder Mine are parallel to a major northwest-trending fault, the Rogers Breccia Reef (Lovering and Goddard, 1950). Folding during the Proterozoic caused a tectonic thickening of the transition zone garnet-biotite gneiss and quartzite. Subsequent faulting generated a complex and permeable fault system in these brittle transition- zone rocks. During the Laramide tectonic event the fault system became the conduit for fluids that left behind massive uranium deposits (Wallace and Karlson, 1985). The richest ore in the mine has been found in two different structural positions along the main veins: where the vein branches, and where the dip of the vein changes abruptly (Downs and Bird, 1965).

A uranium-lead age date of 73 ± 5 Ma was obtained from a sample of pitchblende from the Mena Mine (Sheridan and others, 1967, p.80). Ludwig and others (1985) studied lead isotopes and uranium-lead isochrons from the Illinois and Titan vein ores from the Schwartzwalder Mine. They concluded the age of mineralization for both veins was 69.3 ± 1.1 Ma and that the metals in Schwartzwalder ore bodies were derived from sources of 1,730 ± 130 Ma.

Two stages of alteration, a carbonate-sericite alteration and a later hematite-adularia alteration, are observed around the veins. The largest percentage of uranium ore is associated with the late stage hematite-adularia alteration. Wallace and Whelan (1986) studied alteration, mineralization, and stable isotopes and concluded that the uranium, base metals, and other minerals were not consistent with a source from an unrecognized magma or from the overlying Phanerozoic rocks. They proposed that the uranium-bearing hydrothermal fluids formed from prolonged interaction with the Proterozoic rocks and the regolith developed on these rocks. The loss of carbon dioxide engendered by increased fluid flow in the fracture zones led to the precipitation of the uranium, base metals, and other minerals from the hydrothermal fluids.

The Laramide age of the uranium deposits is a strong indicator that the mineralization is related to the same intrusive event that formed the precious and base metal vein deposits of the Front Range mineral belt. However, there are no exposed Laramide intrusive rocks in the Ralston Buttes area that can be related to the ores.

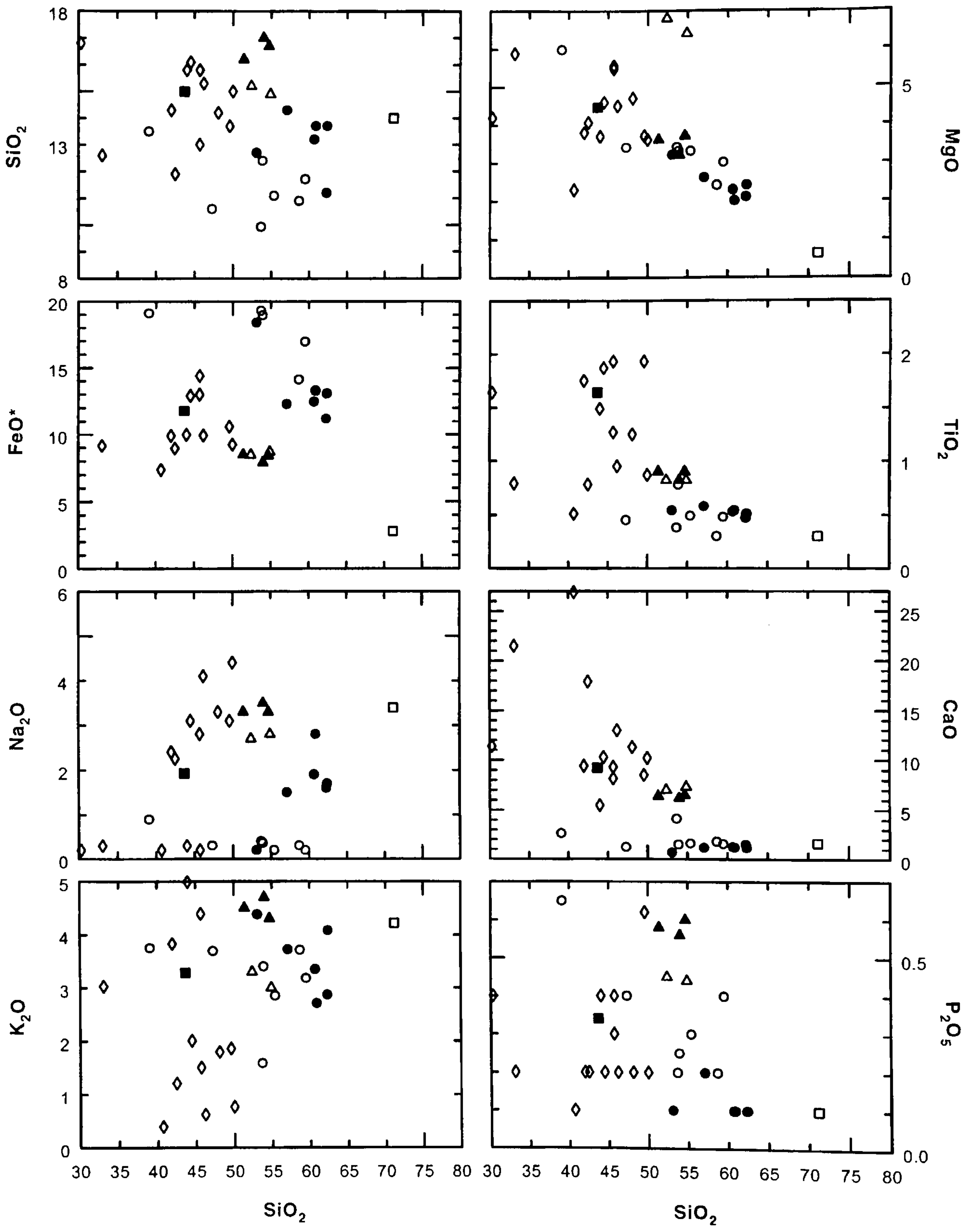

*Figure 47. Harker variation diagram of representative rock samples from the Ralston Buttes district. Refer to the explanation on Fig. 46. (*includes Fe_2O_3)*

REFERENCES

Adams, J.W., Gude, A.J., 3rd, and Beroni, E.P., 1953, Uranium occurrences in the Golden Gate Canyon and Ralston Creek areas, Jefferson County, Colorado: U.S. Geological Survey Circular 320, 16 p.

Downs, G.R., and Bird, A.G., 1965, The Schwartzwalder uranium mine, Jefferson County, Colorado: Mountain Geologist, v. 2, no. 4, p. 183–191.

Hills, F.A., and Houston, R.S., 1979, Early Proterozoic tectonics of the central Rocky Mountains, North America: University of Wyoming Contributions to Geology, v. 17, p. 89–106.

Lovering, T.S., and Goddard, E.N., 1950, Geology and ore deposits of the Front Range, Colorado: U.S. Geological Survey Professional Paper 223, 319 p.

Ludwig, K.R., Wallace, A.R., and Simmons, K.R., 1985, The Schwartzwalder uranium deposit, II—Age of uranium mineralization and lead isotope constraints on genesis: Economic Geology, v. 80, p. 1858–1871.

Sheridan, D.M., Maxwell, C.H., and Albee, A.L., 1967, Geology and uranium deposits of the Ralston Buttes district, Jefferson County, Colorado: U.S. Geological Survey Professional Paper 520, 121 p., scale 1:24,000.

Sims, P.K., and Sheridan, D.M., 1964, Geology of uranium deposits in the Front Range, Colorado: U.S. Geological Survey Bulletin 1159, 116 p.

Van Horn, R., 1976, Geology of the Golden quadrangle: U.S. Geological Survey Professional Paper 872, 116 p.

Wallace, A.R., 1983, Analytical data from host rocks and ores, Schwartzwalder uranium deposit, Front Range, colorado: U.S. Geological Survey Open File report 83-364, 20 p.

Wallace, A.R., and Karlson, R.C., 1985, The Schwartzwalder uranium deposit, I—Geology and structural controls on mineralization: Economic Geology, v. 80, p. 1,842–1,857.

Wallace, A.R., and Whelan, J.F., 1986, The Schwartzwalder uranium deposit, III—Vein mineralization, light stable isotopes, and genesis of the deposit: Economic Geology, v. 81, p. 872–888.

Young, E.J., 1979, Analytical data on the Schwartzwalder uranium deposit, Jefferson County, Colorado: U.S. Geological Survey Open File Report 79-968, 34 p.

Chapter 11

Other Alkalic Provinces in Colorado

SPANISH PEAKS

The Spanish Peaks of Las Animas and Huerfano Counties (Fig. 1) are part of a regional alkalic and subalkalic igneous province of middle Tertiary age marked by a rich variety of igneous rock types including stocks, laccoliths, plugs, and dikes and sills. Compositions are equally variable and range from lamprophyres to granite porphyries.

The Spanish Peaks are formed by two large stocks of granite, granodiorite, and monzonite (syenodiorite of Johnson [1968] as renamed by Penn [1994]) porphyry. Other intrusive stocks in the region are composed of rocks of similar lithology. Laccoliths in the province are composed of monzonite and syenite porphyries at the Black Hills and Sheep Mountain. Plugs are smaller intrusive bodies composed of latite and monzonite porphyry.

More than 500 dikes were intruded in a radial manner around the central two stocks. The radial pattern of the dikes has been a subject of intense geological interest. The rocks of the dikes and related sills are mostly monzonite porphyries and lamprophyres with lesser amounts of olivine gabbro, basalt, microgranodiorites, syenite porphyry, and diorite. The lamprophyres have been classified as either minettes (dominant phenocrysts are biotite) or vogesites (dominant phenocrysts are augite or hornblende) (Johnson, 1961, 1968; Knopf, 1936). Recent petrographic descriptions and geochemical analyses of whole rocks and trace elements can be found in Penn (1994) and Smith (1975).

Argon-argon dates indicate that the rocks of the Spanish Peaks area were intruded continuously from 26.6 Ma to 21.3 Ma. Many of the alkalic lamprophyre and basalt dikes intruded into pre-existing joints and fractures during the first stage of magmatism. During the second stage the large stocks of monzonite porphyry and granite were intruded, and during the third stage lamprophyres were again intruded (Penn, 1994).

The Tertiary sedimentary rocks in the Spanish Peaks province are extensively altered by the intrusives. A concentric alteration pattern and haloes were described by Utada and Vine (1985). Characteristic minerals of these zones from the center to the periphery are amphibole, prehnite-pumpellyite, plagioclase, laumontite, and zeolites.

Placer gold deposits have been described around the Spanish Peaks, but production has been very small. Several silver occurrences are reported in the monzonite porphyry and in altered Tertiary sedimentary rocks of West Spanish Peak (Hills, 1901). Vanderwilt (1947) describes the veins as containing gold and silver associated with galena, gray copper, chalcopyrite, and sphalerite. Total production prior to 1908 was 168 ounces of gold, 1,176 ounces of silver, 92 pounds of copper, and 1,067 pounds of lead.

TWO BUTTES

The Two Buttes alkalic intrusive complex is located in the far southeastern corner of Colorado in Baca County, about 150 miles east of the Rocky Mountain front (Fig. 1). The igneous rocks at Two Buttes range in composition from trachybasalt to trachyandesite and occur as small isolated dikes and sills. The poor exposures cover an area of about a square mile. The rocks have a porphyritic texture. Xenoliths include pyroxenite, sedimentary rocks, granites, and felsic gneiss. The average potassium-argon age of phlogopites from the Two Buttes complex is 36.8 ± 0.4 Ma (Davis and others, 1996)

The host rocks for the intrusive complex are Permian through Jurassic sedimentary rocks that have been variably hydrothermally altered and bleached. Quartz veins and gossan are common; however, no ore minerals have been described in the literature (Davis and others, 1996; Davis, 1993).

NORTH AND SOUTH TABLE MOUNTAIN

North and South Table Mountains, three alkalic lava flow units separated by clastic rocks of the Denver Formation, are located near Golden in Jefferson County, Colorado (Fig. 1) (Van Horn, 1957; Scott, 1972). These flows are shoshonites consisting of augite, plagioclase, olivine, and magnetite in a fine-grained matrix (Scott, 1972). The source of the Table Mountain flows is hypothesized to be the Ralston Dike located about 4 miles north of Golden. E.E. Larson in Scott (1972) reported a potassium-argon date of 63 ± 2.5 Ma from the Ralston Dike.

The only economic mineral occurrences in the area are several zeolite species on North Table Mountain and to a lesser extent on South Table Mountain. The zeolites occur mostly as vesicle fillings in the monzonite flows (Waldschmidt, 1939).

UTE MOUNTAIN

The Ute Mountain laccolith complex is located in the far southwestern corner of the state in Montezuma County (Fig. 1). The intrusive rocks of the Ute Mountain area are Late Cretaceous age and form a differentiated calc-alkalic series of rocks ranging from microgabbro through quartz monzonite. Rare alkalic lamprophyres are associated with the Ute Mountain stocks. Small deposits of copper, uranium, and vanadium occur in the Mesozoic sedimentary rocks of the area and, rarely, in breccias associated with the laccolith (Ekren and Houser, 1965).

MIDDLE PARK–PARK RANGE

Igneous rocks of alkalic affinity named the Rabbit Ears Volcanics occur in the Park Range, northern Gore Range, and Rabbit Ears Range of Jackson, Park, and Routt Counties (Fig. 1). The Rabbit Ears Volcanics consist primarily of trachybasalt and trachyandesite with lesser amounts of tuff breccia, ash flow tuff, and breccia of rhyolitic and quartz latite composition. A potassium argon date of 33 ± 3 Ma was obtained from a sanidine crystal from the tuff north of Hot Sulphur Springs (Izett, 1968); however, a fission track date from a zircon obtained from a trachyandesite porphyry intrusive from near Rabbit Ears Pass yielded a date of only 17.0 ± 1.5 Ma (Naeser in Snyder, 1980).

Other less voluminous alkalic rocks of Late Cretaceous-early Tertiary age also occur in parts of this region. These rocks include the fragmental andesites and trachyandesites of the Windy Gap Volcanic Member of the Middle Park Formation and small intrusive bodies of trachyandesite and syenite (Izett, 1968). No economic mineral deposits have been found in these alkalic volcanic and intrusive rocks (Hail, 1968; Izett, 1968; Izett and Venable-Barclay, 1973; and Snyder, 1980).

PIKES PEAK BATHOLITH

The Pikes Peak batholith is exposed over a large area, 2,800 square kilometers, of the Colorado Front Range from Colorado Springs to just southwest of Denver (Fig. 1). The batholith is largely granitic and contains several local stocks of subalkalic to alkalic rocks. The Pikes Peak batholith at 1,040 ± 13 Ma marked the culmination of the three Proterozoic intrusive events; the oldest at about 1,700 Ma, the second at about 1,400 Ma, and the Pikes Peak event at about 1,000 Ma (Hutchinson, 1976).

Coeval alkalic to subalkalic stocks associated with the Pikes Peak batholith include the Spring Creek syenite, the gabbro of Lake George (Barker and others, 1976), the potassic granites of the Rampart Range, the Tarryall intrusive center, and the Sugarloaf stock (Wobus, 1976). These alkalic centers range in composition from gabbro to syenite.

There are no reported metallic mineral occurrences of note in the Pikes Peak batholith or its associated alkalic to subalkalic stocks. Fluorite deposits of the Saint Peters Dome area in the southern part of the batholith are thought to be related to the intrusion of Tertiary age lamprophyre dikes associated with the nearby Cripple Creek volcanic diatreme complex (Steven, 1949).

REFERENCES

Barker, F., Hedge, C.E., Millard, H.T., Jr., and O'Neil, J.R., 1976, Pikes Peak batholith—Geochemistry of some minor elements and isotopes, and implication for magma genesis, *in* Epis, R.C., and Weimer, R.J., eds., Studies in Colorado field geology: Professional Contributions of the Colorado School of Mines, no. 8, p. 44–56.

Davis, L.L., 1993, Potassic mafic rocks at Two Buttes: Austin, University of Texas, Ph.D. dissertation, 312 p.

Davis, L.L., 1996, Smith, D., McDowell, F.W., Walker, N.W., and Borg, L.E., 1996, Eocene potassic magmatism at Two Buttes Colorado, with implications for Cenozoic tectonics and magma generation in the western United States: Geological Society of America Bulletin, v. 108, p. 1567–1579.

Ekren, E.B., and Houser, F.N., 1965, Geology and petrology of the Ute Mountains area, Colorado: U.S. Geological Survey Professional Paper 481,74 p.

Hail, W.J., Jr., 1968, Geology of southwestern North Park and vicinity, Colorado: U.S. Geological Survey Bulletin 1257, 119 p., scale 1:24,000.

Hills, R.C., 1901, Description of the Spanish Peaks quadrangle, Colorado: U.S. Geological Survey Geological Atlas, Spanish Peaks Folio 71, scale 1:125,000.

Hutchinson, R.M. 1976, Granite tectonics of the Pikes Peak batholith, *in* Epis, R.C., and Weimer, R.J., eds., Studies in Colorado field geology: Professional Contributions of the Colorado School of Mines, no. 8, p. 32–43.

Izett, G.A., 1968, Geology of the Hot Sulphur Springs quadrangle, Grand County, Colorado: U.S. Geological Survey Professional Paper 586, 79 p., scale 1:62,500.

Izett, G.A., and Venable-Barclay, C.S., 1973, Geology of the Kremmling quadrangle, Grand County, Colorado: U.S. Geological Survey Geological Quadrangle Map GQ-1115, scale 1:62,500.

Johnson R.B., 1961, Patterns and origin of radial dike swarms associated with West Spanish Peak and Dike Mountain, south-central Colorado: Geological Society of America Bulletin, v. 72, p. 579–590.

_____1968, Geology of the igneous rocks of the Spanish Peaks region, Colorado: U.S. Geological Survey Professional Paper 594-G, 47 p.

Knopf, A., 1936, Igneous geology of the Spanish Peaks region, Colorado: Geological Society of America Bulletin, v. 47, p. 1727–1784.

Penn, B.S., 1994, An investigation of the temporal and geochemical characteristics, and the petrogenetic origins of the Spanish Peaks intrusive rocks of south-central Colorado: Golden, Colorado School of Mines, Ph.D. dissertation, 199 p.

Scott, G.R., 1972, Geologic map of the Morrison quadrangle, Jefferson County, Colorado: U.S. Geological Survey Miscellaneous Investigation Map I-790A, scale 1:24,000.

Smith, R.P., 1975, Structure and petrology of Spanish Peaks dikes, south-central Colorado: Boulder, University of Colorado Ph.D. dissertation, 191 p.

Snyder, G.L., 1980, Geologic map of the northernmost Gore Range and southernmost northern Park Range, Grand, Jackson, and Routt Counties, Colorado: U.S. Geological Survey Miscellaneous Investigation Map I-1114, scale 1:48,000.

Steven, T.A., 1949, Geology and fluorspar deposits of the Saint Peters Dome district, Colorado: Colorado Scientific Society Proceedings, v. 15, no. 6, p. 259–284.

Utada, M., and Vine, J.D., 1985, Zonal distribution of zeolites and authigenic plagioclase, Spanish Peaks region, southern Colorado: Conference Proceedings, Sixth International Zeolite Conference, 10–15 July, 1983, Reno, Nevada, p. 604–615.

Van Horn, R., 1957, Bedrock geology of the Golden quadrangle, Colorado: U.S. Geological Survey Geological Quadrangle Map GQ-103, scale 1:24,000.

Vanderwilt, J.W., 1947, Mineral resources of Colorado: Denver, State of Colorado Mineral Resources Board, 547 p.

Waldschmidt, W.A., 1939, The Table Mountain lavas and associated igneous rocks near Golden, Colorado: Colorado School of Mines Quarterly, v. 34, no. 3, 62 p.

Wobus, R.A., 1976, New data on potassic and sodic plutons of the Pikes Peak batholith, central Colorado, *in* Epis, R.C., and Weimer, R.J., eds., Studies in Colorado field geology, Professional Contributions of the Colorado School of Mines, no. 8, p. 57–67.

Appendix A

Tables of Geochemical Analyses and CIPW Norms of Rock Samples from Colorado Mining Districts

Note: CIPW norms were calculated using the Igpet program by Terra Softa Inc., Somerset, New Jersey. The numbers on the "K" header line of each table refers to the major rock type group described at the end of each table.

Table 1. Chemical analyses and CIPW norms of rock samples from the Front Range mineral belt.

Sample **K**	**1** **3**	**2** **3**	**3** **3**	**4** **3**	**5** **1**	**6** **9**	**7** **1**	**8** **5**
SiO_2	56.64	53.95	52.1	51.43	44.26	36.77	30.47	27.71
Al_2O_3	17	18.56	19.35	19.35	13.95	10.29	9.04	2.92
Fe_2O_3	3.11	3.86	4.63	5.32	7.84	10.54	16.37	21.8
FeO	5.06	4.23	4.16	4.7	8.87	12.11	14.91	15.7
MgO	2.79	2.35	3.19	3.05	6.59	9.34	7.86	17.98
CaO	6.2	6.58	7.15	7.09	10.41	12.26	9.33	6.83
Na_2O	3.16	3.36	3.39	3.54	1.81	1.16	0.77	0.19
K_2O	3.4	3.88	3.77	3.52	1.75	1.38	2.89	0
H_2O-	0.31	0.3	0.06	0.08	0.33	0.36	0.32	0.54
H_2O+	0.7	0.68	0.13	0.35	1.54	1.7	1.32	3.51
TiO_2	0.81	0.76	0.94	0.85	1.41	2.49	2.52	2.69
CO_2	0	0.85	0	0	0.33	0.18	0.21	0.22
P_2O_5	0.44	0.6	0.71	0.6	0.85	1.4	2.87	0
S	0	0.06	0	0	0.13	0.33	0.69	0.04
MnO	0.2	0.17	0.1	0	0.19	0.23	0.39	0.22
BaO	0.06	0.13	0	0	0.03	0.04	0.09	0
SrO	0	0.07	0	0	0.03	0.02	0.04	0
Total	99.88	100.39	99.68	99.88	100.32	100.6	100.09	100.35
%AN	43.86	44.42	46.5	45.88	60.56	100	100	100
Q	6.39	1.12	0	0	0	0	0	0
or	20.53	23.46	22.46	21.02	10.87	0	0	0
ab	28.99	30.87	30.7	31.62	16.96	0	0	0
an	22.65	24.67	26.68	26.81	26.05	20.04	14.05	7.89
lc	0	0	0	0	0	6.95	12.35	0
ne	0	0	0	0.3	0.08	6.66	4.6	1.13
kal	0	0	0	0	0	0	2.08	0

Sample **K**	**1** **3**	**2** **3**	**3** **3**	**4** **3**	**5** **1**	**6** **9**	**7** **1**	**8** **5**
di	4.68	3.78	3.54	3.83	17.94	25.4	0	0
hy	12.2	11.31	3.5	0	0	0	0	0
ol	0	0	7.74	11.46	20.96	28.68	46.79	65.86
mt	2.47	2.42	2.57	2.48	3.2	4.45	4.66	4.86
il	1.15	1.08	1.32	1.2	2.07	3.7	3.89	4.15
ap	0.94	1.28	1.5	1.27	1.87	3.12	6.65	0
wus	0	0	0	0	0	0	0	7.2
COS	0	0	0	0	0	0.99	4.94	8.91

Sample **K**	**9** **10**	**CC1** **6**	**CC2** **7**	**11-107** **11**	**14-165B** **11**	**24-165D** **11**	**15-2** **11**	**14-164B** **11**
SiO_2	9.6	60.3	66.44	58.1	63.8	62.09	63.6	65.4
Al_2O_3	6.27	18.12	14.98	18.4	16.2	17.62	16.6	16.8
Fe_2O_3	44.72	2.45	1.57	4.3	2.7	2.66	2.7	2.6
FeO	25.31	1.25	0.43	2.8	2.4	2.09	3	2
MgO	5.16	0.28	0.18	2	1.5	1.35	1.6	1.08
CaO	3.75	3.89	2.47	4.6	5	5.29	3.8	3.23
Na_2O	0.15	5.83	1.12	4.1	3.5	4.34	3	3.3
K_2O	0	5.01	3.32	1.7	3.2	2.81	3.1	3.6
H_2O-	0	0.75	4.6	1.2	0.22	0.12	0.6	0.47
H_2O+	0.51	0.77	4.06	1.2	0.22	0.35	0.6	0.47
TiO_2	4.48	0.55	0.2	0.79	0.58	0.51	0.5	0.39
ZrO_2	0	0.01	0.01	0	0	0	0	0
CO_2	0	0	0.67	0.05	0.01	0.02	0	0
P_2O_5	0.08	0.25	0.11	0.48	0.44	0.29	0.32	0.29
SO3	0	0.06	0	0	0	0	0	0
Cl	0	0	0	0.02	0.03	0.02	0.03	0.03
F	0	0	0	0.12	0.08	0.07	0.06	0.08
S	0	0	0.02	0	0	0.07	0	0.1
MnO	0	0.12	0.16	0.08	0.1	0.14	0.02	0.02
BaO	0	0.26	0.11	0	0	0	0	0
Total	100.03	99.9	100.45	99.94	99.98	99.84	99.53	99.86
%AN	100	13.94	53.43	34.85	37.74	34.25	38.36	32.29
Q	0	0.82	44.02	13.2	17.66	12.35	21.74	22.28
or	0	29.71	22.21	10.38	19.2	16.75	18.91	21.78
ab	0	52.55	11.39	38.05	31.92	39.31	27.81	30.34
an	20.34	8.51	13.07	20.35	19.35	20.48	17.31	14.47
ne	1	0	0	0	0	0	0	0
C	0	0	6.57	2.94	0	0	2.44	2.57
di	0	2.53	0	0	2.35	3.27	0	0
hy	0	0	0.56	10.43	5.55	4.4	8.24	5.37
wo	0	2.42	0	0	0	0	0	0
ol	6.99	0	0	0	0	0	0	0

Sample K	9 10	CC1 6	CC2 7	11-107 11	14-165B 11	24-165D 11	15-2 11	14-164B 11
mt	7.74	2.15	1.08	2.47	2.21	2.12	2.16	2.02
il	7.72	0.77	0.32	1.14	0.82	0.72	0.72	0.56
hem	0	0	0.52	0	0	0	0	0
ap	0.21	0.52	0.26	1.04	0.93	0.61	0.69	0.62
wus	55.39	0	0	0	0	0	0	0
COS	0.61	0	0	0	0	0	0	0

Sample K	210-1 11	24-196 11	110-31B 11	38-133 3	14-165A 4	E1-10 3	2P-195 3	2P-917 3
SiO_2	68.62	66.32	69.4	65.7	76.4	50.04	50.7	52
Al_2O_3	15.82	16.22	16.2	15.4	12.4	17.36	17.3	17.8
Fe_2O_3	1.2	2.23	1.5	1.5	1.4	4.07	4.2	4
FeO	1.34	1.99	0.93	1.2	0.72	4.63	4.2	3.9
MgO	0.67	1.05	0.57	0.76	0.18	3.19	3	2.3
CaO	2.98	2.35	1.6	2.8	0.64	8.19	7.3	6.5
Na_2O	3.75	3.76	4.6	4	2.3	4.99	5.5	6
K_2O	3.66	3.76	3.8	3.6	5.9	4.65	4.6	4.8
H_2O-	0.45	1.1	0.49	0.45	0.25	0.05	0.23	0.27
H_2O+	0.11	0.29	0.49	1	0.25	0.52	0.23	0.27
TiO_2	0.27	0.38	0.3	0.29	0.08	0.93	0.9	0.84
CO_2	0.31	0.01	0.01	2.6	0	0.11	0.2	0.22
P_2O_5	0.14	0.23	0.18	0.18	0.02	0.69	0.68	0.56
Cl	0.02	0.01	0	0	0.02	0.14	0	0
F	0.06	0.04	0.04	0	0.01	0.11	0	0
S	0.03	0	0	0	0	0.03	0	0
MnO	0.03	0.05	0.02	0.16	0	0.22	0.22	0.22
Total	99.46	99.79	100.13	99.64	100.57	99.92	99.26	99.68
%AN	29.18	23.13	14.07	26.15	12.85	47.18	34.89	27.21
Q	23.94	21.93	22.71	21.05	36.75	0	0	0
or	22.07	22.74	22.63	22.3	35.61	27.45	27.16	28.17
ab	34.37	34.56	41.63	37.66	21.1	12.57	16.66	19.83
an	14.16	10.4	6.82	13.33	3.11	11.23	8.93	7.41
ne	0	0	0	0	0	19.32	19.62	20.21
C	0.68	2.51	2.25	0.3	1.24	0	0	0
di	0	0	0	0	0	19.9	18.27	16.79
hy	2.82	4.82	1.59	2.89	0.54	0	0	0
ol	0	0	0	0	0	4.25	4.18	2.83
mt	1.28	2.01	1.58	1.64	1.5	2.54	2.51	2.43
il	0.38	0.54	0.42	0.42	0.11	1.29	1.25	1.16
ap	0.3	0.49	0.38	0.39	0.04	1.44	1.42	1.16

Sample	2P-570	E1-33	E1-39	E1-48	E1-53	E2-78	3P-913	3P-914
K	3	3	3	3	3	3	3	3
SiO_2	49.4	54.7	47	53.9	57	58.13	54.4	54.2
Al_2O_3	15.6	18.5	16.56	17.6	17.6	19.09	18.5	18.5
Fe_2O_3	6.1	4.1	6.19	3.2	4	3.17	3.6	3.7
FeO	5.1	3.4	5.36	3.8	2.8	1.79	3.3	3.4
MgO	3.7	2.3	4.54	2.6	1.8	1.11	2.1	1.9
CaO	8.6	6.4	11.93	7	5.3	4.79	6.5	6.4
Na_2O	4.1	4.6	3.29	4.4	4.6	5.14	4.3	5.2
K_2O	4	4.2	1.5	4.5	4.8	5.02	4.3	4.1
H_2O-	0	0.35	0.15	0.45	0.29	0.17	0	0.38
H_2O+	0	0.34	0.65	0.45	0.28	0.27	0.8	0.38
TiO_2	1	0.89	1.31	0.9	0.86	0.68	0.81	0.7
CO_2	0	0.01	0.19	0.02	0.01	0.01	0	0.4
P_2O_5	0.83	0.49	0.87	0.49	0.45	0.21	0.5	0.4
Cl	0	0.03	0.02	0.08	0.04	0.02	0	0
F	0	0.08	0.1	0.11	0.1	0.09	0	0
S	0	0	0	0	0	0.01	0	0
MnO	0.24	0.19	0.24	0.2	0.16	0.19	0.16	0.18
Total	98.67	100.58	99.9	99.7	100.09	99.89	99.27	99.84
%AN	42.42	32.69	56.16	32.92	24.22	24.59	34.05	30.84
or	24.05	24.75	9.08	26.79	28.44	29.51	25.69	24.29
ab	17.07	35.8	20.78	30.78	41.42	43.31	36.21	33.81
an	12.57	17.39	26.62	15.1	13.24	14.12	18.69	15.08
ne	12.24	3.24	5.68	5.42	0	1.56	1.7	7.81
di	20.27	8.88	22.55	13.34	8.15	6.53	8.5	11.32
hy	0	0	0	0	1.67	0	0	0
ol	7.95	5.19	8.55	3.74	2.46	1.32	4.57	3.56
mt	2.66	2.49	3.01	2.53	2.47	2.27	2.44	2.31
il	1.42	1.24	1.87	1.26	1.2	0.94	1.14	0.98
ap	1.77	1.02	1.86	1.03	0.94	0.44	1.06	0.84

Sample	E2-60	15-51	E-23	E-119	E-68	E-23	E-119	E-68
K	3	3	3	3	3	3	3	3
SiO_2	57.73	58.2	45.87	47.09	39.83	45.87	47.09	39.83
Al_2O_3	20.31	17.4	7.03	5.5	11.68	7.03	5.5	11.68
Fe_2O_3	3.05	4.2	5.19	5.25	7.87	5.19	5.25	7.87
FeO	1.35	2.8	6.59	6.11	11.68	6.59	6.11	11.68
MgO	0.75	2	9.38	9.83	7.59	9.38	9.83	7.59
CaO	5.3	5.3	20.5	22.09	12.6	20.5	22.09	12.6
Na_2O	5.28	4.5	1.51	1.11	2.49	1.51	1.11	2.49
K_2O	4.22	3.3	0.61	0.19	1.84	0.61	0.19	1.84
H_2O-	0.33	0.28	0	0.02	0.01	0	0.02	0.01
H_2O+	0.27	0.29	0.26	0.07	1.1	0.26	0.07	1.1
TiO_2	0.73	0.84	1.46	1.6	1.87	1.46	1.6	1.87

Sample	E2-60	15-51	E-23	E-119	E-68	E-23	E-119	E-68
K	3	3	3	3	3	3	3	3
CO_2	0.03	0.01	0	0	0	0	0	0
P_2O_5	0.16	0.5	0.72	0.45	0.49	0.72	0.45	0.49
Cl	0.02	0.05	0.03	0.01	0.05	0.03	0.01	0.05
F	0.07	0.11	0.11	0.04	0.4	0.11	0.04	0.4
S	0.01	0	0	0	0	0	0	0
MnO	0.16	0.13	0.49	0.64	0.6	0.49	0.64	0.6
Total	99.77	99.91	99.75	100	100.1	99.75	100	100.1
%AN	29.09	30.27	100	100	100	100	100	100
Q	0	4.97	0	0	0	0	0	0
or	24.85	19.68	0	0	0	0	0	0
ab	46.79	40.78	0	0	0	0	0	0
an	19.2	17.7	10.87	9.69	15.91	10.87	9.69	15.91
lc	0	0	2.95	0.92	9.06	2.95	0.92	9.06
ne	0.28	0	8.34	6.12	13.98	8.34	6.12	13.98
di	4.78	4.44	67.55	74.14	30.15	67.55	74.14	30.15
hy	0	7.73	0	0	0	0	0	0
wo	0	0	0	2.06	0	0	2.06	0
ol	0.44	0	2.25	0	20.98	2.25	0	20.98
mt	2.32	2.47	3.17	3.32	3.67	3.17	3.32	3.67
il	1.01	1.18	2.08	2.28	2.71	2.08	2.28	2.71
ap	0.33	1.06	1.54	0.96	1.07	1.54	0.96	1.07
COS	0	0	1.24	0.5	2.47	1.24	0.5	2.47

Sample	IP-912	29-33A	E3-83	E4-84	28-12	28-127A	15-51	11-111
K	3	3	3	3	3	3	12	12
SiO_2	62.3	62.4	65.9	65.44	66.6	61.5	65.4	70.8
Al_2O_3	16.4	16.8	17.5	18.06	17.4	18.2	17.8	16.5
Fe_2O_3	2.6	3.6	2.2	1.62	1.7	3	3.3	0.85
FeO	1.7	2	0.78	0.52	0.42	1.5	0.58	0.14
MgO	1.2	1.2	1	0.08	0.14	0.65	0.58	0.14
CaO	3	2.5	1.3	0.46	1.9	2.4	0.14	0.28
Na_2O	4.9	5.1	5.7	5.57	5.6	4.5	4.9	4.6
K_2O	3.8	3.8	4.7	7.43	4.4	6.6	4.3	6.2
H_2O-	0.6	0.35	0.28	0.13	0.26	0.14	1.3	0.39
H_2O+	0.6	0.8	0.28	0.3	0.52	0.48	1.3	0.39
TiO_2	0.52	0.64	0.3	0.16	0.24	0.6	0.43	0.1
CO_2	0.94	0.11	0.02	0.01	0.39	0.05	0.01	0
P_2O_5	0.3	0.44	0.1	0.01	0.06	0.28	0.15	0.02
Cl	0	0	0.02	0.02	0	0	0.01	0.01
F	0	0	0.01	0.01	0	0	0.16	0.09
S	0	0	0	0	0	0	0.02	0
MnO	0.1	0.14	0.06	0.03	0.03	0.12	0.02	0.01
Total	98.96	99.88	100.15	99.85	99.66	100.02	100.4	100.52

Sample **K**	**1P-912** **3**	**29-33A** **3**	**E3-83** **3**	**E4-84** **3**	**28-12** **3**	**28-127A** **3**	**15-51** **12**	**11-111** **12**
%AN	20.77	17.23	10.17	4.24	15.23	19.79	-0.65	2.96
Q	10.84	10.01	9.77	3.22	12.14	3.68	18.16	18.04
or	23.07	22.71	27.47	43.31	26.06	39	25.92	36.47
ab	45.2	46.31	50.64	49.35	50.4	40.42	44.89	41.12
an	11.85	9.64	5.74	2.19	9.06	9.97	-0.29	1.25
C	0	0.89	0.99	0.05	0.13	0	5.78	1.91
di	1.14	0	0	0	0	0.09	0	0
hy	4.34	6.35	2.92	0.22	0.39	3.22	2.55	0.38
mt	2.17	2.26	1.86	0.93	0.55	2.2	2.06	0.14
il	0.74	0.9	0.41	0.22	0.34	0.84	0.61	0.14
hem	0	0	0	0.49	0.82	0	0	0.5
ap	0.64	0.93	0.21	0.02	0.13	0.59	0.32	0.04

Sample **K**	**11-134** **12**	**14-32** **12**	**24-108** **12**	**18-2** **12**	**110-21** **12**	**14-83** **13**	**A-1** **6**	**P-42** **3**
SiO_2	63.2	61.1	65.99	60	61.2	62.4	60.3	66.78
Al_2O_3	18.4	17.3	17.42	19	17.2	18.5	18.12	16.05
Fe_2O_3	3.1	2.8	2.96	2.1	2.5	2.9	2.45	1.69
FeO	1.1	0.32	0.13	0.97	2.1	0.1	1.25	2.09
MgO	0.62	0.33	0.26	0.52	1	0.21	0.28	0.46
CaO	0.59	2.9	0.75	2.7	2.6	0.1	3.89	1.65
Na_2O	6.9	4.3	5.86	6	4.4	0.3	5.83	5.49
K_2O	4.2	6	3.68	4.6	4.9	13.5	5.01	4.74
H_2O-	1.2	0.75	0.45	0.6	0.7	0.7	0.75	0.1
H_2O+	1.2	0.75	1.04	0.6	0.7	0.7	0.77	0.32
TiO_2	0.44	0.32	0.34	0.4	0.52	0.31	0.55	0.32
ZrO_2	0	0	0	0	0	0	0.01	0
CO_2	0.01	2.2	0.36	1.4	1.6	0	0	0.04
P_2O_5	0.17	0.11	0.14	0.1	0.24	0.1	0.25	0.13
SO_3	0	0.27	0	0	0	0	0.06	0
Cl	0.01	0	0	0.01	0.01	0.01	0	0
F	0.04	0.1	0.08	0.09	0.08	0.06	0	0
S	0	0	0.02	0	0	0	0	0
MnO	0.1	0.14	0.15	0.14	0.16	0.08	0.12	0.09
BaO	0	0	0	0	0	0	0.26	0
Total	101.28	99.69	99.63	99.23	99.91	99.97	99.9	99.95
%AN	2.85	20.87	5.06	17.38	22.29	-6.2	13.94	9.47
Q	4.1	7.01	15.09	1.37	8.93	8.26	0.82	11.43
or	24.58	36.83	22.02	27.56	29.8	81.95	29.71	27.92
ab	61.37	40.12	53.29	54.64	40.66	2.77	52.55	49.15
an	1.8	10.58	2.84	11.49	11.66	-0.16	8.51	5.14
C	1.99	0	3.06	0	0.57	3.87	0	0
di	0	2.66	0	1.15	0	0	2.53	1.74

Sample K	11-134 12	14-32 12	24-108 12	18-2 12	110-21 12	14-83 13	A-1 6	P-42 3
hy	3.19	0	0.97	1	4.94	0.71	0	2.15
wo	0	0.12	0	0	0	0	2.42	0
mt	2.01	1.98	1.95	2.01	2.17	1.94	2.15	1.76
il	0.61	0.46	0.48	0.57	0.75	0.44	0.77	0.44
ap	0.35	0.24	0.3	0.21	0.52	0.21	0.52	0.27

Sample K	P-6 12	P-118 12	P-108 12	Go-51A-55 8	Al-27B-55 8	Al-25A-55 8	G-1 4	G-2 4
SiO_2	67.41	68.1	68.56	51.9	72	58.1	71.86	67.56
Al_2O_3	16.23	15.89	15.88	8.8	11.9	14.3	13.19	14.38
Fe_2O_3	0.85	1.43	3.06	11.3	1.9	4.5	1.24	0.78
FeO	1.14	2.49	1.19	14.5	3.2	5.4	1.8	1.86
MgO	0.15	0.08	0.1	3.3	1.5	3	0.55	1.12
CaO	0.14	0.22	0	4.2	1.7	5.2	1.29	0.98
Na_2O	3.95	4.95	4.8	0.1	2.6	1.2	2.22	1.93
K_2O	7.19	5.65	5.44	1.15	2.2	2.6	5.85	7.05
H_2O-	0.67	0.18	0.2	0.4	0.5	0.9	0.04	0.1
H_2O+	0.88	0.7	0.64	0.4	0.5	0.9	0.57	0.79
TiO_2	0.16	0.1	0.14	0.42	0.58	1.4	0.41	0.36
ZrO_2	0.11	0	0	0	0	0	0	0
CO_2	0.56	0.21	0.01	0.19	0.64	0.7	0.34	2.78
P_2O_5	0.05	0.14	0.04	0.65	0.15	0.62	0.24	0.11
F	0	0	0	0	0	0	0.07	0.06
S	0	0	0	0	0	0	0.01	0
MnO	0.16	0.12	0.03	3.4	0.12	0.14	0.03	0.04
BaO	0	0	0	0	0	0	0.05	0.07
Total	99.65	100.26	100.09	100.71	99.49	98.96	99.76	99.97
%AN	1.03	0.4	-0.61	94.87	24.2	66.87	19.51	19.3
Q	15.04	14.81	17.19	14.13	40.29	23.55	31.52	24.26
or	43.42	33.54	32.39	7.51	13.66	16.55	35.76	43.87
ab	36.25	44.66	43.44	0.99	24.54	11.61	20.62	18.25
an	0.38	0.18	-0.26	18.33	7.84	23.43	5	4.36
C	2.03	1.72	2.41	1.58	2.88	1.81	1.62	2.36
hy	1.65	3.15	2.83	53.1	7.52	16.29	3.02	5.26
mt	0.91	1.5	1.73	2.22	2.09	3.27	1.34	0.86
il	0.23	0.14	0.2	0.65	0.85	2.1	0.59	0.53
ap	0.11	0.29	0.08	1.5	0.33	1.4	0.52	0.24

Sample K	G-3 4	G-4 11	G-5 11	G-6 11	G-7 11	G-8 11	G-9 8	G-10 8
SiO_2	58.66	60.2	55.47	57.19	52.05	49.77	76.3	75.4
Al_2O_3	16.59	14.51	16.87	15.55	16.37	16.8	12.2	12.7
Fe_2O_3	0.96	3.56	4.11	4.47	3.28	1.62	0.9	1

Sample K	G-3 4	G-4 11	G-5 11	G-6 11	G-7 11	G-8 11	G-9 8	G-10 8
FeO	3.28	5.26	5.03	5.34	7.58	8.16	2	1.6
MgO	1.56	2.33	2.36	2.23	2.71	1.68	0.48	0.5
CaO	2.75	4.84	2.77	1.4	1.53	1.62	1.7	1.6
Na_2O	0.22	2.93	1.57	0.16	0.08	0.08	3.7	3.4
K_2O	6.86	2.71	2.58	2.66	5.71	6.92	1.1	1.2
H_2O-	0.38	0.02	1.95	1.75	0.57	0.52	0.41	0.9
H_2O+	2.38	0.7	2.92	3.88	3.34	2.02	0.42	0.9
TiO_2	0.51	1.48	1.37	1.66	1.69	1.78	0.22	0.18
CO_2	4.76	0.2	1.61	2.16	3.12	6.48	0.2	0.17
P_2O_5	0.39	0.63	0.51	0.69	0.99	0.99	0.06	0.05
F	0.14	0.21	0.3	0.34	0.35	0.39	0	0
S	0.28	0.15	0.32	0.17	0.18	0.47	0	0
MnO	0.16	0.14	0.14	0.16	0.24	0.7	0.02	0.02
BaO	0.16	0.12	0.07	0.09	0.14	0.12	0	0
Total	100.04	99.99	99.95	99.9	99.93	100.12	99.71	99.62
%AN	84.89	41.21	42.48	62.92	60.98	68.6	19.49	19.96
Q	22.55	17.62	26.07	41.08	22.04	15.14	43.3	44.71
or	45.12	16.63	16.96	18.08	38.11	47.16	6.72	7.41
ab	2.2	27.33	15.68	1.65	0.81	0.83	34.37	31.93
an	12.35	19.16	11.58	2.81	1.27	1.81	8.32	7.96
C	5.76	0	9.33	14.46	11.9	10.83	2.23	3.45
di	0	1.21	0	0	0	0	0	0
hy	9.2	11.31	13.74	13.8	17.11	17.03	3.64	3.08
mt	1.12	3.24	3.34	3.8	3.77	1.95	0.97	1.09
il	0.79	2.14	2.12	2.66	2.66	2.86	0.32	0.26
ap	0.91	1.37	1.19	1.66	2.34	2.39	0.13	0.11

Sample K	G-11 8	G-12 8	G-13 8	G-14 11	G-15 11	G-16 2	G-17 2	G-18 2
SiO_2	71.2	75.5	65.3	64.09	54.29	52.61	51.98	48.06
Al_2O_3	14.1	12.1	13.8	14.03	13.53	15.63	16.88	15
Fe_2O_3	2.5	2.3	6.7	3.44	5.28	2.71	4.69	8.77
FeO	1.4	0.68	0.82	2.71	5.1	6.46	4.77	3.68
MgO	0.55	0.44	0.74	1.14	2.42	5.67	2.9	2.08
CaO	1.4	0.12	0.37	3.91	7.22	6.16	3.41	5.87
Na_2O	2.7	0.11	0.11	2.81	2.64	2.13	0.47	0.99
K_2O	1.2	4.6	4.7	4.18	2.4	2.85	2.66	1.43
H_2O-	1.7	0.8	0.75	0.16	0.22	0.12	1.3	2.94
H_2O+	1.7	0.8	0.75	0.38	0.72	1.61	4.01	3.45
TiO_2	0.2	0.16	0.43	1.31	2.37	0.91	1.33	1.91
CO_2	0.54	0.05	0.05	0.12	0.44	2.08	4.25	4.72
P_2O_5	0.04	0.06	0.2	0.56	2.02	0.33	0.62	0.46
Cl	0	0	0	0.05	0	0	0	0

Sample	**G-11**	**G-12**	**G-13**	**G-14**	**G-15**	**G-16**	**G-17**	**G-18**
K	**8**	**8**	**8**	**11**	**11**	**2**	**2**	**2**
F	0	0.61	0.22	0.59	0.43	0.32	0.3	0.24
S	0	2	5.2	0.03	0.36	0.22	0.16	0.32
MnO	0.05	0.01	0.02	0.09	0.13	0.15	0.18	0.18
BaO	0	0	0	0.24	0.17	0.04	0.06	0.02
Total	99.28	100.34	100.16	99.84	99.74	100	99.97	100.12
%AN	21.62	17.07	34.88	34.56	43.14	56.34	75.31	74.61
Q	46.08	56.7	44.08	22.18	14.93	5.11	27.54	19.78
or	7.64	29.61	31.39	25.72	15.07	17.76	18.18	10.08
ab	26.13	1.08	1.12	26.27	25.19	20.17	4.88	10.6
an	7.21	0.22	0.6	13.88	19.11	26.02	14.88	31.15
C	6.95	8.17	10.29	0	0	0	10.75	2.93
di	0	0	0	2.01	3.95	3.15	0	0
hy	3.68	1.96	9.1	3.76	9.45	23.07	16.71	16.89
mt	1.92	1.89	2.28	3.06	4.3	2.66	3.42	4.25
il	0.3	0.24	0.68	1.9	3.51	1.34	2.14	3.17
ap	0.09	0.14	0.47	1.22	4.49	0.73	1.5	1.15

Sample	**G-19**	**G-20**	**G-21**	**G-22**	**G-23**	**G-24**	**G-25**	**G-26**
K	**8**	**8**	**8**	**8**	**8**	**8**	**8**	**8**
SiO_2	71.76	64.69	65.61	68.61	72.12	76.33	75.1	53.68
Al_2O_3	14.37	13.74	13.05	14.1	9.83	12.3	13.47	17.35
Fe_2O_3	1.13	3.56	3.4	2.33	0.39	1.08	1.11	5.06
FeO	1.8	3.6	4.05	1.72	6.99	1.75	1.32	0.54
MgO	0.58	1.11	0.77	0.64	0.52	0.59	0.65	2.43
CaO	2.05	3.09	1.88	2.51	0.03	2.41	2.24	2.65
Na_2O	4.95	4.16	3.17	3.6	0.08	3.13	2.57	0.05
K_2O	2.02	1.61	1.5	1.15	3.69	1.02	0.98	1.63
H_2O-	0.03	0.16	1.19	1.71	0.15	0.17	0.49	8.35
H_2O+	0.33	0.85	1.31	1.22	1.29	0.42	1.32	4.63
TiO_2	0.27	0.59	0.66	0.54	0.2	0.27	0.29	1.41
CO_2	0.54	2.37	2.78	1.49	0.82	0.01	0.01	0.01
P_2O_5	0.04	0.16	0.17	0.11	0.03	0.03	0.04	1.43
F	0	0	0	0	0	0	0	0.44
S	0	0	0	0	4.96	0	0	0
MnO	0.06	0.17	0.3	0.14	0.11	0.03	0.02	0.02
Total	99.93	99.86	99.84	99.87	101.21	99.54	99.61	99.68
%AN	18.23	27.36	22.4	26.64	-7.03	29.5	31.99	89.45
Q	27.36	22.97	33.79	36.23	53.39	45.48	48.9	46.9
or	12.09	10.03	9.66	7.25	24.57	6.24	6.08	11.64
ab	45.03	39.39	31.03	34.51	0.81	29.12	24.24	0.54
an	10.04	14.83	8.96	12.53	-0.05	12.19	11.4	4.6
C	0.45	0	3.81	3.07	7.04	1.97	4.82	18.62

Sample	G-19	G-20	G-21	G-22	G-23	G-24	G-25	G-26
K	8	8	8	8	8	8	8	8
di	0	0.19	0	0	0	0	0	0
hy	3.36	9.06	8.91	3.08	13.4	3.38	2.83	8.11
mt	1.2	2.3	2.46	2.28	0.46	1.17	1.22	3.45
il	0.38	0.87	1	0.8	0.31	0.39	0.42	2.37
hem	0	0	0	0	0	0	0	0.15
ap	0.08	0.35	0.39	0.25	0.07	0.06	0.09	3.61

Sample	G-27	G-28	G-29	G-30	G-31	G-32	G-33	G-34
K	8	8	8	8	14	14	14	8
SiO_2	72	65.5	58.1	59.5	55.27	48.19	51.39	54.62
Al_2O_3	11.9	17.7	14.3	14.9	16.17	15.66	21.8	18.97
Fe_2O_3	1.9	1.3	4.5	4.9	2.27	3.86	5.87	5.41
FeO	3.2	2.5	5.4	4.2	6.3	9.08	0.45	0.16
MgO	1.5	0.92	3	3.2	3.42	7.17	1.62	1.54
CaO	1.7	0.5	5.2	1.5	7.49	8.68	1.54	1.28
Na_2O	2.6	0.04	1.2	0.07	4.65	0.92	0.6	0.22
K_2O	2.2	4.6	2.6	2.6	1.31	1.07	0.62	0.54
H_2O-	0.5	2	0.9	2.8	0.03	0.67	7.96	10.21
H_2O+	0.5	2	0.9	2.8	0.99	3.17	6.77	5.68
TiO_2	0.58	0.85	1.4	1.3	0.98	0.75	0.94	0.79
CO_2	0.64	2	0.7	1.2	0.48	0.01	0.01	0.01
P_2O_5	0.15	0.06	0.62	0.53	0.24	0.26	0.18	0.16
F	0	0	0	0	0.17	0	0	0
S	0.25	0.09	0.19	0.29	0.01	0	0	0
MnO	0.12	0.17	0.14	0.14	0.19	0.26	0.01	0.01
BaO	0	0	0	0	0.02	0	0	0
Total	99.74	100.23	99.15	99.93	99.99	99.75	99.76	99.6
%AN	24.2	85.33	66.87	86.36	31.71	81.1	54.55	72.87
Q	40.29	45.13	23.55	41.27	2.26	3.81	43.91	52.65
or	13.66	29.91	16.55	17.34	7.87	6.74	4.46	3.97
ab	24.54	0.4	11.61	0.71	42.44	8.81	6.55	2.46
an	7.84	2.3	23.43	4.49	19.71	37.79	7.86	6.61
C	2.88	14.28	1.81	12.96	0	0	23.6	21.86
di	0	0	0	0	13.18	5.05	0	0
hy	7.52	5.05	16.29	16.62	10.23	33.61	8.46	7.68
mt	2.09	1.5	3.27	3.3	2.41	2.51	3.1	2.98
il	0.85	1.3	2.1	2.04	1.39	1.11	1.59	1.37
ap	0.33	0.14	1.4	1.25	0.51	0.58	0.46	0.42

Sample	G-35	G-36	G-37	G-38	G-39	G-40
K	8	8	8	8	8	8
SiO_2	52.4	51.4	49.7	43.1	52.8	49.7
Al_2O_3	8.2	9.4	7.8	9.7	11.1	10.5

Sample K	G-35 8	G-36 8	G-37 8	G-38 8	G-39 8	G-40 8
Fe_2O_3	11.7	10.9	11	7.6	3.4	4.9
FeO	13.9	15	13.9	17.9	16.5	16.8
MgO	2.8	3.8	1.9	2.4	2	2
CaO	5.4	3	2.4	2.4	2.4	2.3
Na_2O	0.1	0.09	0.06	0.06	0.05	0.09
K_2O	0.49	1.8	1.2	0.91	0.21	0.31
H_2O-	0.37	0.44	0.61	0.6	0.6	0.7
H_2O+	0.37	0.43	0.62	0.7	0.6	0.7
TiO_2	0.32	0.52	0.3	0.42	0.42	0.38
CO_2	0.25	0.13	6.4	9.6	5.6	8
P_2O_5	0.7	0.59	0.94	0.76	0.89	0.52
S	1.2	0.94	1.2	0.86	1.3	1.2
MnO	3.5	3.2	3	3.7	3.5	3.5
Total	101.7	101.64	101.03	100.71	101.37	101.6
%AN	95.8	93.17	91.46	92.8	93.14	90.84
Q	15.92	13.01	21.53	13.09	31.73	25.98
or	3.22	11.7	8.56	6.69	1.45	2.21
ab	1	0.89	0.65	0.67	0.53	0.97
an	22.78	12.13	6.96	8.64	7.14	9.67
C	0	3.92	5.65	8.25	10.94	9.32
di	1.55	0	0	0	0	0
hy	51.3	53.88	51.49	57.45	43	47.53
mt	2.12	2.32	2.27	2.5	2.35	2.37
il	0.5	0.8	0.5	0.73	0.69	0.64
ap	1.63	1.36	2.37	1.98	2.18	1.31

Major rock types (K): 1 = gabbro, 2 = diorite, 3 = monzonite, 4 = granite, 5 = peridotite, 6 = syenite, 7 = latite, 8 = gneiss, 9 = hornblendite, 10 = iron ore, 11 = granodiotite, 12 = bostonite, 13 = sanidinite, 14 = amphibolite.

Samples: 1 to 9, CC1and CC2, Front Range mineral belt (FRMB); Bastin and Hill, 1917.
11-107 to Al-24A-55 (FRMB); Braddock, 1969.
G1 to G40 (FRMB); Tooker, 1963.

Table 2. Chemical analyses and CIPW norms of rock samples from the Cripple Creek district.

Sample K	L45I 2	L45II 2	L53 5	L66I 6	L66II 6	L79I 6	L79II 4	L90 3
SiO_2	77.03	66.2	51.88	58.98	58.78	56.01	58.05	49.84
TiO_2	0.13	0.65	0.76	0.24	0.29	1.2	0.91	1.43
Al_2O_3	12	14.33	23.86	20.54	20.03	17.92	17.66	17.78
Fe_2O_3	0.76	2.09	7.24	1.65	1.87	4.2	3.51	5.86
FeO	0.86	1.93	1.89	0.48	0.49	2.52	1.65	2.62
MnO	0	0.13	0	0.26	0.15	0.13	0.13	0.21
MgO	0.04	0.89	1.43	0.11	0.16	2.04	1.55	3.02
CaO	0.8	1.39	0.21	0.67	0.83	4.8	4.58	7.35
Na_2O	3.21	2.58	0.68	9.95	9.36	4.92	5.8	5.2
K_2O	4.92	7.31	5.55	5.31	5.5	4.21	4.06	3.04
P_2O_5	0	0.25	0.07	0.04	0.03	0.55	0.4	0.76
H_2O+	0.3	0.83	0	0.97	1.57	1.1	0.87	2.02
H_2O-	0.14	0.48	0	0.19	0.31	0.31	0.35	0.34
CO_2	0	0.36	0	0	0	0	0	0.52
Other	0.36	0.32	6.05	0.68	0.87	0.28	0.33	0.43
Total	100.55	99.74	99.62	100.07	100.24	100.19	99.85	100.42
%AN	11.66	18.51	8.74	0	0	24.56	16.55	35.48
Q	35.34	18.39	20.72	0	0	0	0	0
or	29.61	44.74	35.97	30.18	31.64	25.1	24.06	18.36
ab	29.36	24	6.7	38.24	38.05	44.59	51.4	30.1
an	3.88	5.45	0.64	0	0	14.52	10.19	16.56
ne	0	0	0	23.67	22.07	0	0.5	10.57
C	0	0.28	19.78	0	0	0	0	0
di	0.13	0	0	2.16	2.23	4.72	7.98	12.52
hy	0.68	3.41	12.27	0	0	3.52	0	0
wo	0	0	0	0.1	0.41	0	0	0
ol	0	0	0	0	0	1.86	1.24	5.1
ac	0	0	0	4.43	4.86	0	0	0
mt	0.81	2.26	2.59	0	0	2.85	2.53	3.13
il	0.18	0.94	1.16	0.32	0.39	1.69	1.27	2.04
ap	0	0.54	0.16	0.08	0.06	1.16	0.84	1.62
NMS	0	0	0	0.82	0.28	0	0	0

Sample K	L93 3	CC004 6	CCPH1 6	CC009 7	CC007 11	CC010 10	CC005 6	CC008 9
SiO_2	48.76	59.1	60	57.9	53	50	47.9	51.3
TiO_2	0.69	0.34	0.2	0.65	1.2	1.26	1.49	1.24
Al_2O_3	17.04	19.6	19.7	19.4	17.4	18.5	16.1	18.1
Fe_2O_3	5.04	1.93	1.76	2	4.19	3.64	4.83	4.61
FeO	3.47	0.65	0.36	1.36	2.32	3.04	3.91	2.57
MnO	0.08	0.24	0.2	0.17	0.19	0.17	0.24	0.19

Sample K	L93 3	CC004 6	CCPH1 6	CC009 7	CC007 11	CC010 10	CC005 6	CC008 9
MgO	4.57	0.31	0.15	0.72	2.14	2.59	4.55	2.55
CaO	8.64	1.25	0.65	2.83	6.04	6.18	8.69	6.51
Na_2O	4.27	8.26	8.83	6.89	5.09	5.95	3.98	4.94
K_2O	3.39	5.72	5.45	5.41	3.69	4.52	3.56	4.01
P_2O_5	0.79	0.06	0.05	0.2	0.57	0.59	0.81	0.72
H_2O+	0.69	0.44	0.67	0.38	0.9	1.66	1.7	1.95
H_2O-	1.84	0.31	0.25	0.13	0.29	0.25	0.35	0.33
CO_2	0.22	0.03	0.01	0.08	1.91	0.02	1.09	0.67
Other	0.34	0.34	0.34	0.34	0.34	0.34	0.34	0.34
Total	99.83	98.58	98.62	98.46	99.27	98.71	99.54	100.03
%AN	47.92	0	0	12.25	26.12	33.99	45.87	33.81
or	20.5	33.22	31.55	31.78	22.55	27.08	21.81	24.26
ab	19.27	43.85	45.74	42.98	40.18	20.53	19.03	30.82
an	17.73	0	0	6	14.21	10.57	16.13	15.75
ne	11.99	16.86	16.84	11.12	4.26	20.19	10.81	8.76
di	16.7	1.68	1.36	4.1	10.35	13.29	18.47	10.01
wo	0	1.44	0.45	0.62	0	0	0	0
ol	8.79	0	0	0	2.58	2.37	6.6	4.15
ac	0	0.77	3.1	0	0	0	0	0
mt	2.34	1.53	0.58	2.08	2.92	2.93	3.24	2.93
il	0.98	0.47	0.27	0.9	1.73	1.78	2.15	1.77
hem	0	0.05	0	0	0	0	0	0
ap	1.69	0.12	0.1	0.42	1.23	1.25	1.76	1.54

Sample K	CCTM1 8	B-150* 8	B-CR85* 8	B-127* 9	CCS-27† 9	B-130* 9	CCS-24† 9	B-165* 10
SiO_2	36.5	36.45	42.23	48.83	48.83	48.46	48.86	50.67
TiO_2	1.9	1.91	1.55	1.29	1.45	1.46	1.52	1.22
Al_2O_3	10.9	10.05	10.76	17.46	16.63	16.21	17.46	18.71
Fe_2O_3	4.82	5.05	4.37	5.29	4.59	4.75	4.27	3.78
FeO	5.38	5.87	5.3	3.06	4.25	4.34	5.01	2.99
MnO	0.19	0.19	0.24	0.18	0.19	0.18	0.18	0.16
MgO	14.3	16.83	13.62	2.9	4.56	4.31	4.43	2.53
CaO	13.8	14.76	13.22	7.56	8.79	8.59	9.42	6.02
Na_2O	2.96	1.06	2.63	4.88	4.82	4.47	4.05	6.52
K_2O	1.18	1.16	1.02	3.12	3.25	3.41	2.53	4.5
P_2O_5	1.26	1.22	0.68	0.81	0.81	0.81	0.88	0.59
H_2O+	2.88	4.35	2.53	1.68	0	1.82	0	1.54
H_2O-	0.75	0.31	0	0.19	0	0.15	0	0.1
CO_2	0.34	0.09	0.75	2	0	0.2	0	0.2
Other	0.34	0.34	0.34	0.34	2.4	2.4	1.06	1.06
Total	97.5	99.64	99.24	99.59	100.57	101.56	99.67	100.59

Sample K	CCTM1 8	B-150* 8	B-CR85* 8	B-127* 9	CCS-27† 9	B-130* 9	CCS-24† 9	B-165* 10
%AN	100	100	99.36	37.77	42.31	41.86	46.64	29.37
or	0	0	6.17	19.21	19.36	20.65	15.13	26.52
ab	0	0	0.1	28.37	19.45	20.07	25.47	20.39
an	13.54	19.96	14.89	17.22	14.26	14.45	22.27	8.48
lc	5.82	5.69	0	0	0	0	0	0
ne	16.64	5.92	14.45	10.37	14.51	12.64	6.8	22.81
di	18.85	14.69	38.18	13.08	19.5	19.05	15.38	13.98
ol	28.2	35.81	19.27	5.08	6.06	6.16	7.74	2.05
mt	3.71	3.7	3.27	3.04	3.11	3.17	3.2	2.84
il	2.76	2.76	2.21	1.87	2.04	2.08	2.14	1.7
ap	2.75	2.65	1.46	1.76	1.71	1.74	1.86	1.23
COS	7.73	8.82	0	0	0	0	0	0

Sample K	B-120* 7	B-128* 7	B-152* 6	B-159* 6	B-124* 6	CCN-9† 6	B-CR1-64* 11	CCN-5 6
SiO_2	54.3	58.5	59.95	58.6	59.38	57.32	54.2	58.99
TiO_2	1.06	0.63	0.22	0.19	0.37	0.21	1.08	0.29
Al_2O_3	19.3	19.55	19.95	20.55	19.75	20.28	19.38	19.69
Fe_2O_3	2.87	2.09	1.86	2.09	2.15	1.95	6.17	1.83
FeO	2.01	1.35	0.51	0.17	0.69	0.42	1.16	0.55
MnO	0.18	0.16	0.19	0.23	0.26	0.27	0.18	0.17
MgO	1.09	0.62	0.11	0.1	0.27	0.09	1.34	0.26
CaO	4.2	2.69	0.77	0.68	1.3	0.66	4.12	0.85
Na_2O	6.85	7.29	8.92	8.51	8.48	10.5	5.03	9.34
K_2O	4.85	5.33	5.33	5.41	5.77	5.37	4.1	5.66
P_2O_5	0.3	0.16	0.03	0.02	0.03	0.02	0.61	0.04
H_2O+	2	0.59	1.29	2.18	0.81	0	1.56	0
H_2O-	0.15	0.15	0.28	0.21	0.03	0	0	0
CO_2	0.03	0.12	0.16	0.28	0.1	0	1.32	0
Other	1.06	1.06	1.06	1.06	1.06	0.98	0.98	1.16
Total	100.25	100.29	100.63	100.28	100.45	98.07	101.23	98.83
%AN	18.13	9.84	0	3.91	0	0	26.71	0
or	28.73	30.98	30.71	31.61	33.17	30.72	24.78	32.51
ab	34.38	44.03	46.41	46.11	41.2	33.06	46.21	37.37
an	7.61	4.8	0	1.88	0	0	16.84	0
ne	16.37	12.23	17.44	17.68	18.31	26.05	0	20.77
C	0	0	0	0	0	0	0.71	0
di	7.17	3.38	1.21	0.55	2.49	2.44	0	2.89
hy	0	0	0	0	0	0	0.46	0
wo	0.94	1.23	0.81	0.26	1.19	0	0	0.09
ol	0	0	0	0	0	0.08	5.39	0
ac	0	0	2.1	0	1.89	4.62	0	4.85
mt	2.68	2.15	0.97	1.36	1.19	0	2.76	0

Sample K	B-120* 7	B-128* 7	B-152* 6	B-159* 6	B-124* 6	CCN-9† 6	B-CR1-64* 11	CCN-5 6
il	1.48	0.86	0.3	0.26	0.5	0.28	1.54	0.39
hem	0	0	0	0.26	0	0	0	0
ap	0.63	0.33	0.06	0.04	0.06	0.04	1.3	0.08
NMS	0	0	0	0	0	2.72	0	1.05

Sample K	CCN-6A 4	CCN-9 6	BBM-2 6	BBM-3 6	BBM-4 3	BBM-5 6	BBM-7 6	BBM-8 6
SiO_2	52.39	57.32	58.83	57.91	56.47	59.17	58.94	59.05
TiO_2	1.16	0.21	0.23	0.25	0.84	0.28	0.2	0.2
Al_2O_3	16.67	20.28	19.94	19.62	17.37	19.83	19.66	19.81
Fe_2O_3	4.34	1.95	1.65	2.43	2.91	1.68	1.86	1.74
FeO	3.74	0.42	0.53	0.22	1.69	0.6	0.33	0.46
MnO	0.17	0.27	0.24	0.35	0.16	0.22	0.28	0.28
MgO	3.01	0.09	0.19	0.17	1.21	0.2	0.14	0.18
CaO	7.28	0.66	0.85	0.66	3.81	0.96	0.67	0.65
Na_2O	3.55	10.5	9.16	9.79	6.14	8.76	9.35	9.4
K_2O	3.46	5.37	5.7	5.26	4.29	5.88	5.36	5.34
P_2O_5	0.6	0.02	0.02	0.02	0.3	0.03	0.02	0.02
Other	3.77	0.98	1.09	2.19	4.79	1.28	2.17	1.34
Total	100.14	98.07	98.43	98.87	99.98	98.89	98.98	98.47
%AN	37.76	0	0	0	12.98	0	0	0
Q	0.21	0	0	0	0	0	0	0
or	21.32	30.72	32.86	30.45	26.1	33.93	31.06	30.83
ab	33.24	33.06	37.32	37.56	49.48	38.17	40.64	40.55
an	20.16	0	0	0	7.38	0	0	0
ne	0	26.05	21.62	22.15	4.38	20.17	20.13	20.57
di	10.73	2.44	2.74	2.46	8.06	2.53	2.51	2.42
hy	8.44	0	0	0	0	0	0	0
wo	0	0	0.23	0	0	0.52	0	0
ol	0	0.08	0	0.52	0.23	0	0	0.14
ac	0	4.62	4.49	4.78	0	4.03	4.65	4.63
mt	2.9	0	0	0	2.52	0.2	0	0
il	1.69	0.28	0.31	0.34	1.21	0.38	0.27	0.27
ap	1.31	0.04	0.04	0.04	0.65	0.06	0.04	0.04
NMS	0	2.72	0.39	1.7	0	0	0.7	0.56

Sample K	BBM-10 3	CCS-15 3	CCS-16 3	CCS-18 3	CCS-20 3	CCS-23A 3	CCS-23B 3	CCS-23C 3
SiO_2	59.04	53.07	58.04	50.57	53.41	59.11	58.25	57.39
TiO_2	0.48	1.14	0.64	1.2	0.97	0.8	0.85	0.76
Al_2O_3	19.18	17.6	19.34	18.67	18.21	18.58	18.71	17.85
Fe_2O_3	1.86	4.25	1.92	3.63	2.98	3.01	3.35	3.07
FeO	0.91	2.11	1.42	2.91	2.05	1.51	1.63	1.12

Sample	BBM-10	CCS-15	CCS-16	CCS-18	CCS-20	CCS-23A	CCS-23B	CCS-23C
K	3	3	3	3	3	3	3	3
MnO	0.19	0.19	0.17	0.17	0.2	0.11	0.11	0.17
MgO	0.46	2.01	0.73	2.46	1.59	0.97	1.07	1.07
CaO	1.8	5.98	2.79	5.97	4.71	2.3	2.63	2.31
Na_2O	7.57	5.36	7.14	6.54	4.82	5.67	5.66	6.26
K_2O	5.76	3.71	5.45	4.55	5.84	5.25	4.45	5.09
P_2O_5	0.1	0.58	0.19	0.56	0.39	0.26	0.29	0.21
Other	1.66	4.27	1.01	2.09	3.92	1.33	1.46	3.73
Total	99.01	100.27	98.84	99.32	99.09	98.9	98.46	99.03
%AN	2.89	25.35	9.8	28.88	27.49	16.02	18	10.3
Q	0	0	0	0	0	0	1.13	0
or	33.69	22.58	31.86	26.92	35.73	31.28	26.72	30.84
ab	44.82	39.47	42.15	20.11	29.52	51.35	51.65	49.8
an	1.33	13.4	4.58	8.16	11.19	9.8	11.34	5.72
ne	13.48	6.06	12.77	23.22	9.18	0	0	4.71
C	0	0	0	0	0	0.01	0.55	0
di	2.51	10.61	4.46	14.27	8.3	0	0	3.7
hy	0	0	0	0	0	3.38	4.29	0
wo	1.49	0	0.93	0	0	0	0	0
ol	0	2.15	0	1.64	1.17	0.08	0	1.27
mt	1.54	2.84	1.99	2.83	2.67	2.43	2.5	2.42
il	0.66	1.64	0.88	1.67	1.4	1.12	1.2	1.09
hem	0.25	0	0	0	0	0	0	0
ap	0.21	1.25	0.39	1.17	0.84	0.55	0.62	0.45

Sample	CCS-26	CCS-30A	CCS-34	CCS-35	CCS-36	CCS-41	CCS-45	CCS-46
K	4	4	1	1	1	4	3	6
SiO_2	51.74	51.34	52.13	53.64	54.06	54.31	51.12	59.21
TiO_2	1.36	1.18	1.36	1.27	1.25	1.16	1.24	0.28
Al_2O_3	17.63	17.78	17.95	17.96	18.26	16.82	18.29	20.04
Fe_2O_3	3.44	3.52	3.9	3.3	3.36	3.68	4.38	1.74
FeO	3.64	2.62	3.65	3.71	3.5	2.5	3.05	0.42
MnO	0.18	0.19	0.16	0.14	0.14	0.18	0.19	0.23
MgO	2.77	1.95	3.51	3.01	3.08	2.21	2.54	0.25
CaO	6.38	5.63	6.78	6.18	6.18	5.19	6.57	0.85
Na_2O	4.96	6.64	5.27	5.46	5.39	5.16	5.25	9.28
K_2O	4.14	3.01	2.99	3	3.09	4.3	4.01	5.71
P_2O_5	0.65	0.49	0.86	0.77	0.75	0.53	0.75	0.03
Other	2.81	6.08	1.48	0.91	0.94	3.6	2.11	1.1
Total	99.7	100.43	100.04	99.35	100	99.64	99.5	99.14
%AN	30.99	21.09	30.73	26.72	27.72	20.01	33.98	0
or	24.97	18.42	17.71	17.78	18.19	26.17	24.05	32.67
ab	30.97	38.07	37.28	43.02	42.91	41.33	28.6	37.34

Sample	CCS-26	CCS-30A	CCS-34	CCS-35	CCS-36	CCS-41	CCS-45	CCS-46
K	4	4	1	1	1	4	3	6
an	13.91	10.17	16.54	15.69	16.45	10.34	14.72	0
ne	8.71	14.21	6.1	3.69	3.19	3.84	11.55	21.56
di	11.27	12.35	9.24	8.02	7.38	10.1	10.72	2.54
wo	0	0	0	0	0	0	0	0.29
ol	3.81	1.11	6.43	5.51	5.71	2.56	4.11	0
ac	0	0	0	0	0	0	0	4.7
mt	3.05	2.9	3	2.9	2.87	2.86	2.91	0
il	1.93	1.7	1.9	1.77	1.74	1.66	1.75	0.38
ap	1.39	1.06	1.8	1.61	1.56	1.14	1.59	0.06
NMS	0	0	0	0	0	0	0	0.47

Major rock types (K): 1 = andesite, 2 = granite, 3 = trachyte, 4 = latite, 5 = gneiss, 6 = phonolite, 7 = plagioclase phonolite, 8 = monchiquite, 9 = phonotephrite, 10 = tephriphonolite, 11 = trachyandesite, 12 = basalt.

Samples: L451 to L93, Cripple Creek District (CCD); Lindgren and Ransome, 1906.
CC004 to CCTMI (CCD); Kelley, 1996.
* from Birmingham, 1987.
† from Eriksson, 1987.
CCN-5 to CCS-46 (CCD); Eriksson, 1987.

Table 3. Chemical analyses and CIPW norms of rock samples from the State Line district.

Sample K	SL1 1	SL2 2	SL3 3	SL4 3	SL5 3	SL6 4	SL7 5	SL8 5
SiO_2	48.71	54.09	53.5	55.88	64.87	72.68	73.33	70.82
Al_2O_3	19.24	13.75	15.23	13.28	14.35	12.62	12.33	13.49
Fe_2O_3	1.85	3.64	3.69	4.74	2.36	2.11	1.2	0.97
FeO	5.11	9.04	7.07	7.56	3.94	1.46	2.17	1.92
MgO	6.92	3.42	3.84	2.24	1.24	0.24	0.16	0.14
CaO	12.55	5.72	5.83	5.37	3.26	0.83	0.97	1.14
Na_2O	2.68	3.17	3.51	3.06	3.54	3.53	3.61	3.77
K_2O	0.26	2.39	2.32	2.34	3.86	5.47	5.01	5.19
H_2O+	1.46	1.63	1.75	1.55	1.05	0.75	0.37	1.44
H_2O-	0.26	0.29	0.62	0.72	0.32	0.06	0.17	0.21
TiO_2	0.45	2.09	1.8	2.34	1.05	0.34	0.29	0.36
P_2O_5	0.11	0.57	0.46	0.61	0.27	0.05	0.04	0.06
MnO	0.12	0.17	0.14	0.18	0.09	0.04	0.01	0.05
Cl	0.04	0.05	0.03	0.06	0.03	0	0.02	0.02
F	0.01	0.07	0.09	0.05	0.09	0	0	0.02
Total	99.77	100.09	99.88	99.98	100.32	100.18	99.68	99.6
%AN	62.27	36.32	37.55	36.21	27.19	7.14	7.54	11.87
Q	0	7.51	4.88	13.33	19.31	27.42	28.63	24.51
or	1.55	14.77	14.27	14.65	23.43	32.99	30.29	31.6
ab	24.31	29.77	32.8	29.12	32.66	32.36	33.17	34.88
an	40.12	16.98	19.73	16.53	12.2	2.49	2.71	4.7
di	17.65	7.05	5.8	5.99	2.09	1.11	1.56	0.58
hy	4.02	15.69	15.32	11.31	5.7	1.09	1.86	2.04
ol	9.53	0	0	0	0	0	0	0
mt	1.95	3.93	3.59	4.26	2.54	1.96	1.28	1.04
il	0.63	3.05	2.61	3.46	1.5	0.48	0.41	0.52
ap	0.23	1.25	1	1.35	0.58	0.11	0.09	0.13

Sample K	SL9 5	SL10 5	SL11 5	SL12 4	SL13 4	SL14 4	SL15 4	SL16 5
SiO_2	76.35	75.93	75.02	68.09	71.76	75.19	75.75	73.61
Al_2O_3	11.58	11.89	12.21	14.06	13.88	11.13	12.52	13.91
Fe_2O_3	1.96	0.83	1.11	2.27	13.88	1.24	0.83	0.89
FeO	0.79	1.42	1.35	2.2	1.81	2.3	0.78	0.63
MgO	0.08	0.11	0.13	53	1.16	0.7	0.07	0.22
CaO	0.47	0.71	0.73	2.18	0.42	1.37	0.39	0.83
Na_2O	3.25	3.01	3.2	3.42	1.33	2.73	3.99	3.3
K_2O	5.15	5.28	5.31	4.88	2.49	3.75	5.16	5.31
H_2O+	0.44	0.31	0.7	0.96	5.25	0.42	0.68	0.59
H_2O-	0.14	0.08	0.22	0.33	0.29	0.1	0.15	0.11
TiO_2	0.2	0.18	0.27	0.76	0.46	0.53	0.07	0.16

Sample **K**	**SL9** **5**	**SL10** **5**	**SL11** **5**	**SL12** **4**	**SL13** **4**	**SL14** **4**	**SL15** **4**	**SL16** **5**
P_2O_5	0.06	0.02	0.01	0.17	0.1	0.14	0.01	0.18
MnO	0.01	0.05	0.04	0.06	0.04	0.07	0.01	0.03
Cl	0.01	0.02	0.02	0.02	0.01	0.03	0.01	0.01
F	0.01	0.09	0.06	0.08	0.11	0.2	0.2	0.15
Total	100.5	99.93	100.38	152.48	112.99	99.9	100.62	99.93
%AN	5.81	11	10.22	100	10.7	19.35	2.75	9.03
Q	34.71	33.96	32.08	0	39.37	38.58	29.77	30.59
or	31.04	31.94	32.08	14.2	14.64	22.93	30.85	31.99
ab	29.77	27.67	29.38	0	11.89	25.37	36.25	30.21
an	1.84	3.42	3.35	5.07	1.42	6.09	1.03	3
lc	0	0	0	2.24	0	0	0	0
ne	0	0	0	10.86	0	0	0	0
C	0	0	0	0	9.21	0.48	0	1.84
di	0.11	0.04	0.23	0.52	0	0	0.69	0
hy	0.31	1.77	1.28	0	20.58	4.14	0.4	0.8
ol	0	0	0	64.88	0	0	0	0
mt	1.81	0.89	1.19	1.39	2.04	1.34	0.88	0.95
il	0.28	0.26	0.38	0.62	0.64	0.76	0.1	0.23
ap	0.13	0.04	0.02	0.21	0.21	0.3	0.02	0.38

Sample **K**	**3-23b** **6**	**3-500** **6**	**KL1-5** **6**	**KL1-6** **6**	**KL2-1** **6**	**KL2-4** **6**	**KL2-1** **6**	**0-ED-1** **6**
SiO_2	31.42	32.24	36.86	44.04	41	38	39	29.6
Al_2O_3	2.2	3.05	4.71	3.62	4.85	5.07	4.08	2.7
Fe_2O_3	5.58	7.41	4.97	1.69	4.51	5.86	7.43	5.6
FeO	1.58	1.09	0	0	0	0	0	5
MgO	27.94	27.03	12	3.84	14.9	18.7	25.5	23.1
CaO	9.92	8.63	17.56	22.89	13.2	10.2	6	10.2
Na_2O	0.1	0.06	0.13	0.05	0.11	0.19	0.06	0.03
K_2O	1.27	0.84	1.27	1.5	1.35	0.49	0.35	0.94
H_2O+	10.42	9.74	20.3	20.46	18.15	18.27	15.24	8.9
H_2O-	2.23	2.65	0	0	0	0	0	0
TiO_2	0.85	1.08	0.58	0.24	0.55	0.81	1.13	5.2
P_2O_5	0.42	0.54	0	0	0	0	0	0.09
MnO	0.13	0.15	0.09	0.08	0.1	0.09	0.15	0.25
Total	94.06	94.51	98.47	98.41	98.72	97.68	98.94	91.61
%AN	100	100	100	92.09	89.86	87.12	94.81	100
Q	0	0	0	8.08	0	0	0	0
or	0	0	0	11.66	9.69	3.52	2.34	0
ab	0	0	0	0.59	1.2	2.07	0.61	0
an	2.06	6.37	10.79	6.87	10.63	14.02	11.13	5.23
lc	6.84	4.54	7.6	0	0	0	0	5.21

Sample	3-23b	3-500	KL1-5	KL1-6	KL2-1	KL2-4	KL2-1	0 -ED-1
K	6	6	6	6	6	6	6	6
ne	0.61	0.37	0.89	0	0	0	0	0.19
di	1.66	9.93	55.1	27.89	55.14	37.98	18.06	13.41
hy	0	0	0	0	6.99	12.65	27.91	0
wo	0	0	0	42.79	0	0	0	0
ol	69.02	64.85	12.63	0	12.82	25.45	35.05	51.11
mt	2.8	3.08	2.75	0	2.6	2.93	3.11	1.57
il	1.35	1.72	1.02	0.17	0.93	1.37	1.78	8.5
hem	0	0	0	1.55	0	0	0	3.53
ti	0	0	0	0.41	0	0	0	0
ap	1	1.29	0	0	0	0	0	0.22
COS	14.65	7.84	9.21	0	0	0	0	11.01

Sample	FD2-2	NX-4-16	NX-1-8	NX-3S-1	SD-1-86	SD2-L186	NX-4-7	SL-17
K	6	6	6	6	6	7	8	9
SiO_2	36.3	34.2	28	24.8	30.4	42.7	42.5	47.7
Al_2O_3	2.9	2.7	3.2	3.1	1.9	3.7	18.8	14.5
Fe_2O_3	9	3.4	6.3	7	4	0.09	0.67	0
FeO	0.85	1.5	0.78	1.3	2	8.5	7	11.2
MgO	32.7	30.7	26	22.2	25.9	42.3	20.5	9.8
CaO	0.67	6.8	11.8	16.2	14.8	1.75	10.5	12.4
Na_2O	0.07	0.09	0.03	0.07	0.04	0.16	0.63	2.79
K_2O	0.23	0.42	0.18	0.16	0.18	0	0	0
H_2O+	12.8	14.1	10.3	10	9.7	0	0	0
TiO_2	1.9	0.95	1.4	1.4	0.9	0.06	0.38	1.79
P_2O_5	0.07	0.3	0.3	1.4	0.35	0	0	0
MnO	0.16	0.14	0.15	0.15	0.13	0.21	0.21	0.21
Cr_2O_3	0	0	0	0	0	0.62	0.11	0
CO_2	0	0	0	10.5	8.9	0	0	0
Total	97.65	95.3	88.44	98.28	99.2	100.09	101.3	100.39
%AN	82.02	100	100	100	100	85.8	94.82	54.14
or	1.49	0	0	0	0	0	0	0
ab	0.69	0	0	0	0	1.3	2.5	22.7
an	3.14	6.44	9.65	9.42	5.18	7.83	45.71	26.8
lc	0	2.23	0	0	0.99	0	0	0
ne	0	0.55	0.19	0.46	0.25	0	1.7	1.27
kal	0	0	0.76	0.7	0	0	0	0
C	1.77	0	0	0	0	0.25	0	0
di	0	19.02	0	0	3.13	0	2.73	27.33
hy	33.36	0	0	0	0	9.67	0	0
ol	52.62	65.04	63.1	48.72	63.24	80.78	46.2	16.03
mt	3.89	2.88	3.63	3.72	2.91	0.08	0.66	3.41
il	2.9	1.49	2.33	2.39	1.45	0.08	0.5	2.47
ap	0.16	0.71	0.75	3.59	0.85	0	0	0

Sample K	FD2-2 6	NX-4-16 6	NX-1-8 6	NX-3S-1 6	SD-1-86 6	SD2-L186 7	NX-4-7 8	SL-17 9
wus	0	0	2.18	7.59	0	0	0	0
COS	0	1.66	17.41	23.41	22.01	0	0	0

Sample K	KL1-7 6
SiO_2	41.6
Al_2O_3	5.4
Fe_2O_3	7.4
MgO	21.7
CaO	7.09
Na_2O	0.38
K_2O	0.76
H_2O+	12.17
TiO_2	1.4
MnO	0.15
Total	98.05
%AN	75.97
or	5.03
ab	3.82
an	12.09
di	21.87
hy	29.33
ol	22.28
mt	3.4
il	2.19

Major rock types (K): 1 = gabbro, 2 = andesite, 3 = diorite, 4 = monzonite, 5 = granite, 6 = kimberlite, 7 = peridotite, 8 = websterite, 9 = eclogite.

Samples: SL1 to SL6, SD-1-86, and SD2-L186, State Line District (SLD); Eggler and others, 1987.
3-23b and 3-500 (SLD); McCallum and Nabarek, 1976.
KL1-5 to KL2-10 (SLD); Coopersmith, 1991.
ED-1-1, FD-2-2, NX-4-16 to NX-32-1, and SD-1-86 (SLD); McCallum and Smith, 1978.
Sl-17 (SLD); Ater and others, 1984.

Table 4. Chemical analyses and CIPW norms of rock samples from the La Plata district.

Sample	**1**	**9**	**14**	**24**	**46**	**50**	**64**	**32**
K	**1**	**1**	**1**	**1**	**1**	**1**	**1**	**1**
SiO_2	61.89	60.22	63.81	61	64.26	57.29	54.87	54.6
Al_2O_3	17.78	20.07	19.01	17.15	16.33	18.55	16.61	15.62
Fe_2O_3	0.99	0.96	2.79	1.98	1.05	2.51	4.04	4.92
FeO	0.28	3.82	0.27	0.4	1.17	2.25	1.88	2.36
MgO	0.05	0.33	0.08	0.02	0.45	1.01	0.95	2.05
CaO	1.75	0.87	0.06	0.27	1.92	3.38	2.68	5.51
Na_2O	2.1	4.85	1.02	0.47	4	5.42	1.87	3.55
K_2O	12.2	6.92	9.39	12.06	6.95	4.65	10.56	6.51
H_2O+	0.34	0.7	2.99	1.64	0.42	0.67	0.55	0.46
H_2O-	0.19	0.24	0.34	0.25	0.06	0.11	0.11	0.07
TiO_2	0.3	0.58	0.32	0.34	0.38	0.62	0.72	0.73
P_2O_5	0.09	0.15	0.04	0.45	0.16	0.25	0.34	0.92
MnO	0.05	0.22	0.01	0.01	0.06	0.1	0.14	0.22
CO_2	1.68	0.1	0.03	0.01	1.88	0.12	2.48	0.25
Total	99.69	100.03	100.16	96.05	99.09	96.93	97.8	97.77
%AN	13.95	7.12	0.4	-61.11	14.48	20.51	32.85	20.95
Q	0.47	0.93	21.14	12.73	9.73	0	0	0
or	73.59	40.8	58.17	76.7	42.18	28.18	66.44	39.8
ab	19.25	43.46	9.6	4.54	36.9	49.92	12.5	29.13
an	3.12	3.33	0.04	-1.72	6.25	12.88	6.11	7.72
ne	0	0	0	0	0	0	3.23	2.31
C	0	3.68	8.19	4.59	0	0	0	0
di	0.28	0	0	0	1.97	2.12	4.54	11.48
hy	0	5.68	0.31	0.06	0.95	1.73	0	0
wo	1.92	0	0	0	0	0	0	0
ol	0	0	0	0	0	1.47	2.88	4.11
mt	0.14	1	2	0.58	1.13	2.27	2.47	2.41
il	0.43	0.81	0.47	0.51	0.54	0.89	1.07	1.05
hem	0.61	0	0	1	0	0	0	0
ap	0.19	0.31	0.09	1.01	0.34	0.54	0.76	1.99

Sample	**68**	**69**	**11**	**59**	**15**	**16**	**47**
K	**2**	**2**	**1**	**1**	**3**	**3**	**4**
SiO_2	72.16	64.72	63.61	59.23	54.54	47.27	60.43
Al_2O_3	13.81	16.62	14.85	17.03	11.8	2.44	20
Fe_2O_3	0.05	1.89	2.77	1.08	0.9	9.36	1.43
FeO	0.36	1.04	0.76	1.23	3.08	3.14	0.03
MgO	0.04	0.17	0.1	0.61	1.17	3.57	0.11
CaO	0.6	0.37	1.53	2.43	7.92	15.81	0.02
Na_2O	2.13	0.4	0.72	3.32	1.56	1.44	0.67
K_2O	9.35	11.69	11.55	10.11	7.96	1.53	14.63

Sample **K**	**68** **2**	**69** **2**	**11** **1**	**59** **1**	**15** **3**	**16** **3**	**47** **4**
H_2O+	0.43	0.8	0.43	0.49	0.44	0.36	0.92
H_2O-	0	0.35	0.17	0.07	0.05	0.1	0.09
TiO_2	0.4	0.41	0.49	0.36	0.13	0.17	0.21
P_2O_5	0.33	0.15	0.17	0.11	0.16	0.06	0.03
MnO	0.01	0.07	0.04	0.12	0.48	1.14	0.14
CO_2	0.07	0	1.1	4.05	9.2	11.69	0.04
Total	99.74	98.68	98.29	100.24	99.39	98.08	98.75
%AN	2.58	19.24	32.95	6.92	10.75	0	-1.64
Q	22.27	16.46	12.55	0	2.18	5	0.39
or	56.2	72.09	72.02	61.74	53.03	11.1	88.41
ab	19.46	3.75	6.82	23.74	15.79	5.25	6.15
an	0.52	0.89	3.35	1.77	1.9	0	-0.1
ne	0	0	0	4.25	0	0	0
C	0	3.41	0	0	0	0	3.46
di	0.22	0	1.13	5.22	17.92	66.26	0
hy	0	0.49	0	0	0	0	0.31
wo	0.02	0	0.83	1.37	7.53	5.19	0
ac	0	0	0	0	0	5.71	0
mt	0.02	1.8	2.2	1.17	1.06	0	0
il	0.57	0.6	0.72	0.52	0.2	0.29	0.27
hem	0.02	0.17	0	0	0	0	1.02
ap	0.7	0.33	0.38	0.24	0.38	0.15	0.06
ru	0	0	0	0	0	0	0.01
NMS	0	0	0	0	0	1.04	0

Major rock types (K): 1 = syenite, 2 = breccia, 3 = pegmatite, 4 = trachyte.
All samples: La Plata District (LPD); Werle and others, 1984

Table 5. Chemical analyses and CIPW norms of rock samples from the Hahns Peak district.

Sample	1	2	3	4	5	6	7	8
K	4	4	2	5	3	1	6	7
SiO_2	73.3	74.4	49.2	41.0	71.3	68.1	69.1	72.4
Al_2O_3	13.6	11.6	18.3	21.7	14.3	16.9	15.4	14.8
Fe_2O_3	0.72	1.6	2	4.7	0.32	1.2	1.7	0.91
FeO	1.8	2.9	7.6	10.4	3.8	1.5	0.56	0.72
MgO	0.6	1.3	6.1	3.5	2.1	1	0.8	0.38
CaO	1.9	1.7	10.4	4.4	0.69	3.8	1.1	1.1
Na_2O	2.1	2.9	2.6	1.6	1.9	4	2.4	3.7
K_2O	5	2.2	0.8	6.1	3	0.83	6	4
H_2O+	0.46	0.72	0.78	2.4	1.2	1.1	0.9	0.91
H_2O-	0.22	0.26	0.22	0.35	0.08	0.24	1.5	0.39
TiO_2	0.25	0.32	0.89	2.2	0.47	0.26	0.33	0.19
P_2O_5	0.05	0.06	0.13	0.98	0.11	0.08	0.17	0.1
MnO	0.04	0.08	0.17	0.26	0.08	0.05	0.02	0.03
CO_2	0.05	0.05	0.08	0.1	0.05	0.15	0.05	0.05
Total	100.09	100.09	99.27	99.69	99.4	99.21	100.03	99.68
%AN	32.55	23.6	60.6	77.21	13.69	33.79	16.79	12.64
Q	34.32	40.33	0	0	40.3	30.13	27.96	31.1
or	30.37	13.46	4.82	38.02	18.5	5.05	36.77	24.21
ab	19.39	26.97	23.81	4.81	17.8	36.98	22.35	34.03
an	9.36	8.33	36.63	16.28	2.82	18.88	4.51	4.92
ne	0	0	0	6.21	0	0	0	0
C	1.57	1.7	0	7.85	7.9	3.04	3.81	2.93
di	0	0	12.12	0	0	0	0	0
hy	3.76	6.88	13.65	0	11.41	4.08	2.29	1.34
ol	0	0	5.3	17.36	0	0	0	0
mt	0.77	1.73	2.13	4.08	0.35	1.29	0.68	0.97
il	0.36	0.46	1.26	3.23	0.68	0.37	0.48	0.27
hem	0	0	0	0	0	0	0.77	0
ap	0.11	0.13	0.28	2.16	0.24	0.17	0.37	0.21

Sample	9	10	11	12	13	14	15	16
K	7	7	7	7	8	9	6	10
SiO_2	63.3	62.3	68.7	67.9	59.1	55.7	69.19	61.64
Al_2O_3	15.6	15.8	15	15	16	15.2	15.57	13.96
Fe_2O_3	3.8	3.8	1.8	1.8	6.5	4.9	2.43	2.15
FeO	0.92	0.92	0.76	0.84	1.2	3.9	0.18	3.06
MgO	2.6	2.7	1.1	0.65	2.5	2.5	0.32	2.86
CaO	4	4.3	1.6	2.9	3.9	4.7	0.32	2.65
Na_2O	4.1	4.1	3.6	2.1	3.2	4.2	2.9	4.1
K_2O	3.2	3.3	3.7	4.2	3.3	2.6	6.24	4.88
H_2O+	0.77	0.91	1.2	1.9	1.1	1.1	1.34	0.65

Sample **K**	**9** **7**	**10** **7**	**11** **7**	**12** **7**	**13** **8**	**14** **9**	**15** **6**	**16** **10**
H_2O-	0.43	0.39	1.6	0.53	0.26	0.72	0.37	0.31
TiO_2	0.81	0.86	0.45	0.39	1.5	1.7	0.46	0.92
P_2O_5	0.38	0.36	0.28	0.23	0.71	0.83	0.21	0.63
MnO	0.11	0.1	0.03	0.06	0.08	0.23	0.02	0.14
CO_2	0.05	0.05	0.05	0.93	0.52	2.4	0	1.21
F	0	0	0	0	0	0	0.11	0.21
BaO	0	0	0	0	0	0	0.18	0.37
S	0	0	0	0	0	0	0.02	0.05
Total	100.07	99.89	99.87	99.43	99.87	100.68	99.86	99.79
%AN	28.56	28.9	15.9	40.6	33.86	28.39	0.82	12.54
Q	14.92	13.22	28.19	32.53	15.7	8.01	26.68	10.09
or	19.16	19.79	22.69	26.35	20.25	16.11	38.1	29.68
ab	37.31	37.36	33.55	20.02	29.84	39.55	26.91	37.89
an	14.91	15.19	6.34	13.68	15.28	15.67	0.22	5.43
C	0	0	3.21	2.64	2.01	0	4.48	0
di	2.15	3.26	0	0	0	2.48	0	3.09
hy	7.15	6.69	3.15	1.91	9.95	10.38	0.91	8.82
mt	2.45	2.5	0.93	1.36	3.26	3.51	0.5	2.31
il	1.14	1.22	0.65	0.58	2.17	2.48	0.66	1.32
hem	0	0	0.68	0.43	0	0	1.08	0
ap	0.81	0.76	0.61	0.51	1.54	1.82	0.45	1.36

Sample **K**	**17** **11**	**18** **12**
SiO_2	54.7	46.4
Al_2O_3	14.3	11.6
Fe_2O_3	4.2	3.2
FeO	3.3	4.7
MgO	6.7	8.5
CaO	7.4	8
Na_2O	3.7	2.7
K_2O	2.6	2.1
H_2O+	0.89	1.3
H_2O-	0.41	0.61
TiO_2	1.2	1.1
P_2O_5	0.5	0.57
MnO	0.14	0.16
CO_2	0.05	8.5
S	0.05	0.05
Total	100.15	99.49

Sample **K**	**17** **11**	**18** **12**
%AN	30.73	35.48
Q	0.7	0
or	15.45	13.81
ab	33.42	26.98
an	14.82	14.84
di	15.06	20.16
hy	14.97	7.73
ol	0	10.42
mt	2.84	3.03
il	1.68	1.71
ap	1.05	1.33

Major rock types (K): 1 = quartz dioite gneiss, 2 = amphibolite, 3 = schist, 4 = felsic gneiss, 5 = biotite gneiss, 6 = rhyolite, 7 = quartz latite, 8 = rhyodacite, 9 = trachyandesite, 10 = alkali trachyte, 11 = andesine trachybasalt, 12 = olivine andesine trachybasalt.

All samples: Hahns Peak District (HPD); Segerstrom and Young, 1972.

Table 6. Chemical analyses and CIPW norms of rocks from the Powderhorn District.

Sample **K**	**G2300a** **5**	**G4500** **2**	**Ih-71** **4**	**U1026a** **3**	**U718** **5**	**U2015** **5**	**U1199** **6**	**U1877** **6**
SiO_2	76.3	73.1	62.55	65.1	38.57	38.04	40.25	47.88
TiO_2	0.12	0.22	0.15	0.2	1.71	1.98	4.76	0.32
Al_2O_3	13.8	13.2	15.07	16.6	5.79	6.34	2.74	8.34
Fe_2O_3	0.8	1.2	2.42	2	5.41	8.45	10.83	3.27
FeO	0.27	0.96	2.03	1.1	3.33	5.9	7.38	3.83
MnO	0.02	0.04	0.29	0.1	0.16	0.23	0.16	0.18
MgO	0.14	0.45	1.33	0.2	8.44	7.81	12.04	9.5
CaO	0.36	1.2	4.09	1.5	30.72	27.19	20.21	19.52
Na_2O	3.3	3.5	5.8	7.3	2.34	2.16	0.42	3.84
K_2O	4.8	4.7	5.68	5.1	0.42	0.12	0	1.74
H_2O+	0.48	0.56	0.13	0.3	0.62	0.48	0.46	0.42
H_2O-	0	0.06	0.05	0.3	0.34	0.22	0.46	0
P_2O_5	0	0.1	0.14	0	0.83	0.24	0.45	1.45
CO_2	0.07	0.14	0.03	0.03	1.28	0.3	0.07	0
Total	100.46	99.43	99.76	99.83	99.96	99.46	100.23	100.29
Other	0	0	0	0	0.68	0.28	0.09	0.05
%AN	5.69	14.43	0	0	100	100	100	100
Q	35.41	29.96	0	1.2	0	0	0	0
or	28.72	28.45	33.19	29.6	0	0	0	0
ab	30.01	32.2	46.98	59.42	0	0	0	0
an	1.81	5.43	0	0	4.17	7.54	5.9	0.38
lc	0	0	0	0	2.04	0.59	0	8.09
ne	0	0	0.71	0	12.97	12.1	2.39	20.36
C	2.79	0.46	0	0	0	0	0	0
di	0	0	15.16	4.68	32.19	30.61	63.48	64.14
hy	0.39	1.69	0	0	0	0	0	0
wo	0	0	0.09	0.59	0	0	0	0
ol	0	0	0	0	8.89	14.11	8.09	0.11
ac	0	0	2.67	3.98	0	0	0	0
mt	0.43	1.29	0.7	0.25	3.45	3.78	6.91	1.87
il	0.17	0.31	0.21	0.27	2.45	2.87	7	0.44
hem	0.28	0	0	0	0	0	0	0
ap	0	0.21	0.29	0	1.79	0.52	0.99	2.98
COS	0	0	0	0	32	28	5	2

Sample **K**	**U2011** **7**	**441A** **14**	**449** **14**	**489** **14**	**573** **14**	**741** **14**	**514D** **7**	**517** **7**
SiO_2	35.82	13.53	5.25	2.98	14.96	1.01	43.73	39.81
TiO_2	4.41	1.11	0.14	0.38	1.1	0.11	0.6	1.15
Al_2O_3	18.04	3.66	0.35	0.16	1.32	0.6	9.72	18.05
Fe_2O_3	9.92	2.18	2.83	2.21	6.53	0.46	2.95	6.51

Sample	**U2011**	**441A**	**449**	**489**	**573**	**741**	**514D**	**517**
K	**7**	**14**	**14**	**14**	**14**	**14**	**7**	**7**
FeO	2.02	6.13	6.43	1.45	3.13	20.28	3.75	3.02
MnO	0.19	0.24	1.35	0.3	0.36	1.47	0.26	0.24
MgO	0.77	3.75	13.57	3.89	7.04	9.62	10.04	3.12
CaO	17.18	35.42	22.78	46.02	30.4	22.8	19.7	13.11
Na_2O	6.3	0.55	0.14	0.22	2.28	0.07	3.34	9.61
K_2O	3.04	2.11	0.8	0.5	1.44	0.05	1.71	3.11
H_2O+	0.82	1.62	0.14	0.3	1.18	0.19	1.63	1.3
H_2O-	0.42	0.12	0.14	0.05	0.12	0.07	0.05	0.28
P_2O_5	0.08	1.65	0.11	1.73	2.33	0.38	1	0.46
CO_2	0.48	26.98	41.54	39.47	26.81	41.81	0.31	0.41
ZrO_2	0	0.05	0.01	0.01	0.15	0	0.44	0.25
BaO	0	0.72	2.29	0.15	0.11	0.23	0.06	0.02
SrO	0	0.54	0.19	0.46	0.3	0.05	0.19	0.08
Total	99.49	100.36	98.06	100.28	99.56	99.2	99.48	100.53
Other	0.13	0.13	0.13	0.13	0.13	0.13	0.13	0.13
%AN	100	100	0	0	0	100	100	0
an	12.26	1.87	0	0	0	2.13	6.55	0
lc	14.71	0	0	0	0	0	8.17	14.26
ne	34.76	4.3	0	0	0	0.68	18.19	46.67
kal	0	10.86	2.05	0.88	6.1	0.32	0	0
di	4.35	0	0	0	0	0	45.26	2.42
wo	4.18	0	0	0	0	0	0	0
ol	0	-34.13	-40.39	-101.47	-25.60	-57.93	7.91	11.34
ac	0	0	1.8	2.66	10.23	0	0	4.77
mt	4.41	3.31	2.39	2.31	0	0.87	2.22	0.9
il	6.29	2.25	0.35	0.89	2.16	0.28	0.85	1.55
hem	1.28	0	0	0	0	0	0	0
ap	0.17	5.01	0.41	6.08	6.88	1.44	2.11	0.93
wus	0	35.21	71.69	78.13	37.39	92.76	0	0
KMS	0	0	1.51	1.05	0.55	0	0	0
NMS	0	0	0	0	4.83	0	0	0
COS	18	71	60	109	57	59	9	17

Sample	**475**	**777**	**1**	**2**	**3**	**4**	**5**	**6**
K	**12**	**12**	**8**	**5**	**7**	**5**	**9**	**10**
SiO_2	55.26	56.35	44.13	38.04	34.3	40.01	42.05	33.02
TiO_2	0.36	0.22	0	1.98	5.08	1	0	0
Al_2O_3	16.41	18.42	10.8	6.34	4.46	5.41	5.19	14.02
Fe_2O_3	4.55	3.09	0	8.45	12	7.12	1.5	3.43
FeO	1.12	1.65	2.04	5.9	12.09	1.08	1.76	0.21
MnO	0.18	0.14	0.16	0.23	0	0.11	0.09	0
MgO	0.41	0.24	4.35	7.81	0.52	8.89	9.52	4.69
CaO	5.43	2.45	33.81	27.19	31.06	30.99	34.68	35.72

Sample	475	777	1	2	3	4	5	6
K	12	12	8	5	7	5	9	10
Na_2O	3.23	7.89	3.4	2.16	0	0.6	1.06	2.57
K_2O	8.15	6.22	0	0.12	0	0	0.14	0
H_2O+	2.52	1.54	0.49	0.48	0	2	2.22	6.26
H_2O-	0.29	0.26	0	0.22	0	0.52	2.23	0
P_2O_5	0.04	0.02	0	0.24	0	0.88	0	0
CO_2	1.02	0.61	0	0.3	0	1.51	0	0
ZrO_2	0.05	0.03	0	0	0	0	0	0
S	0	0	0	0.02	0	0.06	0	0
BaO	0.12	1.01	0.03	0	0	0	0	0
SrO	0.54	0.14	0.82	0.26	0	0.21	0	0
Total	99.68	100.28	100.03	99.74	99.51	100.39	100.44	99.92
Other	0.13	0.13	0.13	0.13	0.13	0.13	0.13	0.13
%AN	25.23	0	100	100	100	100	100	100
or	50.72	36.64	0	0	0	0	0	0
ab	19.38	24.95	0	0	0	0	0	0
an	6.54	0	14.21	7.54	13.61	12.8	9.3	28.14
lc	0	0	0	0.59	0	0	0.68	0
ne	6.7	23.19	18.31	12.1	0	3.43	5.9	14.58
di	10.75	9.59	24.56	30.61	35.9	42.96	40.45	0
wo	3.25	0	18.05	0	2.96	0	0	0
ol	0	0.17	0	14.11	0	7.5	6.63	0.71
ac	0	4.78	0	0	0	0	0	0
mt	2.05	0	1.57	3.78	7.69	2.77	1.62	1.65
il	0.53	0.31	0	2.87	7.91	1.48	0	0
ap	0.09	0.04	0	0.52	0	1.95	0	0
wus	0	0	0	0	0	0	0	7.38
NMS	0	0.32	0	0	0	0	0	0
COS	0	0	23	28	32	27	35	48

Sample	1A	2A	A	A1	A2	A3	A4	A5
K	5	5	5	6	6	6	6	6
SiO_2	38.57	38.04	38.3	40.25	36.82	22.02	31.28	47.88
TiO_2	1.71	1.98	1.8	4.76	9.02	8.79	6.6	0.32
Al_2O_3	5.79	6.34	6.1	2.74	2.9	10.8	5.18	8.34
Fe_2O_3	5.41	8.45	6.9	10.83	8.32	8.82	12.11	3.27
FeO	3.33	5.9	4.6	7.38	6.18	6.44	5.44	3.83
MnO	0.16	0.23	0.2	0.16	0.06	0.15	0.06	0.18
MgO	8.44	7.81	8.1	12.04	11.68	13.02	23.15	9.5
CaO	30.72	27.19	29	20.21	21.38	13.58	10.26	19.52
Na_2O	2.34	2.16	2.2	0.42	0.68	0.7	0.25	3.84
K_2O	0.42	0.12	0.3	0	0.45	4.75	1.88	1.7
H_2O+	0.62	0.22	0.3	0.46	0.53	2.7	3.22	0.42
H_2O-	0.34	0.48	0.5	0.46	0	1.51	0	0

Sample K	1A 5	2A 5	A 5	A1 6	A2 6	A3 6	A4 6	A5 6
P_2O_5	0.83	0.24	0.5	0.45	0	6.35	0.03	1.49
CO_2	1.28	0.3	0.8	0.07	1.34	0	0	0
ZrO_2	0.02	0	0	0	0	0	0	0
SO_3	0	0	0	0	0.31	0	0.24	0.05
S	0.03	0.02	0	0.02	0	0.02	0	0
BaO	0.28	0	0.3	0.03	0.08	0.48	0.04	0
SrO	0.35	0.26	0.3	0	0.06	0.17	0.02	0
F	0	0	0	0	0.1	0.07	0.04	0
CL	0	0	0	0	0	0.04	0	0
Total	100.64	99.74	100.2	100.28	99.91	100.41	99.8	100.34
Other	0.13	0.13	0.13	0.13	0.13	0.06	0.06	0.06
%AN	100	100	100	100	100	100	100	100
an	4.17	7.54	6.09	5.9	3.79	13.25	7.71	0.49
lc	2.04	0.59	1.47	0	2.28	0	9.18	7.91
ne	12.97	12.1	12.27	2.39	3.93	4.06	1.39	20.36
kal	0	0	0	0	0	18.13	0	0
di	32.19	30.61	30.99	63.48	54.94	0	3.27	64.45
wo	0	0	0	0	0	0	0	0.03
ol	8.89	14.11	11.69	8.09	5.32	25.05	48.31	0
mt	3.45	3.78	3.57	6.91	0	0	7.62	1.87
il	2.45	2.87	2.6	7	10.36	11	9.5	0.44
hem	0	0	0	0	6.22	6.62	0.75	0
ap	1.79	0.52	1.08	0.99	0	14.3	0.06	3.07
pero	0	0	0	0	3.11	2.19	0	0
wus	0	0	0	0	0	2.65	0	0
COS	32	28	30	5	10	3	12	1

Sample K	A6 6	B1 7	B2 7	B3 7	B4 7	B5 7	B6 3	B7 3
SiO_2	47.1	43.5	47.88	38.89	35.82	31.55	65.08	56.74
TiO_2	1.7	5.35	0.32	2.45	4.41	4.86	0.2	0.4
Al_2O_3	8.16	3.97	8.34	12.69	18.04	9.85	16.65	19.32
Fe_2O_3	6.38	3.42	3.27	7.46	9.92	5.27	2.01	2.37
FeO	6.62	4.41	3.83	2.96	2.02	5.9	1.08	1.65
MnO	0.36	0.19	0.18	0.16	0.19	0.11	0.13	0.07
MgO	3.97	8.12	9.5	5.01	0.77	7.45	0.21	0.27
CaO	17.3	24.69	19.52	18.65	17.18	15.22	1.49	1.98
Na_2O	3.15	1.55	3.84	4.9	6.3	3.69	7.31	8.05
K_2O	2.15	0.14	1.7	2.19	3.04	3.9	5.14	5.88
H_2O+	1.1	0.34	0.42	0.7	0.82	1.82	0.32	1.12
H_2O-	0	0.58	0	0.36	0.42	0.92	0.3	0.32
P_2O_5	1.49	3.11	1.45	1.78	0.08	2.34	0.04	0.03
CO_2	0	0.66	0	0.66	0.48	5.27	0	1.5

Sample	**A6**	**B1**	**B2**	**B3**	**B4**	**B5**	**B6**	**B7**
K	**6**	**7**	**7**	**7**	**7**	**7**	**3**	**3**
ZrO_2	0	0	0	0.02	0.05	0	0.03	0.02
SO_3	0.07	0	0.05	0.25	0	1.52	0	0.12
S	0	0.03	0	0.6	0.03	0.27	0.02	0.05
BaO	0.05	0	0	0	0	0.07	0.03	0.16
SrO	0	0.13	0	0	0	0.09	0.03	0.12
F	0.25	0	0	0	0	0	0	0
Total	99.85	100.19	100.3	99.73	99.57	100.1	100.07	100.17
Other	0.06	0.06	0.06	0.06	0.05	0.05	0.05	0.05
%AN	15.22	22.28	100	100	100	0	0	0
Q	0	0	0	0	0	0	1.03	0
or	13.29	0.87	0	0	0	0	29.79	34.51
ab	10.36	12.66	0	0	0	0	59.37	34.18
an	1.86	3.63	0.49	6.33	12.26	0	0	0
lc	0	0	7.91	10.63	14.71	20.45	0	0
ne	11.54	1.16	20.36	27.1	34.76	20.45	0	21.64
di	45.22	47	64.4	31.85	4.35	7.68	4.81	4.96
wo	8.49	17.56	0	0	4.18	0	0.4	1.34
ol	0	0	0.03	1.45	0	14.23	0	0
ac	0	0	0	0	0	2.14	4.02	1.24
mt	3.5	0	1.87	4.24	4.41	4.23	0.24	1.51
il	2.48	7.47	0.44	3.5	6.29	7.51	0.27	0.55
hem	0	2.5	0	0	1.28	0.72	0	0
ap	3.26	6.82	2.98	3.82	0.17	5.43	0.08	0.06
pero	0	0.34	0	0	0	0	0	0
COS	0	0	2	11	18	17	0	0

Sample	**B8**	**B9**	**B10**	**B11**	**B12**	**B13**	**B14**	**B15**
K	**1**	**3**	**11**	**6**	**7**	**3**	**3**	**1**
SiO_2	47.94	54.99	50.86	35.5	39.5	65.1	56.7	47.9
TiO_2	1.12	0.99	0.84	7.4	2.9	0.2	0.4	1.1
Al_2O_3	22.56	12.98	11.14	4.1	14	16.6	19.3	22.6
Fe_2O_3	2.02	3.13	2.93	9.4	7.6	2	2.4	2
FeO	4.77	3.92	5.21	6.9	2.8	1.1	1.6	4.8
MnO	0.11	0.13	0.13	0.1	0.2	0.1	0.1	0.1
MgO	2.06	5.5	11.26	11.9	4.3	0.2	0.3	2.1
CaO	12.08	5.67	6.97	19.7	18.3	1.5	2	12.1
Na_2O	4.02	2.83	1.73	0.6	5.2	7.3	8	4
K_2O	0.84	7.08	5.85	1	2.4	5.1	5.9	0.8
H_2O+	1.3	0.58	0.95	0.62	0.6	0.3	0.7	0.7
H_2O-	0.24	0.41	0.64	0.61	0.6	0.3	0.7	0.8
P_2O_5	0.25	1	0.79	1.3	1.2	0	0	0.3
CO_2	0.16	0	0	0.2	0.5	0	1.5	0.2
$Zr0_2$	0.02	0.04	0.02	0	0	0	0	0

Sample K	B8 1	B9 3	B10 11	B11 6	B12 7	B13 3	B14 3	B15 1
S	0.03	0.05	0.02	0.1	0.4	0	0.1	0
BaO	0.39	0.47	0.31	0.1	0	0	0.2	0.4
SrO	0.31	0.17	0.22	0.1	0	0	0.1	0.3
CL	0	0	0	0.1	0	0	0	0.1
Total	100.22	99.94	99.87	99.73	100.5	99.8	100	100.3
Other	0.05	0.05	0.15	0.05	0.05	0.05	0.05	0.05
%AN	62.06	7.22	31.99	100	100	0	0	61.93
Q	0	0	0	0	0	1.2	0	0
or	5.05	42.44	34.87	0	0	29.6	34.65	4.81
ab	25.54	23.54	11.48	0	0	59.42	34.06	25.87
an	41.78	1.83	5.4	5.91	7.87	0	0	42.09
lc	0	0	0	5.04	11.49	0	0	0
ne	6.72	1.34	2.51	3.45	28.38	0	21.61	6.41
di	14.06	16.07	19.42	45.39	28.11	4.68	5.07	13.61
wo	0	0	0	0	2.18	0.59	1.41	0
ol	2.58	8.61	21	9.26	0	0	0	2.88
ac	0	0	0	0	0	3.98	1.07	0
mt	2.15	2.64	2.47	1.98	4.66	0.25	1.57	2.13
il	1.59	1.4	1.18	11	4.09	0.27	0.55	1.56
hem	0	0	0	5.3	0	0	0	0
ap	0.53	2.12	1.67	2.9	2.54	0	0	0.64
COS	0	0	0	10	11	0	0	0

Sample K	B16 1	B17 13	B18 13	B19 9	B20 10
SiO_2	52.2	33.64	33.7	42.3	33.02
TiO_2	1.5	0.07	0	0	0
Al_2O_3	14.7	29.82	29.4	5.41	14.02
Fe_2O_3	1.5	0	0	2.68	3.43
FeO	9.9	0	0	0.56	0.21
MnO	0.2	0	0	0.1	0
MgO	5.4	0.39	0	9.07	4.69
CaO	8.8	8.64	4.18	34.84	35.72
Na_2O	2.6	15.41	18.52	0.95	2.57
K_2O	1.2	0.5	1.45	0.09	0
H_2O+	0.7	2.3	4.24	4.06	6.26
H_2O-	0.6	2.31	0.72	0.18	0
P_2O_5	0.2	0	0	0.04	0
CO_2	0	6.79	0	0	0
SO_3	0	0.03	4.65	0	0
S	0.1	0	0	0	0
SrO	0	0	0.08	0	0
CL	0.1	0.1	0.1	0.1	0.1
Total	99.7	100	97.04	100.38	100.02

Sample K	B16 1	B17 13	B18 13	B19 9	B20 10
Other	0.05	0.05	0.05	0.05	0.05
%AN	51.61	100	0	100	100
Q	3.02	0	0	0	0
or	7.33	0	0	0	0
ab	24.13	0	0	0	0
an	25.74	10.6	0	10.62	28.14
lc	0	0	0	0.44	0
ne	0	82.09	88.99	5.31	14.58
kal	0	1.75	5.02	0	0
di	14.44	0	0	42.58	0
hy	21.13	0	0	0	0
ol	0	-13.61	-12.87	4.78	0.71
mt	1.62	0	0	1.63	1.65
il	2.16	0	0	0	0
ap	0.43	0	0	0.09	0
pero	0	0.1	0	0	0
wus	0	9.6	8.58	0	7.38
NMS	0	0	4.21	0	0
COS	0	9	6	35	48

Major rock types (K): 1 = gabbro, 2 = granite, 3 = syenite, 4 = fenite, 5 = uncompahgrite, 6 = pyroxenite, 7 = ijolite, 8 = melilite, 9 = juanite, 10 = cebollite, 11 = shonkinite, 12 = nepheline syenite, 13 = cancrinite, 14 = carbonatite.

Samples: G2300a, G4500, and 1H-71, Powderhorn District (PD); Olson and Hedlund, 1981.
U1206a to U2011 (PD); Larsen, 1942.
441A to 777 (PD); Nash, 1972.
1 to B20 (PD); Larsen, 1942.

Table 7. Chemical analyses and CIPW norms of rock samples from the Silver Cliff and Rosita districts.

Sample	1	2	3	4	5	6	7	8
K	4	5	5	1	2	6	3	5
SiO_2	66.46	70.87	71.2	57.01	50.47	58.94	66.03	71.56
Al_2O_3	17.91	15.18	13.7	18.4	18.73	17.19	18.49	13.1
Fe_2O_3	2.42	2.18	0.9	3.69	4.19	2.63	2.18	0.66
FeO	0.35	0.12	0	2.36	4.92	1.98	0.22	0.28
MgO	0.49	0.6	0.2	2.34	3.48	1.52	0.39	0.14
CaO	2.89	1.58	0.5	4.29	8.82	4.45	0.96	0.74
Na_2O	4.79	3.47	2.9	4.95	4.62	4.2	5.22	3.77
K_2O	3.74	5.04	4.9	3.72	3.56	3.9	5.86	4.06
H_2O+	1.01	1.08	4.9	2.29	0.58	4.53	0.85	5.52
TiO_2	0	0	0.1	0.27	0.51	0.27	0	0
P_2O_5	0	0	0	0.42	0.1	0.23	0	0
MnO	0	0	0	0.21	0.11	0.1	0	0.16
Total	100.06	100.12	99.3	99.95	100.09	99.94	100.2	99.99
%AN	25	20.1	8.7	27.67	55.67	30.49	9.23	9.79
Q	15.75	25.48	33.93	0.08	0	7.52	9.62	31.74
or	22.18	30.26	31.01	22.26	20.93	24.04	34.34	25.55
ab	43.17	31.66	27.89	45.01	15.74	39.35	46.49	36.06
an	14.39	7.97	2.66	17.22	19.76	17.26	4.72	3.91
ne	0	0	0	0	15.32	0	0	0
C	0.8	1.27	3.18	0	0	0	1.97	1.35
di	0	0	0	1.25	18.51	3.37	0	0
hy	2.14	1.77	0.59	11.04	0	5.63	1.31	0.65
ol	0	0	0	0	6.74	0	0	0
mt	1.57	1.59	0	1.87	2.09	1.93	1.56	0.74
il	0	0	0	0.38	0.71	0.39	0	0
hem	0	0	0.67	0	0	0	0	0
ap	0	0	0	0.89	0.21	0.5	0	0
ru	0	0	0.07	0	0	0	0	0

Major rock types (K): 1 = gabbro, 2 = andesite, 3 = trachyte, 4 = rhyodacite, 5 = rhyolite, 6 = latite.

Samples: 1 and 2, and 4 to 8, Rosita Hills and Silver Cliff District (RSD); Cross, 1896.
3 (RSD); Anderson and others, 1956.

Table 8. Chemical analyses and CIPW norms of rock samples from the Wet Mountains district.

Sample	WM-64-843	WM-64-859	WM-64-875	WM-62-131	WM-62-140	WM-62-142	WM-62-143	WM-62-114
K	2	1	3	2	2	2	2	2
SiO_2	62.27	39.19	45.31	59.7	59.9	57.71	59.8	55.95
Al_2O_3	17.41	13.72	7.03	20.04	18.64	19.18	18.64	21.43
Fe_2O_3	3.87	7.5	3.98	1.41	1.65	1.86	1.46	1.28
FeO	0.79	9.79	6.05	1.8	1.8	2.09	1.93	2.09
MgO	0.59	6.68	12.84	0.96	1.09	1.28	1.11	0.69
CaO	0.7	12.12	19.99	2.69	2.55	3.34	2.34	2.49
Na_2O	7.63	2.56	0.82	5.98	5.37	5.39	5.82	7.36
K_2O	3.97	0.45	0.17	5.25	6.6	5.64	5.91	6.32
H_2O+	1.1	1.06	0.63	0.32	0.27	0.28	0.38	0.38
H_2O-	0.66	0.1	0.21	0.32	0.27	0.29	0.38	0.39
TiO_2	0.72	4.42	2.5	0.86	0.92	1.15	0.88	0.56
P_2O_5	0.29	1.06	0.14	0.32	0.41	0.5	0.31	0.18
MnO	0.04	0.21	0.15	0.08	0.11	0.1	0.12	0.11
CO_2	0.02	0.99	0.4	0.07	0.43	0.45	0.5	0.24
Cl	0.02	0.04	0.02	0.02	0.01	0.02	0.01	0.21
F	0.12	0.12	0.04	0.1	0.15	0.14	0.15	0.1
Total	100.2	100.01	100.28	99.92	100.17	99.42	99.74	99.78
%AN	2.19	65.38	100	17.94	14.01	20.67	13.07	19.4
Q	0.54	0	0	0	0	0	0	0
or	23.3	2.81	0	30.59	38.65	33.32	34.75	36.45
ab	68.07	13.79	0	50.78	44.19	44.07	48.22	27.47
an	1.52	26.04	15.26	11.1	7.2	11.49	7.25	6.61
lc	0	0	0.82	0	0	0	0	0
ne	0	6.32	4.49	1.31	2.16	2.59	2.27	22.22
C	0	0	0	0.43	0	0	0	0
di	0.04	24.19	65.36	0	2.15	1.46	1.83	3.44
hy	2.63	0	0	0	0	0	0	0
ol	0	11.44	5.09	2.5	1.83	2.48	2.3	1.38
mt	2.31	6.55	4.23	1.45	1.71	1.94	1.52	1.31
il	1	6.51	3.54	1.18	1.27	1.6	1.22	0.76
ap	0.6	2.34	0.3	0.66	0.85	1.05	0.65	0.37
COS	0	0	0.9	0	0	0	0	0

Sample	75-201X	78-496	78A-498A	75A-363	75A-369	75A-373	75A-381	75A-299
K	4	4	4	2	2	2	2	1
SiO_2	46.9	43	37.7	67.7	74.3	66.8	74.9	52.8
Al_2O_3	16.2	16.5	11.3	15.4	13.4	15.7	12.7	9.3
Fe_2O_3	4.7	3.1	6.2	1.3	0.88	1.6	1	1.2
FeO	4.7	7.4	10.6	2.2	0.72	1.9	0.28	6.5
MgO	3.5	5.6	7.3	0.12	0.01	0.01	0.01	16.8

Sample **K**	**75-201X** **4**	**78-496** **4**	**78A-498A** **4**	**75A-363** **2**	**75A-369** **2**	**75A-373** **2**	**75A-381** **2**	**75A-299** **1**
CaO	9.9	9.6	12.5	0.47	0.39	0.52	0.25	10.5
Na_2O	6.7	5.4	2.4	6.8	5.1	6.8	4.8	1.3
K_2O	3.6	3.6	3.8	4.9	4.2	4.7	4.1	0.22
H_2O+	0.52	0.59	1.02	0.26	0.14	0.21	0.23	0.41
H_2O-	0.52	0.59	1.02	0.26	0.14	0.2	0.24	0.41
TiO_2	2.1	3.4	3.4	0.08	0.03	0.12	0.02	0.34
P_2O_5	1.2	2.2	2.2	0.03	0.02	0.04	0.02	0.08
MnO	0.23	0.31	0.31	0.12	0.03	0.12	0.02	0.13
CO_2	0.02	0.02	0.02	0	0	0.02	0.12	0.02
Cl	0	0	0	0	0	0.01	0.02	0
F	0	0	0	0.25	0.36	0.37	0.1	0.1
Total	100.79	101.31	99.77	99.89	99.72	99.12	98.81	100.11
%AN	31.91	76.53	100	0	2.69	0	2.27	61.81
Q	0	0	0	7.9	25.78	7.48	29.15	0
or	20.94	21	0	28.68	25.01	27.74	24.74	1.28
ab	7.35	3.07	0	54.6	46.16	57.87	44.01	11.5
an	3.44	10.03	9.27	0	1.28	0	1.02	18.61
lc	0	0	18.83	0	0	0	0	0
ne	31.13	26.88	13.55	0	0	0	0	0
di	26.39	18.25	27.38	1.69	0.43	1.85	0.06	25.75
hy	0	0	0	2.93	0.32	1.57	0	39.08
wo	1.68	0	0	0	0	0	0.02	0
ol	0	8.35	13.88	0	0	0	0	1.91
ac	0	0	0	3.59	0	2.5	0	0
mt	3.71	3.2	5.37	0	0.93	0.73	0.67	1.24
il	2.88	4.68	4.96	0.11	0.04	0.17	0.03	0.47
hem	0	0	0	0	0	0	0.27	0
ap	2.47	4.54	4.82	0.06	0.04	0.08	0.04	0.16
NMS	0	0	0	0.42	0	0	0	0
COS	0	0	1.94	0	0	0	0	0

Sample **K**	**75A-300** **3**	**75A-302** **1**	**75A-297** **3**	**IM-10-64** **6**	**WM-64-827** **5**	**IM-20-64** **7**	**WM-62-73** **6**	**WM-64-828** **5**
SiO_2	52.6	53.1	53.4	40.31	42.81	43.28	46.74	46.88
Al_2O_3	4.8	7.4	4.8	7.31	17.08	24.82	21.1	11.18
Fe_2O_3	3	0.5	1.9	2.81	5.53	1.54	1.51	3.47
FeO	6.5	7.8	7.8	15.61	7.49	3.22	4.93	5.12
MgO	22.2	18.2	22.5	25.22	6.53	9.41	7.48	10.61
CaO	8.2	10.1	7.5	5.34	13.59	12.44	13.62	19.47
Na_2O	0.59	0.97	0.67	0.88	2.18	1.55	2.41	1.07
K_2O	0.15	0.11	0.34	0.14	0.22	0.19	0.21	0.09
H_2O+	0.28	0.34	0.33	0.62	0.35	1.45	0.37	0.18

Sample	**75A-300**	**75A-302**	**75A-297**	**IM-10-64**	**WM-64-827**	**IM-20-64**	**WM-62-73**	**WM-64-828**
K	**3**	**1**	**3**	**6**	**5**	**7**	**6**	**5**
H_2O-	0.29	0.34	0.33	0.62	0.34	1.44	0.37	0.18
TiO_2	0.39	0.45	0.38	0.54	2.57	0.11	0.72	1.83
P_2O_5	0.05	0.08	0.09	0.05	0.37	0.03	0.13	0.08
MnO	0.17	0.13	0.18	0.29	0.15	0.07	0.1	0.13
CO_2	0.01	0	0.04	0.38	0.78	0.39	0.33	0.02
Cl	0	0	0	0.01	0.02	0.02	0.03	0
F	0.1	0.1	0.1	0.01	0.04	0.01	0.02	0.02
Total	99.33	99.62	100.36	100.14	100.05	99.97	100.07	100.33
%AN	65.39	64.05	60.17	70.91	72.6	83.72	72.55	86.27
or	0.87	0.64	1.96	0.81	1.34	1.13	1.24	0.53
ab	5.22	8.61	5.86	6.28	14.1	11.8	17.41	4.07
an	9.86	15.34	8.85	15.3	37.36	60.68	46.01	25.59
ne	0	0	0	0.89	3.67	1.33	2.5	3.35
di	23.91	26.95	21.46	8.31	23.83	1.06	16.42	56.83
hy	55.42	46.45	56.81	0	0	0	0	0
ol	2.13	0.7	2.44	65.47	10.8	22.16	13.58	3.39
mt	1.95	0.52	1.91	2.09	4.39	1.62	1.57	3.5
il	0.54	0.62	0.52	0.74	3.7	0.15	1	2.56
ap	0.1	0.17	0.18	0.1	0.8	0.06	0.27	0.17

Sample	**WM-64-829**	**WM-64-824**	**IM-28-64**	**IM-31-64**	**WM-64-896A**
K	**5**	**3**	**3**	**8**	**5**
SiO_2	46.99	44	46.07	51.05	46.59
Al_2O_3	11.47	9.67	8.73	26.94	23.32
Fe_2O_3	3.09	4.36	4.07	0.8	1.92
FeO	4.73	4.95	3.83	1.08	3.01
MgO	10.68	13.66	11.95	1.29	4.89
CaO	20.02	20.01	21.42	12.47	15.26
Na_2O	0.94	0.47	0.94	3.78	2.69
K_2O	0.07	0.12	0.18	0.62	0.26
H_2O+	0.14	0.35	0.24	0.5	0.35
H_2O-	0.15	0.34	0.24	0.5	0.35
TiO_2	1.71	1.57	1.81	0.28	0.74
P_2O_5	0.03	0.04	0.06	0.02	0.14
MnO	0.13	0.13	0.11	0.03	0.07
CO_2	0.03	0.56	0.37	0.48	0.57
Cl	0	0.01	0.02	0.01	0.03
F	0.02	0.02	0.04	0.02	0.16
Total	100.2	100.26	100.08	99.87	100.35

Sample K	WM-64-829 5	WM-64-824 3	IM-28-64 3	IM-31-64 8	WM-64-896A 5
%AN	91.22	100	100	62.35	77.5
or	0.42	0	0	3.66	1.54
ab	2.6	0	0	33.04	14.75
an	27	24.14	19.26	54.72	50.81
lc	0	0.57	0.86	0	0
ne	3.53	2.55	5.11	0.54	5.64
di	58.07	47.54	62.24	5.62	19.21
ol	2.69	14.75	3.41	1.14	4.73
mt	3.24	3.24	3.49	0.84	2.01
il	2.39	2.21	2.55	0.39	1.03
ap	0.06	0.08	0.13	0.04	0.29
COS	0	4.9	2.96	0	0

Major rock types (K): 1 = gabbro, 2 = syenite, 3 = pyroxenite, 4 = clinopyroxene, 5 = plagioclase pyroxene, 6 = clinopyroxene plagioclase olivine, 7 = plagioclase olivine, 8 = anorthosite.

Samples: WM-64-859, WM-64-875, and WM-64-843: Wet Mountain District (WMD); Parker and Sharp, 1970.
All other samples: (WMD); Armbrustmacher, 1984.

Table 9. Chemical analyses and CIPW norms of rock samples from the Ralston Buttes district.

Sample	G22	G7	G8	RD-1	RD-2	RD-3	79S28	79S31
K	2	1	2	2	1	2	5	5
SiO_2	54	52.4	51.4	54.7	54.9	51.4	40.7	45.7
Al_2O_3	17	15.2	16.2	16.7	14.9	16.2	4.8	13
Fe_2O_3	4.1	4.4	6.2	4	4.1	6.2	1.57	2.55
FeO	4.2	4.5	2.9	4.8	5	2.9	5.95	10.7
MgO	3.2	6.8	3.6	3.7	6.4	3.6	2.3	5.48
CaO	6.2	7	6.4	6.5	7.3	6.4	26.9	9.31
Na_2O	3.5	2.7	3.3	3.3	2.8	3.3	0.2	0.2
K_2O	4.7	3.3	4.5	4.3	3	4.5	0.39	4.39
TiO_2	0.82	0.82	0.9	0.9	0.82	0.9	0.51	1.27
P_2O_5	0.56	0.45	0.58	0.6	0.44	0.58	0.1	0.4
MnO	0.16	0.15	0.18	0.16	0.15	0.18	0.27	0.08
H_2O+	0	0	0	0.43	0.73	1.8	0	0
H_2O-	1.3	2.2	3.6	0.3	0.62	1.8	0	0
CO_2	0.05	0.08	0.36	0.01	0.01	0.36	0	0
Total	99.79	100	100.12	100.4	101.17	100.12	83.69	93.08
%AN	34.83	44.72	35.99	37.87	43.34	35.99	98.1	92.33
Q	0	0	0	0	1.94	0	0	0
or	28.27	19.94	27.8	25.61	17.81	27.8	2.88	28.76
ab	31.99	24.79	29.94	29.87	25.26	29.94	0.27	1.99
an	17.1	20.06	16.84	18.21	19.32	16.84	13.82	23.96
ne	0	0	0.62	0	0	0.62	1.19	0
di	8.39	9.96	9.92	8.29	11.35	9.92	35.48	19.49
hy	3.49	17.42	0	12.23	19.82	0	0	14.99
wo	0	0	0	0	0	0	43.17	0
ol	5.93	3.23	9.68	0.73	0	9.68	0	4.97
mt	2.47	2.48	2.62	2.53	2.44	2.62	2.05	2.96
il	1.16	1.17	1.31	1.26	1.15	1.31	0.89	1.96
ap	1.19	0.96	1.27	1.26	0.92	1.27	0.26	0.93

Sample	80S8	80S15	80S28	80S31	80S35	80S40	80S67	80S81
K	5	5	5	5	5	5	5	5
SiO_2	33.1	42	50	45.7	44.5	46.2	48.1	30.3
Al_2O_3	12.6	14.3	15	15.8	16.1	15.3	14.2	16.8
Fe_2O_3	1.63	2.2	1.98	3.22	2.78	2.21	0	0
FeO	7.69	7.93	7.46	11.5	10.4	7.94	0	0
MgO	5.89	3.8	3.6	5.56	4.6	4.5	4.7	4.2
CaO	21.5	9.42	10.2	8.15	10.3	13	11.3	11.4
Na_2O	0.3	2.4	4.4	2.8	3.1	4.1	3.3	0.2
K_2O	3.03	3.83	0.77	1.51	2.01	0.62	1.8	5.93
TiO_2	0.79	1.75	0.87	1.93	1.87	0.95	1.25	1.64
P_2O_5	0.2	0.2	0.2	0.3	0.2	0.2	0.2	0.4

Sample	80S8	80S15	80S28	80S31	80S35	80S40	80S67	80S81
K	5	5	5	5	5	5	5	5
MnO	0.13	0.18	0.16	0.2	0.13	0.11	0.7	0.16
Total	86.86	88.01	94.64	96.67	95.99	95.13	85.55	71.03
%AN	100	88.08	34.74	50.93	65.58	56.57	39.52	100
or	0	25.97	4.81	9.39	12.52	3.84	12.17	0
ab	0	2.63	37.53	26.45	13.32	17.34	32.61	0
an	28.05	19.44	19.98	27.45	25.39	22.58	21.31	37.86
lc	10.42	0	0	0	0	0	0	25.84
ne	1.88	13.26	2.53	0	9.61	12.78	0.78	1.49
kal	4.69	0	0	0	0	0	0	9.63
di	0	26.16	25.7	10.43	21.69	34.99	29.7	0
hy	0	0	0	2.52	0	0	0	0
wo	0	0	0	0	0	0	0.96	0
ol	22.82	6.62	5.54	16.72	11.22	4.22	0	12
mt	1.98	2.64	2.19	3.54	3.06	2.42	0	0
il	1.28	2.8	1.28	2.83	2.75	1.39	1.26	0.35
ap	0.49	0.48	0.44	0.66	0.44	0.44	0.48	1.15
pero	0	0	0	0	0	0	0.74	2.81
COS	28.39	0	0	0	0	0	0	8.87

Sample	80S90	80S124	S1	S2	S3	S4	S5	S6
K	5	5	4	5	3	6	7	8
SiO_2	44	49.6	43.7	42.5	71.2	94.7	53.9	60.7
Al_2O_3	15.8	13.7	15	11.9	14	0.79	12.4	13.2
Fe_2O_3	1.78	3.4	2.66	1.85	0	0.57	3.5	7.73
FeO	8.38	7.54	9.4	7.3	2.79	1.69	15.8	5.51
MgO	3.7	3.7	4.47	4.07	0.62	0.47	3.3	2.28
CaO	5.47	8.53	9.24	17.9	1.62	0.58	1.5	1.26
Na_2O	0.3	3.1	1.93	2.25	3.4	0.2	0.36	1.9
K_2O	4.99	1.86	3.28	1.21	4.22	0.12	3.4	3.35
TiO_2	1.49	1.93	1.64	0.78	0.3	0.03	0.78	0.53
P_2O_5	0.4	0.62	0.34	0.2	0.1	0.1	0.25	0.1
MnO	0.1	0.13	0.18	0.17	0.04	0.02	0.66	0.39
Total	86.41	94.11	91.84	90.13	98.29	99.27	95.85	96.95
%AN	90.1	39.24	67.89	100	19.48	33.48	64.25	24.71
Q	1.92	3.11	0	0	29.57	91	18.63	22.9
or	35.04	11.9	21.48	5.52	25.63	0.77	22.29	21.33
ab	3.2	30.13	11.84	0	31.39	1.95	3.59	18.38
an	29.15	19.46	25.03	21.13	7.59	0.98	6.45	6.03
lc	0	0	0	2.01	0	0	0	0
ne	0	0	4.42	13.62	0	0	0	0
C	1.19	0	0	0	1.27	0	7.27	5.17
di	0	17.58	18.66	45.93	0	1.15	0	0

Sample K	80S90 5	80S124 5	SI 4	S2 5	S3 3	S4 6	S5 7	S6 8
hy	23.82	9.66	0	0	1.97	3.23	37.34	22.88
wo	0	0	0	7.92	0	0	0	0
ol	0	0	12.16	0	0	0	0	0
mt	2.21	3.85	3.08	2.17	1.93	0.65	2.65	2.29
il	2.47	2.91	2.53	1.22	0.43	0.05	1.21	0.8
ap	0.99	1.4	0.79	0.47	0.21	0.23	0.58	0.23

Sample K	79S21 8	79S22 8	79S25 8	80S95 8	80S10 3 8	79S19 7	80S19 7	80S25 7
SiO_2	60.9	62.4	53.1	62.3	57.1	59.5	39.1	58.7
Al_2O_3	13.7	13.7	12.7	11.2	14.3	11.7	13.5	10.9
Fe_2O_3	10	10	2.89	5.39	5.48	4.4	4.11	4
FeO	4.28	4.07	15.8	6.34	7.36	13	15.4	10.5
MgO	2	2.4	3.2	2.1	2.6	3	5.99	2.4
CaO	1.2	1.16	0.67	1.5	1.18	1.56	2.6	1.8
Na_2O	2.8	1.7	0.2	1.6	1.5	0.2	0.9	0.3
K_2O	2.71	4.08	4.38	2.87	3.72	3.18	3.75	3.71
TiO_2	0.54	0.51	0.54	0.47	0.58	0.48	3.9	0.3
P_2O_5	0.1	0.1	0.1	0.1	0.2	0.4	0.65	0.2
MnO	0.31	0.25	0.62	0.27	0.71	0.48	1.06	0.66
Total	98.54	100.37	94.2	94.14	94.73	97.9	90.96	93.47
%AN	17.41	25.05	59.8	32.09	25.24	74.06	51.71	73.89
Q	19.9	21.87	16.72	29.82	20.56	27.72	0	27.12
or	16.94	25.15	29.12	18.87	24.16	20.46	25.55	24.88
ab	26.6	15.93	2.02	15.99	14.8	1.96	9.32	3.06
an	5.61	5.32	3.01	7.56	5	5.58	9.98	8.66
C	4.87	5.26	8.17	3.61	7.37	7.19	6.03	4.46
hy	22.81	23.32	37.47	20.9	24.37	33.21	28.47	28.74
ol	0	0	0	0	0	0	7.85	0
mt	2.26	2.19	2.4	2.29	2.39	2.25	4.96	2.14
il	0.8	0.74	0.85	0.73	0.89	0.73	6.27	0.47
ap	0.22	0.22	0.24	0.23	0.46	0.91	1.57	0.47

Sample K	80S48 7	80S71 7	80S77 7
SiO_2	53.7	55.4	47.3
Al_2O_3	9.93	11.1	10.6
Fe_2O_3	4.44	0.56	3.6
FeO	15.3	20.5	17.1
MgO	3.4	3.3	3.4
CaO	4.12	1.61	1.22
Na_2O	0.4	0.2	0.3
K_2O	1.59	2.85	3.69

Sample K	80S48 7	80S71 7	80S77 7
TiO_2	0.38	0.49	0.45
P_2O_5	0.2	0.3	0.4
MnO	1.05	1.03	1.18
Total	94.51	97.34	89.24
%AN	84.2	77.05	56.08
Q	18.22	18.7	10.44
or	10.66	18.51	26.11
ab	4.07	1.97	3.23
an	21.71	6.63	4.12
C	0.67	6.57	6.34
hy	41.37	45.53	45.57
mt	2.23	0.64	2.44
il	0.6	0.75	0.75
ap	0.47	0.69	1

Major rock types (K): 1 = diorite, 2 = monzonite, 3 = gneiss. 4 = amphibolite, 5 = biotite gneiss, 6 = quartzite, 7 = garnet biotite gneiss, 8 = schist.

Samples: G22 and G7, Ralston Buttes District (RBD); Van Horn, 1976.
G8 and RD-3 (RBD); Sheridan and others, 1967.
RD-1 and RD-2 (RBD); Young, 1972.
79S28 to 80S77 (RBD); Wallace, 1983.